THE UNIVERSITY
of EDINBURGH

Notch/Wnt signalling and the hepatic progenitor response in hepatocellular regeneration

Sarah Minnis-Lyons

Doctor of Philosophy

University of Edinburgh

2016

Declaration

I declare that:

(a) the thesis has been composed by myself,

(b) the work is my own, or where a contribution has been made by other members of the research group, such contribution is clearly indicated, and

(c) that the work has not been submitted for any other degree or professional qualification.

Signed,

Sarah Minnis-Lyons

Abstract

Chronic liver disease remains a significant cause of morbidity and mortality globally. Transplantation is the only effective treatment for end-stage disease but is limited by organ availability, surgical complications and risks of long term immunosuppression. Novel therapies for advanced disease are therefore required. The liver has a remarkable capacity to regenerate through division of mature hepatocytes, however in chronic or severe disease hepatocyte replication fails, senescence occurs and liver failure ensues. Ductular reactions (DRs), containing hepatic progenitor cells capable of repopulating the parenchyma, arise in chronic liver injury when hepatocyte regeneration is impaired. Enhancing this endogenous repair mechanism is a key therapeutic goal. Notch and Wnt are key signals required for liver regeneration, however to date they have principally been characterised in end-point disease and the temporal kinetics of these signalling pathways not known.

I sought to identify if these signals control expansion of DRs after hepatocyte injury and whether they can be therapeutically manipulated. I examined the dynamics of Notch and Wnt activity using a genetic model of hepatocellular injury and ductular-mediated regeneration whereby induction of injury could be timed, synchronising the regenerative response. Using lineage tracing, small molecules, blocking antibodies and genetic loss of function experiments I defined distinct time-sensitive Notch and Wnt signatures where early regeneration is driven by Notch and the later response by Wnt. I demonstrated that inhibition of Notch1 and Notch3 but not Notch2 reduces the generation of DRs. I identified that DRs were a source of potent growth hormone IGF1 and this production was Wnt driven. Notch driven expression of IGF1-receptor within DRs identified this axis as a node for cooperation between Notch and Wnt signals. Blocking the IGF1 axis prevented DR expansion, which conversely could be enhanced by administration of recombinant IGF1.

Here, I functionally defined complex temporal dynamics controlling of DRs and identified therapeutic pathways to enhance liver regeneration.

Lay summary

Chronic liver disease remains a significant cause of death and poor health worldwide. Liver transplantation is a treatment for advanced disease but there are insufficient organs available and significant risks of surgery and long term use of anti-rejection drugs. This means new types of treatment need to be developed. The liver has a remarkable ability to repair itself by replication of liver cells or hepatocytes, however in the case of severe or long-term damage this can become overwhelmed. The liver also contains a further type of cell called hepatic progenitor cells (HPCs) that can behave like 'stem cells' and contribute to liver regeneration when the hepatocytes fail. Understanding this process may help identify targets for drugs to enhance this method of liver repair. I focused my work on investigating chemical signalling pathways used by the developing liver to see if they controlled expansion of HPCs after injury. I identified that these pathways behave in a dynamic way, taking turns to control expansion. I also identified that these pathways can cooperate and took advantage of this to enhance the regenerative response. This work identifies targeting strategies for future therapies.

Acknowledgements

I wish to thank my supervisors for their support over the past few years. Professor Stuart Forbes for his faith and encouragement and Professor Owen Sansom for his unshakable optimism, and always being inspiring.

I would like to thank Professors Iain McInnes and David Webb for the opportunity to work with the MRC Scottish Clinical Pharmacology and Pathology scheme, and the assistance that this has resulted in.

I wish to thank Janet Man for her excellent stewardship of my (copious) mouse lines, without whom this thesis would be considerably slimmer and Luke Boulter for his seemingly limitless patience with me on all matters scientific. I extend further thanks to members of the Forbes group past and present whose help and good humour have ensured the time has flown by. On a more personal note I would like to thank Rachel Guest and Joanna Moore for the conversation (scientific and otherwise), travel, and being there in challenging times.

This thesis is dedicated to Peter, whose support means everything, and Felix, whose early arrival added to the challenge.

Contents

Table of Figures

List of Abbreviations

2/3 PH	two-thirds partial hepatectomy
2AAF	2-acetylaminofluorene
AAV	adeno-associated virus
ABC	active beta-catenin
Ah	aryl hydrocarbon
Akt	thymoma viral proto-oncogene
Alb	albumin
ALD	alcoholic liver disease
ALT	alanine transaminase
ANOVA	analysis of variance
APAP	acetaminophen, paracetamol
APC	adenomatous polyposis coli
Ascl2	achaete Scute-Like 2
BDL	bile duct ligation
BMP	bone morphogenetic protein
BNF	beta-naphthoflavone
BrdU	bromodeoxyuridine
BSA	bovine serum albumin
CBF	c-promotor binding factor
CBP	CREB-binding protein
CCl4	carbon tetrachloride
CDE	choline-deficient, ethionine-supplemented
CK19	cytokeratin 19
Cre	cyclic recombinase
CREB	cAMP response element-binding
CSL	CBF/Suppressor of hairless/Longevity-assurance gene family member
CV	central vein
DAB	3,3'-Diaminobenzidine
DAPI	4',6-diamidino-2-phenylindole
DAPT	N-[N-(3,5-Difluorophenacetyl)-L-alanyl]-S-phenylglycine t-butyl ester
DDC	3,5-diethoxycarbonyl-1,4-dihydrocollidine

Dll	delta-like ligand
DMSO	dimethyl sulfoxide
DNA	deoxyribonucleic acid
DR	ductular reaction
DSL	delta, serrate and lag domain
Dvl	dishevelled
EdU	ethynyldeoxyuridine
EGF	epidermal growth factor
ELISA	enzyme-linked immunosorbent assay
EpCAM	epithelial cell adhesion molecule
ER	oestrogen receptor
Fah	fumarylacetoacetate hydrolase
FAP	familial adenomatous polyposis
FCH	fibrosing cholestatic hepatitis
FCS	foetal calf serum
FGF	fibroblast growth factor
Fox	forkhead box protein
Gapdh	glyceraldehyde-3-Phosphate Dehydrogenase
GFAP	glial fibrillary acidic protein
GFP	green fluorescent protein
GGT	gamma-glutamyltranspeptidase
GH	growth hormone
GSK3b	glycogen synthase kinase 3 beta
GS	glutamine synthetase
H2B	histone 2B
HCC	hepatocellular carcinoma
HGF	hepatocyte growth factor
HIF	hypoxia inducible factor
HNF	hepatic nuclear factor
HPC	hepatic progenitor cell
i.p.	intra-peritoneal
ICD	intracellular domain

IGF1	insulin-like growth factor 1
IGF1R	type 1 IGF receptor
IGFBP	IGF binding protein
IRS	insulin receptor substrate
IVC	inferior vena cava
Krt19	cytokeratin 19
Lgr5	leucine-rich repeat-containing G-protein coupled receptor 5
MAML	mastermind like
MCD	methionine-choline deficient
MCDE	methionine-choline deficient, ethionine supplemented
MDM2	mouse double minute 2 homolog
Mdr	multidrug resistance gene
MMP	matrix metalloproteinase
MMT	3-(4,5-dimethylthiazol-2-yl)-2,5-diphenyltetrazolium bromide
mTOR	mechanistic target of rapamycin
MTT	3-(4,5-dimethylthiazol-2-yl)-2,5-diphenyltetrazolium bromide
NASH	non-alcoholic steatohepatitis
NICD	notch intracellular domain
NPC	non-parenchymal cell
Nrarp	Notch-regulated ankyrin repeat protein
NTBC	2-(2(-nitro-4-trifluoromethylbenzoyl)-1,3-cyclohexanedione
NTR	nitroreductase
OCT	optimal cutting temperature
OPN	osteopontin
panCK	pancytokeratin
PBC	primary biliary cirrhosis
PBS	phosphate buffered saline
PCNA	proliferating cell nuclear antigen
PI3K	Phosphoinositide 3-kinase
PV	portal vein
qPCR	quantitative polymerase chain reaction
RBP-Jk	recombination signal-binding protein kappa

RFP	red fluorescent protein
RNA	ribonucelic acid
SEM	standard error of the mean
Shh	sonic hedgehog
siRNA	small interfering ribonucleic acid
SOX9	SRY-related HMG box transcription factor 9
SV	simian virus
TAA	thioacetamide
TAD	transactivation domain
TBG	thyroid binding globulin
TCF/LEF	T-cell factor/lymphoid enhancer factor
TGF	transforming growth factor
TIMP	tissue inhibitor of matrix metalloproteinases
TM	tamoxifen
Ttr	transthyretin
TWEAK	tumour necrosis factor-like weak inducer of apoptosis
YFP	yellow fluorescent protein

1 Introduction

1.1 Liver disease – the clinical problem

Chronic liver disease is a significant cause of morbidity and mortality globally (1). In the United Kingdom disease incidence continues to rise with an approximately 50% increase between 1998 and 2009 (2). An evolutionary necessity in an organ whose principal roles include removal of toxins, the liver possesses a remarkable capacity to repair and regenerate itself. However in cases of severe or chronic injury these processes become overwhelmed and liver failure ensues. Transplantation is the only effective treatment for end-stage disease but is limited by organ availability, surgical complications and risks of rejection and long-term immunosuppression. Novel therapies for advanced disease are therefore required.

1.2 Liver development

An appreciation of liver development and the structure of the adult organ are helpful to understanding liver injury and repair. Anatomically the lobes of the adult liver are divided into lobules, a classical hexagonal arrangement of sheets or plates of hepatocytes radiating around a central draining vein (see Figure 1.1). Located along the lobule perimeter, the portal triad consists of a small portal vein, hepatic artery and bile duct. Blood flows from the portal tract through hepatic sinusoids towards the central vein. Highly specialised sinusoidal fenestrated endothelium permits contact between the basolateral surface of hepatocytes and the blood. Associated with the sinusoids are macrophages with key immune and repair functions and resting stellate cells, which maintain extracellular matrix but transform into activated myofibroblasts after injury and are responsible for scar deposition. Tight junctions between the apical surfaces of hepatocytes form bile canaliculi which drain newly synthesised bile into ducts lined with biliary epithelial cells also known as cholangiocytes. The area of interface between bile duct and canaliculus is termed the Canal of Hering and has been proposed to represent the location of hepatic progenitor cells (HPCs) (3).

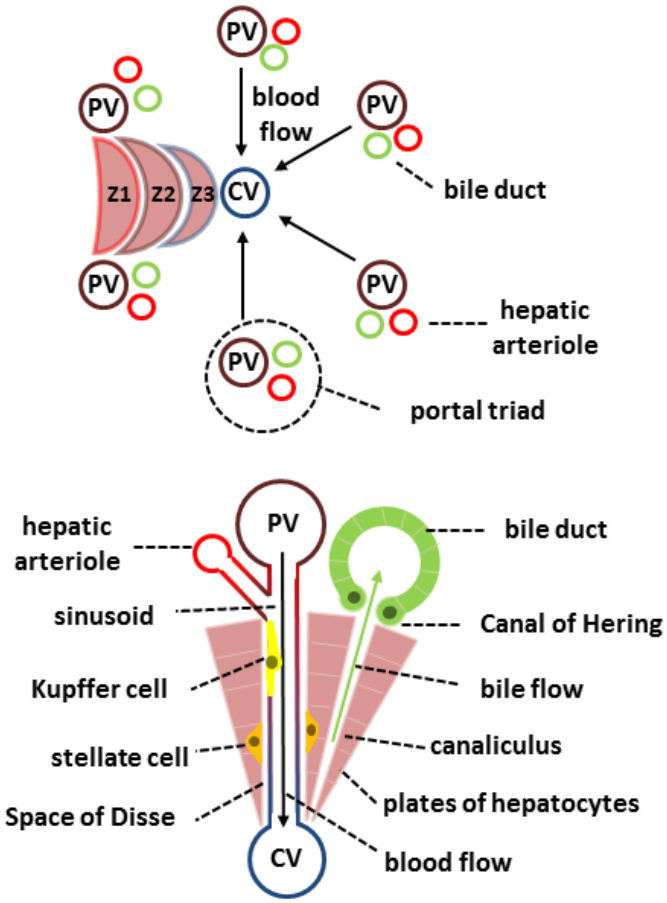

Figure 1.1: Structure of the liver lobule: Sheets of plates of hepatocytes radiate around the central vein (CV). At the periphery of the lobule are the portal triads, consisting of a branch of the portal vein (PV), hepatic artery and a bile duct. The most peripheral hepatocytes, receiving the most oxygenated blood are termed zone 1 (Z1) hepatocytes. Those closest to the central vein are in zone 3 (Z3). Blood enters the liver from the portal vein and hepatic artery, flowing through sinusoids towards the central vein. Hepatocytes form sheets with their basolateral surface associated with sinusoidal fenestrated endothelium permitting contact between blood and hepatocytes. Closely associated with the sinusoids are numerous macrophages or Kupffer cells and in the space of Dissé separating hepatocytes from sinusoids are extracellular matrix components and stellate cells. The hepatocytes' apical surface forms a bile canaliculus which drains newly synthesised bile into ducts lined by biliary epithelial cells or cholangiocytes. The junction between canaliculus and duct is termed the Canal of Hering. PV, portal vein; CV, central vein

The two mature liver epithelial cell types, hepatocytes and cholangiocytes share a common embryonic liver progenitor cell termed hepatoblast. These cells derive from three domains within the endoderm that migrate to fuse into a single prehepatic domain adjacent to the cardiogenic medosderm. At this stage the first molecular evidence of liver 'specification' occurs: the expression of albumin, transthyretin and alpha-fetoprotein (4, 5). Subsequently a liver diverticulum forms from the specified cells, now designated hepatoblasts, expressing the markers Dlk, E-cadherin and Liv2 (6-8). These cells proliferate and form a tissue bud within a basement membrane of laminin, collagen IV, nidogen, fibronectin and heparin sulfate proteoglycan (9). The hepatoblasts then migrate through the basement membrane, leaving the endoderm for the septum transversum. Here, under control of growth factors including hepatocyte growth factor (HGF) (10), continuing proliferation and liver expansion occurs.

Ultimately the hepatoblasts make a fate decision: hepatocyte or cholangiocyte lineage (11). Cells adopting the cholangiocyte lineage align around branches of the portal vein to form a single layered ring called the ductal plate. Areas within the ductal plate become asymmetrical bi-layered arrangements which mature under the influence of SRY-related HMG box transcription factor 9 (SOX9) (12) to form luminal structures giving rise to bile ducts. Each ductal plate gives rise to an average of two bile ducts per portal tract (13) and it was initially proposed that the ductal plate cells that did not become bile ducts apoptose. Subsequently the ductal plate has been shown to also generate canals of Hering and hepatocytes of the periportal region (14). Cells adopting the hepatocyte lineage undergo a process of maturation involving a set of transcription factors, commonly referred to as liver-enriched factors including hepatic nuclear factor (HNF)-1 alpha and HNF-4 alpha that form a network of auto-regulatory and cross-regulatory loops (15).

Functions of all hepatocytes (e.g. gene expression and biochemical activities) are not equivalent and depends on their physical location within the lobule and this maturation continues in the first weeks after birth (16). From a metabolic perspective, rather than the anatomically defined lobular unit, the functional unit of the liver is the hepatic acinus. This represents all liver parenchyma supplied by a terminal branch of the portal vein and hepatic artery. Zone one (periportal) hepatocytes are located nearest to the entering vascular supply and thus receive the most oxygenated blood, zone 3 (pericentral) hepatocytes are

located closest to the central vein and therefore most sensitive to ischaemia. The metabolic functions of hepatocytes from each zone are distinct (17). For example zone 1 hepatocytes are specialised for oxidative functions such as gluconeogenesis, cholesterol synthesis and express urea cycle enzymes for the conversion of ammonia. Zone 3 cells are important for glycolysis, cytochrome P450-based drug detoxification, express glutamine synthase (GS) and utilise ammonia to generate glutamine (18). One key mechanism by which this functional zonation is maintained is via signalling molecules or morphogens (19). Wnt/beta-catenin signalling was the first identified 'zonation keeper' (20). Further examples include members of the fibroblast growth factor (FGF) family (21), the transforming growth factor (TFG)-beta family (22), including bone morphogenetic proteins (BMPs), Notch (23-25), hepatocyte growth factor (HGF) (26, 27) and possibly Hedgehog signalling (28). Not surprisingly roles for these same morphogens have been implicated in liver development and regeneration.

1.3 Liver regeneration – potential methods

Two modes of liver regeneration have been demonstrated and are illustrated in Figure 1.2. In the first, for example after surgical removal of up to two-thirds of the liver (2/3 partial hepatectomy (PH)), the remaining hepatocytes and other liver cells are not injured and enlarge and divide to rapidly regenerate the liver in a process known as 'compensatory hypertrophy' (29, 30). Provided the ability of hepatocytes and cholangiocytes to divide remains intact, similar methods are also responsible for regeneration after a range of acute and chronic insults (31-33). There is evidence that the ability of mature hepatocytes to replicate declines in advanced disease. In rodent models there is reduction of hepatocyte DNA synthesis after partial hepatectomy in animals with cirrhosis (34, 35). In humans, cirrhosis is associated with expression of markers of cell cycle arrest in hepatocytes (36, 37) which suggests they may be less able to contribute to regeneration.

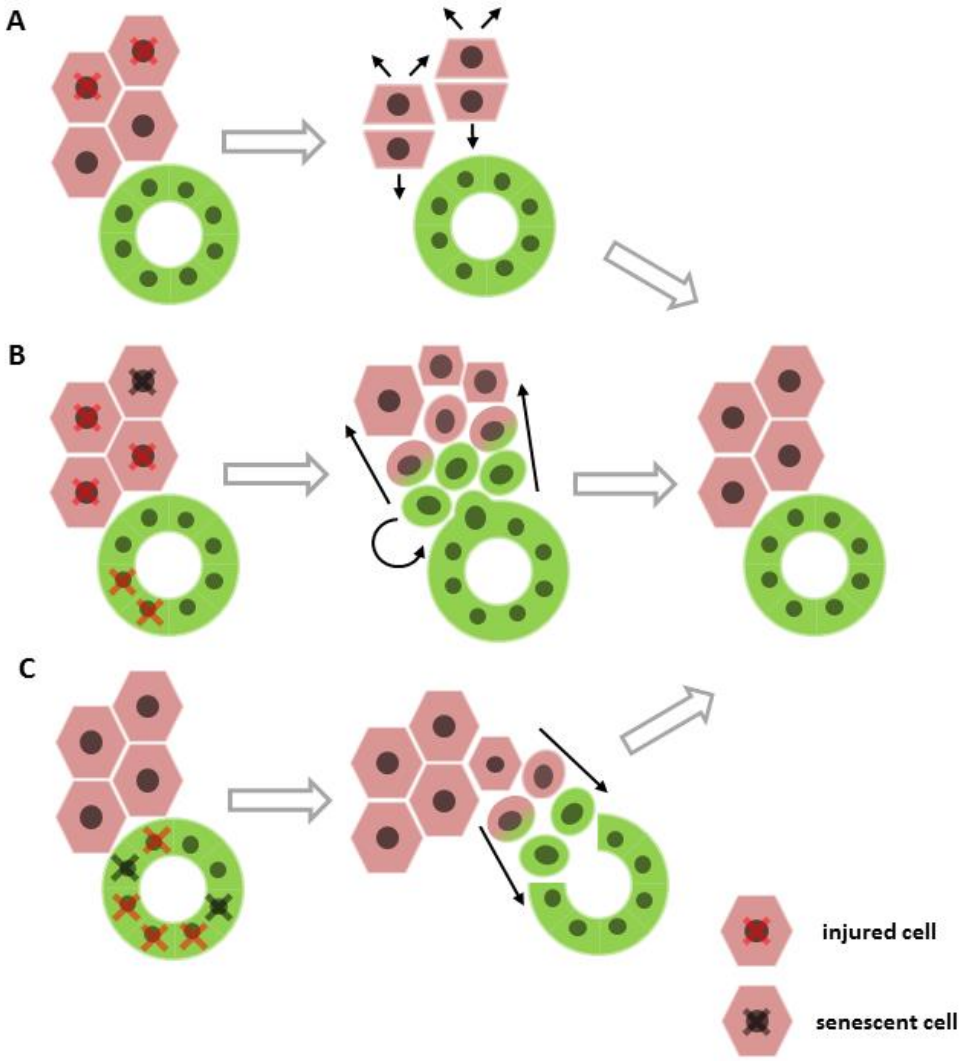

Figure 1.2: Methods of liver regeneration: (A) After hepatocyte injury, remaining hepatocytes reconstitute the liver mass by a combination of hypertrophy and proliferation. **(B**) In instances of severe or chronic injury, ultimately the regenerative capacity of hepatocytes becomes impaired. Facultative stem cells derived from the biliary compartment become activated, producing bipotential progenitor cells which are capable of expanding and differentiating into hepatocytes or cholangiocytes as required. **(C)** After severe biliary injury it is also likely that this process can happen in reverse, with hepatocytes giving rise to ductular-like cells, although whether this is permanent is not yet established.

The second regenerative strategy, proposed to contribute to regeneration after severe or chronic injury involves the activation of 'stem cells'. The term 'stem cell' is probably not entirely appropriate in the liver. The strict definition of cells that are resident clonal precursors of both more stem cells of the same type, as well as a defined set of differentiated progeny, confirmed through in vivo transplantation and reconstitution assays (38-40) has not been met. There is no cell type visible routinely in the uninjured adult liver that has the functions of a fully committed tissue-specific stem cell akin to the cells of the intestinal crypts (41), the basal layer or the epidermis (42), bone marrow (43, 44) or bone (45). However, even in tissues with a clearly defined resident stem cell population such as skin and intestine, other populations of cells can act as stem cells, such as label retaining bulge cells in the hair follicle (46) and the label retaining +4 cell in the intestine (47-49). The +4 position intestinal stem cell is considered the prototype of a 'facultative' tissue stem cell, i.e. only active when required in very specific circumstances. These cells have subsequently been shown to have a bidirectional relationship with Lgr5+ classical intestinal stem cells (47).

The term 'facultative' stem cell is also preferred when applied to the liver. Although here rather than a resident dedicated tissue stem cell that can be called upon to form multiple cell types should the need arise, the mature and apparently terminally differentiated hepatocyte and cholangiocyte epithelia serve to regenerate themselves and each other through what is probably a bipotent 'progenitor' intermediate (33). Investigators disagree whether this process represents transdifferentiation or 'stem cell'-like activity and whether either mature epithelial type, or both, and whether all, or only a subset have this capacity. Descriptive studies support that progenitor mediated regeneration occurs in humans (50, 51), and regeneration of hepatocytes from cells of biliary origin has been demonstrated in zebrafish (52, 53), the rat (54, 55) and the mouse (56-59). In these settings there is activation and expansion of ductular cells. Within this ductular expansion are cells known differentially as hepatic progenitor cells (HPCs), liver progenitor cells (LPCs), oval cells, or sometimes ductular hepatocytes in humans. For consistency I will use the term HPC throughout this thesis. As not all the cells in these ductular expansions are confirmed bipotent progenitors, the term 'ductular reaction' has been coined (60, 61), although technically speaking this term should include any associated inflammatory niche (62). These cells form ductular structures extending from the terminal biliary ductules, the interface

between hepatocytes and duct known as the canals of Hering (3, 63, 64). First described in the portal areas of rat livers after chemical injury, these cells express markers of hepatocytes (albumin) and biliary epithelial cells (cytokeratin 19) in a similar manner to foetal hepatoblasts (65-67). This led to speculation that these cells may be common precursors for both hepatocytes and biliary cells after injury in the adult although disagreement persists as to whether it is only this canal of Hering subset, or potentially all or at least more cholangiocytes that have this capacity as demonstrated by several independent studies (52, 68-70). The degree of contribution of biliary derived HPCs to hepatocyte regeneration is likely determined by the degree to which hepatocyte regeneration is impaired. Indeed the number of HPCs correlates with disease severity in human chronic liver diseases (71). Use of this second repair mechanism may be dependent on inhibition of hepatocyte proliferation following induction of p21 (59, 72) and thus animal models that do not replicate this feature of human disease will not demonstrate significant repopulation of the parenchyma by HPCs of biliary origin (33). The now strong evidence of the potential for cells of biliary origin to regenerate hepatocytes supports the study of HPCs as an in situ or ex vivo resource that can be targeted by novel therapies to enhance liver repair.

1.4 Defining HPCs

A limitation of studies using adult HPCs is their lack of unique cell surface markers, and lack of consensus regarding which combination of non-specific markers identifies those with repopulation capacity (36, 73). Historically HPCs were identified based on their morphology and location within tissue, as well as the co-expression of hepatocyte and biliary markers. This however is clearly not equivalent to demonstration of repopulation, is confounded by presence of markers that may be transiently or dynamically expressed and does not confirm cell of origin or hierarchy within the progenitor population. Clonogenic assays and in vitro differentiation protocols have been used to identify isolated putative HPCs (74), along with their ability to engraft and repopulate the parenchyma after transplantation (75). However biological function may be altered by the process of isolation and culture.

Markers used to identify HPCs in tissue such as cytokeratin 19 (CK19), pancytokeratin (panCK), OV-6 and epithelial cell adhesion molecule (EpCAM) are also present on mature cholangiocytes. EpCAM -positive cells can be differentiated along both lineages in vitro and

form both hepatocytes and cholangiocytes after transplant (55, 75, 76). However as this marker also labels mature cholangiocytes, this strategy will not necessarily mark a pure population of repopulating HPCs. The repopulation capability of EpCAM positive cells may reflect either an ability of all EpCAM expressing mature cholangiocytes to be repopulating cells, but this transformation might occur at very low frequency, or alternatively EpCAM marks a larger population which includes the specific HPC sub-population. Using a combination of surface markers for prospective isolation enables identification of populations with the most 'stem-like' activity, and helps clarify a hierarchy within the subpopulations of cells. For example cells positive for EpCAM, CD133 (a marker usually associated with haematopoietic cells) and CD24 identify a population capable of generating more frequent colonies when plated at clonal density than EpCAM+ or EpCAM and CD24+ dual positive cells (59). In addition these triple positive cells are capable of differentiation down the hepatocytic and biliary route in vitro and after transplantation in vivo. Other markers of clonogenic HPCs include MIC1-1C3, used in combination with other markers including CD133 (74), and Lgr5 which marks cells visible in rodent (77) and human livers (78) after injury. These Lgr5+ cells are capable of bi-directional differentiation and engrafting in mouse livers after in vitro hepatocytic differentiation. The number of proposed markers and repopulating capability of a range of defined populations likely reflects that HPCs within the DR represent a heterogeneous population containing cells from the most primitive progenitors to more hepatocyte-like cells (79). A single DR appears to demonstrate distinct polarity with biliary differentiated cells at one end and hepatocytic differentiated cells at the other (80).

1.5 HPCs and fibrosis

An association between DRs and the severity of fibrosis has long been established in a range of human liver diseases including alcoholic steatohepatitis (81), chronic hepatitis C (82), genetic haemochromatosis (83) and most dramatically in recurrence of hepatitis C virus after liver transplantation (84) where extremely florid DRs accompany severe fibrosis in a condition termed fibrosing cholestatic hepatitis (FCH). It remains unclear however if these processes occurs in parallel as two independent parts of the response to injury, if HPCs stimulate fibrosis, or if fibrosis supports HPCs (85, 86). Evidence favouring HPCs as the driver of fibrosis includes the finding that administration of TNF-like weak inducer of apoptosis (TWEAK), which is a mitogen for HPCs via the Fn14 receptor (87), to fibrotic mice

undergoing partial hepatectomy resulted in both an increase in HPC numbers and collagen deposition (88). When TWEAK stimulation was prevented with a blocking antibody both HPC number and collagen accumulation decreased. However direct activation of the TWEAK/Fn14 pathway in cultured myofibroblasts from the heart or intestine can promote their activation and collagen production, therefore the effect of TWEAK on collagen production in the liver could also be direct, rather than a secondary consequence of HPC expansion (89, 90). Activated myofibroblasts have been found to be the source of a mitogenic ligand, Jagged-1, directly signalling to HPCs and promoting their proliferation after liver injury (91). Another study that looked at the timing of fibrosis and matrix deposition relative to HPC expansion found that after hepatocellular injury the appearance of collagen appeared to precede growth of DRs, suggesting fibrosis may be required for, rather than be consequent of HPC expansion (92). There is additional evidence that matrix components themselves, and their turnover can influence HPCs (86). Administration of an agent that reduces production of matrix components collagen and laminin after hepatocellular injury, was associated with an increase in generation of HPC-derived hepatocytes, while the number of remaining HPCs fell, suggesting their enhanced differentiation (56). Additionally when macrophages were administered to mice receiving fibrosis-inducing hepatotoxins, there was upregulation of proteins promoting collagen turnover (MMP-9 and MMP-13) with an associated fall in fibrosis, but interestingly numbers of HPCs rose and there was an increase in serum albumin levels, suggestive of improved regeneration (93). While activated myofibroblasts and matrix components may be intricately associated in the development of DRs, this study does suggest that fibrosis may not be a necessary accompaniment to HPC expansion. Ultimately novel pro-regenerative therapies directed at HPCs should not exacerbate fibrosis.

1.6 Modelling liver regeneration

1.6.1 Lineage tracing

Early studies designed to investigate which cells were responsible for hepatocyte repopulation after injury involved administration of a pulse of H^3–thymidine or 5-bromo-2'-deoxyuridine (BrdU) to label proliferating cells (pulse) and then analysis of the tissue following regeneration to identify cells 'tagged' as having derived from those proliferating cells (chase). While this tagging has been shown to be reliable, the label retention cannot

identify distant progeny as detection of label becomes difficult after three cell divisions (94) and this technique has largely been superseded by the development of transgenic technologies in which involve genomic alterations to permanently tag cells of a particular lineage.

Formal tracing of genetically tagged cells remains the gold standard for defining cell fate, however conflicting results from experiments have led to controversies about the capacity of liver cells to switch fate (95). Genetic cell tracing involves the generation of mouse lines containing two transgenes. The first is cyclization recombinase (Cre), under the control of a cell-specific promotor, usually fused to a ligand-binding domain of the oestrogren receptor (ER) rendering expression sensitive to administration of tamoxifen, such as SOX9-CreER, osteopontin (OPN)-CreERT2, CK19-CreER, LGR5-CreER. There are several variants of the tamoxifen-induced Cre system utilised in the liver for example the *Mx1-Cre* in which Cre is induced in Mx-1 expressing cells after exposure to interferon or synthetic double stranded RNA such as poly(I:C) and *AhCre* in which Cre expression is inducible from a cytochrome P450 promotor element that is transcriptionally up-regulated in response to lipophilic xenobiotics such as beta-naphthoflavone (96-98). The second transgenic element is usually under control of the ROSA26 locus and involves a *loxP*-flanked STOP cassette preceding a reporter protein (usually *lacZ*, YFP or RFP). Thus when a cell expressing the specific promotor is exposed to the inducing agent it irreversibly expresses the reporter protein and passes this on to its progeny, thus labelling the lineage. High fidelity lineage tracing experiments require the tissue-specific promotor to be truly tissue-specific and the Cre-induction regimen to result in recombination only within the intended cells, and no recombination to occur in the absence of either the promotor or inducing agent. Further transgenes can be added, where *loxP*- flanked areas (denoted $^{fl/fl}$) are inserted into a gene of interest. The precise arrangement can result in loss of this gene or alteration in its structure or degradability after administration of the inducing agent, to generate loss of function or over-expression mutants to assess target gene function.

After administration tamoxifen persists in the organism with low level induction of Cre-ER being been demonstrated up to four weeks after injection (99). This may be shortened by altering the solvent used to administer the agent (100). As tamoxifen also can be excreted in faeces, this can result in inadvertent exposure and of untreated animals housed in the

same cage (101). Tamoxifen is directly toxic to hepatocytes (57) and administration can alter gene expression. For example SOX9-CreER is intended to label biliary epithelium, however exposure of mice to tamoxifen results in increased expression of SOX9 in hepatocytes and therefor there is the potential for inadvertent labelling of hepatocytes (14) which after injury could result in aberrant lineage labelling. The possibility that Cre specificity is further altered by the injury model must also be considered (see Chapter 3).

An alternative strategy involves viral-mediated delivery of Cre. Adeno-associated virus 2 and 8 infect hepatocytes with a specificity that is enhanced by inserting the Cre-encoding sequence downstream of a hepatocyte-specific promoter such as transthyretin (Ttr) and thyroid binding globulin (TBG) (102, 103). This too is not without potential confounding factors as the viral vectors do induce liver toxicity and inflammatory responses which may alter the behaviour of the marked cells (104).

True tissue specificity has also been an issue with lineage tracing experiments. For example albumin-CreER is active not just in hepatocytes but in a proportion of cholangiocytes (58, 104). Likewise, glial fibrillary acidic protein (GFAP)-Cre was intended to label only stellate cells, however is also expressed in cholangiocytes (105-107) which may have contributing to the controversy as to whether stellate cells can generate epithelial cells.

Lineage tracing the cell of origin for regenerating hepatocytes can be ‘negative’ or ‘positive’. Negative lineage tracing involves labelling of all hepatocytes prior to injury and observing the appearance of unlabelled hepatocytes (negative patches) suggestive of a non-hepatocyte origin. If labelling remains consistent all cells are of hepatocyte lineage. Robust negative lineage tracing requires near 100% hepatocyte labelling in order that negative patches are not simply expansions of hepatocytes that were not pre-labelled. While this method can identify cells not of hepatocyte lineage, it does not demonstrate their origin. Positive lineage tracing involves labelling cells of the alternative proposed lineage (such as cholangiocytes) and observing the appearance of positively labelled hepatocytes after injury. For this method to be robust, labelling of cholangiocytes does not need to be extensive, however crucially the level of mislabelling of hepatocytes must be negligible if not zero to be sure positive patches of hepatocytes do not represent expansion of aberrantly labelled hepatocytes.

1.6.2 Traditional models for the study of liver regeneration

The best characterised model used in the experimental study of liver regeneration is partial hepatectomy (2/3 PH) (29). This is achieved surgically due to the multi-lobe structure of rodent livers whereby three of the five lobes can be removed without causing any tissue damage to the residual lobes. The remaining two lobes grow to restore liver mass within 5-7 days. Similarly, after resection of liver lobes in humans to remove lesions or after trauma, liver volume is restored in 8-15 days. The high degree of reproducibility of 2/3PH in rodents has enabled the timing and sequence of ensuing regenerative events to be precisely studied. A highly orchestrated series of orderly cellular events have been characterised from the first 5 minutes to completion of regeneration from existing hepatocytes and cholangiocytes at 5-7 days. When the replicative potential of hepatocytes is not impaired, DRs are not seen in this model. Positive lineage tracing experiments using OPN-CreER or HNF1-beta Cre have failed to identify a contribution from the biliary or HPC compartment (56-58). A negative lineage tracing study by Malato et al found 1.4% of hepatocytes were unlabelled after 2/3PH but it remains unclear if this is due to incomplete primary labelling or an alternative cell origin (102).

Loss of liver mass can also be induced by administering hepatotoxic chemicals such as carbon tetrachloride (CCl4). CCl4 causes injury to pericentral hepatocytes through the formation of toxic intermediates via the cytochrome P450 pathway and alteration of calcium homeostasis (108). With chronic delivery it induces hepatic fibrosis however neither the acute or chronic injury model classically results in a DR. Results from lineage tracing studies have demonstrated with positive lineage tracing no biliary contribution to hepatocyte regeneration and with negative tracing only a small contribution after chronic administration, again potentially reflecting incomplete labelling (56, 57, 102, 109).

Paracetamol (acetaminophen, APAP) poisoning is one of the most clinically relevant of the injury models as it remains one of the commonest causes of acute liver failure in Europe and the USA (110). In humans DRs are seen in cases of massive hepatic necrosis (36). In mice a dose and time-dependent bi-phasic expansion of DRs is seen with change in HPC number visible within the first 10 hours post-APAP administration (111), however in the one published lineage tracing experiment, hepatocytes of biliary (HNF1b-CreER labelled) origin were not seen (57).

Oral administration of thioacetamide results in formation of toxic metabolites within zone 3 (pericentral) hepatocytes (112, 113). Prolonged administration results in ductular reaction, hepatic fibrosis and in the rat, ultimately dysplasia and biliary carcinoma (114). In the mouse, when combined with conditional loss of tumour suppressor gene p53, chronic administration of TAA also results in biliary cancer (115, 116). This model has been used to lineage trace the cell of origin in cholangiocarcinoma (116), but not the origin of hepatocytes after shorter term administration.

Hepatocyte proliferation in rats can be blocked by administration of the chemical 2-acetylaminofluorene (AAF), triggering replicative arrest by accumulation of p53 and p21 (117). When administered prior to 2/3 PH, hepatocytes fail to proliferate and instead cholangiocytes, in particular located at the canals of Herring, expand markedly and express a mix of biliary and hepatocytic genes (118, 119). These cells take on the 'oval cell' morphology (ovoid nuclear shape and high nuclear to cytoplasmic ratio). They subsequently become basophilic hepatocytes and eventually mature hepatocytes, restoring liver volume (54, 94, 120). As described above the precise timing of 2/3PH makes careful analysis of dynamic processes of regeneration possible, however current genetic technology does not permit the accurate permanent tissue-specific labelling in rats as performed in transgenic mouse lines. Unfortunately when the same protocol is applied to mice, they fail to generate convincing regenerative DRs, likely because al lack of a sulfotransferase means blockade of DNA replication is not achieved (67, 121).

Several models involving the incorporation of toxins or manipulation of the nutritional content of mouse diets have been described. The choline-deficient, ethionine supplemented (CDE) diet is frequently used to generate DRs. It involves choline-mediated hepatocyte steatosis and injury and ethionine-mediated replicative block and the two agents are traditionally given separately in food and water (122). Injury is predominantly hepatocytic and HPCs generated in response to this typically form a niche surrounded by macrophages (123) after 3 weeks. In lineage tracing studies using OPN-CreER and HNF1b-CreER 1.81-2.45% were found to be biliary derived using what is known as the CDE-STOP or CDE-recovery protocol where experimental choline deficient diet and ethionine 0.15% in drinking water is given for three weeks followed by a 2 week recovery period where animals receive chow and the majority of HPC differentiation occurs (56-59). In these

studies the age of animals used varied widely from 3-4 weeks to 12-24 weeks at time of Cre-induction with diet commenced 1-2 weeks after the final tamoxifen dose. Injury resulting from the CDE diet has been found to be highly sensitive to animal age and background strain with a very much reduced HPC response in older animals and those of a mixed genetic background (124), which may explain the range in results and failure of lineage tracing in older animals. Interestingly while two of the groups generated very similar results (2.45 vs 2.12% hepatocytes), the authors of one paper concluded this demonstrated the potential of HPCs and the other concluded this reflected minimal relevance of HPCs (56, 58).

Espanol-Suner et al report lineage tracing with CDE diet is much reduced in the OPN-CreER strain when animals are older and weigh over 20-22g at the start of injury (56). One study using a K19CreER found no biliary contribution to hepatocytes however the injury period was shortened to 2 weeks (109). A second study using the K19CreER with a 3 week diet protocol and negligible lineage tracing was seen however animals were at least 12 weeks old before commencing diet (59). The Stanger group used a combination of positive lineage tracing with a K19CreER and negative lineage tracing with an AAV8-TBG-Cre (hepatocyte-specific promotor) to trace lineages with CDE diet (103). Animals were different ages at the time of commencing diet as the AAV8 group received virus at 6-8 weeks followed by a 2 week 'washout' period, commencing two weeks of experimental diet at 10 weeks. The K19CreER group commenced diet at age 6-8 weeks and again received only 2 weeks injury, however received 3-5 doses of tamoxifen during the second week of diet, rather than being labelled prior to commencing injury as in other studies. They found no hepatocytes labelled as being of biliary origin. Furthermore the Willenbring group also used a combination of positive and negative lineage tracing (K19CreER and AAV8-Ttr-Cre) to perform lineage tracing using the CDE diet (125). They found in the negative lineage tracing group 0.76% of hepatocytes were unlabelled and therefore potentially of HPC origin, however the positive lineage tracing group only labelled a negligible proportion of hepatocytes (<0.1%) leading authors to conclude that the unlabelled cells in the negative trace group reflected sub-100% labelling by the virus, rather than contribution from biliary lineage. Finally, a group using a SOX9-CreER traced <1% of hepatocytes however their protocol used a lower percentage of ethionine (0.1%) than the standard (0.15%).

The importance of a significant CDE-related injury in generating biliary lineage labelled hepatocytes is emphasised by the recent publication of a study by Shin et al. In this study HPCs appearing after onset of injury using a Foxl1-Cre labelling system were traced. When analysis was restricted to animals experiencing >14% weight loss (an indication of significant injury), the number of labelled hepatocytes rose to 5% after 15 days diet and 29% after 4 further days of recovery (126). The authors subsequently demonstrated, by introducing a diphtheria toxin-sensitive element to their genetic construct so Foxl1+ cells could be ablated, that this population was essential for proper regeneration. As the traditional CDE diet involves uncoupling the choline deficiency from the ethionine supplementation so each component could be altered independently to better suit the tolerability and sensitivity of different strains (122), this does introduce variability as the intake of each component varies between individuals. This has led to the optimisation of an alternative protocol in which the ethionine is included in the modified diet, reducing variability between animals and generating a robust HPC response without animal welfare concerns (127).

The methionine-choline deficient (MCD) diet causes some features similar to human non-alcoholic steatohepatitis (NASH) (128, 129) with hepatocyte specific injury, however not the full spectrum of the condition as insulin resistance is not induced (130). It does however generate a robust ductular reaction and fibrosis (131) but formal lineage tracing studies have not yet been published. One study has shown a variant of this diet, in which ethionine is given in addition (MCDE), gives rise to DRs and biliary derived hepatocytes, although concerns have since been raised regarding the specificity of the SOX9-Cre used (70). Huch et al have identified Lgr5+ HPCs from animals fed the MCDE diet and demonstrated that they differentiate into hepatocytes (77).

By contrast the 3,5-diethoxycarbonyl-1,4-dihydro-collidine-supplemented (DDC) diet induces a predominantly biliary injury with deposition of porphyrins causing occlusion of small ductules, although there is associated hepatocyte damage (132). HPCs generated in this model are typically intimately associated with activated myofibroblasts (123) and have not been shown to be capable of hepatocellular differentiation (56-58). Interestingly when the source of cells of the DRs generated in response to DDC diet were analysed, a proportion were shown to be of hepatocyte rather than biliary lineage using the AAV8-TBG-

Cre (103). Suzuki et al also identified cells they determined as cholangiocytes after DDC diet to be of hepatocyte origin using an Alb-CreER (104). However due to difficulties distinguishing de novo DR cells from mature cholangiocytes, particularly given the morphology of DRs in this injury model it is not clear whether these cells represent fully differentiated cholangiocytes of hepatocyte origin, particularly as at peak injury 60-70% of cells were positive for the hepatocyte lineage marker, yet after recovery this number fell to 1.1%. In addition the Alb-CreER has been shown to also label a proportion of biliary cells (58). Tarlow et al went on to demonstrate the wide scale conversion of hepatocytes to HPC-like cells of the DRs generated in response to DDC diet (133). In order to do this they generated chimeric animals by transplanting hepatocytes positive for the red fluorescent protein (RFP) variant Tomato into *Fah*$^{-/}$ mice. *Fah*$^{-/-}$ mice are deficient in fumarylacetoacetate hydrolase (Fah), involved in the catabolism of phenylalanine. The animals develop fatal tyrosinaemia unless they receive 2-(2(-nitro-4-trifluoromethylbenzoyl)-1,3-cyclohexanedione (NTBC) and this strain is frequently used as a recipient when assessing the repopulation capacity of hepatocytes or HPCs in the liver as when sufficient Fah positive hepatocytes engraft, NTBC treatment is not required. In these experiments, engrafted and lineage tagged hepatocytes were shown to be the cell of origin of many cells of the DR and that these cells reverted to hepatocyte phenotype on removal of the injury. A similar result was obtained when human hepatocytes were transplanted into immunodeficient mice. This led the authors to conclude that hepatocytes undergo a reversible ductal metaplasia in response to injury, and then contribute to restoration of hepatocyte mass.

An alternative model to study biliary injury and regeneration is bile duct ligation (BDL). Surgical induction of biliary obstruction results in injury, biliary proliferation, myofibroblast activation, the appearance of DRs and an intense fibrotic response comparable to human biliary cirrhosis (134-136). Lineage tracing studies using this model have demonstrated the cell of origin of DRs lies within the biliary compartment and that there is no contribution to hepatocyte lineages (58, 102).

1.6.3 Transgenic models of liver injury and regeneration

Transgenic technology has also been used to induce regenerative responses in the liver. Multidrug resistance gene (Mdr2) (also known as Abcb4) deletion in mice results in failure of secretion of phospholipid into bile and regurgitation of bile acids from leaky ducts resulting in periductal inflammation, a DR, severe ductular fibrosis and ultimately obliterative cholangitis due to death of cholangiocytes and duct atrophy (137, 138). Negligible contribution to new hepatocytes from biliary lineages has been identified in this model (58).

In the zebrafish, genetic incorporation of the bacterial nitroreductase (NTR) gene under the control of a tissue-specific promotor results in conditional ablation of the cell type after exposure to the NTR substrate metronidazole (139). Zebrafish engineered to have the NTR gene under the control of a hepatocyte specific promotor (lfabp) exhibit extreme ablation of hepatocytes after incubation with metronidazole for 24 hours. The liver regenerates to 50% of normal size at 48 hours and fully regenerates within the next 36-48 hours from cells of biliary origin (52). These findings were independently corroborated in a second paper using positive and negative lineage tracing under control of a Tp1 biliary and a fabp10a hepatocyte promotor (53). Authors of the first study term this hepatocyte repopulating capacity of biliary cells 'transdifferentiation'. This term classically refers to direct conversion of one cell type to another, avoiding a pluripotent state, however can include a de-differentiation step into an intermediate precursor stage (140). He et al demonstrate expression of hepatoblast markers Hhex and Foxa3, and Choi et al expression of Prox1, consistent with a dedifferentiated bipotential intermediate state.

A key point in both zebrafish papers in demonstrating substantial regeneration of hepatocytes from the biliary compartment was the severity of the hepatocyte injury and failure of hepatocyte-mediated regeneration. As discussed above, in rats combination of 2AAF and 2/3PH results in failure of hepatocyte replication and regenerative DRs (94, 120). In advanced human liver disease, hepatocyte-mediated regeneration fails and cells become senescent, indicated by expression of markers p21 or p16. DRs are seen in this setting, but in the absence of lineage tracing, their functional role in contributing to regeneration is unclear (36). One explanation of the apparent discrepancy in findings between murine dietary model studies versus zebrafish and rat are differences in the extent to which hepatocyte regeneration is impaired. When expression of p21 was analysed in the

hepatocytes of mice undergoing dietary models of liver injury such as CDE, hepatocyte senescence was found to be minimal (59). To recreate the widespread senescence seen in humans and rats, a novel mouse model has been generated in which hepatocyte senescence is induced (59). Mouse double minute 2 homolog (MDM2) is an E3 ubiquitin-protein ligase that degrades p53. In its absence, p53 accumulates resulting in senescence and death of the cell. Use of the hepatocyte-specific Cre *AhCre* in combination with a MDM2 locus in which exons 5 and 6 are deleted and rendered inactive following Cre induction results in hepatocyte senescence and death, massive expansion of DRs and repopulation of the parenchyma by ductular derived HPCs. This study using the *AhCre MDM2*$^{fl/fl}$ strain provides the most compelling evidence to date for the potency of DRs in regenerating the liver in mice, although formal lineage tracing using this model has not yet been possible.

1.6.4 The plastic liver hypothesis

Reliability of labelling, differing definitions of stem and stem-like activity, protocol variation, reproducibility of models, clinical relevance of models and differing conclusions drawn from similar results have together rendered the field of investigation of the capacity of liver cells to switch fate and repopulate highly controversial.

A most plausible explanation for some of the grossly divergent results from apparently well designed and accurate lineage tracing studies using different systems and models that is gaining ground within the field is that of the highly plastic liver (33, 141-145), although acceptance is not universal (32, 109, 125). This organ has so many vital roles in the maintenance of body homeostasis, and in addition is the principal barrier to ingested toxins. Therefore it would seem an evolutionary necessity that many if not all cell types, particularly cells with common developmental precursors, may retain some potential to contribute to regeneration of the whole organ. Thus the results obtained through formal lineage tracing experiments reflect the type of cell injured, the degree of injury, and the degree to which this cell type's ability to regenerate is impaired and therefore the degree of stimulus applied to other cell types to contribute. Collectively these studies demonstrate the diversity and potency of regenerative strategies that the liver can employ, rather than conflicting views on the correct representation of a single consistent process. Instead of a strictly definable entity, the 'HPC' represents an indistinct transitional form; it does not

conform to a traditional stem cell model and instead represents a milieu that can encompass protective metaplasia through to regenerative potential.

1.7 Liver homeostasis

It is perhaps not surprising that there is so much controversy regarding how the liver can regenerate when even in homeostasis evidence for which cells are responsible for routine tissue turnover is conflicting.

Early rodent DNA labelling studies using thymidine gave rise to the 'streaming liver' hypothesis: hepatocytes migrate from the portal area to the central area (69, 146). This has been further supported by description of a 'maturation gradient' along the same axis (147), and clonal expansion of hepatocytes originating in the portal areas (148) in humans. One study took the streaming liver hypothesis a step further, demonstrating that biliary cells (lineage tagged via expression of Sox9) were the source of hepatocytes under normal homeostatic conditions, replacing over 90% of hepatocytes along the portal-central axis in a year (70). However subsequent studies have failed to confirm this data: cells positive for Sox9 at the time of ductal plate formation were able to subsequently generate periportal hepatocytes only (14), and during adult homeostasis no contribution was found from labelled biliary Sox9 positive cells (102). While not distinguishing the axis of hepatocyte replacement in homeostasis, further tracing studies labelling either hepatocytes or ductal cells have demonstrated that existing hepatocytes are responsible for hepatocyte renewal (56, 57, 102, 109). Font-Burgada et al have recently demonstrated a population of periportal cells that express low levels of Sox9 but not biliary marker CK19 and instead express hepatocyte marker HNF4a (149). The role of these cells in homeostasis was not the focus of this paper; the authors reporting the number of Sox9-GFP labelled HNF4a positive cells remaining stable for at least nine months. However they went on to demonstrate that after hepatocyte injury, these cells were responsible for hepatocyte renewal along the portal-central axis. In sharp contrast to the concept of new hepatocytes 'streaming' from the portal tract to the central vein, Wang et al have recently described how streaming may actually occur in the opposite direction (150). It has previously been established that Wnt signalling is responsible for formation and maintenance of hepatic zonation with pericentral expression of Wnt target genes such as GS (20). In this new study authors observed expression of Wnt target gene Axin2 in the same cells and used a tamoxifen-inducible

Axin2-CreERT2 to permanently pulse label Axin2 expressing cells with GFP and their progeny. These cells were shown to self-renew and generate expanding clones that populate the entire lobule over time, although on average 40% of hepatocytes were labelled. The central vein endothelium was identified as a local source of Wnt. Most hepatocytes are polyploid (151), which may limit replicative potential (152). However, the Axin2 positive cells were predominantly diploid, a characteristic of stem cells that may be necessary for unlimited duplication (153). This model does however contrast with the observation that zone 3 hepatocytes do not show a higher proliferative rate than other areas (154), unlike the Axin2 and Lgr5 positive stem cells in the gut.

1.8 Pathways involved in regeneration

1.8.1 Notch signalling

A relatively small set of highly conserved signalling pathways including the sonic hedgehog (Shh), Wnt, protein/transforming growth factor beta (BMP/TGFb), phosphatidylinositol 3-kinase/thymoma viral proto-oncogene (PI3K/AKT) and Notch pathways are used by cells to sense cues from their environment and integrate this information into an appropriate developmental or physiological response. Most of these pathways involve a 'core' signalling pathway of components required for signal transduction and a more varied set of 'auxiliary' proteins that have the capability of modifying the signal (155). The Notch pathway is uniquely able to permit cells to communicate with their direct neighbours by ligand-receptor interactions between adjacent cells to direct a transcriptional response (156).

1.8.1.1 Notch pathway

There are four known Notch receptors in mammals (Notch1-4) and five ligands from the Jagged (Jagged1 and 2) and Delta-like (Delta-like ligand (Dll) 1, 3 and 4) families. The ligands are characterised by the presence of a Delta, Serrate and Lag2 (DSL) domain.

Notch receptors are generated as a single transmembrane receptor that is cleaved by Furin-like convertase in the *Trans*-Golgi (S1 cleavage) to yield heterodimeric Notch receptor containing an intra- and extracellular domain, which is exocytosed to the cell surface (see Figure 1.3).

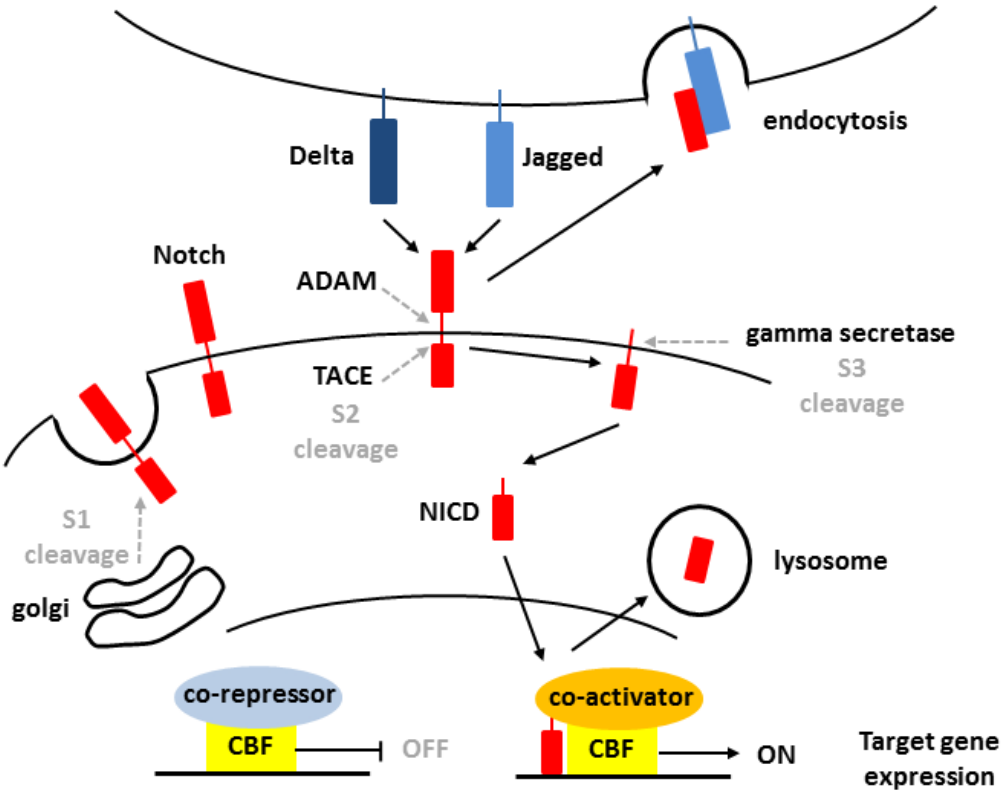

Figure 1.3: Core components of the Notch signalling pathway: Following manufacture, Notch receptors undergo their first proteolytic cleavage by Furin-like convertase and transported and exocytosed onto the plasma membrane. Here ligand from the signal sending cell, of either the Delta or Jagged families, binds the extracellular domain of the receptor. This then triggers cleavage of the extracellular domain by ADAM and TACE metalloproteases and this extracellular domain remains bound to the ligand and is endocytosed by the signal-sending cell. Further cleavage within the transmembrane domain to yield the Notch intracellular domain (NICD) is performed by gamma secretase. The NICD enters the nucleus where is associates with a member of the CSL family and co-activators such as mastermind like (MAML) and target gene expression ensues.

CBF, C-promotor binding factor; CSL, CBF/Suppressor of hairless/Longevity-assurance gene (LAG); ADAM, a disintegrin and metalloproteinase; TACE, TNF alpha converting enzyme

In canonical signalling ligand binds membrane-bound receptor leading to proteolytic cleavage of the extracellular domain by ADAM10/TACE metalloprotease (S2 cleavage) and this outer portion is then subjected to lysosomal degradation by the ligand-presenting cell. The remaining receptor portion is cleaved within its transmembrane domain by the gamma-secretase complex (S3 cleavage) as it is endocytosed by the signal-receiving cell, resulting in release and nuclear translocation of the Notch intracellular domain (NICD). Here is associates with a CSL (CBF1 (C promotor-binding factor)/Suppressor of hairless/Longevity-assurance gene-1 (LAG-1)) family member. CBF1 is also known as recombination signal-binding protein kappa (RBP-Jk) in mammals. NICD binding converts it from a transcriptional repressor to an activator, resulting in Notch target gene expression. The NICD is rapidly consumed and degraded by the proteasome, terminating the signal. There is no signal amplification step in this pathway, unlike many others where for example phosphorylation of core components occurs. This results in signal transduction in a 1:1 ratio and therefore the relationship between signalling input and output and signalling strength is important for generating the appropriate cellular response, and explains the sensitivity of the pathway to gene dosage deviations (155).

Notch signalling can also occur independently from canonical ligands and/or from CSL/RBP-Jk-mediated transcription (non-canonical pathway) (157). Delta-like 1 (Dlk1) is one of the first reported non-canonical ligands for Notch (158). This ligand is lacking a DSL domain and evidence supports that it interacts in *cis*, inhibiting Notch signalling (159) although may be able to activate Notch signalling via an alternative domain (160). Other non-canonical ligands include members of the microfibril-associated glycoprotein family (161) and connective tissue growth factor/cysteine-rich 61/nephroblastoma overexpressed gene family member CCN3 (162). Additionally Notch signalling can be transmitted in a CSL/RBP-Jk independent manner (163), including through cross-talk with other signalling pathways (see 1.8.1.2 and 1.10).

1.8.1.2 Notch actions and regulation

Despite the small number of core components, Notch signalling is able to affect cell fate decisions across a wide range of species and cell types and at different stages in lineage progression (164). The outcome of Notch signal is strictly dependent on the cellular context

and can influence differentiation, proliferation, migration and apoptosis of cells (165). A variety of methods exist to permit both tight control of Notch signalling and generate diversity of responses from activating the core conserved pathway.

Notch receptors share a similar basic structure with an extracellular domain including epidermal growth factor (EGF)-like repeats, and a transmembrane region and an intracellular region containing at least three conserved domains. These are the RBP-Jk-associated molecule domain, consecutive Ankyrin repeat domains and a C-terminal proline-glutamic acid-serine-threonine (PEST) sequence (166). A full transactivation domain (TAD) is only found in Notch1 and 2, the structure of the third identified paralog, Notch3, displays distinct structural differences most marked in this area which may explain the weak transactivation activity of Notch3-ICD (167). In addition these and other structural differences could affect interactions with coactivators or repressors (168).

Tissue distribution of the different paralogs and ligands varies, suggesting difference in functionality. This can be seen through the range of phenotypes seen in developmental defects and diseases in humans accompanying mutation of pathway components. For example mutations in either Jagged1 or Notch2 result in Alagille syndrome, characterised by bile duct paucity and to a variable extent cardiac and spine defects and deafness (169-171). Absence of Dll3 is associated with a disorder of the segmentation of the axial skeleton (172), and activating mutations of Notch3 causes cerebral autosomal dominant arteriopathy with subcortical infarcts and leukoencephalopathy (CADASIL), a hereditary young-onset stroke disorder (173, 174).

Post-translational modifications of Notch receptors by proteins such as Fringe family members modulate the relative responsiveness of receptors of the Delta versus Jagged classes (175-177). Limiting the distribution of Notch ligands and receptors only to certain parts of the cell can also contribute to signalling specificity as communication will only occur with certain neighbours (155). This enables Notch signalling to generate lateral inhibition – a cell adopts a certain fate and prevents its immediate neighbours from doing the same. Ligands tend not to be expressed only on the signal-receiving cell. Relatively small concentration differences in ligand and receptor establish directionality of signalling. This is assisted by the fact that ligands activate receptors on contacting cells (trans-activation) but inhibit receptors on the same cell (cis-inhibition) (178-181).

Ligand-receptor combinations do not seem to influence signal output with the exception of Dll3 which is the most structurally divergent ligand (182). It is not capable of activating Notch receptors in *trans* and may exclusively act through cis-inhibition of receptors (183). There does however appear to be evidence of ligand-receptor specific interactions, particularly in the context of cancer cell survival and growth (184, 185).

Diversity in signalling response can also be generated at the transcriptional level. Hairy and enhancer of split (Hes) and hairy/enhancer-of-split related with YRPW motif (Hey) genes encode basic helix-loop-helix transcriptional repressors. These are considered to be the key Notch target genes, however it now appears that the immediate Notch transcriptome is larger, with many genes activated in parallel, rather than secondary to *Hes* and *Hey* genes (155). The transcriptome output differs by cell type, stage in cell cycle and lineage progression (186, 187) with no 'obligatory' Notch target upregulated in all cell types. Other genes activated in parallel include *c-myc*, *cyclin D1* and *p21* (188-190). There is some evidence that the different notch receptors are capable of generating diversity in the downstream response, consistent with distinct expression patters of the four paralogs in most tissues. For example the configuration of CSL binding sites within Notch target genes influences the likelihood of recruiting the NICD of Notch1 or Notch3 (191).

A number of auxiliary proteins have been shown to affect Notch signalling at various stages of the pathway such as proteins that affect ligand intracellular trafficking in the signal-sending cell such as Mind bomb (Mib) and those that regulate interactions between NICD and CSL/RBP-Jk such as Mastermind-like (MAML), contributing to adjustment of signal strength (192-194). Numb is an endocytic adaptor protein that suppresses Notch signalling (195, 196). It recruits Itch, an E3 ubiquitin ligase, to promote ubiquitination degradation of the Notch receptor (197, 198) and regulate post-endocytic trafficking and degradation (199). Not all Notch receptors are equal targets for Numb with the absence of key lysine residues in Notch3 rendering it relatively resistant to the effects of Numb compared with Notch1 and Notch2 (197). Interactions between Notch and Numb are discussed further below (see 1.10.1) Notch can be further regulated by phosphorylation, ubiquitylation or hydroxylation of the NICD (200-203).

The Notch signalling pathway can also interact with and be modified by other signalling pathways. Interactions with the Wnt pathway are discussed below (see 1.10). Notch can

interact with the TGFb signalling pathway – NICD interacts with mothers against decapentaplegic (SMAD) transcription factors, and TGFb signalling enhances canonical Notch signalling (204, 205). Notch signalling is also linked to the cellular response to hypoxia. It can interact directly with hypoxia inducible factor 1 alpha (HIF1a), controls gene expression synergistically with HIF1a, and hypoxia itself can lead to stabilisation of the NICD (206-208). Hypoxia regulates Notch3 expression in pulmonary artery hypertension, important for disease development (209) and hypoxia also maintains colorectal cancer cells in a stem-like phenotype in a Notch-dependent manner (210).

1.8.1.3 Notch and liver development

Identification of mutations in the Jagged1 gene in most patients with Alagille syndrome, and subsequently Notch2 in the remainder, established Notch signalling as key for liver development (169-171). Mice compound heterozygote for Jagged1 and a hypomorphic Notch2 allele, or mice homozygous for hypomorphic Notch2 exhibit several features of Alagille's syndrome including intrahepatic bile duct paucity (211).

Notch1-ICD and Notch2-ICD overexpression models demonstrate conversion of bipotential hepatoblasts to biliary lineage and the formation of the three-dimensional architecture of intrahepatic ducts (12, 212). Notch1 versus Notch2 effects are largely redundant in hepatoblasts, however Notch2 appears to be more prominent and mediates many of the Notch effects during intrahepatic biliary duct development (212, 213). The Jagged1 signal-sending cells are likely to be the portal mesenchyme (214). Interestingly even in the absence of canonical Notch signal from early development (such as in inducible *Rbpj*$^{fl/fl}$ mice), specification of ductal plate cells still occurs, although at a lower rate (215). The key biliary fate-determining properties of Notch are further demonstrated by the over-expression of Notch1-ICD in adult hepatocytes which results in upregulation of Sox9 and ultimately their reprograming into biliary cells (103, 215).

Further distinct roles have been attributed to the different Notch paralogs during development with Notch2 and Notch4 associated with proliferation of hepatoblast cell lines and Notch3 associated with a more hepatocyte-like morphology (216). While Notch1, 2 and 4 impeded hepatocytic differentiation *in vitro* Notch3 expression was conducive to differentiation.

While several key Notch regulated genes including Sox9, HNF1b and Hes1 are critical for biliary development, there is no single factor exclusively downstream of Notch mediating all effects on biliary development (156) and instead a complex network exists involving communication with other signalling pathways including TGFb and Wnt to define the transcriptome that directs biliary specification and maturation (217).

1.8.1.4 Notch and liver injury

In the rat after 2/3 PH NICD migrates to hepatocyte nuclei within 15 minutes. Notch effectors Hes-1 and Hes-5 are upregulated by 30 minutes (218). RNA interference to Jagged1 or Notch1 partially suppressed regeneration and delivery of recombinant Jagged1 to cultured hepatocytes induced DNA synthesis, demonstrating a pro-proliferative role for Notch signalling in liver regeneration (218), however some of this effect may be indirect *in vivo* due to effects of Notch signalling on liver sinusoidal epithelial cells (219, 220).

Following liver injury when DRs are generated, vital roles for Notch, along with the other important developmental morphogens such as Wnt and Shh have been proposed. In human disease, the type of injury appeared important as to the activation status of these pathways (123, 221). Expansion of DRs in various rodent injury models is sensitive to Notch pathway inhibition with gamma-secretase inhibitors (GSIs) (123, 222). Genetic interference with Notch signalling in the biliary/HPC compartment through conditional deletion of RBP-Jk impedes their expansion after injury (58) and Notch2 specifically is required for proper tubular morphogenesis (223). Similarly, genetic over-expression of the Notch2-ICD within this compartment in the absence of injury results in spontaneous generation of DRs (224). Specific interaction has also been identified between Jagged1 expression on myofibroblasts and Notch1 on biliary cells, directly causing their proliferation and generation of DRs (91). When this axis is disrupted in mice, they were unable to survive biliary injury from bile duct ligation, the impaired DRs associated with massive hepatic necrosis and mortality, providing evidence of a further role for DRs in supporting the parenchyma, even if not contributing directly to repopulation. In the ablative zebrafish model of liver regeneration, after extreme loss of hepatocytes, remaining biliary cells underwent de-differentiation losing their tubular morphology, proliferated and expressed hepatocyte markers, repopulating the parenchyma (52). This process was Notch dependent.

Notch signalling has also been proposed to direct fate of HPCs along the cholangiocyte route akin to the developmental specification of the hepatoblast during development with Jagged1 ligand provided by activated myofibroblasts in the surrounding inflammatory niche in response to biliary injury (123). Administration of DDC diet to mice has been shown to result in upregulation of the Notch pathway within hepatocytes, akin to forced over-expression of Notch1-ICD, both resulting in their conversion to biliary cells (103). Likewise forced activation of Notch2-ICD in hepatocytes results in biliary lineage conversion (224). On the other hand, inducible conditional deletion of canonical Notch signalling in HNF1b-positive (i.e. biliary) cells did not result in conversion to hepatocytes, however it is not clear if this is due to absence of effect on fate or failure of DR activation and expansion (58).

Provision of Jagged1 ligand to ductular cells by activated stellate cells results in ductal proliferation, however may also influence the biology of the stellate cell itself, inducing production of alpha-smooth muscle actin and collagen (225). Myofibroblasts have also been shown to upregulate Notch3 in rat CCl4-induced liver fibrosis and when transduced with a viral vector interfering with Notch3 production, fibrosis was attenuated (226).

1.8.1.5 Notch and liver cancer

Roles for Notch signalling have been proposed in both major types of liver cancer, hepatocellular carcinoma (HCC) and intrahepatic cholangiocarcinoma (ICC). There is evidence to date that ICC can derive from both biliary and hepatocyte lineages (103, 116, 227, 228). Genetic over-activation of Notch1 (by transgenic insertion of constitutively active N1-ICD) in hepatocytes not only re-directs them to the biliary lineage, but also activates the cancer program: it appears that in this context too, Notch not only determines fate but promotes proliferation (104, 227, 229). With regard to HCC, lineage tracing suggests it arises principally, if not exclusively from hepatocytes (58, 230). Activation of Notch1 or N2-ICD in hepatoblasts also results in HCC (231, 232).

1.8.2 Wnt signalling

In development Wnt signalling is crucial for the generation of patterned tissues during embryogenesis by acting as a symmetry-breaking signal. In vertebrates this signalling system also functions in pattern maintenance: by fuelling stem cell activity in many organs they sustain tissue renewal. In addition when some stem cells are ablated, they are

replaced by more differentiated cells that under the influence of Wnt signalling regain characteristics of their stem cell origin to effect tissue repair (233).

1.8.2.1 Canonical Wnt pathway

After production in the signal sending cell, the palmitoyltransferase Porcupine induces addition of a palmitate group to Wnts. This lipidated state both tethers it to membranes or receptors and permits binding to transmembrane protein Wntless (Wls) which conveys it to the cell membrane for secretion or externalisation (234). The classical description of Wnt is as a long-range signal in *Drosophila* development, however recent evidence suggests a non-diffusible membrane-tethered form of the protein may instead be the principal mode of action (235). Within the context of the stem cell niche, action is primarily short-range between adjacent cells (233).

Wnt ligand binds Frizzled receptors on the target cell via the palmitate group and the Lrp5/6 co-receptor (low density lipoprotein receptor-related protein 5 and 6), inducing it to form a complex with Frizzled, enabling phosphorylation by associated protein kinases. The phosphorylated cytoplasmic domain of Lrp inhibits glycogen synthase kinase 3 beta (GSK3b) and binds Axin (see Figure 1.4). In the absence of Wnt signal, a complex of proteins including Axin, adenomatous polyposis coli (APC) and GSK3b, known as the 'destruction complex' phosphorylates b-catenin, continuously targeting it for degradation by the proteasome. Wnt-induced inhibition of the destruction complex leaves beta-catenin available for translocation to the nucleus where it associates with T-cell factor/lymphoid enhancer factor (TCF/LEF) transcription factors, inducing target gene expression. Target genes include pro-proliferative *myc* and *cyclin*. R-spondin proteins enhance Wnt signalling strength; their binding to Lgr family receptors, most notably Lgr5, itself a Wnt-responsive gene, results in inhibition of E3 ubiquitin ligases usually responsible for degradation of Frizzled resulting in a more stable Wnt/Frizzled complex (236).

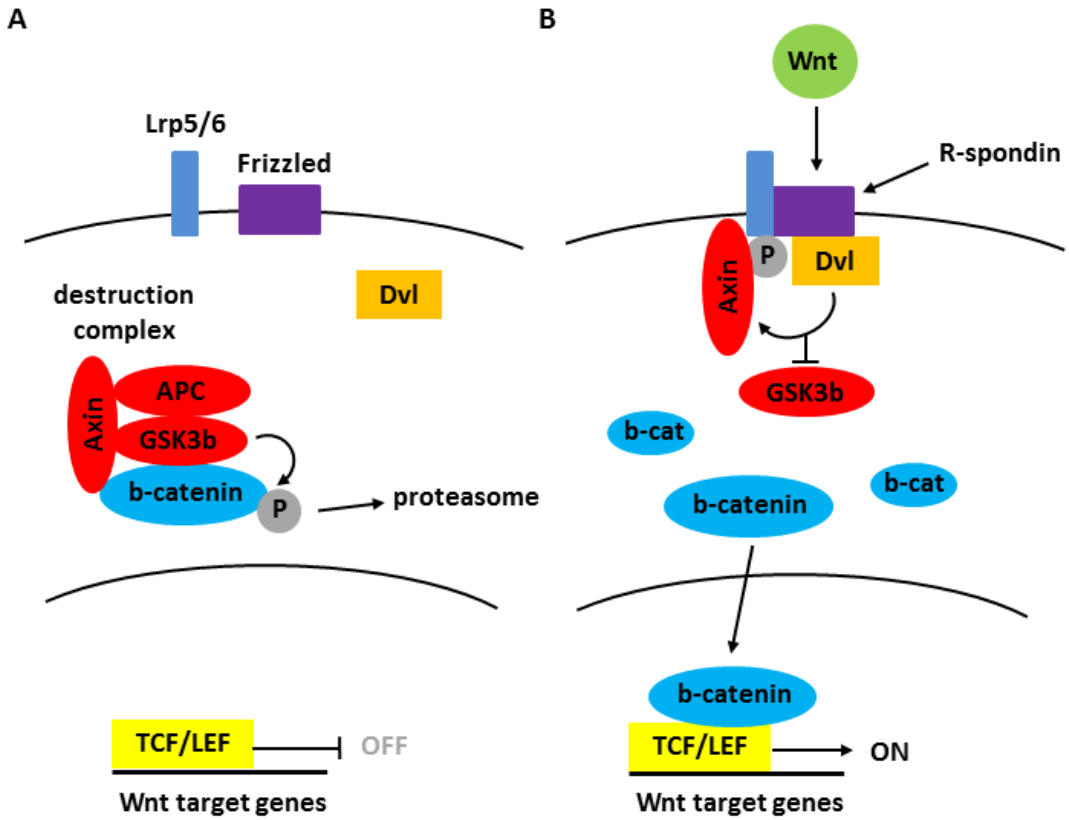

Figure 1.4: The canonical Wnt pathway: (A) in the absence of Wnt signal the destruction complex which includes Axin, APC and GSK3b phosphorylates beta-catenin. This identifies it for ubiquitination and degradation in the proteasome. **(B)** When Wnt ligand is present it binds Frizzled receptor and the Lrp5/6 co-receptor resulting in phosphorylation of the cytoplasmic domain of Lrp5/6 by associated kinases. The phosphorylated version of Lrp binds and sequesters Axin and with dishevelled (Dvl) inhibits GSK3b. This permits cytoplasmic accumulation of active (un-phosphorylated) beta-catenin which translocates to the nucleus and associates with TCF/LEF transcription factors to induce target gene expression.

Lrp5/6, low density lipoprotein receptor-related protein 5 and 6; APC, adenomatous polyposis coli; GSK3b, glycogen synthase kinase 3 beta; Dvl, dishevelled; TCF/LEF, T-cell factor/lymphoid enhancer factor.

This thesis focuses on canonical Wnt signalling; however Wnt signalling can also occur via non-canonical pathways. Beta-catenin is a multifunctional protein and can interact with additional proteins such as cadherins, and is therefore involved in cell adhesion (237). Wnt signalling can also occur independent of beta-catenin and is mediated by jun N-terminal kinase (JNK) or intracellular calcium with cell polarity and motility the main outcomes of signalling.

1.8.2.2 Wnt functions

Wnt signalling has key and myriad roles in development, homeostasis and regeneration. Mutations in pathway components have been shown to generate diverse phenotypes from problems with bone mass, virilisation, and tooth agenesis to type II diabetes (238). One of the most studied areas is the role of Wnt signalling in intestinal homeostasis and malignancy after the genetic loss of a negative regulator of Wnt signalling (subsequently designated APC) was identified as the cause of hereditary cancer syndrome familial adenomatous polyposis (FAP) as well as sporadic cancers (239, 240). The gut epithelium undergoes rapid turnover, largely replaced every 4-5 days (241). Cells from the absorptive surface, the protruding villi, are continuously shed into the gut lumen and are replaced by cells generated from *Lgr5+* stem cells located in the crypts at the villus base (41). Disruption of Wnt signal results in abrupt cessation of proliferation within the crypts, loss of villi, and gut failure (242, 243). Addition of Wnt agonist R-spondin, or loss of negative pathway regulators, stimulates proliferation (233, 244). Labelling Axin2 or Lgr5 positive cells in a range of other tissues including mammary gland (245, 246), skin (42, 247), brain (248) and liver (150) has demonstrated crucial roles for 'Wnt responding' cells in tissue renewal.

In addition to effects driven through direct induction of genes related to cell growth and proliferation, Wnt/beta-catenin signalling interacts with a number of other pathways and cell-regulatory molecules, for example Wnt stimulates the activation of the tyrosine kinase Src (via Dishevelled-2) (249) which in turn enhances Wnt signalling and it may promote serine/threonine kinase mTOR activity through direct effects on ligand production, stimulating PI3K and Ras pathways, or through inactivating GSK3b promoting mTOR activity (250, 251).

1.8.2.3 Wnt and liver development

During the patterning of the endoderm, Wnt signalling must be supressed to allow expression of early liver transcription factors (252), however subsequently during the early stages of hepatic morphogenesis, Wnt signalling is required for liver specification and growth (252, 253), highlighting changing temporal requirements for this pathway during development. The requirement for Wnt signal persists with beta-catenin being required for proliferation and differentiation of hepatoblasts into the hepatocyte fate (254), but even at this later stage there is likely to be careful regulation of signal as when beta-catenin is depleted from E9.5 onwards hepatoblast proliferation and differentiation is impaired, whereas when negative regulator of Wnt-signal APC is deleted starting from E11.5 proliferation and differentiation were also reduced. As discussed above, Wnt/beta-catenin signalling is responsible for establishing appropriate zonation of hepatocytes late in development, and maintaining that zonation through adult life with negative regulator APC most strongly expressed in zone 1 and 2 hepatocytes and Wnt target genes including GS expressed exclusively in zone 3 (20). Recently the Lemaigre group have demonstrated that beta-catenin is not required for differentiation of hepatoblasts into cholangiocytes and bile duct morphogenesis. They also found that excessive beta-catenin activity in developing ducts actively stimulated biliary development, however ducts showed aberrant morphology and perturbed differentiation, reinforcing the importance of tight control of levels of Wnt signalling (255).

1.8.2.4 Wnt, liver regeneration and cancer

The pro-proliferative and fate determining functions of Wnt signalling suggest potential further roles in liver regeneration. However, unchecked proliferation might result in malignant transformation.

Wang and colleagues' model of liver homeostasis driven by Wnt-responsive Axin2-positive zone 3 hepatocytes has yet to be interrogated in the injury setting, however a role for Wnt signalling has been established in other regenerative models. After 2/3 PH beta-catenin is visible in the nucleus of hepatocytes after 5-10 minutes and for up to 6 hours (256). Hepatocyte growth factor (HGF) is a principal early driver of liver regeneration (257-260). In cultured hepatocytes HGF induces dose-dependent nuclear translocation of beta-catenin, independent of Wnt ligand and thus beta-catenin is thought to be responsible for some of the multifunctionality of HGF in liver regeneration (261).

HPC-mediated regeneration in rats undergoing the 2AAF 2/3PH protocol is accompanied by expression of active beta-catenin in the DRs (262). After induction of biliary injury with DDC diet DRs report Wnt activity and when the HPCs are isolated, they proliferate in response to administration of Wnt3a (263). Deletion of beta-catenin abrogates the ductular response to DDC injury (262). Periductal cells positive for Wnt-dependent marker Lgr5 have been identified after liver injury. These cells have been lineage traced into hepatocytes and when isolated expand and differentiate in the presence of Wnt agonist and Lgr5 ligand R-spondin. Once transplanted into a non-competitive model (*Fah*$^{-/-}$ mice) they behave as functional hepatocytes (77). Furthermore the mass repopulation of hepatocytes from biliary cells demonstrated in the ablative zebrafish models has been shown to require Wnt (in this case Wnt2bb) (53).

Aberrant activation of beta-catenin pathway is observed in 30-40% cases of human HCC, principally due to mutations in beta-catenin itself or Axin (264, 265). Viral mediated Cre-inactivation of APC results in nuclear accumulation of beta-catenin in hepatocytes, and induction of target genes including GS. This accompanies hepatomegaly, hepatocyte hyperplasia and rapid mortality (266). When the dose of adenoviral-delivered Cre is reduced, compatible with both survival and persistence of beta-catenin activated cells, 2/3 of mice develop HCC. Promotion of beta-catenin signalling by its core protein is one mechanism by which hepatitis C virus is thought to drive HCC (267). In addition to HCC, activation of Wnt signalling has been identified in cholangiocarcinoma. In this condition when associated with liver fluke infestation, mutations in a negative regulator of Wnt signalling (*RNF43*) have been detected (268). In cases of sporadic disease, a 'high-Wnt' state has also been identified, in this case driven by inflammatory macrophages in the surrounding cancer stroma, reflecting an aberrant injury repair mechanism (115).

In addition to pro-proliferative effects of Wnt signalling, roles in hepatocytic differentiation of HPCs have been established in the mouse, rat and human (77, 78, 123, 269). In vitro differentiation protocols in all three species involve Wnt agonism and interference with Wnt signalling in vivo prevents hepatocytic differentiation.

1.9 Systems where Notch and Wnt signalling co-exist

In the gut Wnt signalling is essential for maintenance of the stem cell compartment with pathway inhibition or genetic ablation resulting in loss of the Lgr5 stem cell population (41,

242). In addition Notch signalling, in particular via Dll1 and Dll4 ligands, are required to maintain this same population (270). There is also a requirement for an intact Wnt signalling cascade within cells to respond to Notch-dependent mitogenic stimulus (271), thus further demonstrating a requirement for both pathways in stem cell maintenance.

As discussed above Wnt signalling can be involved in fate decisions and in the gut is involved in Paneth cell differentiation (272, 273) while overexpression of Wnt inhibitor *Dkk1* leads to loss of all secretory cells (274). In contrast Notch signalling negatively regulates secretory cell differentiation in favour of generation of absorptive cells (enterocytes) with goblet cell hypertrophy occurring in response to Notch inhibition (275, 276). Again careful regulation of these two pathways is required for maintenance of effective organ function and cell differentiation (277).

Effective regeneration in any tissue requires a switch from progenitor cell proliferation to differentiation. In muscle Notch has been identified as a key driver of activation and expansion of myogenic progenitors (278). Subsequently it has been determined that a temporal switch from Notch to Wnt signalling is required for these cells to differentiate. These signals in the correct sequence permit the regulated proliferation then differentiation required for effective muscle regeneration (279). Crosstalk between these two pathways appears to be mediated by GSK3b.

1.10 Interactions between Notch and Wnt pathways

1.10.1 Numb

Numb can act as a juncture between Notch and Wnt signalling. Numb is a direct transcriptional target of the Wnt signal (280), and binds to the NICD, recruiting the E3 ubiquitin ligase Itch leading to polyubiquitination and degradation by the proteasome (198, 281). Numb can also disrupt trafficking of Notch receptor, re-directing it to an endocytic compartment for degradation (199). Finally, Numb supresses Shh signal (282); Shh regulates Notch activity and when inhibited, accumulation of ductular cells after biliary injury is impaired (107, 283).

Previous work has proposed a model for hepatocellular regeneration in which HPCs enter a window where Wnt signal results in Numb expression which inhibits Notch and results in hepatocyte fate (123). In this setting Wnt ligand is supplied by inflammatory macrophages

within the niche in response to the engulfment of dead hepatocytes. In the absence of hepatocyte death (for example in the case of predominantly biliary injury), there is no Wnt signal from macrophages and Notch signal is unopposed and HPCs proceed down the biliary fate.

The Notch receptor paralogs are not equivalent targets for Numb-mediated ubiquitination and degradation: the loss of a number of conserved lysine residues in Notch3ICD makes it a poor target for the Numb/Itch complex (197) and correlates with the finding that Notch3 is not degraded by the proteasome (284). The concept of Notch3 a more 'permissive' Notch in the context of Wnt signalling is supported from the finding in liver development where Notch3 is more associated with progenitor cells undergoing hepatocellular differentiation versus the other paralogs (285).

1.10.2 Ascl2

Transcription factor Achaete Scute-Like 2 (Ascl2/MASH2) also occupies a potentially interesting position between the two signalling pathways. In the gut Ascl2, a direct target of canonical Wnt signalling, is required for maintenance of the Lgr5 stem cell pool in adult intestinal epithelium (286, 287). Recently it has been revealed that the continuous Wnt gradient seen along the intestinal crypt is translated to a discrete Ascl2 'on' switch at the crypt base through a Wnt/R-spondin activated auto regulatory loop (288). Interestingly Notch signalling can both induce Ascl2 expression and repress it via Hes-1 in epidermal development (289), further highlighting the tight controls on this Notch/Wnt sensitive system.

1.10.3 IGF1 axis

Several studies have demonstrated interactions between the IGF1 axis and Notch or Wnt signalling. Insulin-like growth factor 1 (IGF1) is principally produced in the liver in response to growth hormone (GH) (290-292). It enters the circulation bound to IGF binding proteins (IGFBPs) which transport it into tissues and regulate bioavailability (293). IGF1 also acts in a paracrine fashion (294). The type 1 IGF receptor (IGF1R) is a transmembrane tyrosine kinase and exerts most of the biological actions of IGF1. This receptor has been identified on ductular cells (295). Following ligand binding the kinase is active, autophosphorylates and can then bind several substrates including the insulin receptor substrates (IRS), initiating phosphorylation cascades resulting in activation of phosphatidylinositol 3-kinase (PI3K) and p70 S6K kinase which results in increasing the active ribosomal pool necessary for cell cycle

entry, and Akt. Akt further enhances proliferative protein synthesis through mechanistic target of rapamycin (mTOR) activation (294). Additional pro-proliferative IGF1R actions include recruitment of Ras and activations of Raf-1/MEK/ERK (296, 297). In muscle where Notch and Wnt are also both important for regeneration, IGF1 is of key importance in proliferation and differentiation of muscle progenitor cells (298).

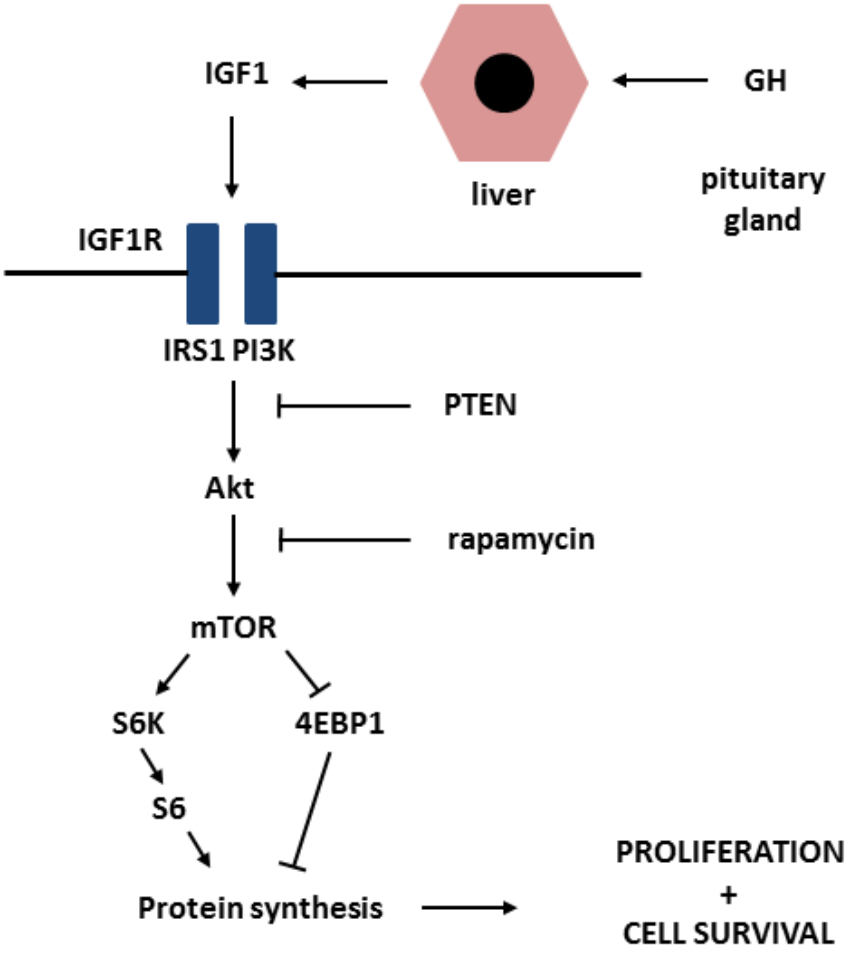

Figure 1.5: The IGF1 axis and mTOR pathway: Growth hormone releasing hormone from the hypothalamus stimulates release of growth hormone from the pituitary gland. This induces expression of IGF1 in the liver which can enter the circulation bound to IGF binding proteins or act in a paracrine fashion. IGF1 binds one of the insulin family receptors, principally the type 1 IGF receptor (IGF1R). Activation of this tyrosine kinase triggers an intracellular phosphorylation cascade mediated via the intracellular adaptor protein IRS1

and PI3K. This results in phosphorylation of Akt, activation of mTOR and the subsequent activation of ribosomes via p70 S6 kinase. In addition negative regulator of translation 4EBP1 is phosphorylated and deactivated. The net effect is increased protein synthesis and cellular proliferation.

GH growth hormone; IGF1 insulin-line growth factor 1; IGF1R type I IGF1 receptor; IRS1 insulin receptor substrate 1; PI3K phosphoinositide 3-kinase; Akt thymoma viral proto-oncogene; mTOR mechanistic target of rapamycin; SK6 ribosomal protein S6 kinase; S6 ribosomal protein S6; 4EBP1 eukaryotic translation initiation factor 4E-binding protein.

The IGF1R is directly induced by Notch1 in hypoxic conditions within lung adenocarcinoma, leading to activation of pro-survival Akt (299). It is also a target of Notch1 in human T acute lymphoblastic leukaemia (T-ALL) initiating cells (300). In addition to directly proliferative actions, Notch can regulate hepatic glucose production and lipid metabolism via forkhead box protein O1 (FoxO1) and Akt/mTOR with Notch inhibition blocking mTOR activity, increasing insulin sensitivity and preventing hepatosteatosis (23, 24). The relationship between Wnt signalling and the IGF1 axis is complex but suggests a positive feedback loop between the two pathways (301). IGF1 can regulate the stability and transcriptional activity of beta-catenin and, via activation of PI3K, stimulate TCF/LEF dependent transcription (302, 303).

In patients with liver cirrhosis plasma levels of total IGF1 and free IGF1 are low while GH is increased, indicating GH resistance and reduced hepatic functional reserve; indeed the degree of IGF1 deficiency correlates with the progression of liver disease (304-306). Some of the clinical manifestations of advanced cirrhosis such as malnutrition and muscle wasting may reflect loss of this anabolic activity (307).

1.10.4 Others

In addition to Numb- and IGF1-mediated cross-talk between Wnt and Notch signalling pathways, other direct and indirect interactions have been reported. For example GSK3b is able to bind and phosphorylate Notch2 resulting in inhibition of Notch target gene expression (200), similarly other components of the beta-catenin destruction complex can influence Notch trafficking (308). Jagged1 has been identified as a beta-catenin target gene (309). Beta-catenin can also act in synergy with the NICD-CSL/RBP-Jk complex on Notch target genes (310, 311). During somite differentiation, beta-1 integrin activity controls both Wnt and Notch signalling, and both signals must be active for downstream gene activation of *cMeso1/MesP2*, involved in the formation of a morphological intersomitic boundary (312). MAML, in addition to its role in stabilising NICD-CSL/RBP-Jk interactions, can also bind GSK3b decreasing MAML transcriptional activity (313) and beta-catenin itself (314), where it behaves as a transcriptional co-activator.

The Notch-regulated ankyrin repeat protein (Nrarp) is induced by Notch signalling and functions as a negative feedback regulator of Notch both by binding the NICD and reducing Notch target gene expression (315, 316). Genetic loss of Notch3 in muscle results in

apparently normal myogenesis (317). However, in Notch3 null animals gross muscle hypertrophy occurs after muscle injury due to unchecked proliferation of progenitors which is largely driven by Notch1 (318). As Notch3-ICD overexpression results in increased *Nrarp* expression it has been proposed as a mechanism by which Notch3 can negatively regulate Notch1.

Further integration between Wnt and Notch pathways is also conferred by Nrarp: in addition to modulating Notch protein turnover it acts independently as a positive regulator of the Wnt signalling pathway (319, 320). This is achieved by stabilising and preventing proteasome-mediated degradation of pivotal Wnt pathway element and transcription factor Lef1.

1.11 Summary

Chronic liver disease remains a significant cause of morbidity and mortality and establishing how the liver regenerates, from which cell types and the potency of those cells, has been hotly debated in recent years. In this most regenerative of organs we are arriving at the concept of a state of regenerative plasticity, where traditional definitions of stem cells may not be appropriate and instead the nature, degree and persistence of liver injury determine which of many potential regenerative avenues are deployed. It has now been established that the bile ducts, and ductular reactions (DRs) generated in response to injury, do contain cells with hepatocyte repopulation capacity. Therefore understanding how they do this is vital for the development of novel therapies that can enhance this endogenous function.

In the gut Wnt signalling is essential for maintenance of the stem cell compartment with pathway inhibition or genetic ablation resulting in loss of the Lgr5 stem cell population (41, 242). In addition Notch signalling, in particular via Dll1 and Dll4 ligands, are required to maintain this same population (270), thus demonstrating a requirement for both pathways. After muscle injury, effective regeneration requires Notch followed by Wnt signal in sequence (279). It has previously been demonstrated that, in end-stage models of liver regeneration, HPCs require differentiation signals through the Notch and Wnt pathways (123) however whether there is a more complex temporal interaction between Notch and Wnt activity in the regenerating liver has not been evaluated.

1.12 Hypothesis

Both Notch and Wnt signalling are required for an effective HPC regenerative response to hepatocellular injury

The roles of these signalling pathways differ with regards to expansion, migration and differentiation

Notch3 has a previously unrecognised role in liver regeneration

Cross-talk between these pathways directs the progenitor response

1.13 Aims

Develop models to further study the HPC response

Characterise the Notch/Wnt axis in hepatocellular regeneration

Characterise the role of Notch3 in the ductular response to hepatocellular injury

Manipulate this axis to identify potentially druggable targets to enhance response to hepatocellular injury

2 Materials and methods

2.1 Animal studies

2.1.1 Generation of animal strains

2.1.1.1 AhCre MDM2 strains:

AhCre MDM2$^{fl/fl}$ (59) was crossed with *Notch3^{d1}* (Notch3$^{-/-}$) (321), *CBF:H2B-Venus* (322) or *TCF/Lef:H2B/GFP* mice (323) (obtained from Jackson Laboratories stock numbers 010547, 020942 and 013752) to give *AhCre MDM2$^{fl/fl}$;Notch3$^{+/+}$, AhCre MDM2 $^{fl/fl}$;Notch3$^{-/-}$, AhCre MDM2$^{fl/fl}$;CBF:H2B-venus* and *AhCre MDM2$^{fl/fl}$;TCF/Lef:H2B-GFP* strains.

2.1.1.2 Krt19-Cre strains:

Krt19-CreER^{T} (324), was crossed with the *Ai14* TdTomato strain (325) (Jackson Laboratories stock number 007914) to give *Krt19-CreER^{T};RCL-tdT* strain.

2.1.1.3 OPN-iCre strains:

OPN-iCreER^{T2};R26R^{YFP} mice (56) (a gift from Frederic Lemaigre, de Duve Institute) were crossed with *Notch3$^{-/-}$* as above to give *OPN-iCreER^{T2};R26R^{YFP};Notch3$^{+/+}$* and *OPN-iCreER^{T2};R26R^{YFP};Notch3$^{-/-}$,* and *Igf1r$^{fl/fl}$* (326) (Jackson Laboratories stock number 012252) to give *OPN-iCreER^{T2};R26R^{YFP};Igf1r$^{fl/fl}$* and *OPN-iCreER^{T2};R26R^{YFP};Igf1r$^{wt/wt}$*.

2.1.1.4 Notch3 null strains:

Notch3^{d1} (Notch3$^{-/-}$) (as above) (321) mice were crossed with C57BL/6 (wild type) mice (Charles River) to give *Notch3$^{-/-}$, Notch$^{+/-}$,* and *Notch3$^{+/+}$* strains.

2.1.1.5 Genotyping:

Genotyping was performed commercially by Transnetyx© (Memphis, TN, USA). Ear notches were taken at the time of weaning at 4 weeks of age. During my maternity leave animal colonies were maintained and bred to usable genotype by Janet Man. She also assisted with the running of animal experiments to my experimental protocols and subsequent tissue harvest.

2.1.2 Induction of Cre and liver injury models

Animals were housed with 12 hour light/dark cycle and given chow and water *ad libitum*.

2.1.2.1 AhCre MDM2 strains:

All *AhCre MDM2*$^{fl/fl}$ strains received 20mg/kg beta-naphthoflavone (BNF) (Sigma-Aldrich) in corn oil intra-peritoneal (i.p.) for Cre induction.

Time course experiment: Animals were harvested at day 0, 3, 5, 7, 10 and 14 post-Cre-induction. This experiment was carried out by Michael Williams. Due to morbidity levels by day 14 all subsequent experiments were terminated at day 10.

Notch inhibition experiments: mice received 50mg/kg/dose DAPT (N-[N-(3,5-Difluorophenacetyl)-L-alanyl]-S-phenylglycine t-butyl ester) (Sigma-Aldrich) or equivalent volume of vehicle daily for 3 days by i.p. injection as outlined in the experimental schematic in Figure 4.5. Animals received DAPT days 2-4 ('early'), days 4-6 ('mid') or days 7-9 ('late') and were harvested 24 hours after the final dose. Notch1 or 2 blocking antibody (clones aN1_E7, aN1_E10, aN2_B6 and aN2_B9) or control antibody (aDesmin) (327) (a gift from John McCafferty, University of Cambridge) was administered by single dose of 10mg/kg by i.p. injection 24 hours after Cre-induction. Animals were culled on day 5 post-Cre induction. *AhCre MDM2*$^{fl/fl}$*;Notch3*$^{+/+}$ and *AhCre MDM2*$^{fl/fl}$*;Notch3*$^{-/-}$ mice received only BNF induction and were culled 7 days later.

Wnt inhibition experiments: mice received 5mg/kg/dose ICG001 (Tocris) or vehicle for 4 days by i.p. injection for the periods demonstrated in the experiment schematic in Figure 5.4. Animals received ICG001 days 1-4 ('early') or days 6-9 ('late'). C59 (Cellagen) was administered at a dose of 20mg/kg/dose or vehicle was administered by i.p. injection day 6 and day 8 post-Cre-induction as per the experimental schematic in Figure 5.4 and 5.7A.

IGF axis experiments: mice received daily i.p. injection of: AG1024 (Santa Cruz Biotechnology) 30ug/dose or vehicle, rapamycin (Tocris) 10mg/kg/dose or vehicle or recombinant murine IGF1 (rIGF1) (Sigma-Aldrich) 0.5mg/dose or vehicle days 6-9 post-Cre induction, as per the schematics in Figures 6.9-12.

2.1.2.2 Krt19-Cre strains:

Six week old *Krt19-CreER*^{T}*;RCL-tdT* mice were given 3 injections of 4 mg tamoxifen in olive oil (Sigma-Aldrich) by i.p. injection 48 hours apart.

When mice reached 22g for females and 25g for males (a minimum of 17 days after the last tamoxifen injection) they received methionine-choline-deficient (MCD) diet (Dyets) for 14

days. During the dietary injury period they received 3 doses per week of DAPT (25mg/kg), ICG001 (5mg/kg) or equivalent volume of vehicle by i.p. injection.

2.1.2.3 OPN-iCre strains:

OPN-iCreER^{T2};R26R^{YFP} mice received the CDE-stop protocol (choline-deficient ethionine-supplemented diet, MP Biomedicals) as previously described (56). This involved commencing Cre-induction with tamoxifen at 21 days old and injury diet at least 14 days after final tamoxifen dose when the mice reached 20g. During the 2 week 'STOP' period DAPT (25mg/kg), ICG001 (5mg/kg) or equivalent volume of vehicle was administered three times per week by i.p. injection. This experiment was conducted by Noemi van Hul at Universite catholique de Louvaine and the tissue and serum shipped to me for analysis.

OPN-iCreER^{T2};R26R^{YFP} strains *OPN-iCreER^{T2};R26R^{YFP};Notch3$^{+/+}$, OPN-iCreER^{T2};R26R^{YFP};Notch3$^{-/-}$, OPN-iCreER^{T2};R26R^{YFP};Igf1r$^{fl/fl}$* and *OPN-iCreER^{T2};R26R^{YFP};Igf1r$^{wt/wt}$* having been generated through crosses with mice on a C57Bl/6 background were smaller than the original CD1 parent strain and less tolerant of CDE diet. Therefore induction of Cre with tamoxifen took place at 5-6 weeks old and CDE diet was commenced 14 days after the last injection once animals reached an acceptable starting weight and were harvested after 3 weeks of diet. *OPN-iCreER^{T2};R26R^{YFP};Igf1r$^{fl/fl}$* and *OPN-iCreER^{T2};R26R^{YFP};Igf1r$^{wt/wt}$* mice also underwent 14 days of the MCD diet with induction of Cre at six weeks of age and commencing diet on reaching 22g for females and 25g for males (a minimum of 17 days after the last tamoxifen injection).

2.1.2.4 DDC diet:

Mice of genotypes *Notch3$^{-/-}$, Notch$^{+/-}$,* and *Notch3$^{+/+}$* aged 12-16 weeks received 7 days of 0.1% w/w 3,5-diethoxycarbonyl-1,4-dihydrocollidine (DDC) in chow (Special Diet Service 824943). This induces biliary injury via accumulation of porphyrins. Due to the predominantly C57Bl/6 background of these mice which results in increased sensitivity to DDC diet, this experiment used older mice for a shorter time period than traditionally used.

2.1.3 Tissue and serum harvest

Mice were euthanized according to UK Home Office regulations by a Schedule 1 procedure (either $C0_2$ asphyxiation or cervical dislocation).

Blood was collected at time of sacrifice by cardiac puncture and the resulting serum analysed by a biochemist using a commercial kit for alanine aminotransferase (ALT; Alpha Laboratories Ltd).

2.2 Cell culture

The HPC cell line BMOL was provided by George Yeoh, University of Western Australia. Cells were maintained in WilliamsE + GlutaMAX-1 medium (Gibco) containing 2% foetal calf serum (FCS) supplemented with 100units/ml penicillin and 100ug/ml streptomycin (PAA). Cells were cultured in a humidified atmosphere wth 5% CO_2 at 37^{o}C.

The SWA cell line was generated by Wei-Yu Lu and Atsunori Tsuchiya from cells from the non-parenchymal cell (NPC) fraction of the livers of mice fed CDE diet for 21 days. NPCs were isolated by centrifugation over a discontinuous Percoll (Sigma-Aldrich) gradient and expanded on rat tail collagen I coated plates (Sigma-Aldrich). When HPC colonies were observed expansion media was changed to a serum free purification media (328) until HPC colonies were exclusively observed. HPCs were then maintained in 1% FCS supplemented purification media and passaged with the diluted trypsin assisted replating method as described previously (59) then weaned onto Williams E medium as above supplemented with 5% FCS generating a similar growth rate to the BMOL line. These cells can be differentiated down the biliary or hepatocyte route as previously described (59).

Cells were tested for the presence of mycoplasma in-house at the beginning of the study and after resuscitation from cryopreservation and were found to be negative.

2.3 Immunohistochemistry

At the time of sacrifice, livers were perfused with 5mls sterile PBS via the IVC before being fixed overnight in 10% buffered formaldehyde. After paraffin embedding tissue sections were cut at 4 µm. Sections were de-waxed in xylene and rehydrated through graduated alcohol. Sections were subject to heat-mediated antigen retrieval performed by microwaving in either 0.01M sodium citrate pH6, Tris-EDTA pH9 or treating with 125ug/ml proteinase K in a waterbath at 37^{o}C.

For colorimetric staining with diaminobenzidine (DAB), endogenous peroxide activity was quenched with Bloxall (Vector) prior to blocking with avidin/biotin (Life technologies). Non-specific binding was blocked by incubation with protein block (Vector). Primary antibody in

Antibody Diluent Reagent Solution (Life technologies) was applied for one hour at room temperature or overnight at 4^{o}C. After washing, slides were incubated with species appropriate biotinylated secondary antibody (Vector) for 30 minutes, followed by ABC reagent (Vector) for 30 minutes. Sections were then treated with DAB (Liquid Dab Substrate Chromogen System, DAKO) for 5 minutes before counterstaining with Harris Haematoxylin and Scott's tap water. Finally sections were dehydrated through graduated alcohols and xylene and mounted in Pertex hard set mounting medium.

For immunofluorescence sections were blocked with protein block prior to incubation with primary antibody. Sections were incubated overnight with primary antibodies at 4°C. After washing, sections were stained with species-appropriate secondary antibodies conjugated to Alexa 488 or Alexa 555 (Life technologies). Where further amplification of signal was required or for dual immunofluorescence where both primary antibodies were in the same species, a Tyramide Signal Amplification kit was used (Perkin Elmer) prior to further heat treatment. Slides were mounted using DAPI Fluoromount-G (Southern Biotech).

For frozen sections a liver lobe was frozen in optimal cutting temperature (OCT) medium (Fischer Scientific) at time of sacrifice and stored at -20^{o}C prior to cutting to 6um. These sections were air dried and fixed in a 1:1 ratio of ice cold methanol and acetone for 10 minutes.

In all cases specificity of staining was confirmed by the use of appropriate isotype controls. For a complete list of primary antibodies, see Table 2.1.

Primary antibodies		
Alpha SMA	Sigma	A5228
Beta-catenin	BD Biosciences	610154
Beta-catenin (active)	Millipore	05-665
CK19	Developmental studies hybridoma bank	Troma-III

Dll-1	R&D systems	AF3970
IGF1	Abcam	ab40657
IGF1 receptor pY1161	Abcam	ab39398
Jagged-1	Santa-Cruz	Sc-8303
Jagged-2	Santa-Cruz	25-255
Ki67	Abcam	ab16667
Notch1-ICD	Abcam	Ab8925
Notch3	Abcam	Ab23426
panCK	DAKO	Z0622
PCNA	Abcam	ab29
pmTOR (Ser2448)	Cell signalling	2976
RFP	SICGEN	AB0081-500
Sox9	Millipore	AB5535
YFP	Abcam	ab6673

Table 2.1 Primary antibodies used in this study

2.4 Immunocytochemistry

For immunocytochemistry cells were fixed in frozen methanol for 10 minutes and permeablised with 0.5% PBS-Tween (Sigma-Aldrich) prior to application of protein block. Fluorescent immunostaining was then performed as above.

2.5 In situ hybridisation

Formalin fixed paraffin embedded samples were analysed using RNAscope 2.0 Reagent Kit-Brown (AdvancedCellDiagnostics#310035) according to manufacturer's instructions. Probes

used were; Mm Axin-2 (#400331); Mm Lgr5 (#312171); positive control Mm Ppib (#313911); negative control Mm DapB (310043). This was performed by central histology services at the Beatson Institute, Glasgow.

2.6 Microscopy and cell counting

2.6.1 Photography and manual cell counting

Images were obtained on a Nikon Eclipse E600 microscope in conjunction with Axiovision Elements software v3.0.

Cell counts were performed manually using Fiji ImageJ (EMBL) on blinded slides and more than 20 consecutive non-overlapping fields at x200 (colorimetric) or x400 (immunofluorescent) magnification. Interlobular bile ducts were excluded from quantification.

2.6.2 Picrosirius red quantification

Picrosirius red quantification was performed on 30 consecutive non-overlapping x200 fields by pixel analysis using Adobe Photoshop CS6.

2.6.3 Automated quantification of cell proliferation

For analysis of PCNA positivity in RFP or YFP-expressing cells after performing immunofluorescent staining for the fluorescent reporter, PCNA and DAPI, slides were scanned using the Operetta high-content analysis system (PerkinElmer). A minimum of 30 10X long working distance objective fields (0.4cm^2) liver tissue was analyzed using the Columbus image data storage and analysis system. Briefly, a sliding parabola was applied to the DAPI channel to remove variation in background level across and between samples. All nuclei were identified using method M standard settings and from this population, cells positive for the reporter were identified based on a common threshold. From this second population those with nuclear PCNA staining were again identified using a common threshold. Results are reported as % RFP/YFP positive cells also PCNA positive. Fields containing artefacts that affected image analysis were excluded manually. 'Pipeline' illustrated in Appendix 1.

2.7 Quantitative PCR analysis

At time of harvest a whole liver lobe was snap frozen on dry ice and stored at -80°C. 2-3mm^3 of liver tissue was defrosted and lysed into Tri-Reagent (Ambion) and homogenized using a tissue tearer. Lysates were mixed with 1:5 chloroform/TriReagent and centrifuged at 12000 rpm for 15 minutes at 4°C. The aqueous RNA containing phase was collected and mixed with an equal volume of 70% molecular grade ethanol. For RNA extraction from cells lysis directly into RLT lysis buffer (Qiagen) was performed before the addition of ethanol.

An RNEasy Mini kit (Qiagen) was used for RNA purification according to the manufacturer's protocol. RNA concentration and purity was determined using a Nanodrop spectrophotometer (ThermoFisher). RNA concentration over 100ng/ul, RNA purity 260/280 ratio >2 and 260/230 ratio 1.8 were taken as an acceptable standard.

1ug RNA was reverse transcribed after concentrations were standardised with RNase free water. Reverse transcription was performed using the Qiagen kit according to manufacturer's instructions, including a genomic DNA wipe-out step.

Real time qPCR was performed using SYBR Green (Qiagen). Reactions were performed in 384 well plates and consisted of 5ul cDNA diluted 1:10 in RNase free water, 6.25ul SYBR and 1.25ul primers. Pre-designed validated primer sets were purchased from Qiagen and are listed in Table 2.3. All samples were run in triplicate. A Roche LightCycler480 was used to run reactions to the following specifications:

Cycles	**Temperature (°C)**	**Duration (s)**
Activation	95	20
40 cycles: denaturation	95	10
anneal/extend	60	30
Melt curve	95	15
	60	15
Cooling	40	30

Table 2.2 Cycling conditions for qPCR using SYBR Green and Roche Lightcycler 480

Specificity of PCR products was confirmed by melting curve analysis. Standard curves for each primer's amplification efficiency was generated using cDNA template from each sample combined and serially diluted in RNase free water. The relative standard curve method was used to estimate changes in gene expression. RNA concentration in experimental sample triplicates was calculated from the generated standard curves and normalised to expression levels of housekeeping gene *Gapdh* as internal control and the mean taken. The values were then normalised to the experimental control group (day 0 expression levels or control blocking antibody or genotype as stated in the individual figure legends).

Primers		
Ascl2	Qiagen	QT01066513
Axin2	Qiagen	QT00126539
CyclinE1 (Ccne1)	Qiagen	Qt00103495
Dll1	Qiagen	QT00113239
Dll3	Qiagen	QT00113477
Dll4	Qiagen	QT01053598
Epcam	Qiagen	QT00248276
Gapdh	Qiagen	QT01658692
Hes1	Qiagen	QT00313537
Hey1	Qiagen	QT00115094
Hey2	Qiagen	QT00129885
HeyL	Qiagen	QT00128954
Igf1	Qiagen	QT00154469
Igf1r	Qiagen	QT00155351
Jagged1	Qiagen	QT00115703
Jagged2	Qiagen	QT01043819
Krt19	Qiagen	QT00156667
Lef1	Qiagen	QT00148834
Lgr5 (Gpr49)	Qiagen	QT00123193

Notch1	Qiagen	QT00156982
Notch2	Qiagen	QT00153496
Notch3	Qiagen	QT01051729
Notch4	Qiagen	QT00135653
Numb	Qiagen	QT00097328
Sox9	Qiagen	QT00163765
Wnt7b	Qiagen	QT00168812
Wnt9a	Qiagen	QT01062250

Table 2.3 Tables of primers used in this study

2.8 MTT assay

For in vitro cell viability assays, cells were plated at $2x10^5$/cm2 density and treated for 48 hours with DAPT, ICG001, AG1024 or recombinant IGF1 or the relevant vehicle at the concentrations shown in the figures. Anti-Notch antibodies or control were used at 10ug/ml. 6 wells were used per concentration per experiment. MTT assay was conducted using 3-(4,5-dimethylthiazol-2-yl)-2,5-diphenyltetrazolium bromide (5 mg/ml) (Sigma-Aldrich) diluted in PBS (Sigma-Aldrich). Cells were treated for 12 hours, and MTT crystals were dissolved in DMSO and read at 570/690 nm using a FluoStar Omega (BMG Labtech).

2.9 EdU assay

EdU incorporation assay (C10337, ThermoFisher Scientific) was conducted as described in the manufacturer's instructions. Cells were plated at 2000 cells per well. After adhering overnight, media was changed to include DAPT (10uM), ICG001 (5uM) or volume-matched DMSO for 24 hours. EdU was added to give a working concentration of 10uM and incubated for 3 hours. Media was removed and cells fixed with 4% formaldehyde for 15 minutes. They were then washed with 3% BSA in PBS and permeabilised by treating with 0.1% triton X for 20 minutes. Clickit reaction buffer and buffer additive were made up as per manufacturer's instructions, added to the wells and incubated in the dark on a rocker for 30 minutes. Nuclear counterstaining was performed with DAPI Fluoromount-G.

2.10 siRNA transfection

Small interfering RNA (siRNA) against Notch3 was obtained from Qiagen (FlexiTube GeneSolution Cat no. 1027416, GS18131). Four independent sequences were obtained (see

Table 2.4) as well as a scrambled sequence control (Qiagen negative Allstars siRNA control). Oligonucleotides were suspended in 100ul RNAse-free water. BMOL cells were plated at 10^5 cells per well. Cells were transfected using HiPerFect (Qiagen) as per manufacturer's instructions. A mastermix of siRNA was prepared to the ratio 75ng siRNA: 6ul HiPerFect: 200ul serum free water, mixed and left for 10 minutes at room temperature to form complexes. This was added a drop at a time onto cells while continuously swirling the plate to ensure even distribution. After 48 hours cells were lysed for RNA extraction to check gene knockdown efficiency. Sequences Notch3_6 and Notch3_3 did not cause significant knock-down compared to untransfected or scrambled controls and therefore were not used for further experiments. The experiment was repeated with sequences Notch3_7 and Notch3_5 and cells lysed for RNA at 24, 48, 72 and 96 hours to confirm effective duration of knockdown. Finally the procedure was repeated with multiple wells (n=4 per sequence) and after 48 hours cells were fixed with ice cold methanol and stained for Ki67 (see above).

siRNA duplexes used in this study	
Mm_Notch3_6	CAGGGCTGCAACACTGAGGA
Mm_Notch3_7	CCACTTCTAATTGTAAATACA
Mm_Notch3_3	CCCAGTCTTCCTTTATTTATA
Mm_Notch3_5	GACAGTTGTGAGGATAATATA

Table 2.4 Notch3 siRNA sequences

2.11 Migration assay

BMOL or SWA cells were trypsinised and incubated with 5ug/ml mitomycin C for 90 minutes to inhibit proliferation. Wells of an Oris migration plate (Platypus Technologies) were coated with 60ul of 20ug/ml human placental laminin (Sigma L6274) for 2 hours at 37^{o}C. Excess solution was removed and central stoppers inserted. 5000 cells were added per well and incubated overnight to allow confluent cell attachment. Stoppers were

removed to create a standardised central defect. Control (time=0) wells were fixed immediately with 5% glutaraldehyde. Media for the remaining wells was changed to contain DAPT (10uM), ICG001 I5uM) or volume matched DMSO and returned to the incubator for 24 hours. The remaining wells were fixed and cells stained with crystal violet and photographed. Quantification of cell migration was performed using Photoshop CS6 to generate standard defect size and ImageJ for pixel analysis.

2.12 ELISA detection of IGF1

Conditioned medium from cells cultured with ICG001 (5uM) or vehicle for 48 hours was tested for IGF1 concentration using an IGF1 Mouse ELISA kit (ab100695 Abcam) following the manufacturer's protocol. This involves using a plate with wells pre-treated with capture antibody. Protein standards and samples were added and incubated for 2.5 hours at room temperature. After washing, biotinylated IGF1 detection antibody was added and incubated for one hour at room temperature. After further washing a HRP-streptavidin solution was added and incubated for 45 minutes. Finally TMB One-Step Substrate Reagent was added for 30 minutes prior to Stop Solution. The plate was read immediately at 450nm using a spectophotometer (SPECTROstar Omega). Test samples were run against the standard curve generated. This concentration was normalised to protein content of secreting cells (determined using a BSA standard and Pierce reagent) as a surrogate for cell number.

2.13 Immunoblotting

Cell extracts were prepared from BMOL or SWA cells treated with DAPT (10uM) or vehicle for 48 hours. Protein content was quantified using a BSA standard and BCA reaction with Pierce reagent. Protein quantity was standardized using lysis buffer before sampled were resolved using precast 4-12% Bis-Tris NuPAGE gels and 1X MOPS running buffer (all ThermoFisher Scientific). Precision Plus Dual Colour ladder (BioRad) was used to assess molecular weight.

Gels were transferred onto nitrocellulose membrane using Toubin's transfer buffer. Protein transfer was confirmed using Ponceau red solution. Blots were washed with TBS-Tween before blocking with 5% powdered fat-free milk (Marvel) in TBS-Tween. Immunoblots were split at the 70kDa mark and incubated at 4°C overnight with primary antibody anti-Igf1R Y116 (Abcam) or anti-beta-actin clone AC-74 (Sigma-Aldrich) as a loading control. Appropriate horseradish peroxidase labelled secondary antibodies were used (Cell

signaling) and signal detected with ECL reagent (Thermo Scientific) on photographic film. Images were scanned and densitometric analysis performed in photoshop and ImageJ.

2.14 Statistical analysis

Prism software (GraphPad Software) was used for all statistical analysis. Data are presented as mean ± s.e.m. *n* refers to biological replicates. Normal distribution of data was determined using the D'Agostino and Pearson omnibus normality test. For parametric data, data significance was analysed using a two-tailed unpaired Student's *t*-test. In cases where more than two groups were being compared, then a one-way ANOVA was used. In instances where the *n* was too small to determine normal distribution or the data were non-parametric then a two-tailed Mann–Whitney *U*-test was used. Kruskall-Wallis test was used when comparing multiple non-parametric data. Levels of significance are denoted as follows: *$p \leq 0.05$; **$p \leq 0.01$; ***$p \leq 0.001$.

2.15 Study approval

All studies involving human tissue were approved by the University of Edinburgh and NHS Lothian Academic and Clinical Central Office for Research Development (ACCORD) tissue governance unit (approval number: 10/S1402/33). Animal studies had local ethical approval and were conducted under license issued by the UK Home Office (Project licence number 70-7874 and personal licence numbers 60/13368 and 60/13368).

3 Characterising the Notch/Wnt axes in progenitor mediated hepatocellular regeneration

3.1 Introduction

Notch and Wnt are key signals in liver development with Notch directing fate of the hepatoblast down the biliary route and Wnt signal directing fate down the hepatocyte route. They are also known to be important in regeneration after liver injury in the adult, but here their roles are less well understood. During HPC-mediated regeneration HPCs within the DR must become activated, proliferate, migrate and differentiate, and in doing so transition from the Notch determined biliary phenotype to the Wnt determined hepatocyte fate. This process likely requires careful regulation of these two signalling pathways. While fate may represent an example of antagonistic functions of Notch and Wnt, other actions such as proliferation and migration are similar. This leads to the questions – 'are these pathways dynamically regulated?' and 'are they capable of cooperation?'

Traditional models used for the generation of hepatocyte injury and ductular reactions involve several weeks of ingestion of toxic diet (122, 329). Continuous exposure to the toxin results in ongoing hepatocellular damage and activation of DRs, limiting our ability to study what signals may drive a DR over time. Lu et al have recently demonstrated that beta-naphthoflavone (BNF) induction of AhCre causing hepatocytic loss of MDM2 in the *AhCre MDM2$^{fl/fl}$* mouse strain results in a florid DR from which HPCs can be isolated and are capable of repopulating the parenchyma in meaningful numbers (59). In this chapter I utilise this strain with a Cre induction regimen that generates a robust DR with low levels of short term morbidity and mortality. I sought to determine if this model could be used to study the ductular response over time. I then go on to determine if Notch and Wnt pathways were present and active, and if this activity appeared to be dynamic, consistent with temporal regulation of these pathways in the regenerative response. I characterise the Notch and Wnt expression profile of two HPC lines (BMOL and SWA) (330) to identify if they are typical of the DRs seen in the *in vivo* models. Finally I examine human tissue to see how representative my models may be and look for evidence of Notch and Wnt activity.

3.2 *AhCre MDM2$^{fl/fl}$* is a model for the temporal study of hepatic progenitor cell response over time

The *AhCre MDM2$^{fl/fl}$* mouse model produces a DR in response to widespread hepatocellular injury and senescence as a consequent of loss of MDM2. This protein acts as a negative regulator of p53 and thus its loss results in accumulation of p53 causing senescence and apoptosis (Figure 3.1A). It has been established in previous work that a dose of 20mg/kg beta napthoflavone is sufficient to induce a ductular reaction within 10 days with a hepatocyte recombination rate of 85.1%. At 10 days 17% of the animals appear unwell and require euthanizing. This dose of BNF was administered and groups of mice harvested over a 14 day period for further analysis of the DR generated and the activity of Notch and Wnt pathways (Figure 3.1B). The animal experiment to generate the *AhCre MDM2$^{fl/fl}$* time-course tissues was conducted by Michael Williams. All subsequent tissue analysis presented in this chapter was performed by myself.

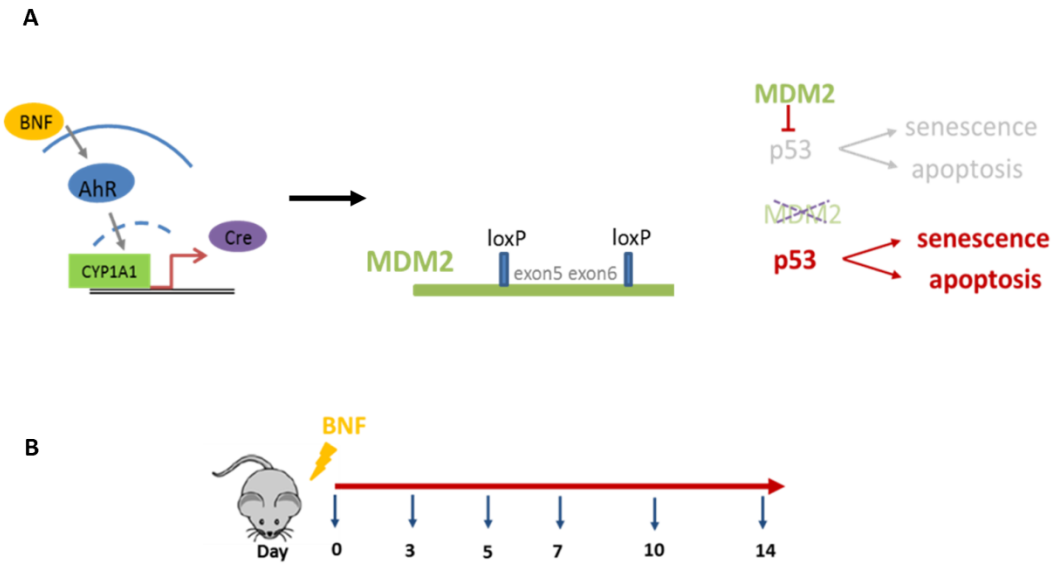

Figure 3.1 Using the *AhCre MDM2$^{fl/fl}$* model of hepatic progenitor cell (HPC) activation to study the ductular reaction over time: (A) The activation of HPCs requires both hepatocellular injury and inhibition of hepatocyte replication. The *AhCre* line contains the rat *Cyp1A1* promotor upstream of Cre recombinase and when combined with a strain

bearing an Mdm2 locus in which exons 5 and 6 are flanked by loxP sites, the *AhCre MDM2$^{fl/fl}$* strain is generated. Following administration of xenobiotic beta-naphthoflavone (BNF), Cre recombinase is expressed in hepatocytes where it results in inactivation of Mdm2. MDM2 is an E3 ubiquitin-protein ligase that degrades p53. Loss of MDM2 results in upregulation of p53 and induces p53-mediated hepatocyte death and senescence. This results in rapid activation of HPCs with the potential to restore liver architecture and function. **(B)** Cre-recombinase was induced with BNF and groups of mice harvested 3, 5, 7, 10 and 14 days later for comparison with day 0 controls.

Following Cre induction, using the ductular markers panCK, cytokeratin 19 (CK19) and SOX9, a highly predictable expansion, morphological change and parenchymal invasion of ductular cells occurs (Figure 3.2A). Quantification of panCK positive cells confirms a predictable and sequential rise in ductular cell number (Figure 3.2C). I observed expression of SOX9 in hepatocytes (Figure 3.2A, middle panel) after injury. SOX9 is traditionally seen as a biliary or HPC marker however can be seen in hepatocytes after tamoxifen administration (14) and also has been reported to be expressed in low levels in uninjured periportal hepatocytes, in one study defining them as the cell responsible for cell turnover in liver homeostasis (149). Analysis of gene expression data shows changes in expression of ductular markers over time with *cytokeratin19 (Krt19)* being the first to rise, accompanying expression of putative HPC marker *Ascl2* (Figure 3.2D). Following induction of hepatocyte senescence there is a rapid rise in proliferation rate of ductular cells which peaks at day 5 (approximately 20%) (Figure 3.3). These data confirm the utility of this model in studying the DR over time. Due to the morbidity beyond day 10, and that 10 days was sufficient to generate a robust DR with cell number by day 14 plateauing, any new animals experiments using the *AhCre MDM2$^{fl/fl}$* system were designed to last no longer than 10 days, to avoid unnecessary animal morbidity.

Figure 3.2: Single time-point MDM2 deletion from hepatocytes induces a temporal ductular response:

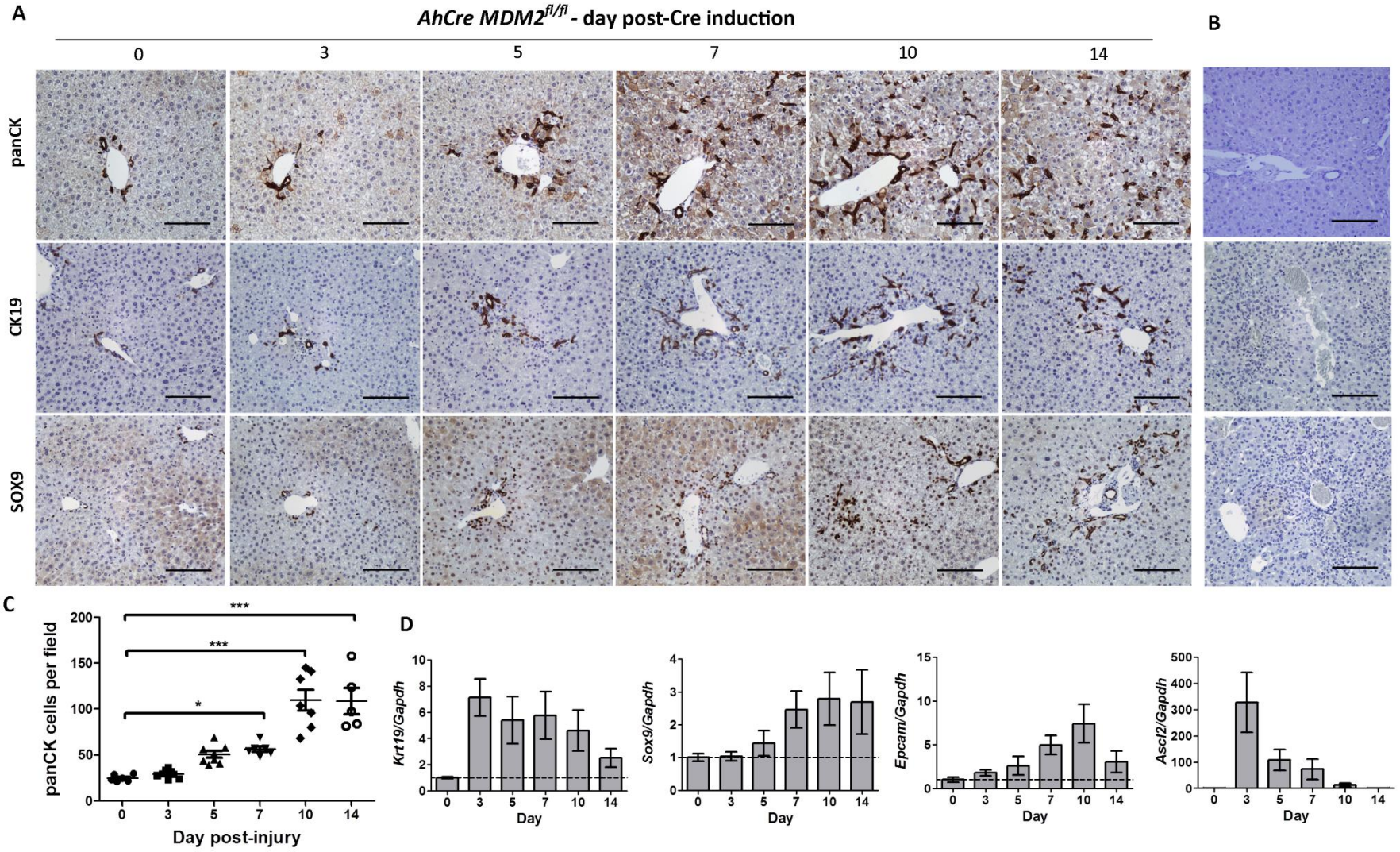

Figure 3.2 Single time-point MDM2 deletion from hepatocytes induces a temporal ductular response: (A) Immunohistochemistry for a range of ductular/HPC markers over 14 days following Cre induction; panCK (upper panels), cytokeratin 19 (CK19) (middle panels) and SOX9 (lower panels). **(B)** Isotype controls. **(C)** Quantification of panCK positive cells following Cre induction ($p<0.0001$) (*n*=5-8 per time-point). **(D)** Gene expression of ductular/progenitor markers cytokeratin 19 *(Krt19)*, *Sox9, Epcam* and *Ascl2* following Cre-induction relative to *Gapdh* normalised to day 0 levels (*n*=5-8 per time-point). Data are presented as mean ± SEM. Kruskal-Wallis test was used for comparison of multiple groups (p value shown in legend above) with Dunn's multiple comparison post-test analysis included in the figure *$p<0.05$; ***$p<0.001$. Photomicrograph scale bars: 100uM.

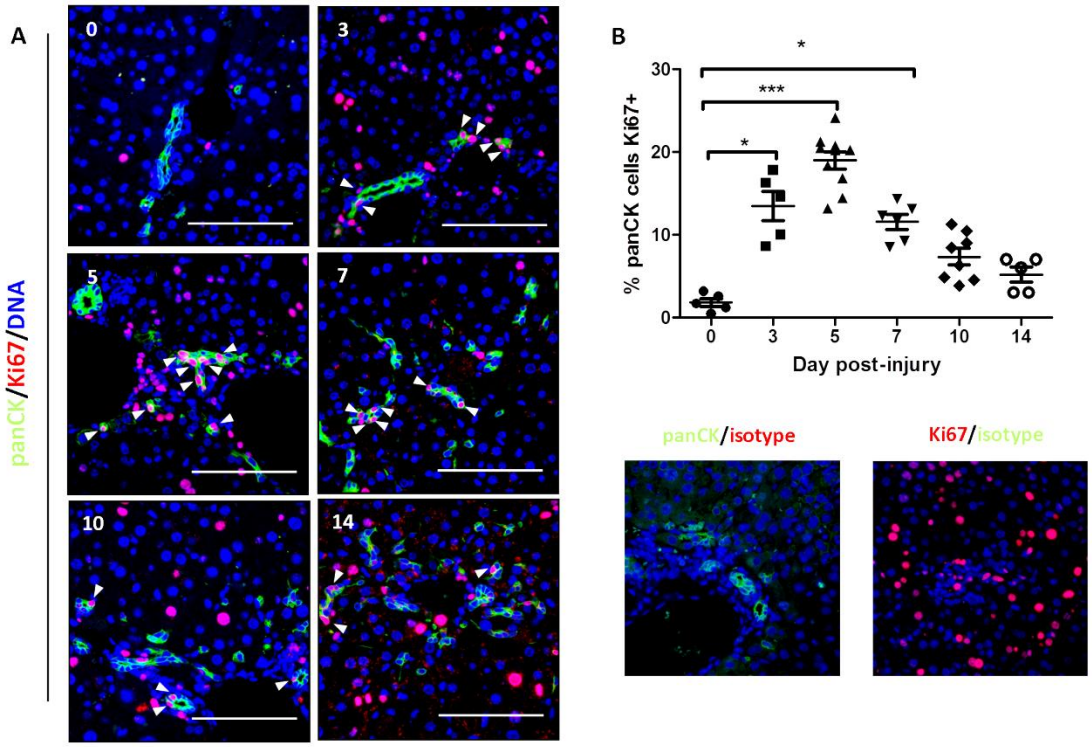

Figure 3.3 Single time-point MDM2 deletion from hepatocytes induces predictable ductular proliferation: (A) Immunohistochemistry for panCK (green) and Ki67 (red) following Cre induction (day post-induction inset). Dual positive cells shown (white arrows). **(B)** Quantification of panCK/Ki67 dual positive cells as a proportion of single positive panCK cells ($p<0.0001$) (*n*=5-8 per time-point). **(C)** Single stain/isotype controls. Data are presented as mean ± SEM. Kruskal-Wallis test was used for comparison of multiple groups (p value shown in legend above) with Dunn's multiple comparison post-test analysis included in the figure *$p<0.05$; ***$p<0.001$. Photomicrograph scale bars: 100uM.

3.3 Notch pathway is active in HPC mediated regeneration in vivo

To assess the involvement of Notch signalling after hepatocyte injury, I began by quantifying the expression of the Notch receptors over the *AhCre MDM2*$^{fl/fl}$ time-course tissue, to identify which receptors were expressed and whether this changed over time. There was an early marked increase in expression of *Notch1* (by day 3), which then steadily fell (Figure 3.4A). *Notch2* was detectable throughout the time-course but expression levels did not vary. *Notch3* showed marked up-regulation, peaking at day 5 and showing more protracted expression than *Notch1*. *Notch4* was undetectable at all time-points. Immunohistochemistry confirmed that expression of Notch1, specifically the active Notch1 intracellular domain (NICD) was detectable within cells positive for ductular marker panCK, confirming expression within the DR (Figure 3.4B). Notch3 also co-localised with ductular marker panCK. Notch1 and Notch3 were both clearly evident within blood vessels, consistent with previous reports (331). Notch2 was just detectable within the major ducts and not within the invading ductular reactions (Figure 3.4D).

Figure 3.4 Expression of Notch receptors after MDM2-mediated hepatocellular injury is dynamic and is identified within ducts: (A) Gene expression of Notch receptors following Cre-induction relative to *Gapdh* normalised to day 0 levels. *Notch4* was undetectable. **(B)** Immunohistochemistry for Notch1 intracellular domain (ICD) on day 3 (upper panel) and Notch3 on day 7 (lower panel) (red) and panCK (green) in *AhCre MDM2*$^{fl/fl}$ model. **(C)** Single stain/isotype staining controls **(D)** Immunohistochemistry for Notch2. For gene expression data n=5-8 per time-point. Data are presented as mean ± SEM. Photomicrograph scale bars: 100uM.

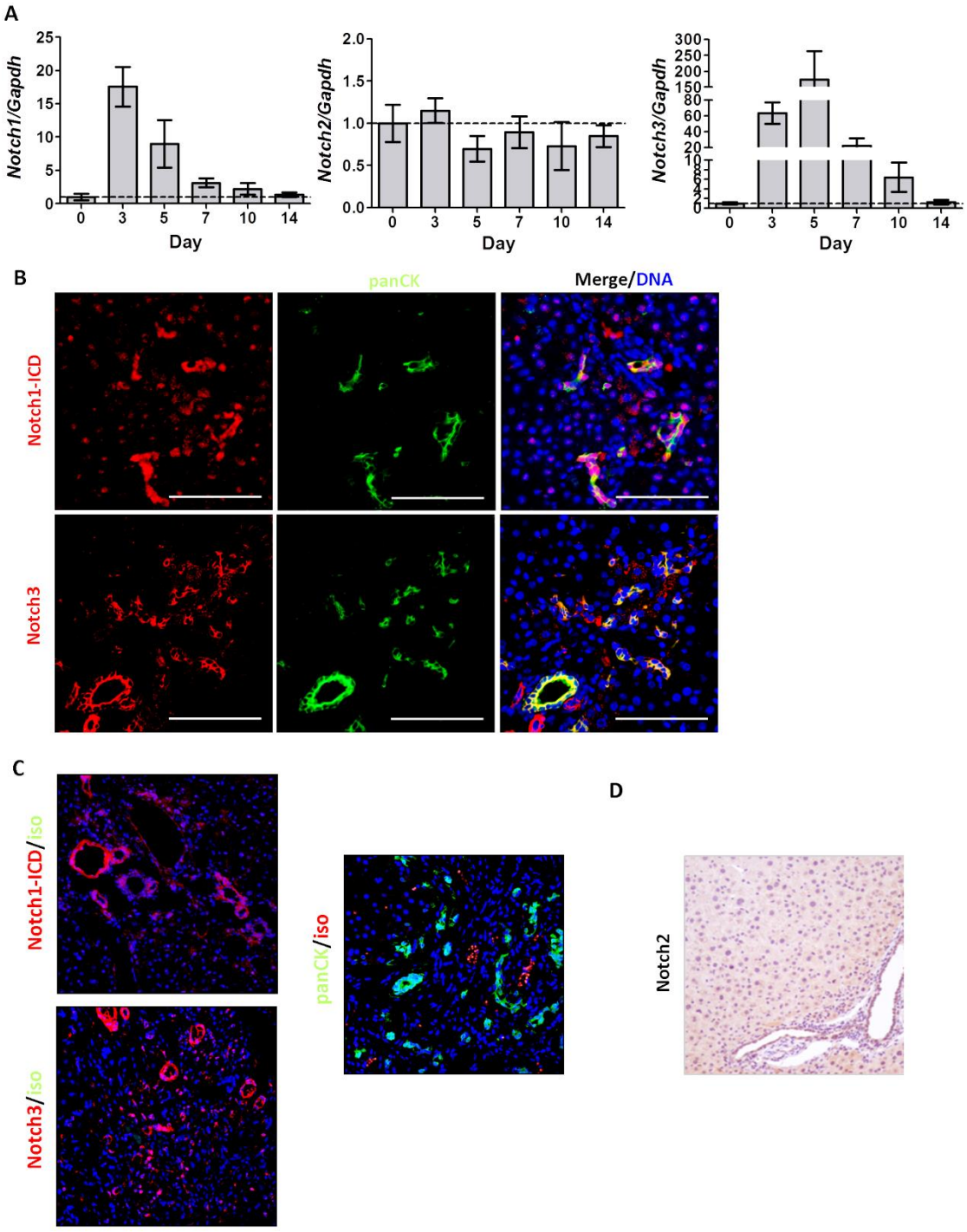
A
Notch1/Gapdh
Notch2/Gapdh
Notch3/Gapdh
Day
B
panCK
Merge/DNA
Notch1-ICD
Notch3
C
Notch1-ICD/iso
Notch3/iso
panCK/iso
D
Notch2

As so little is known about Notch3 in the liver, I was keen to ensure the ductular expression seen in the *AhCre MDM2*$^{fl/fl}$ model was representative of other traditional models of hepatocellular injury. Animals treated with 3 weeks of choline-deficient, ethionine-supplemented (CDE) or 2 weeks methionine-choline deficient (MCD) diet showed also expression of Notch3 within CK19 positive ductular cells (Figure 3.5). In addition there appeared to be staining of blood vessels and cells with a myofibroblast phenotype.

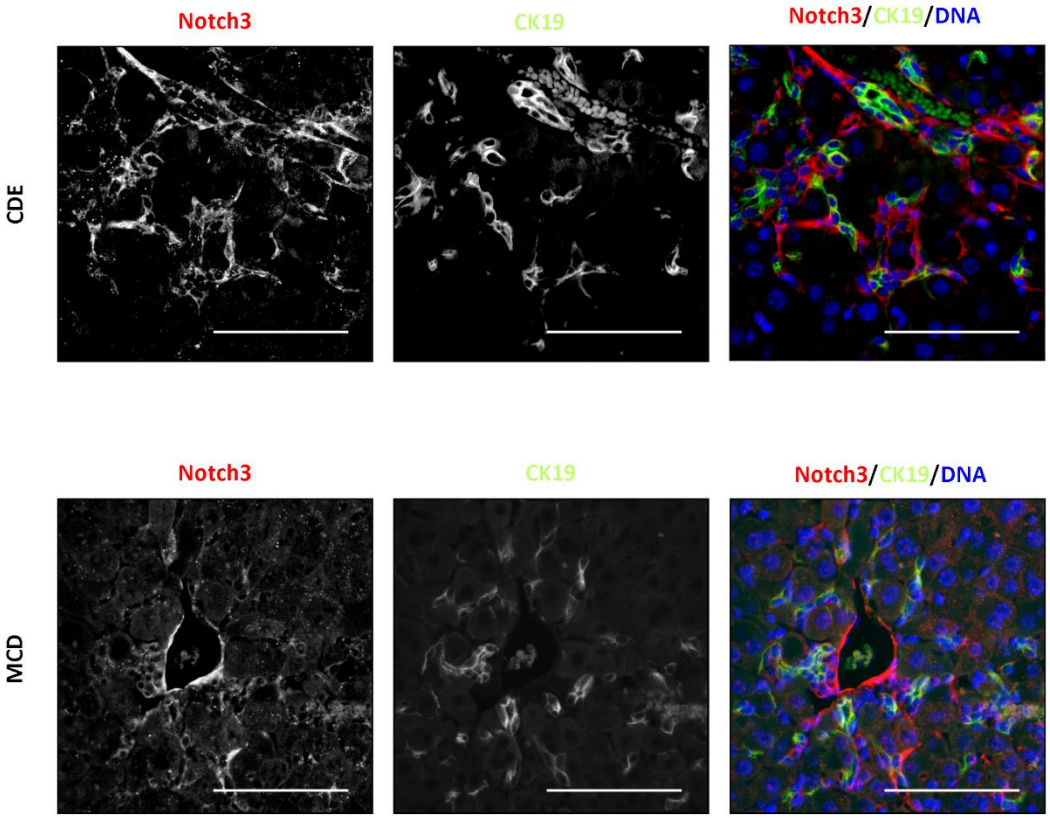

Figure 3.5 Notch3 is expressed in other models of hepatocellular injury: Immunohistochemistry for Notch3 (red) and CK19 (green) in CDE- (top) and MCD- (bottom) diet treated animals. Consistent with *AhCre MDM2*$^{fl/fl}$ model, Notch3 co-localises with ductular cells, blood vessels and some myofibroblasts accompanying the ductular reaction. Photomicrograph scale bars: 100uM.

In order to confirm this, I co-stained tissue from the *AhCre MDM2*$^{fl/fl}$ model and CDE model with myofibroblast marker alpha-smooth muscle actin (aSMA) (Figure 3.6). In both models most animals showed only co-localisation of Notch3 and aSMA in blood vessels, however in a subset of animals, myofibroblasts were Notch3 positive (2 out of 5 animals examined), which would suggest it may have a role in the fibrotic response in these injury models.

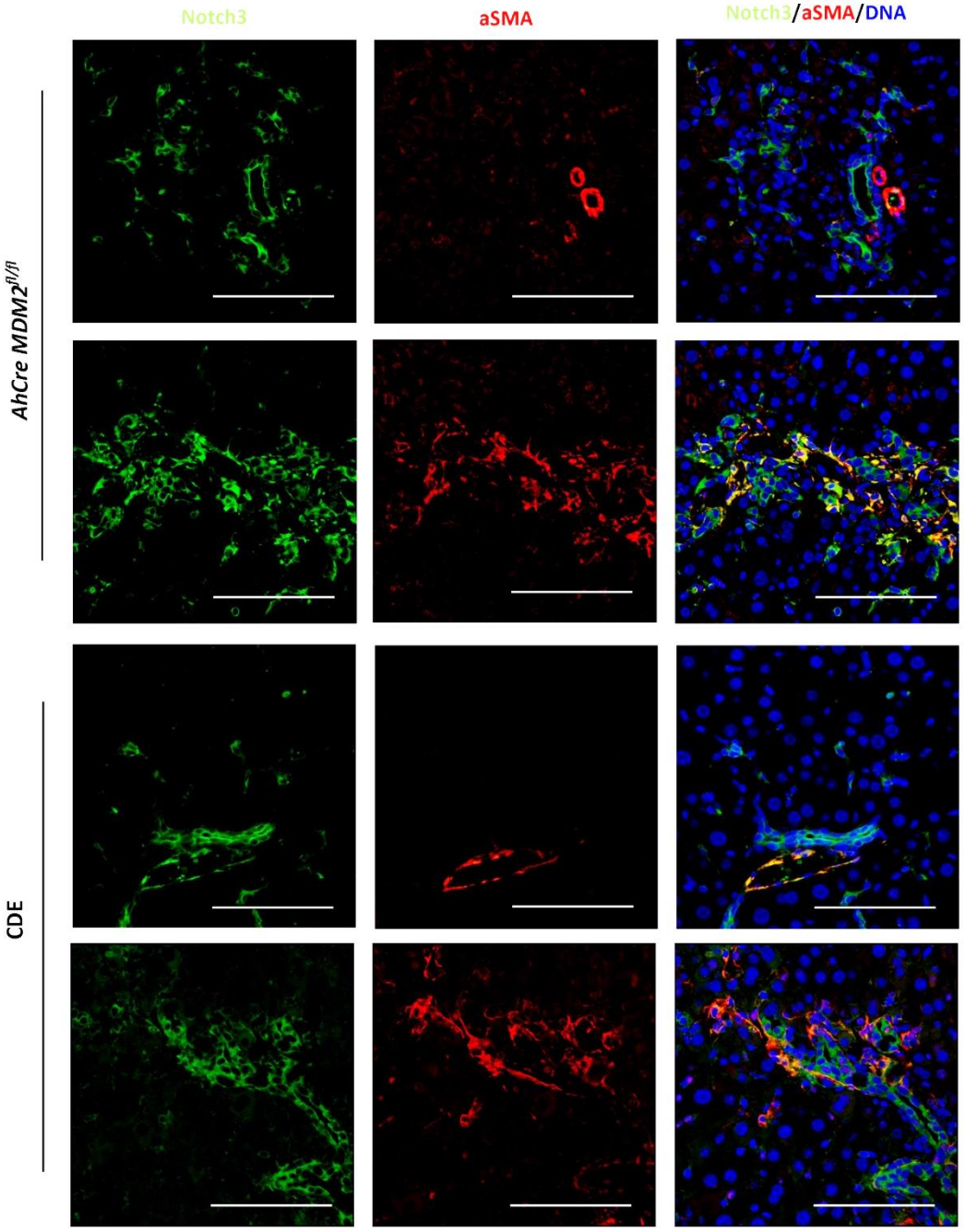

Figure 3.6 Expression of Notch3 in myofibroblasts after hepatocellular injury: Immunohistochemistry for Notch3 (green) and aSMA (red) in *AhCre MDM2*$^{fl/fl}$ model (top) and CDE diet (bottom). Most animals after MDM2 or CDE diet-mediated injury show Notch3 isolated to ductular cells and blood vessels (upper panels) however in a subset of animals, Notch3 positive aSMA positive (myofibroblast) cells are seen (lower panels). Photomicrograph scale bars: 100uM.

To identify which ligands might be signalling to Notch1 and Notch3 I quantified the expression of Notch ligands over the *AhCre MDM2*$^{fl/fl}$ time-course (Figure 3.7A). *Jagged1* rose rapidly, peaking at day 3. *Jagged2* expression also appeared dynamic and peaked at day 5. *Dll1* expression did not change markedly over the time-course. *Dll3* and *Dll4* were not detectable. I went on to confirm expression at the protein level by performing immunohistochemistry for Jagged1, Jagged2 and Dll1. Jagged1 was strongly expressed in blood vessels and around ducts, as was Jagged2. Interestingly Dll1 in addition to staining blood vessels appeared to localise to ducts. This was confirmed by dual staining with ductular marker panCK. This suggests a capacity may exist for local Notch signalling within the ductular compartment.

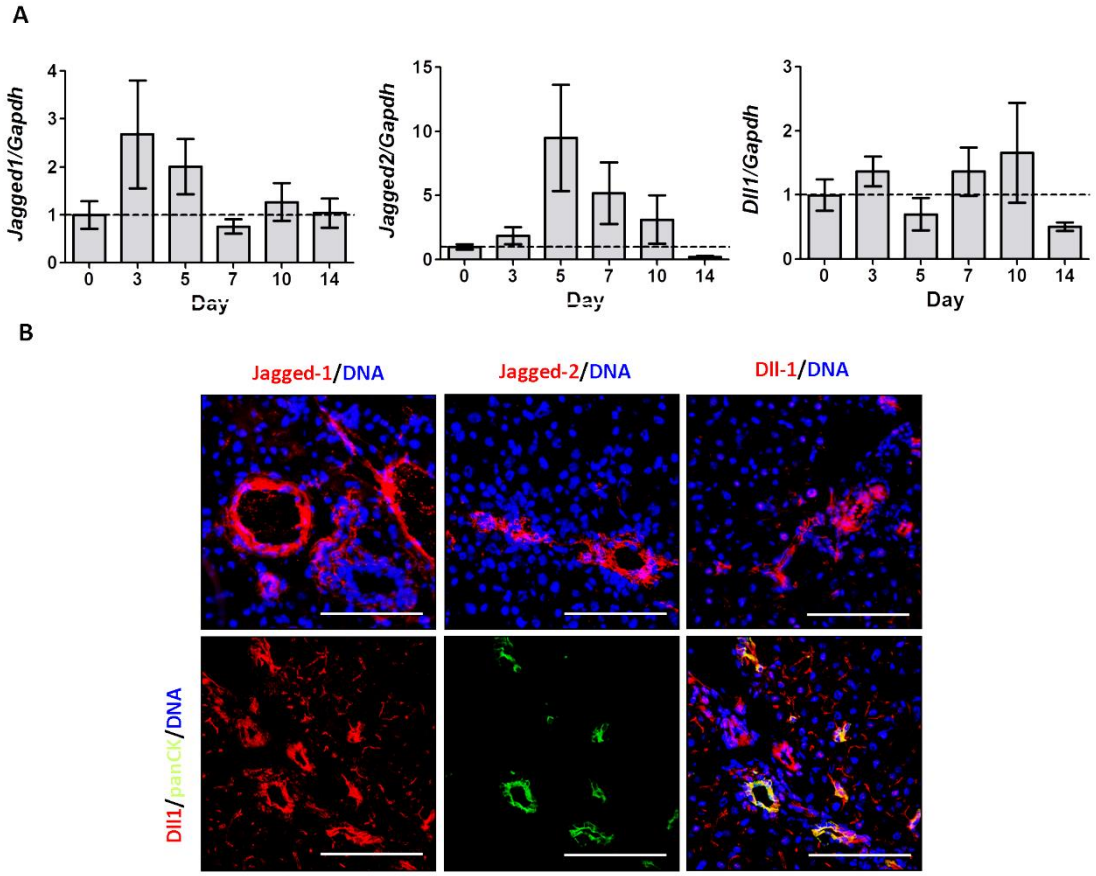

Figure 3.7 MDM2-mediated hepatocellular injury induces dynamic expression of Notch ligands: (A) Gene expression of Notch ligands following Cre induction relative to *Gapdh* normalised to day 0 levels. *Dll-3* and *Dll-4* were undetectable. **(B)** Immunohistochemistry for Notch ligands Jagged-1 (left), Jagged-2 (middle) and Dll-1 (left), (red) and Dll-1 (red) with panCK (green) (lower panel) (all day 5 post-induction). For gene expression data n=5-8 per time-point. Data are presented as mean ± SEM. Photomicrograph scale bars: 100uM.

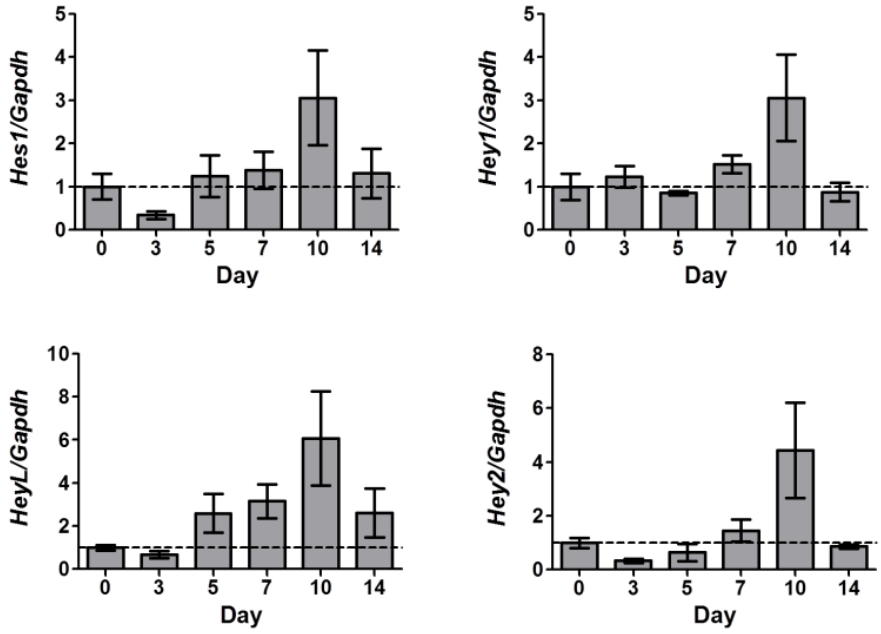

Figure 3.8 Expression of Notch effector genes after MDM2-mediated hepatocyte injury follows a characteristic profile or 'signature': Gene expression of classic canonical Notch target genes after Cre induction *Hes1, Hey1* and *Hey2* relative to *Gapdh* normalised to day 0 levels. n=5-8 per time point. Data are presented as mean ± SEM.

Notch signalling results in the expression of a great many genes. In order to determine if Notch signalling might be active after hepatocellular injury, I began by analysing the expression of genes from the classic canonical Notch effector Hes and Hey families (Figure 3.8). Genes followed a characteristic expression profile, rising from day 3 and peaking at day 10, suggestive of a Notch expression 'signature'.

The presence of dynamic changes in expression of Notch ligands, receptors and effectors would suggest an intact and active signalling pathway after hepatocellular injury. In order to provide further evidence of this and confirm if activity was located within the ductular reaction I crossed the *AhCreMDM2*$^{fl/fl}$ mice with a strain that reports active canonical Notch signalling at single cell resolution *CBF:H2B-venus* (322). A nuclear localised H2B:venus protein, a variant of YFP is expressed when a cell is in receipt of canonical Notch signal. Nuclear translocation of the NICD following ligand binding results in binding of NICD to C

promotor binding factor (CBF) at CBF response elements. This results in transcription from the simian virus (SV) 40 minimal promotor of the transgene *H2B-venus* (Figure 3.9A). In the uninjured *AhCreMDM2$^{fl/fl}$; CBF:H2B-venus* mice, Notch activity was reported in ductular cells as demonstrated by co-localisation of YFP with ductular marker CK19. Cohorts of animals underwent Cre-induction with BNF and were harvested 0, 3, 5, 7 and 10 days later. Immunohistochemistry in these animals confirms Notch signalling within all ductular cells persisting until day 7. At day 7 some ductular cells are negative for the reporter and by day 10 reporter expression is infrequent.

Together these data suggest that there is dynamic regulation of the Notch pathway following hepatocyte injury with differential expression of Notch1 and Notch3, and that Notch signalling is important in the early part of the ductular response.

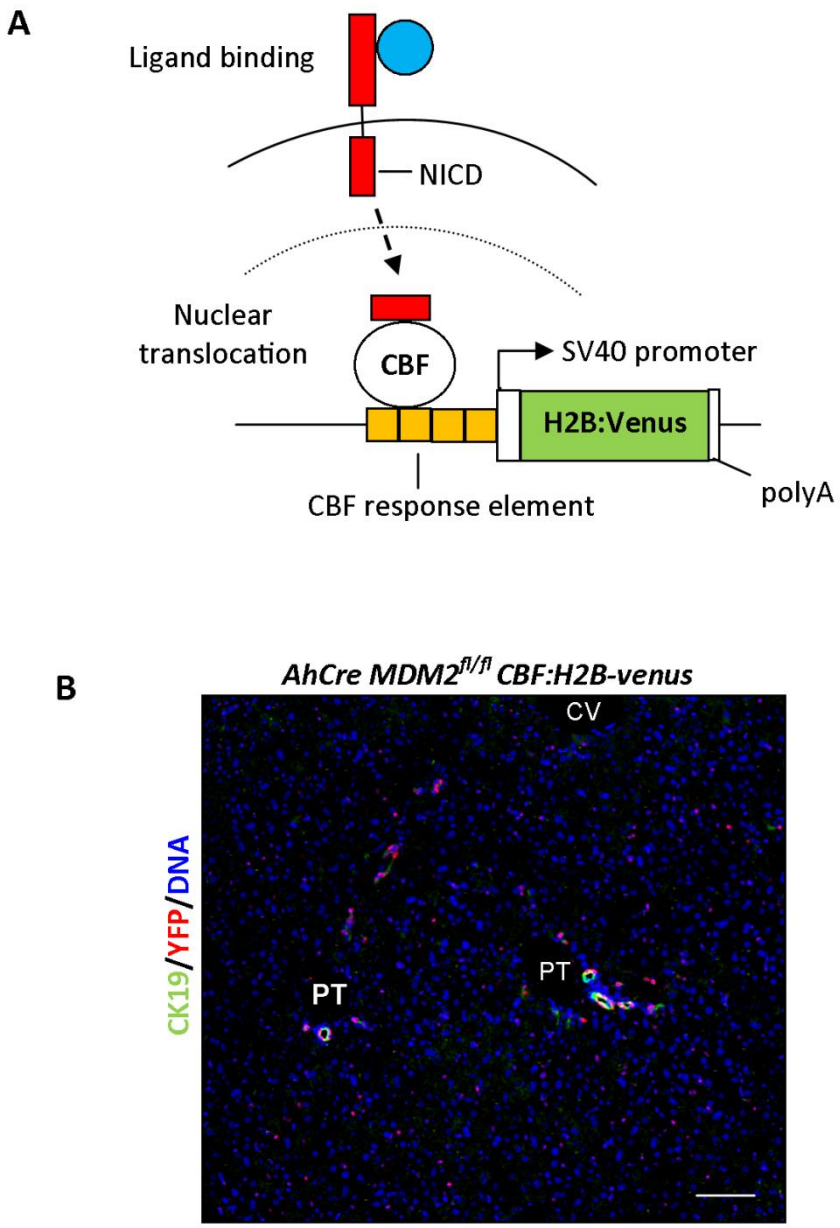

Figure 3.9 *AhCre MDM2$^{fl/fl}$ CBF:H2B-venus* strain permits visualisation of Notch signal within ductular cells: (A) Schematic of *AhCre MDM2$^{fl/fl}$ CBF:H2B-venus* strain. A nuclear localised H2B-YFP venus fusion protein is expressed under control of multiple CBF1 binding sites and SV40 minimal promoter. Canonical Notch signalling results in nuclear translocation of the notch intracellular domain (NICD), association with CBF1 and its binding to the response elements resulting in reporter expression. **(B)** Low power image of *AhCre MDM2$^{fl/fl}$ CBF:H2B-venus* strain for CK19 (green), YFP (red). PT = portal tract, CV = central vein. Photomicrograph scale bars: 100uM.

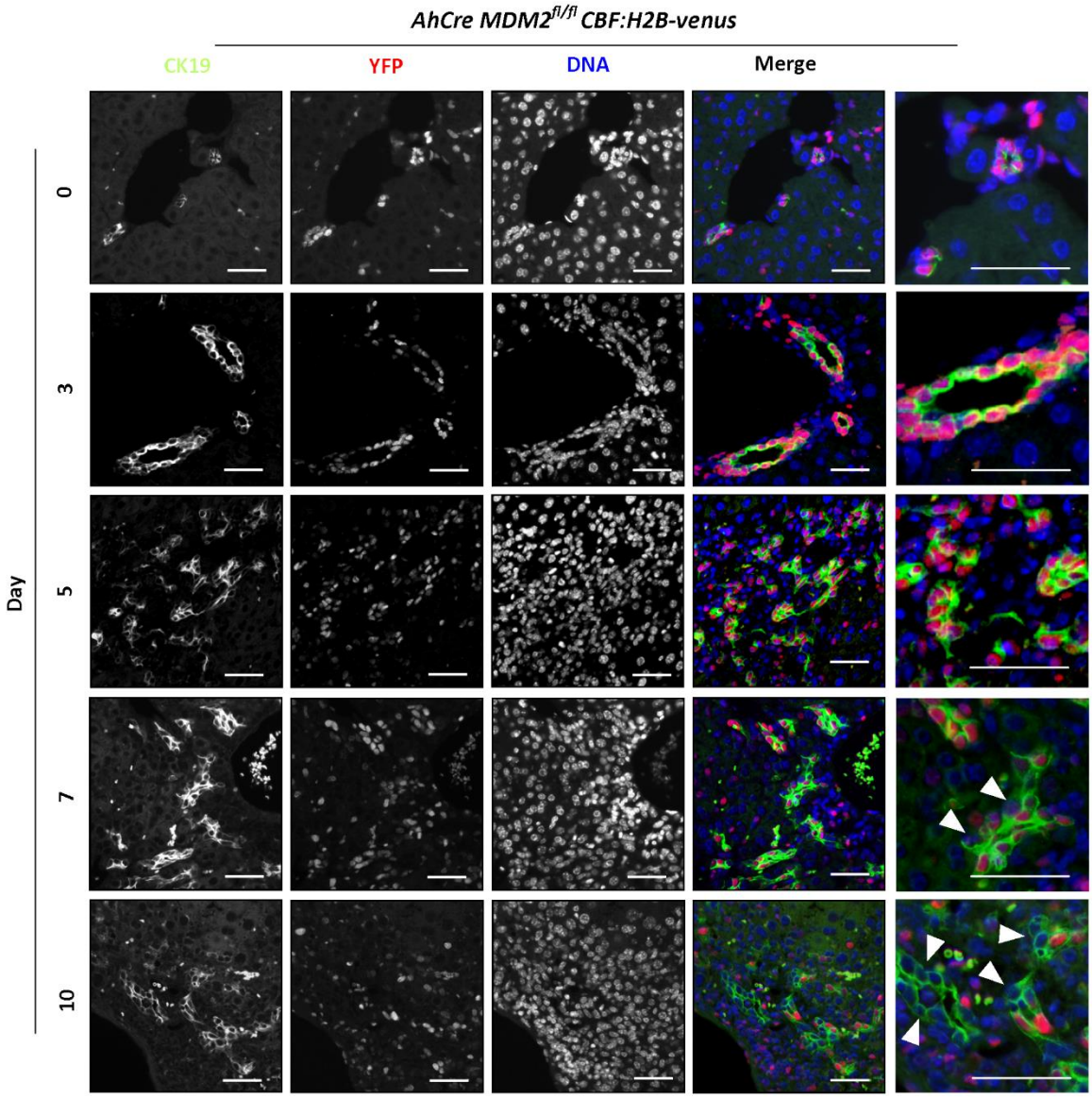

Figure 3.10 Expression of Notch reporter in *AhCre MDM2$^{fl/fl}$ CBF:H2B-venus* strain confirms dynamic Notch activity after hepatocellular injury: Immunohistochemistry for YFP venus (red) and CK19 (green) after Cre induction in Notch reporter strain *AhCre MDM2$^{fl/fl}$ CBF:H2B-venus.* Arrows denote reporter-negative ductular cells. Photomicrograph scale bars: 50uM.

3.4 HPC lines express Notch pathway

Having established *in vivo* that DRs demonstrate Notch activity, I went on to characterise the expression of the Notch pathway in HPC lines to further confirm if HPCs are likely to be sensitive to Notch signalling. In order to determine the direct effects of Notch signalling on HPCs in the absence of direct or indirect influence from other cell types, I used two HPC lines, BMOL (330) and SWA. Both are derived from the livers of mice who have been fed CDE diet to induce a HPC response and can be differentiated along the hepatocyte lineage.

The BMOL cell line was derived from HPCs that have undergone spontaneous immortalisation (330). Digested liver tissue was passed through a Percoll density centrifugation gradient to generate primary cultures which were then serially diluted to obtain single cell cultures, some of which overcame growth inhibition to form clonally-derived lines. Phenotypic markers of both biliary and hepatocytic lineages are expressed and they can be differentiated towards hepatocytes using dexamethasone with insulin-transferrin-selenium and nicotinamide or Wnt3a (123, 330).

SWA cells were generated by Wei-Yu Lu and Atsunori Tsuchiya and differ in that the primary cultures were grown in a highly restrictive media (328) to prevent fibroblast overgrowth and then passaged using a diluted trypsin technique to lift small colonies of cells (59). After 16 passages the cells were weaned onto the standard growth medium used for culturing BMOLs and became tolerant to usual methods of trypsinisation. With similar changes to the growth media differentiation into hepatocytes is possible (59).

Both cell lines expressed Notch1 and Notch3. Notch1-ICD staining was most marked in the smaller cells at the centre of colonies. Notch3 stained all cells within the culture (Figure 3.10). Notch2 was just visible in the BMOL line and weakly stained a small proportion of cells of the SWA line.

Next I stained both HPC lines for the three Notch ligands identified in the *AhCre MDM2*$^{fl/fl}$ time-course (Figure 3.11). Both lines were negative for Jagged1 and Jagged2, however both stained positive for Dll1, consistent with the immunostaining from injured livers and further suggesting that local Notch signalling is possible within the ductular compartment.

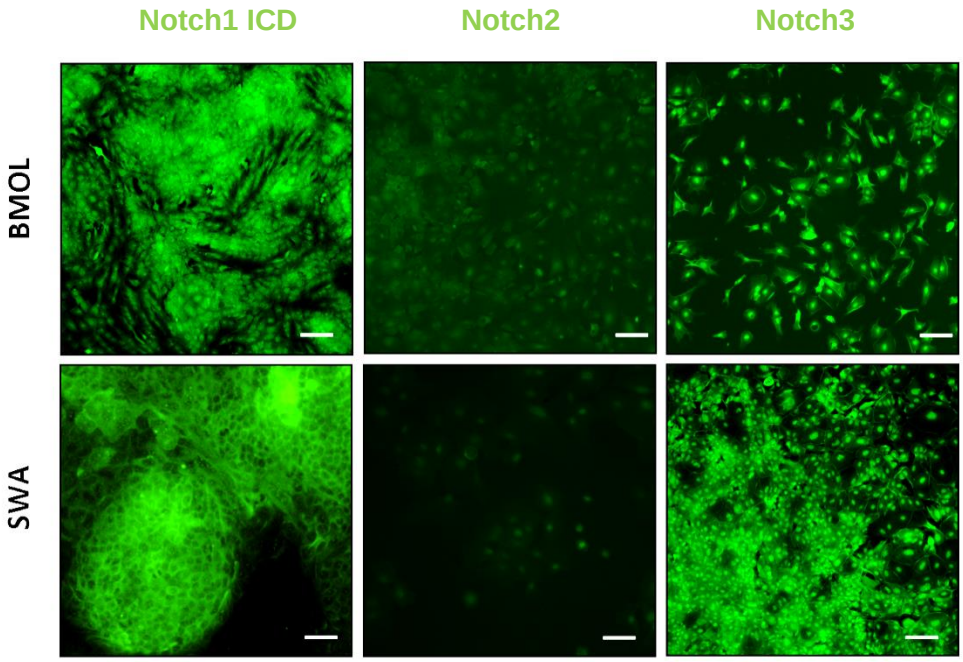

Figure 3.11 Expression of Notch receptors in HPC lines: Immunocytochemistry for Notch1 intracellular domain (Notch1-ICD), Notch2 and Notch3 in BMOL (upper panel) and SWA (lower panel) cell lines. DAPI co-stain omitted to help demonstrate nuclear location of Notch3, all cells were positive for Notch3. Photomicrograph scale bars: 100uM.

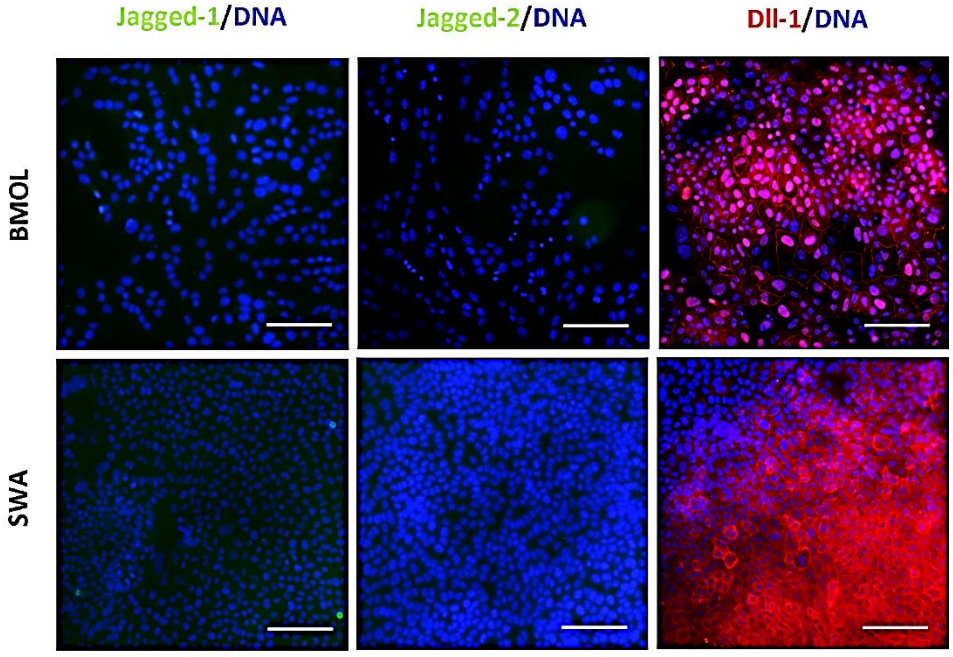

Figure 3.12 Expression of Notch ligands in HPC lines: Immunocytochemistry for Jagged-1 (green), Jagged-2 (green) and Dll-1 (red) in BMOL (upper panel) and SWA (lower panel) cell lines. Photomicrograph scale bars: 100uM.

3.5 Wnt pathway is involved in HPC mediated regeneration *in vivo*

To assess the involvement of Wnt signalling after hepatocyte injury, I began by quantifying the expression of Wnt ligands over the *AhCre MDM2*$^{fl/fl}$ time-course tissue. Wnt ligands 9a and 7b rise rapidly after induction of Cre in *AhCre MDM2*$^{fl/fl}$ mice (Figure 3.13A). Wnt signalling has a vast number of target genes. *Axin2* and *Lef1* are considered classical targets of canonical Wnt signal. Wnt signalling is known to be important in maintenance of hepatocyte function (150, 332) so it was not unexpected that expression of Wnt target effectors including *Lef1* and *Axin2* fall sharply after Cre-mediated induction of hepatocyte senescence and injury. After day 5 expression rapidly returned to pre-injury levels. Wnt target gene and Notch antagonist *Numb* also follows this trajectory. As these genes follow a typical expression profile, akin to the characteristic expression pattern seen amongst the Notch effector genes, this suggests there is also a Wnt expression 'signature'. Interestingly Wnt-sensitive stem cell marker *Lgr5* also follows this expression profile and would be consistent with previous studies identifying a putative Lgr5+ HPC population only after liver injury (77, 78) and also reiterating that *Lgr5* is likely a beta-catenin target.

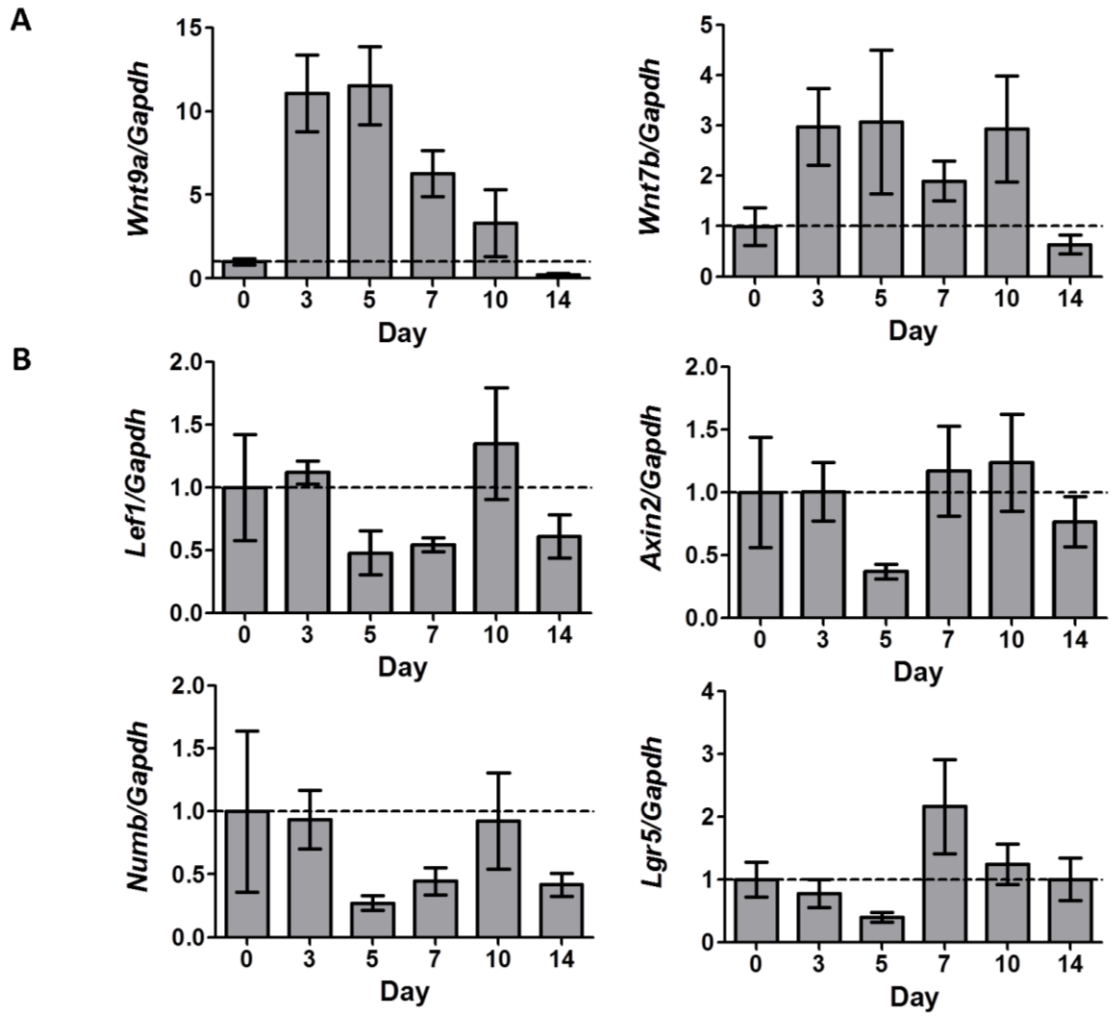

Figure 3.13 Hepatocyte injury induces dynamic changes in expression of the Wnt pathway: (A) Gene expression of Wnt ligands *Wnt9a* and *Wnt7b* following Cre-induction relative to *Gapdh* normalised to day 0 levels. **(B)** Gene expression of Wnt target genes *Lef1, Axin2, Numb* and *Lgr5* following Cre-induction. n=5-8 per timepoint. Data are presented as mean ± SEM.

I went on to demonstrate by in situ hybridisation that Axin2 and Lgr5 were expressed within DRs (Figure 3.14). In the uninjured liver, *Axin2* was detectable in zone 3 hepatocytes (Figure 3.14B) consistent with previous reports (150). However I also observed expression within ductular cells (Figure 3.14A). After injury *Axin2* expression is seen in expanding DRs. *Lgr5* was not visible in uninjured ducts but was present in DRs after injury and in pericentral hepatocytes (Figure 3.14C and D).

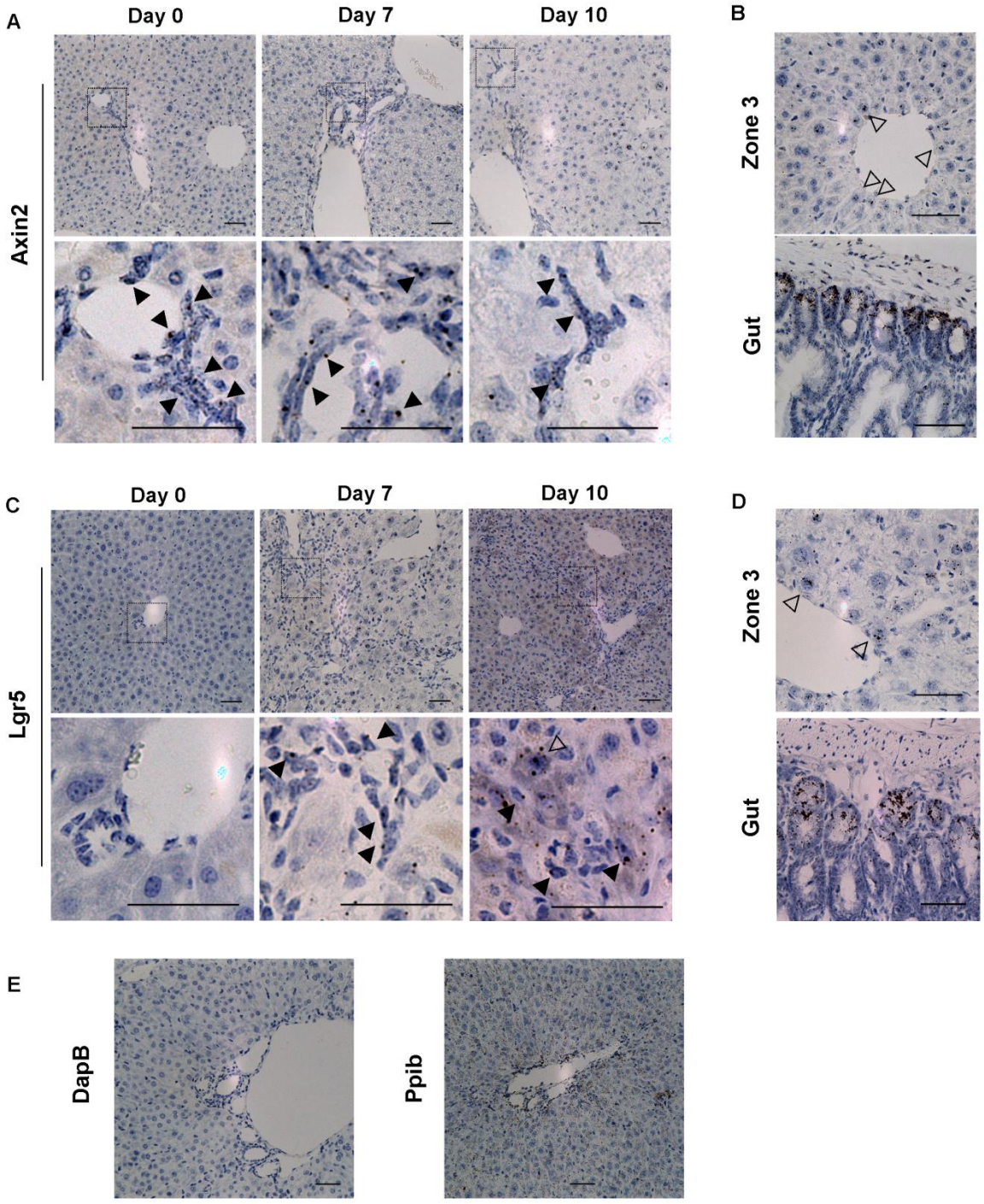
A
Day 0
Day 7
Day 10
Axin2
B
Zone 3
Gut
C
Day 0
Day 7
Day 10
Lgr5
D
Zone 3
Gut
E
DapB
Ppib

Figure 3.14 Wnt target effectors are expressed by ductular cells after MDM2-mediated hepatocellular injury: (A) Expression of *Axin2* RNA in the ducts of uninjured animals and days 7 and 10 after hepatocellular injury (filled arrows). **(B)** Expression of *Axin2* in zone 3 hepatocytes (unfilled arrows) (upper panel) and gut (lower panel). **(C)** *Lgr5* RNA is not detectable in the ducts of uninjured animals but can be detected in expanding DRs after injury (filled arrows) and by day 10 in hepatocytes adjacent to DRs (unfilled arrow). **(D)** Expression of *Lgr5* RNA in zone 3 hepatocytes of uninjured liver (unfilled arrows) (upper panel) and gut (lower panel). **(E)** Staining controls: negative control probe DapB and positive control probe Ppib. Photomicrograph scale bars: 50uM.

The presence of dynamic changes in expression of Wnt ligands and effectors would suggest an intact and active signalling pathway after hepatocellular injury. In order to provide further evidence of this and further confirm activity was located within the ductular reaction I crossed the *AhCreMDM2*$^{fl/fl}$ mice with a second reporter strain, this time one that reports active canonical Wnt signalling at single cell resolution *TCF/LEF:H2B-GFP* (323). This strain expresses a nuclear localised H2B-GFP fusion protein in response to binding of TCF/LEF to its response element. Canonical Wnt signalling results in nuclear translocation of active (de-phosphorylated) beta-catenin which acts as a co-activator of TCF/LEF and thus reporter expression (Figure 3.15A).

In the uninjured *AhCreMDM2*$^{fl/fl}$ *TCF/LEF:H2B-GFP* mice pericentral or zone 3 hepatocytes demonstrated Wnt activity, consistent with previous reports (150, 333) (Figure 3.15B). In uninjured animals, reporter expression was also detected at a reduced intensity in CK19-positive ductular cells, suggesting a tonic level of Wnt signal in biliary homeostasis, similar to the gut. Cohorts of animals underwent Cre-induction with BNF and were harvested 0, 3, 5, 7 and 10 days later. Immunohistochemistry in these animals identified that after injury there is expansion of GFP-negative ductular cells, suggesting Wnt is not required for this early expansion. By day 7 most ductular cells are positive, consistent with progressive upregulation of Wnt activity.

Together these data suggest that Wnt activity, although potentially required to maintain the biliary compartment in a state of readiness to respond to hepatocyte injury, is not involved in the early expansion of the ductular reaction. However as the DR progresses, the Wnt pathway is progressively upregulated and active.

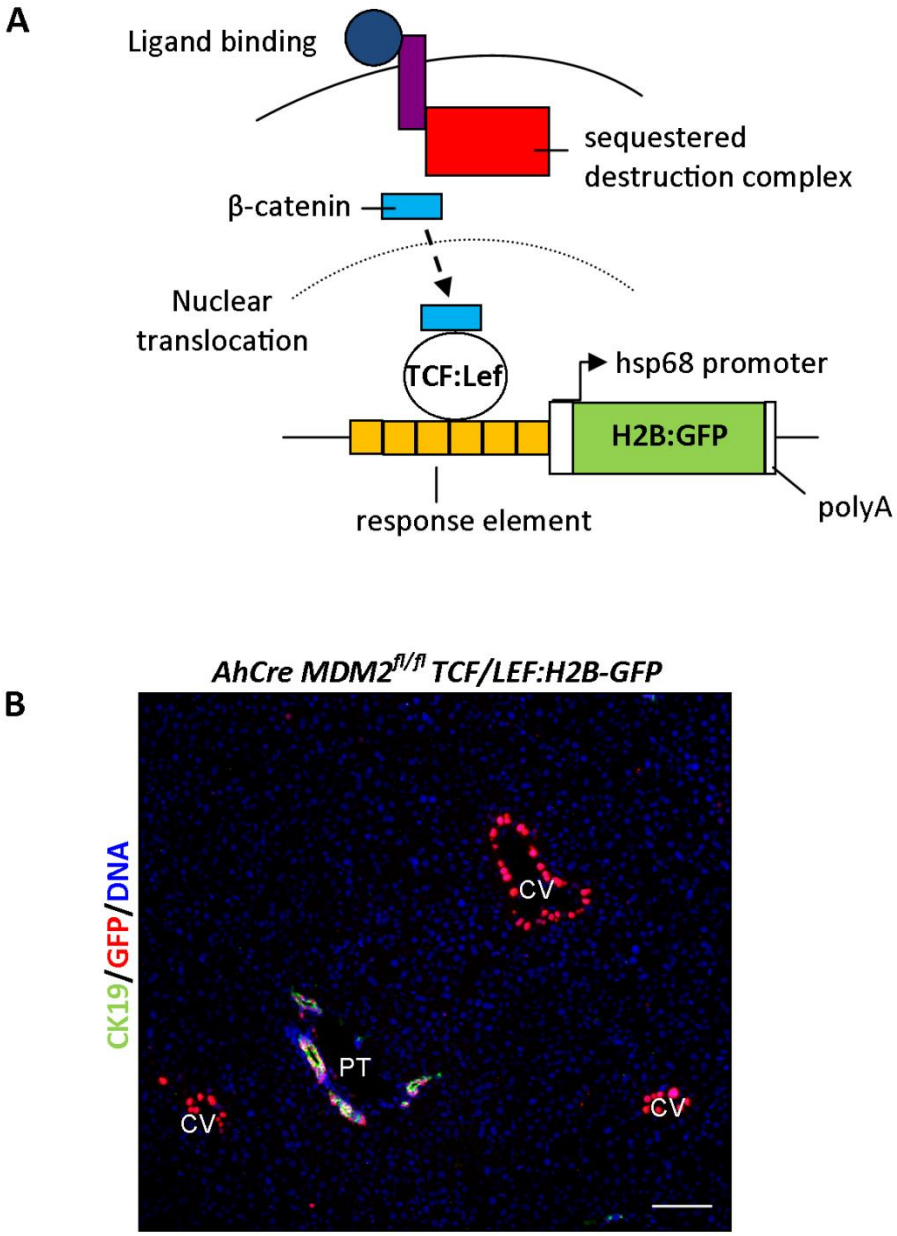

Figure 3.15 ***AhCre MDM2$^{fl/fl}$ TCF/LEF:H2B-GFP*** **strain permits visualisation of Wnt signal within ductular cells: (A**) Schematic demonstrating *AhCre MDM2$^{fl/fl}$ TCF/LEF:H2B-GFP* strain. A H2B-GFP fusion protein is expressed under control of a TCF/Lef1 response element and a heatshock protein 1B minimal promotor. Canonical Wnt signalling results in nuclear translocation of beta-catenin, a co-activator of TCF/LEF, response element binding and expression of the construct. **(B)** Low power image of *AhCre MDM2$^{fl/fl}$ TCF/LEF:H2B-GFP* strain for CK19 (green), GFP (red). PT = portal tract, CV = central vein. Photomicrograph scale bars: 100uM.

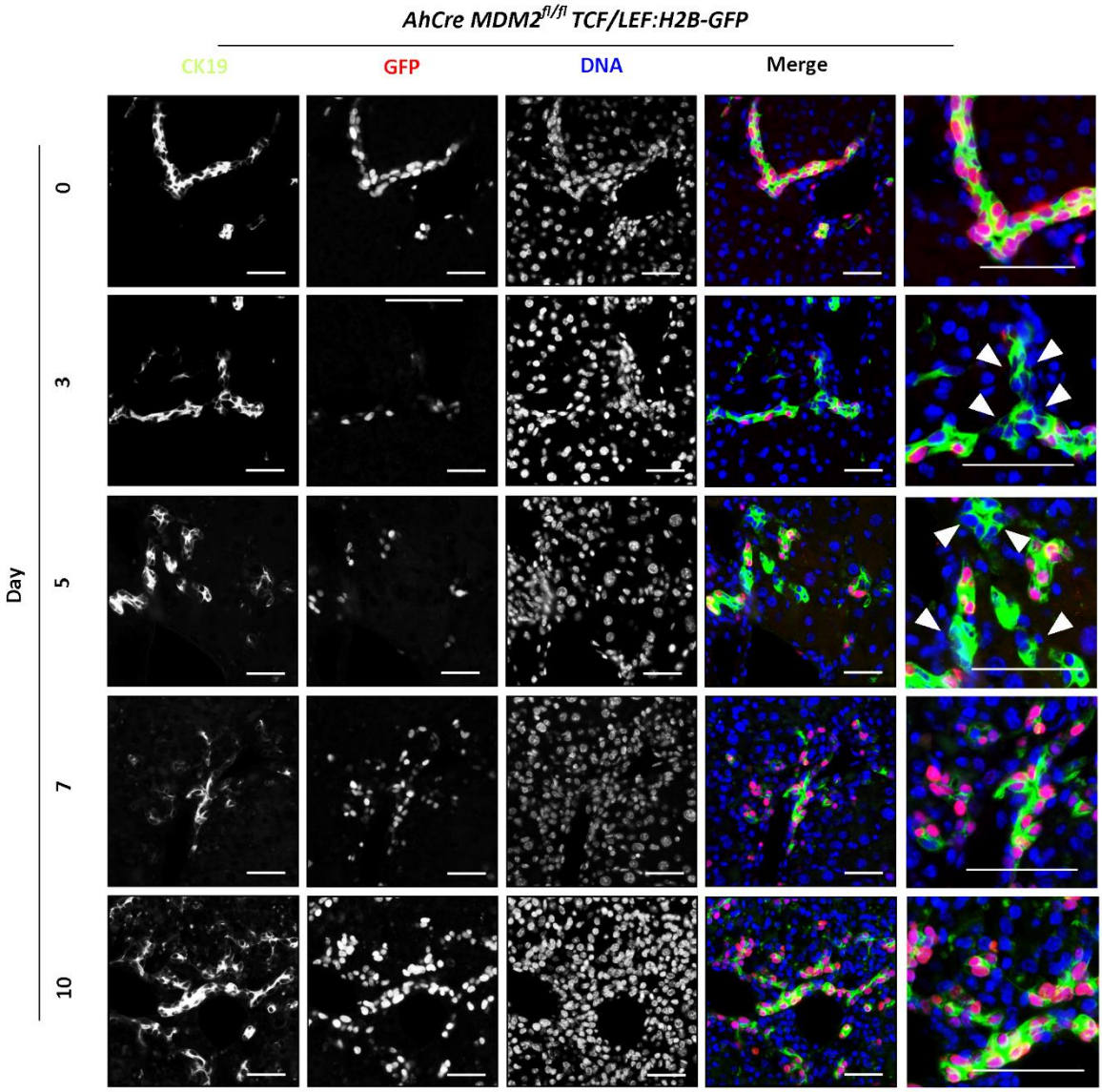

Figure 3.16 Expression of Wnt reporter in *AhCre MDM2$^{fl/fl}$ TCF/LEF:H2B-GFP* strain confirms dynamic Wnt activity after hepatocellular injury: Immunohistochemistry for GFP (red) and CK19 (green) after Cre induction in Wnt reporter strain *AhCre MDM2 $^{fl/fl}$;TCF/LEF:H2B-GFP.* Arrows denote reporter-negative ductular cells. Photomicrograph scale bars: 50uM.

3.6 HPC lines express Wnt pathway

To determine if my HPC lines were representative of the cells of the DRs seen *in vivo*, I performed immunocytochemical staining for beta-catenin. All cells of both BMOL and SWA lines were positive (Figure 3.17). In addition, cells were positive for an antibody that identifies the dephosphorylated (i.e. active) form of beta-catenin. This form was seen within the nuclei in both HPC lines suggesting Wnt activation.

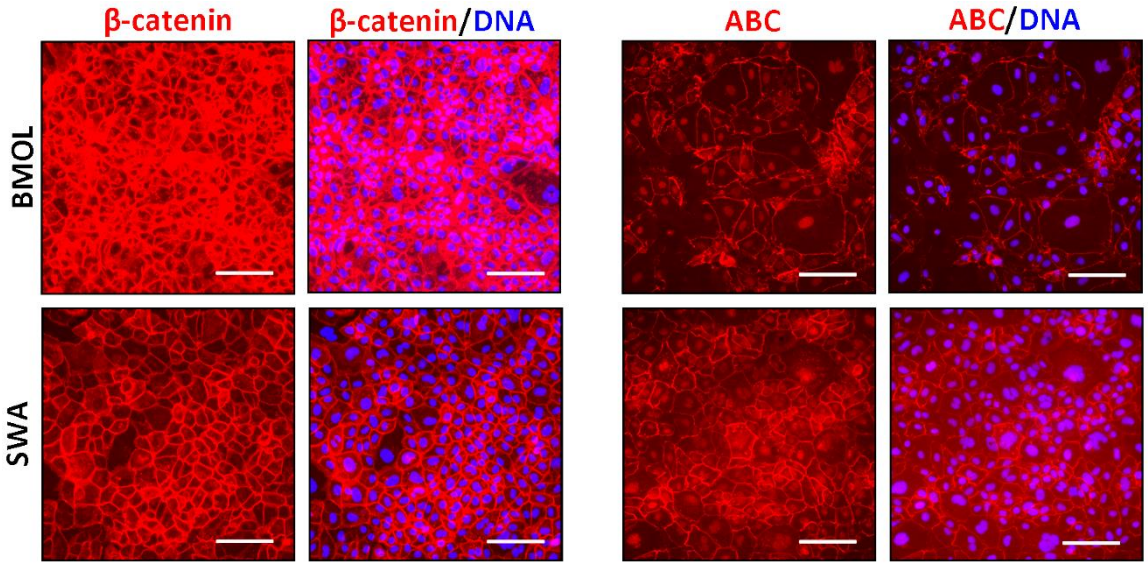

Figure 3.17 The Wnt pathway is identified in HPC lines: Immunocytochemistry for total beta-catenin (red) and dephosphorylated (active) beta-catenin (ABC) (red) in BMOL (upper panel) and SWA (lower panel cell lines). Photomicrograph scale bars: 100uM**.**

3.7 Notch and Wnt pathways co-exist in HPC-mediated regeneration

As experiments above suggested that DRs express elements of both Notch and Wnt pathways, I was interested to see if both pathways could be expressed in the same cell as was suggested by the frequency of reporter expression at day 7 in *AhCreMDM2$^{fl/fl}$; CBF:H2B-venus* and *AhCre MDM2 $^{fl/fl}$; TCF/LEF:H2B-GFP* mice. I stained tissue from the

AhCre MDM2$^{fl/fl}$ time-course for Notch3 and beta-catenin and dephosphorylated beta-catenin and found dual expression within the DR. While this does not confirm both pathways are active in the same cell in itself, taken with the Notch and Wnt reporter evidence it strongly suggests a Notch-Wnt permissive state. This is further supported by dual staining of HPC lines for beta-catenin and Notch3 (Figure 3.19).

Figure 3.18 The ductular reaction after hepatocellular injury expresses both Notch and Wnt: (A) Immunohistochemistry for Notch3 (red) and beta-catenin (green) in *AhCre MDM2*$^{fl/fl}$ model. **(B)** Immunohistochemistry for Notch3 (red) and dephosphorylated beta-catenin (ABC) after MDM2-mediated hepatocellular injury (day 10 post-induction).

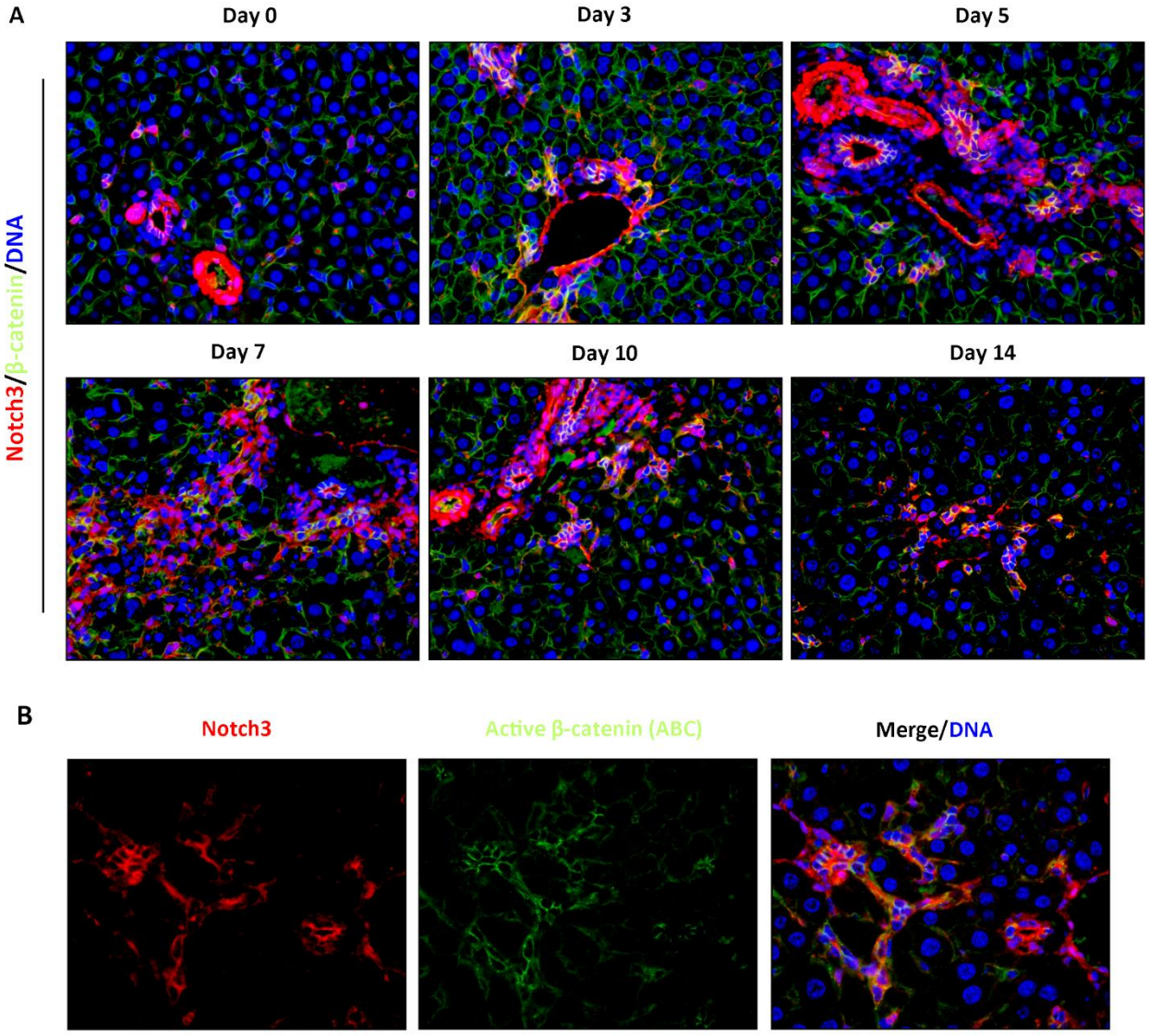
A
Day 0
Day 3
Day 5
Notch3/β-catenin/DNA
Day 7
Day 10
Day 14
B
Notch3
Active β-catenin (ABC)
Merge/DNA

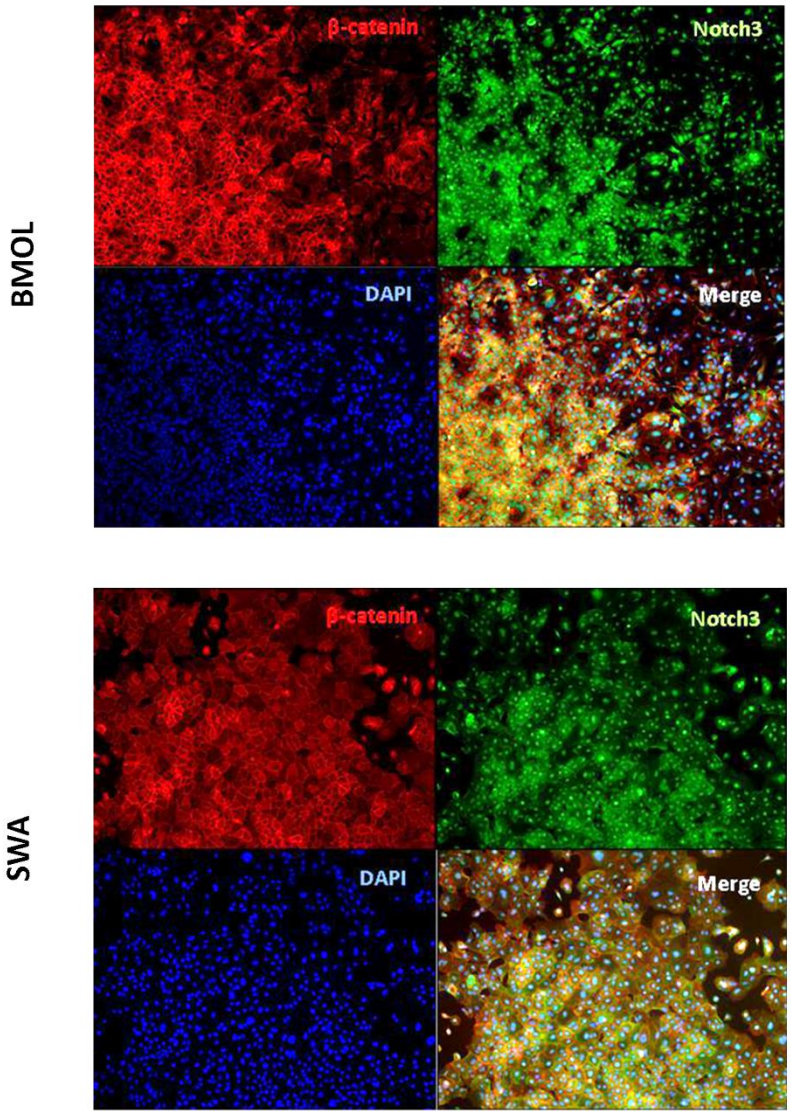

Figure 3.19 Notch and Wnt pathways co-exist in HPC lines: Immunocytochemistry of beta-catenin (red) and Notch3 (green) in BMOL (upper panels) and SWA (lower panels) HPC lines.

3.8 Notch and Wnt pathways are present in human disease

DRs are known to be present in a range of human liver diseases. I received Local ethical approval (number 10/S1402/33) for access to tissue samples held as part of the South East Scotland SAHSC Bioresource. I used tissue from liver explants from patients with hepatocellular disease (both acute and chronic) to identify samples containing DRs. Staining of tissue from these cases of advanced liver disease and identified those with robust DRs

(Figure 3.20). Robust DRs were seen in 2/5 cases fulminant liver failure, 2/3 cases hepatitis C virus and 1/1 case autoimmune hepatitis. I went on to identify if there was evidence of Notch and Wnt pathway presence in these samples. Staining of this tissue identified occasional cells positive for Notch1-ICD but Notch3 was more widely expressed and co-localises with ductular cells, confirming the relevance of Notch3 even in advanced human disease. In the short-term mouse models Notch3 stained all ductular cells, whereas in end-stage human disease while all parent ducts were positive, not all ductular cells within the expanded DR were positive in all samples. This may reflect differences between short-lived and long term disease.

DRs in chronic human disease also stained positive for beta-catenin in all conditions examined. This again supports the relevance of the mouse model to human disease.

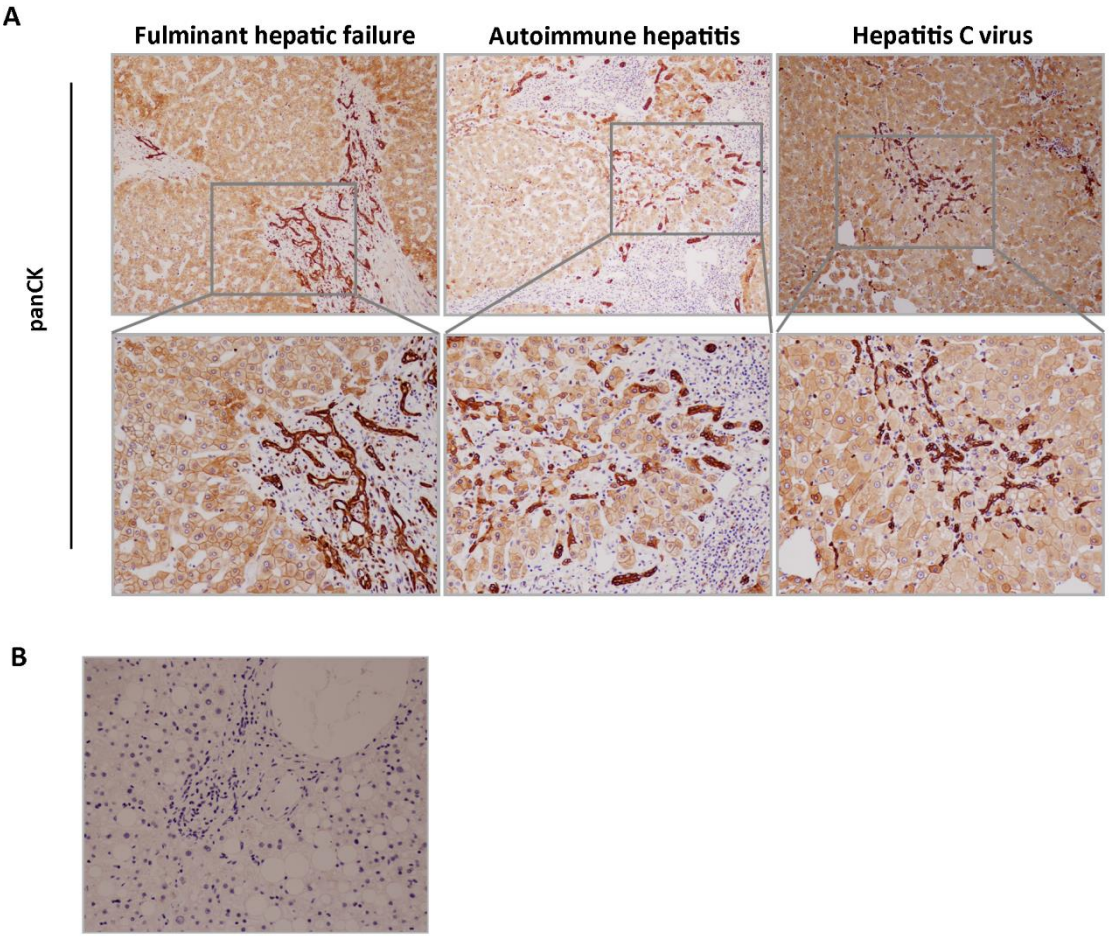

Figure 3.20 Ductular reactions occur in chronic hepatocellular injury in humans: (A) Representative images of immunohistochemistry for panCK in fulminant hepatic failure, autoimmune hepatitis and hepatitis C virus. **(B)** Rabbit isotype control.

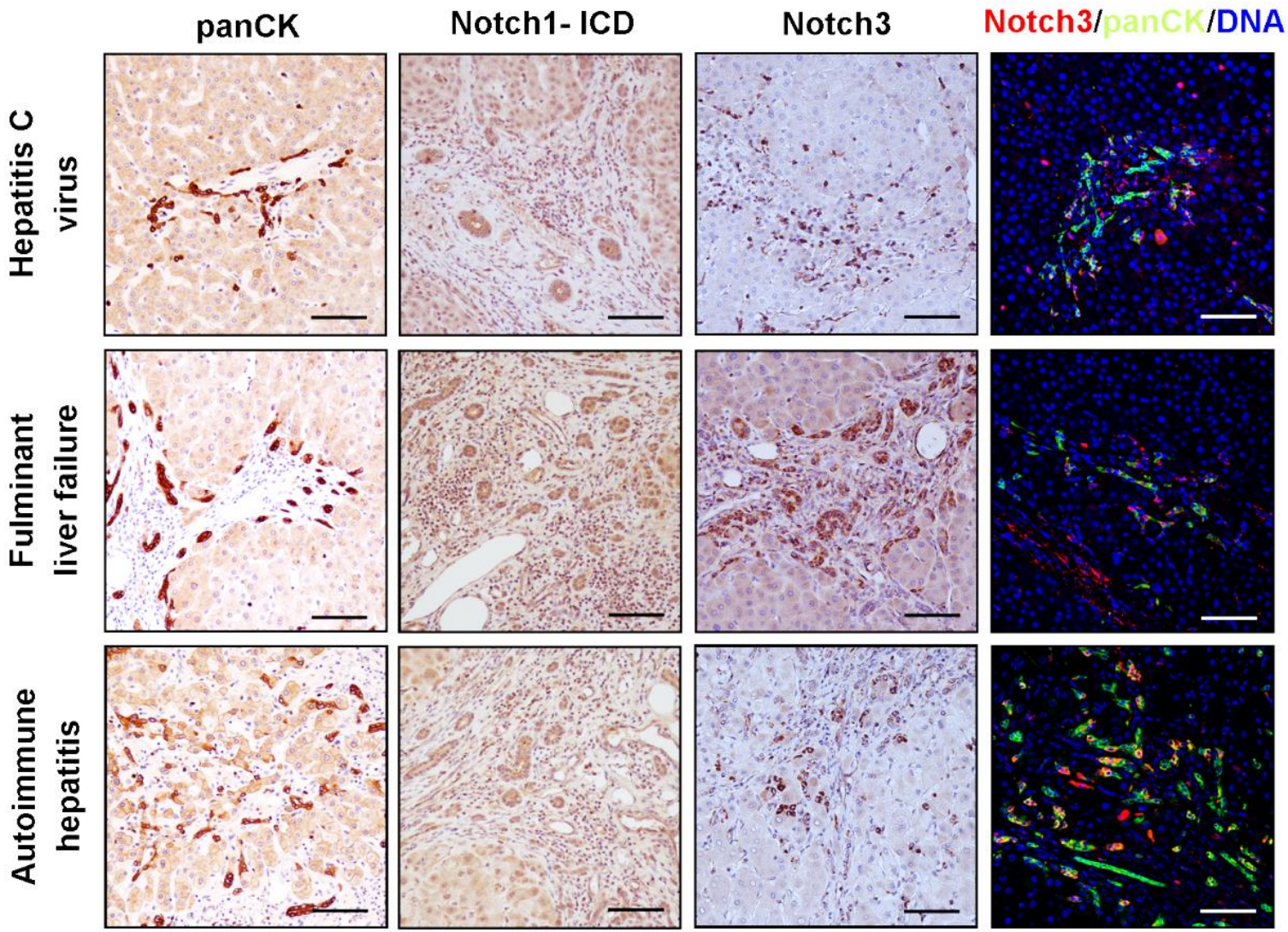
panCK
Notch1- ICD
Notch3
Notch3/panCK/DNA
Hepatitis C virus
Fulminant liver failure
Autoimmune hepatitis

Figure 3.21 Notch is expressed in human chronic hepatocellular injury: Representative images of immunohistochemistry (from left to right) for panCK, Notch1-ICD, Notch3 and co-stain for Notch3 (red) and panCK (green) in human hepatocellular liver diseases: hepatitis C virus infection (upper panel), fulminant liver failure (middle panel) and autoimmune hepatitis (lower panel). Photomicrograph scale bars: 100uM.

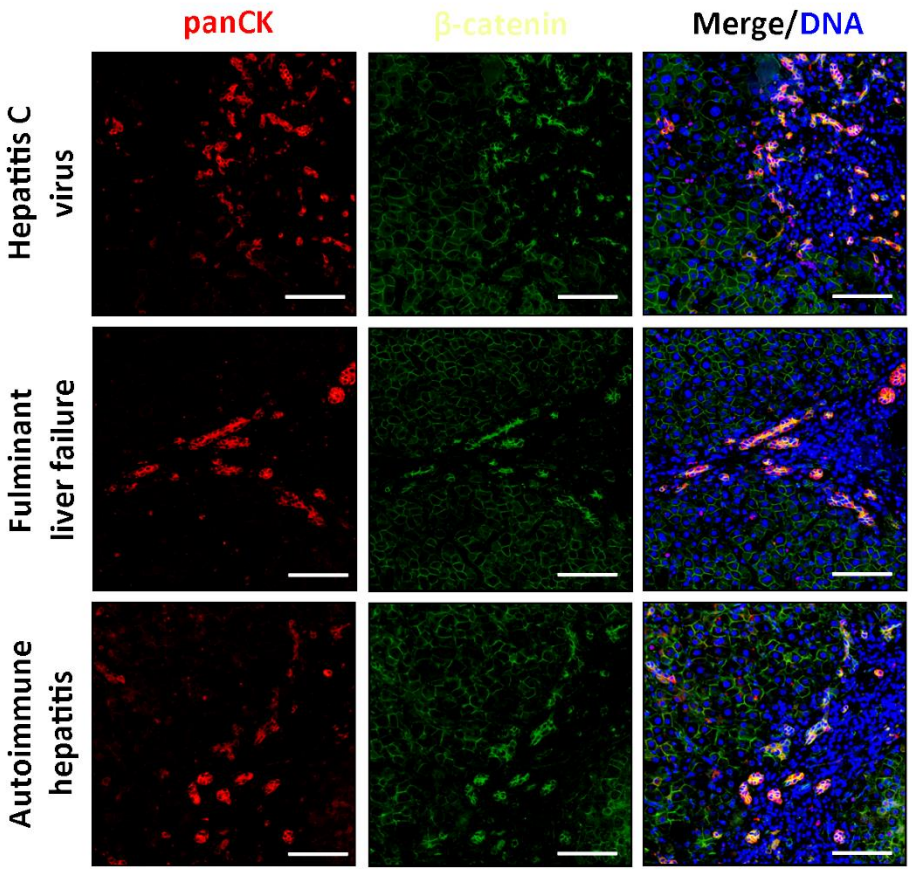

Figure 3.22 Beta-catenin is expressed by the ductular reaction after hepatocellular injury in human disease: Representative images of immunohistochemistry for panCK (red) and beta-catenin (green) in human hepatocellular liver diseases: hepatitis C virus infection (upper panel), fulminant liver failure (middle panel) and autoimmune hepatitis (lower panel). Photomicrograph scale bars: 100uM.

3.9 Discussion

Classic models used to study the response to hepatocellular injury or hepatocyte loss are acetaminophen (APAP) poisoning and 2/3 partial hepatectomy (29, 111). In both these models the insult is administered at a single point in time and thus the dynamics of injury and repair can be studied. DRs are not typically generated in these models and therefore temporal study of the HPC response is not possible. Classic rodent dietary injury models do generate DRs and replicate some of the features of human chronic liver disease, however not the wide scale replicative arrest that appears necessary in rodents for generation of a DR with extensive hepatocytic differentiation of HPCs (59, 118, 119). In addition, studying signalling pathways that may be expressed dynamically as a DR generates is limited when injury is continuous, with temporal changes that may be masked by ongoing injury and HPC activation. In order to study Notch and Wnt signalling after hepatocellular injury further, in this chapter I used a recently established potent model of HPC activation *AhCreMDM2*$^{fl/fl}$ that replicates the hepatocyte senescence seen in advanced human disease. I took advantage of the synchronised injury delivered in the *AhCreMDM2*$^{fl/fl}$ model to study the temporal dynamics of DRs and the signalling pathways involved in generating the HPC response.

Using tissue from *AhCreMDM2*$^{fl/fl}$ animals taken at various time-points after induction of Cre-mediated MDM2 hepatocyte injury, I was able to monitor the DR as it developed. There was a predictable increase in ductular cell numbers which began to plateau between days 10 and 14. Accompanying this increase in cell number was a change in cell morphology from expanding numbers surrounding a ductal lumen to an elongated appearance and then physical migration into the parenchyma away from the parent duct. I also studied the proliferation dynamics confirming a highly proliferative cell type with the peak proliferation rate reached at day 5. Detectable changes in expression of reported HPC markers were also seen over the time-course, further confirming the utility of this model in studying the development of DRs.

I went on to use this model to interrogate expression of the Notch pathway. I identified changes in expression of Notch receptors Notch1 and Notch3 after induction of injury. The expression profile of Notch1 was relatively short lived with localisation of the active intracellular domain within cells of the DR. Expression of Notch3 was more persistent

following injury. Notch3 has not been well studied in the liver. It has a potential role in regulating the activation of hepatic stellate cells and thus may be pro-fibrotic (226, 334), and in the foetal liver, Notch3-expressing cells are more hepatocyte-like with Notch3 activity appearing conducive to hepatocyte differentiation (285). A role in biliary epithelium or HPCs has not been established. I identified expression of Notch3 in the DRs of *AhCreMDM2*$^{fl/fl}$ animals and confirmed this was not model specific by replicating the finding in two traditional dietary models of hepatocellular injury. A subset of animals showed expression of Notch3 within fibroblasts, however this was not universal and therefore the role of Notch3 is unlikely to be restricted to fibrosis. The expression profiles of Notch receptors in my two HPC lines were similar to the *in vivo* models.

I identified dynamic expression of Notch ligands Jagged1 and Jagged2 which localised to the area around ductular cells, most likely expressed by myofibroblasts, consistent with previous reports (91, 123). I was also able to detect expression of Dll1 by ductular cells. This was further supported by identifying Dll1 expression in both HPC lines. This is an interesting observation as it suggests there may be potential for paracrine Notch signalling within the ductular compartment. It also explains how Notch signalling may occur in a HPC line monoculture, given Jagged ligands are not expressed by the HPCs themselves.

I found expression of classical Notch effectors, the Hes and Hey family of genes, followed a distinctive expression pattern in the *AhCreMDM2*$^{fl/fl}$ animals. This leads me to describe a 'signature' expression profile of Notch target genes.

Identifying dynamic changes in ligand, receptor and effectors suggested an intact signalling pathway. To confirm this I added a reporter of Notch activity to my transgenic model. This demonstrated active Notch signalling particularly marked in the early part of the injury response. As the half-life of GFP and its variants is reported to be 24 hours it could be argued that Notch activity was over-estimated. This could be overcome by using GFP variants with a shorter half-life (335, 336).

Using a similar strategy I demonstrated dynamic expression of Wnt pathway components in the *AhCreMDM2*$^{fl/fl}$ model. The canonical Wnt target genes examined followed a characteristic profile or Wnt 'signature' of loss during the first 5 days, followed by rapid return to pre-injury levels. The early fall likely reflects loss of Wnt pathway expression by

injured hepatocytes. Of particular interest was the observance of a similar expression profile of stem cell marker *Lgr5* and localisation of expression to ducts post-injury. The late finding of rising *Lgr5* expression suggests this does not mark a resting resident population, rather is induced in another population after injury. This is consistent with the previous observations that Lgr5+ cells are only identified in the liver after injury (77). The marked rise I identified in *Ascl2* expression, known to be upstream of *Lgr5*, further supports this.

The identification of GFP reporter expression in uninjured *AhCreMDM2$^{fl/fl}$; TCF/LEF:H2B-GFP* mice was a particularly interesting finding. The intensity of signal was lower than in pericentral hepatocytes likely reflecting lower expression levels, but clearly positive. This does however suggest a tonic level of Wnt signal in biliary homeostasis, suggesting parallels to the gut stem cell compartment where both Notch and Wnt are required for maintenance of stem cell populations (41, 242, 270). Expression of reporter in ducts occurred regardless of the animals' age and thus not reflective of residual reporter activity from immature animals. Analysis of HPC lines further supports active Wnt signalling within the DR. Benhamouche et al performed in situ hybridisation for Wnt target gene Axin2 as part of work determining that liver zonation was maintained by a balance of Wnt signalling (20). By in situ hybridisation they identified *Axin2* expression in pericentral hepatocytes but interestingly the ducts also appear to show some expression. Using an RNAScope method for *in situ* hybridisation I was able to identify *Axin2* in both ductular cells and pericentral hepatocytes. A TOPGAL TCF/LEF reporter strain has previously been used to analyse Wnt activity in uninjured and DDC-treated animals in which beta-catenin binding to TCF/LEF response elements results in beta-galactosidase (beta-gal) expression encoded for by the *lac z* gene (263). This study demonstrated minimal beta-gal reporter activity in the portal region of non-injured animals with reporter expression limited to the pericentral hepatocytes. After biliary injury, there was increased beta-gal activity in DRs. In my TCF/LEF reporter system, the use of a bright fluorescent reporter enabling single cell resolution and the construct containing six TCF/LEF binding sites means the sensitivity of this system is higher (323) and may explain the discrepancy in our findings.

Notch and Wnt have antagonistic functions in fate determination of hepatoblasts and HPCs, yet often appear to drive similar cellular processes. I wanted to establish if Notch and Wnt signals represented an either/or state or might be able to coexist. The frequency of

reporter expression in the *AhCreMDM2$^{fl/fl}$; CBF:H2B-venus* and *AhCreMDM2$^{fl/fl}$; TCF/LEF:H2B-GFP* mice suggested a capacity to overlap. Analysis of the HPC lines identified Notch3 and beta-catenin within the same cell. Staining the *AhCreMDM2$^{fl/fl}$* confirmed this *in vivo*. Through the actions of the Wnt target gene *Numb*, Wnt antagonises Notch. The structural differences between the paralog Notch receptors results in differences in their sensitivity to antagonism via Numb. Notch3 is relatively resistant to Numb-mediated degradation and thus is congruent with a Notch/Wnt permissive state possible within adult HPCs. This is highly consistent with the finding that in foetal liver progenitor cells, where Wnt is essential for hepatocyte differentiation of hepatoblasts, Notch3 expression is conducive to hepatocytic differentiation (285).

Finally, I have confirmed that in the DRs of advanced human hepatocellular disease, Notch, in particular Notch3, remains present, as does beta-catenin. In the short-term mouse models Notch3 stained all ductular cells. However, in end-stage human disease, while all parent ducts were positive, not all cells within the DRs were positive in all samples. This may reflect differences between short-lived and long term disease. Spee et al have previously identified expression of Jagged1 and LEF1 accompanying DRs in human acute and chronic hepatocellular injury, suggesting both Notch and Wnt pathways may be involved, although propose Notch pathway is less relevant to hepatocellular injury based on Notch1-ICD staining (221). Further supporting a role for Wnt signalling within the biliary compartment in the regeneration of hepatocytes from HPCs in human disease is the recent publication of a study identifying expression of Wnt target gene glutamine synthetase (GS) in ducts that appear to contribute to hepatocyte replacement (51).

The descriptive work outlines in this chapter identifies dynamic expression and activity of Notch and Wnt pathways after hepatocellular injury and led me to perform further experiments to investigate if these pathways are functional, what these functions might be, and if the dynamic expression patterns are relevant.

4 The functional role of Notch signalling in progenitor mediated hepatocellular regeneration

4.1 Introduction

Canonical Notch signalling involves Jagged or Delta family ligands binding to the extracellular domain of transmembrane Notch receptors on neighbouring cells. This leads to cleavage by ADAM10/TACE metalloprotease releasing the extracellular component, then a further cleavage by the gamma-secretase complex allowing release and nuclear translocation of the Notch intracellular domain (NICD) where it binds RBP-Jk and drives transcription of Notch target genes (see Figure 1.3).

During development Notch signalling is critical for the formation of cholangiocytes and the maturation and patterning of the biliary tree (214, 337). Mesenchymal Jagged-1 signalling via Notch2 results in NICD/RBPJK mediated activation of biliary specification gene HNF6 (338). In the adult liver, Notch continues to direct biliary fate of DRs and HPCs with Notch2 remaining a key paralog for this process (123, 222, 224). These studies also show a role for Notch in expansion of DRs after biliary injury and most recently it has been demonstrated that genetic loss of Notch signalling intermediate RBPJK or specific interference between Jagged1-Notch1 signalling impedes proliferation of cholangiocytes and DRs generated in response to biliary injury (58, 91).

Having established dynamic changes in expression of Notch pathway after hepatocellular injury, I wanted to investigate if these changes reflect temporally regulated functionality within DRs. In order to do this I used a number of techniques to disrupt Notch signalling – small molecule inhibitors, blocking antibodies, small interfering RNA (siRNA) and genetic loss of function.

As key roles identified for Notch in the liver relate to biliary differentiation and proliferation of cholangiocytes and DRs after biliary injury, I have focused on answering whether Notch signalling governs proliferation of the DR after hepatocellular injury.

In this chapter I begin by determining if the proliferation of HPC lines is sensitive to Notch inhibition and determine which Notch paralogs are responsible for this effect. I also

examine a potential role for Notch in the migration of HPC lines. I then go on to determine if the dynamic Notch pathway component and Notch reporter expression demonstrated in chapter 3 reflects changes in functional activity driving the ductular response.

4.2 Notch signalling promotes proliferation of HPC lines

Using my two HPC lines, I began by ascertaining whether their proliferation appeared sensitive to Notch inhibition. I first used a MTT assay which reports the ability of live cells to convert yellow 3-(4,5-dimethylthiazol-2-yl)-2,5-diphenyltetrazolium bromide (MTT) to purple formazan; the rate of conversion reflecting the number of viable cells. However, it should be noted that cell number will be affected by both cell proliferation and cell death. To inhibit Notch I used small molecule gamma secretase inhibitor DAPT (N-[N-(3,5-Difluorophenacetyl)-L-alanyl]-S-phenylglycine t-butyl ester). The gamma secretase complex is responsible for cleavage of the NICD from the membrane, therefore gamma secretase inhibitors prevent cleavage and nuclear translocation and transmission of signal. This small molecule has been confirmed to effectively block Notch signalling in the liver both *in vitro* and *in vivo* in multiple studies (91, 123). Incubating cells with increasing concentrations of DAPT resulted in a dose-dependent decrease in viable cell number (Figure 4.1A). To determine if this reduction in cell number was caused by a drop in proliferation rate, I selected the concentration of DAPT which reduced absorbance in both lines by approximately 50% (10uM) for use in a 5-ethynyl-2'-deoxyuridine (EdU) incorporation assay, a more specific measure of cell proliferation. EdU is an analogue of nucleoside thymidine incorporated into DNA during S-phase. After incubation with DAPT for 48 hours EdU incorporation in BMOLs was reduced from a mean of 48.3% to 25.4% and SWAs from 47.5% to 27.2% (Figure 4.1B). To confirm this reduction in proliferation rate related to Notch inhibition, I measured expression of classical Notch effector genes *Hes1* and *Hey1* in cells exposed to the same concentration of DAPT for 48 hours and found significant reductions in relative expression of both genes in both lines (Figure 4.1C).

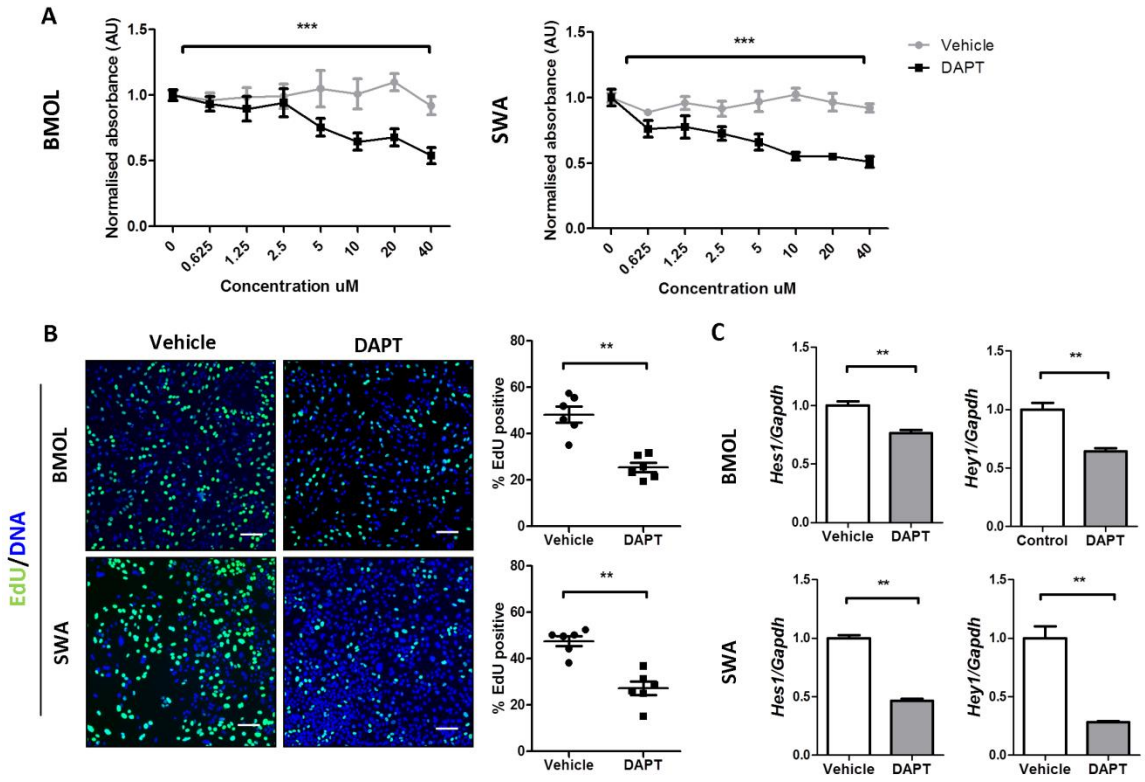

Figure 4.1: Notch inhibition with gamma secretase inhibitor reduces proliferation of HPC lines: (A) MTT assay using BMOL (left) and SWA (right) lines treated with increasing concentrations of DAPT or vehicle. Data presented as mean ± SEM of 6 experimental replicates, experiment was repeated twice. **(B)** Representative images (left) and quantification of EdU incorporation in BMOL (upper panel) and SWA (lower panel) lines treated with DAPT or vehicle (n=6 per group). **(C)** Gene expression of Notch target genes *Hes1* (left) and *Hey1* (right) relative to *Gapdh* in cell lines BMOL (upper panels) and SWA (lower panels) treated with DAPT compared to vehicle (n=6 per group). Data are presented as mean ± SEM. DAPT dose-response experiments were analysed by 2-way ANOVA. Mann Whitney test was used for experiments with two groups. **p<0.01; ***p<0.001. Photomicrograph scale bars: 100uM.

As expression profiles of the different Notch receptors differed both in the cell lines and *in vivo* after hepatocellular injury. I wanted to determine if this Notch-mediated effect on proliferation was receptor-specific. Using blocking antibodies raised against Notch2, Notch2, Jagged1 and a control antibody – raised against an intracellular epitope (desmin) I performed further cell viability assays. Two clones of Notch1 (aN1_E7 and aN1_E10) and Notch2 (aN2_B6 and aN2_B9) blocking antibodies were used to confirm the effect (Figure 4.2). Notch1 reduced cell number of both cell lines. Reductions in viable cell number after Notch2 blockade did not reach significance. Interestingly blocking Jagged1 did not significantly reduce cell number either. This would further support that some part of the Notch signalling effect, at least within these HPC lines, can be mediated via Dll1.

As no blocking antibody was available to Notch3, I used small interfering RNA (siRNA) to knock-down endogenous *Notch3* expression in the BMOL line. I tested four sequences of siRNA to *Notch3*, a scrambled sequence and untransfected cells. As transfection can result in a degree of non-specific knockdown, knockdown efficiencies were expressed as a proportion of expression relative to the scrambled sequence. Two of the *Notch3* siRNAs (*Notch3_5* and *Notch3_7*) resulted in 80-90% knockdown. This effect persisted for 48 hours and expression was returning to normal levels by 96 hours (Figure 4.3). At 48 hours post transfection, I stained cells for proliferation marker Ki67 and found *Notch3* siRNAs reduced proliferation ($p=0.0022$). When compared to scrambled sequence the *Notch3_7* sequence reached statistical significance on post-test analysis. These data suggest Notch1 and Notch3 are responsible for the effect on proliferation of Notch blockade.

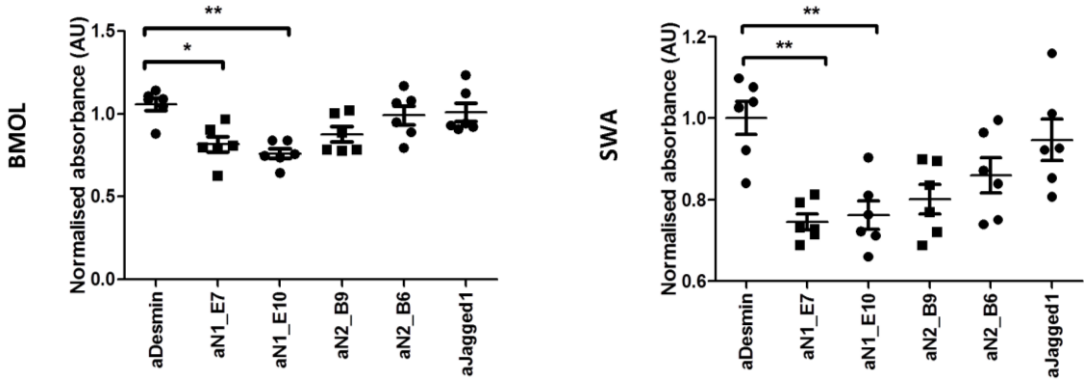

Figure 4.2: Notch1 blockade reduces viability of HPC lines: MTT assay using BMOL (left, p=0.0031) and SWA (right p=0.0049) cell lines treated with one of 2 clones of anti-Notch1 (aN1_E7 and aN1_E10), anti-Notch2 (aN2_B9 or aN2_B6), anti-Jagged1 or control antibody (to intracellular epitope desmin). Data presented as mean ± SEM of 6 experimental replicates, experiment was repeated twice. Significant p value for Kruskal-Wallis test for experiments with multiple groups presented above with Dunn's multiple comparison post-test shown in figure. *p<0.05; **p<0.01.

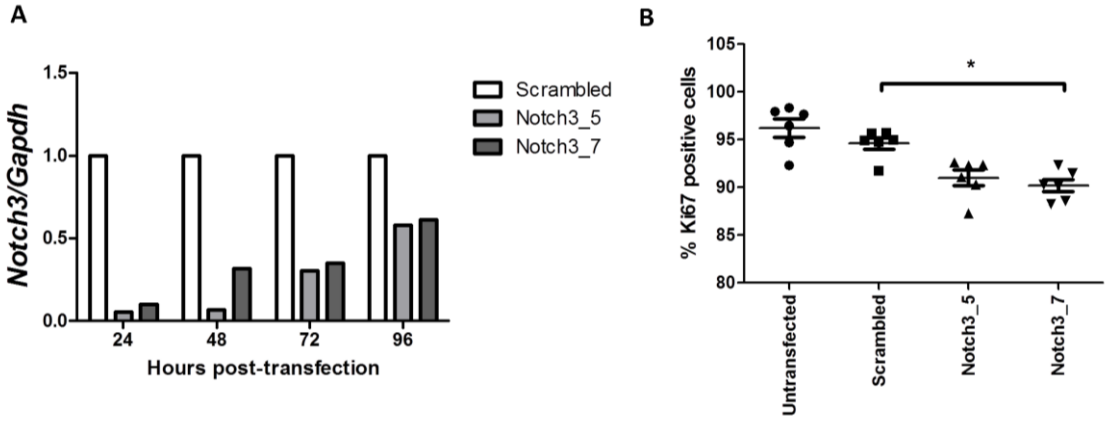

Figure 4.3: Loss of Notch3 results in attenuated proliferation in HPC lines: (A) Expression of *Notch3* relative to *Gapdh* in BMOL cells transfected with two sequences of siRNA to Notch3 (Notch3_5 and Notch3_7) or scrambled sequence 24, 48 and 72 hours post-transfection. Data presented as mean of 3 technical replicates. **(B)** Percentage of BMOL cells positive for Ki67 48 hours after transfection with *Notch3* or scrambled sequence siRNAs as above or addition of transfection vehicle (p=0.0022). Data presented as mean ± SEM of 6 experimental replicates. Significant p value for Kruskal-Wallis test for experiments shown above with Dunn's multiple comparison post-test shown in figure. *p<0.05.

4.3 Notch inhibition does not affect HPC migration in vitro

Functions of Notch can include migration (339-341). When cells proliferate, the area they occupy will expand with cells appearing further from their starting point, unless the daughter cells become progressively smaller. This is clearly distinct from true cell migration. In order to determine if Notch might have an effect on migration of HPCs, I performed an assay in which cell proliferation is blocked, and thus with no change in cell number, migration can be better assessed. This assay involved plating BMOL and SWA cells at confluent density on extracellular matrix (laminin) coated plates around a central plug. The cells had been pre-treated with mitomycin C to inhibit proliferation. Once cells had adhered, the central plug was removed creating a standard circular area into which the cells could migrate. The media was changed to one containing DAPT or vehicle and after 24 hours cells were fixed and stained (Figure 4.4). Images were taken and migrating cells quantified by pixel analysis. Notch inhibition did not reduce migration in either cell line.

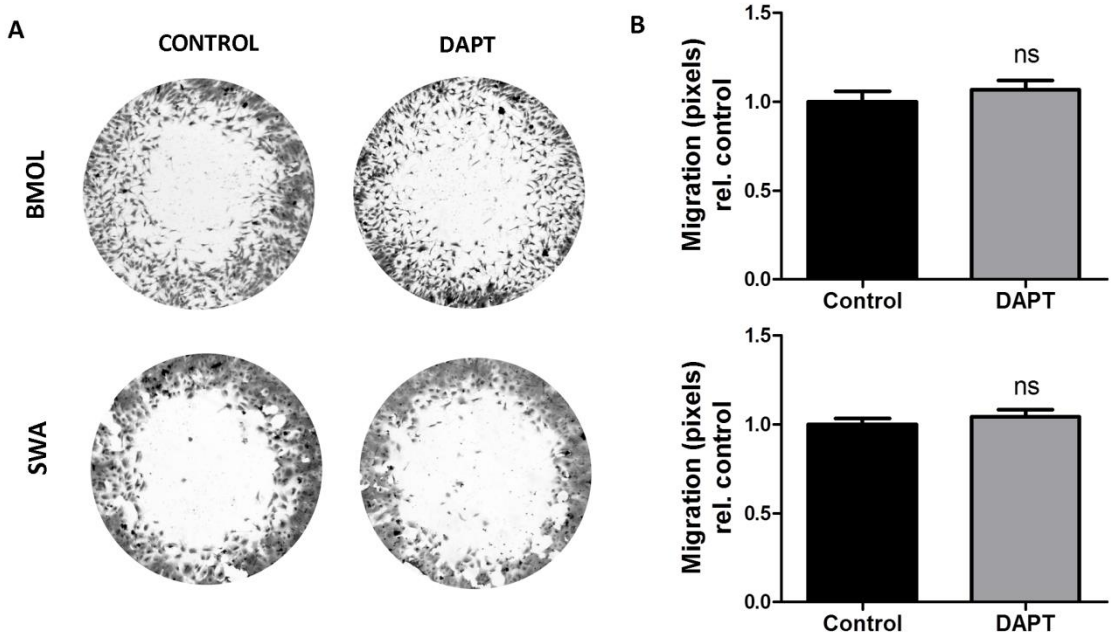

Figure 4.4: Notch inhibition does not prevent migration of HPC lines: (A) Representative images of migration assay of BMOLs (upper panel) and SWA (lower panel) towards the centre of the well after exposure to DAPT 10uM (right) or control media (left). **(B)** Quantification of cell migration by pixel analysis normalised to control conditions. *n*=8 per group. Data are presented as mean ± SEM. Statistical analysis by Student's 2-tailed t test.

4.4 Notch pathway is functionally active during the HPC response in vivo

Having established a functional role for Notch signalling in the proliferation of HPC lines *in vitro*, I sought to confirm this effect *in vivo*. As I have identified temporal changes in expression of Notch pathway components and pathway activity reporting in the *AhCre MDM2*$^{fl/fl}$ strains, I designed experiments to assess the functional relevance of these changes to the expansion of the DR.

4.4.1 Inhibition of Notch reduces HPC number and proliferation in a time-sensitive manner

Experiments were designed to reflect the apparent time-sensitive nature of Notch signalling after hepatocellular injury. *AhCre MDM2*$^{fl/fl}$ mice received DAPT or vehicle by daily i.p. injection to coincide with the peak expression of *Notch1* (days 2-4, 'early') or peak expression of *Notch3* (days 4-6, 'mid-point'), both times when Notch reporter (H2B:venus) expression was high. In a third experiment DAPT or vehicle was administered when Notch receptor and Notch reporter expression were falling (days 7-9, 'late') (Figure 4.5). Animals were harvested 24 hours after the final dose.

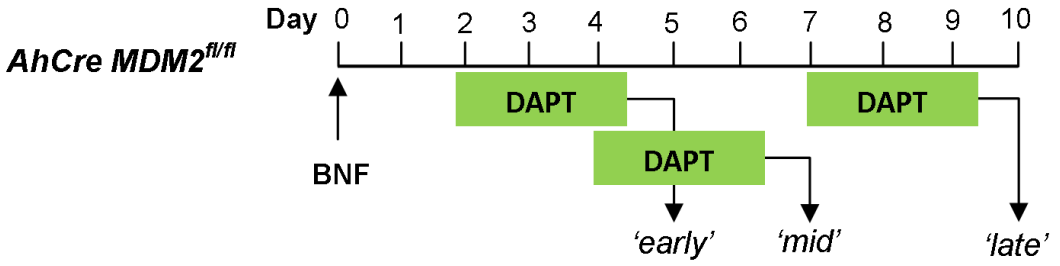

Figure 4.5: Schematic depicting experimental design for Notch inhibition experiments in *AhCre MDM2*$^{fl/fl}$ strain: Notch inhibitor DAPT or vehicle was administered days 2-4 ('early') post Cre-induction to coincide with peak expression of Notch1, days 4-6 ('mid') to coincide with peak expression of Notch3, both time periods when CBF:H2B-venus expression was high. DAPT was then given days 7-9 ('late') when Notch receptor and CBF:H2B-venus expression was falling. Animals were harvested 24 hours after the final dose. (*n*=5 per group).

'Early' inhibition of Notch (Figure 4.6) resulted in a reduction in number of ductular cells (Figure 4.6C), a time when *Notch1* and H2B:venus expression were high. Proliferation as determined by the proportion of ductular cells that stained positive for proliferation marker Ki67 was also affected (8.4% vs 19.5%) (Figure 4.6D). The level of injury as determined by

serum ALT level (Figure 4.6E) was consistent between groups and therefore initiation of injury was equivalent and not responsible for the changes in DR seen.

'Mid-point' inhibition of Notch (Figure 4.7) also resulted in a reduction in number of ductular cells, a time when *Notch3* and H2B:venus expression were high. Ductular proliferation was also reduced (5.7% vs 11.3%). In this experiment ALT levels were again consistent and therefore level of initiating injury not responsible for the change in size of the DR.

'Late' inhibition of Notch (Figure 4.8) did not affect the size or proliferation rate of ductular reactions. This was consistent with the finding of low expression levels of Notch reporter over this period in the *AhCre MDM2$^{fl/fl}$; CBF:H2B-venus*. ALT levels remained consistent.

Taken together these data suggest:

1. The *AhCre MDM2$^{fl/fl}$; CBF:H2B-venus* strain accurately reports active Notch signalling and
2. Ductular proliferation in the early but not the late phase of the ductular response is Notch-sensitive.

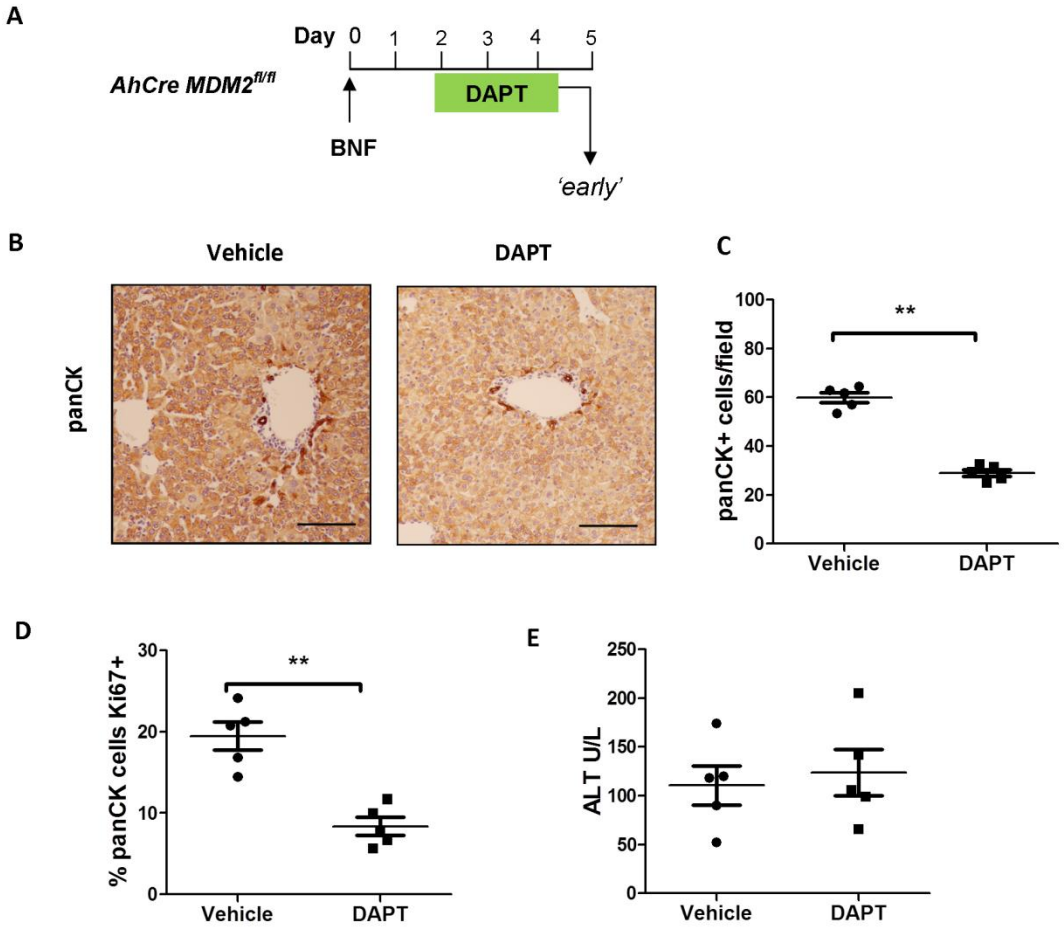

Figure 4.6: Notch signalling drives expansion of the early ductular reaction after hepatocellular injury: (A) Schematic demonstrate the strategy for time-dependent treatment with Notch inhibitor DAPT or vehicle following MDM2-mediated hepatocyte injury. **(B)** Representative images of panCK staining in DAPT and vehicle-treated animals. **(C)** Quantification of effect on ductular response in terms of panCK-positive cell number and (D) Ki67 positive proportion. **(E)** Serum ALT levels. (*n*=5 per group). Data are presented as mean ± SEM. Mann Whitney test was used. **p<0.01. Photomicrograph scale bar: 100uM.

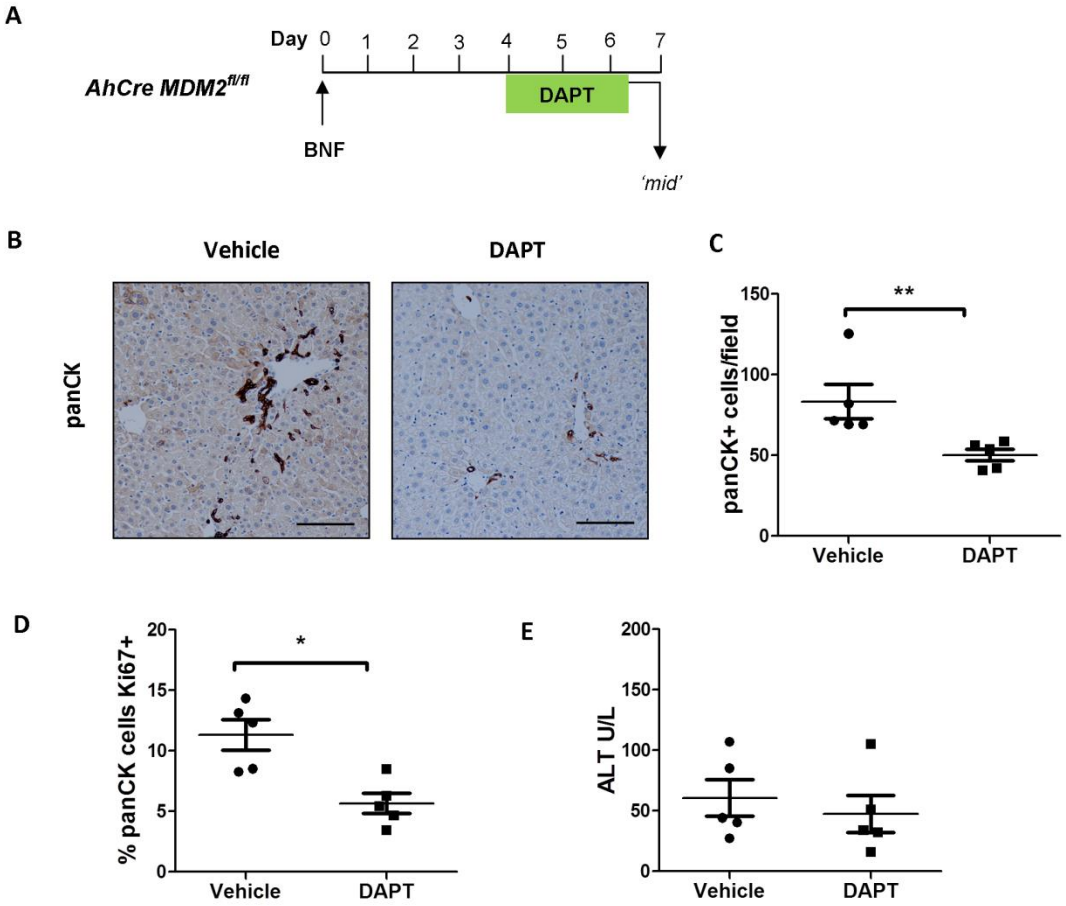

Figure 4.7: Notch signalling drives expansion of the mid-point ductular reaction after hepatocellular injury: (A) Schematic demonstrate the strategy for time-dependent treatment with Notch inhibitor DAPT or vehicle following MDM2-mediated hepatocyte injury**. (B)** Representative images of panCK staining in DAPT and vehicle-treated animals. **(C)** Quantification of effect on ductular response in terms of panCK-positive cell number and **(D)** Ki67 positive proportion. **(E)** Serum ALT levels. (*n*=5 per group). Data are presented as mean ± SEM. Mann Whitney test was used. *p<0.05; **p<0.01. Photomicrograph scale bars: 100uM.

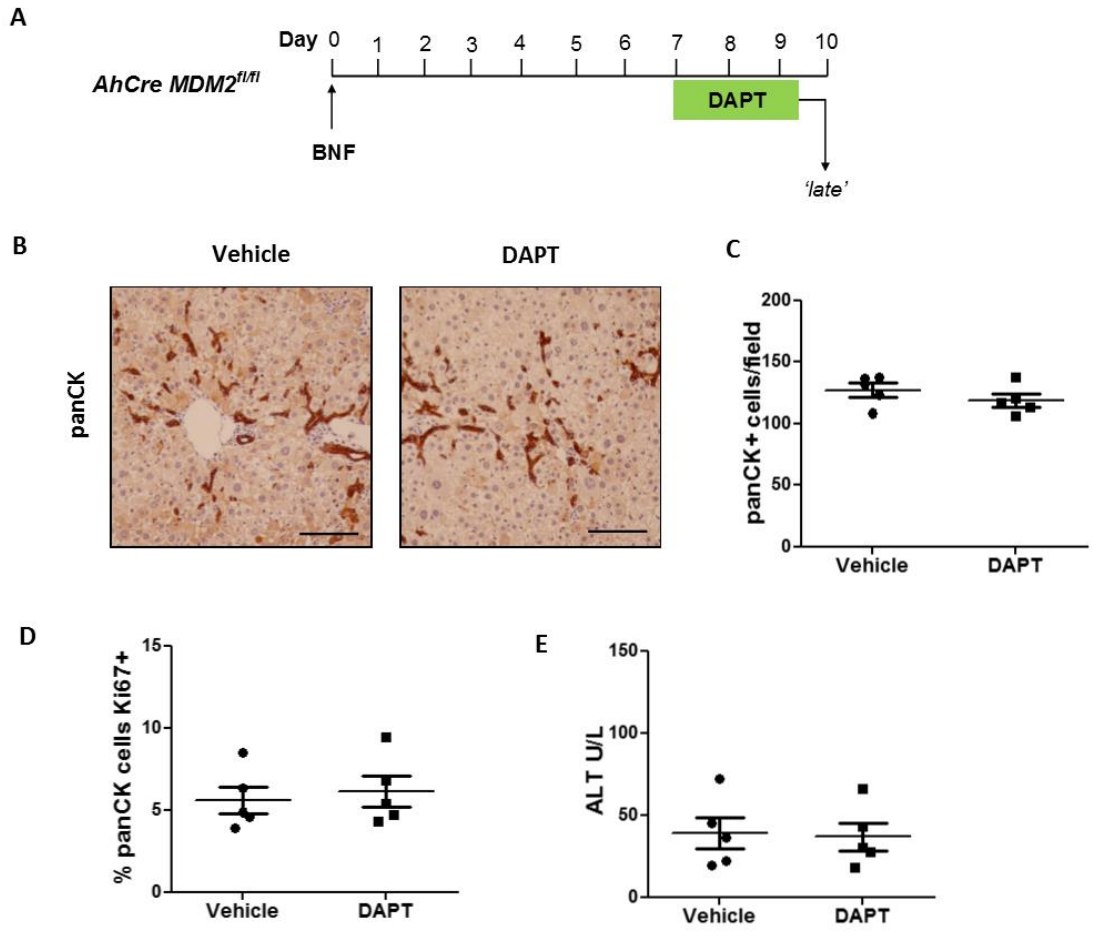

Figure 4.8: Notch signalling does not drive expansion of the late ductular reaction after hepatocellular injury: (A) Schematic demonstrate the strategy for time-dependent treatment with Notch inhibitor DAPT or vehicle following MDM2-mediated hepatocyte injury. **(B)** Representative images of panCK staining in DAPT and vehicle-treated animals. **(C)** Quantification of effect on ductular response in terms of panCK-positive cell number and **(D)** Ki67 positive proportion. **(E)** Serum ALT levels. (*n*=5 per group). Data are presented as mean ± SEM. Mann Whitney test was used. *p<0.05; **p<0.01. Photomicrograph scale bars: 100uM.

4.4.2 Loss of DR is due to loss of proliferation capacity rather than premature differentiation

While the experiments in the *AhCre MDM2$^{fl/fl}$* strain support the loss of ductular cells after Notch inhibition being due to impaired proliferation, given Notch inhibition in HPC lines and primary HPCs promotes differentiation down the hepatocyte lineage (123), it could be argued that differentiation could contribute to the reduction in cell number. As the DRs in the *AhCre MDM2$^{fl/fl}$* model are not lineage labelled, it is not possible to test this with this strain. *OPN-iCreER^{T2};R26R^{YFP}* is a strain in which Cre is induced in osteopontin (OPN) expressing cells (near exclusively ductular cells in the uninjured liver (203)) after administration of tamoxifen. This results in excision of a *loxP*-flanked STOP codon upstream of YFP within the *Rosa26* locus and subsequent YFP labelling of the cell and its progeny (56). This strain has been shown to label ductular cells in liver injury and when induced mice receive three weeks of CDE diet followed by a two week 'STOP' or recovery period on regular chow, approximately 2.45% of hepatocytes are labelled as having been of ductular origin. *Krt19CreER^{T};RCL^{tdT}* is a strain in which Cre is induced in cytokeratin 19 (*Krt19*) expressing cells after administration of tamoxifen resulting in excision of a *loxP*-flanked STOP codon resulting in expression of downstream red fluorescent protein (RFP) variant tdTomato in the cell and its progeny. This strain was generated by crossing the parent strain *Krt19CreER^{T}* (324) with the *Ai14(RCL-tdT)* strain (325). We have confirmed it can lineage label ductular cells in dietary models of liver disease and when mice are given the CDE-stop protocol, small numbers of *Krt19* lineage labelled hepatocytes are seen (59). Using these two strains I designed experiments to determine the effect of Notch inhibition on the ability of DRs to generate hepatocytes and to confirm in another model the effects of Notch on ductular proliferation after hepatocellular injury.

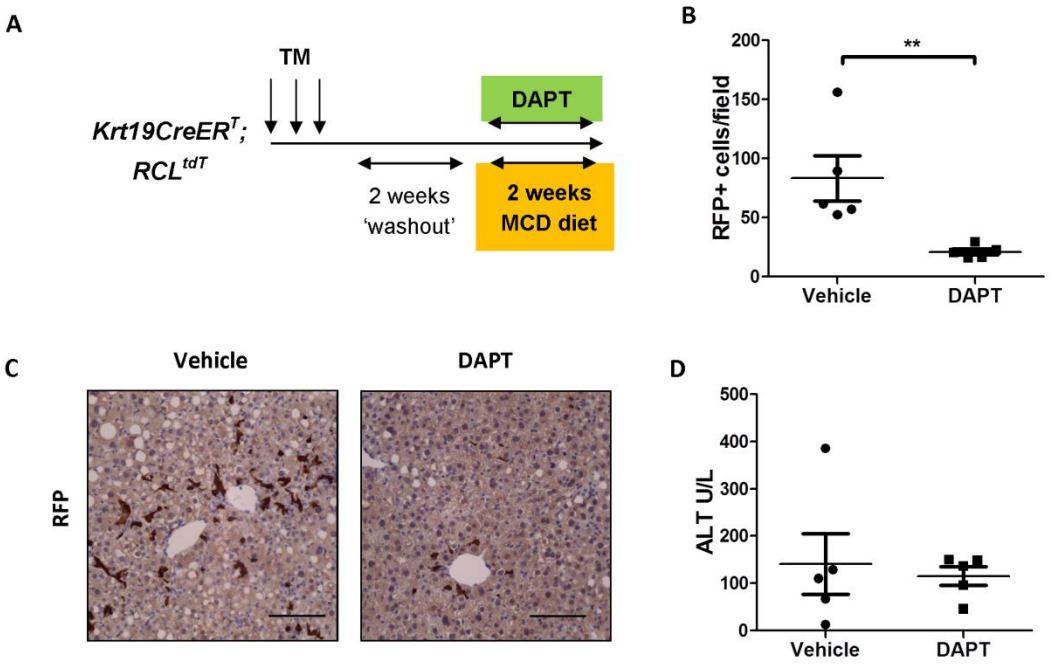

Figure 4.9: Lineage tracing confirms loss of ductular cells after Notch inhibition in hepatocellular injury: (A) Schematic demonstrating experimental strategy for assessment of the effect on the ductular reaction of Notch inhibition using *Krt19-CreER^T;RCL-tdT* strain with MCD diet to induce hepatocellular injury. **(B**) Quantification of RFP-positive cell number. **(C**) Representative immunohistochemistry for RFP label. **(D)** Serum ALT levels. (*n*=5 per group). Data are presented as mean ± SEM. Mann Whitney test was used. **p<0.01. Photomicrograph scale bars: 100uM.

Groups of *Krt19CreER^T;RCL^{tdT}* mice received three doses of tamoxifen i.p. at 5-6 weeks old to induce Cre recombination. After a two-week washout period to reduce the chance of residual tamoxifen mislabelling cells whose expression profile may change in response to injury, the mice received two weeks of MCD diet to induce hepatocellular injury. As the dietary injury models involve continuous exposure to the toxin, DAPT was administered at a frequency of three doses per week for the duration of the injury diet to assess the effect of Notch inhibition on the expanding DR (Figure 4.9A). This experiment was designed to answer the question whether change in numbers of DR cells was due to premature differentiation (and thus loss of ductular marker and not detectable in the *AhCre MDM2$^{fl/fl}$*

model) or reduced proliferation of cells. I then stained the tissue for the RFP lineage label and quantified the cells. There was a marked reduction in lineage labelled cells (Figure 4.9B) and this could not be explained by differences in the level of liver injury as determined by serum ALT levels (Figure 4.9D). The RFP cells all appeared to be of ductular morphology and subsequent co-staining of tissue for RFP with hepatocyte marker HNF4a failed to identify lineage labelled hepatocytes above a negligible frequency (0-1 per section examined). Having established that the RFP positive cells remained ductular and were not hepatocytes, I wanted to confirm if the loss in cell number was due to loss of proliferation consistent with the *AhCre MDM2*$^{fl/fl}$ model. The quantification of Ki67 positive ductular cells had required staining for a ductular marker (panCK), then co-staining for the proliferation marker, then photographing multiple microscopic fields at a high magnification to enable manual counting. The research centre had subsequently acquired a high-content analysis system (Operetta) with a facility for scanning, imaging and analysing whole slides. As the lineage tracing strains both resulted in label expression that involved the nucleus, the site of expression of many proliferation markers, generating an analysis 'pipeline' that could automate the quantification of proliferating reporting cells appeared possible. As the manual identifying, photographing and counting of fields is extremely time consuming, this limits the number of fields analysed. An automated process offers the opportunity to increase the amount of tissue analysed and thus the reliability of the results. Effective staining protocols were in place for both RFP and YFP reporters. Ki67 staining could on occasion vary in intensity across a slide, which could cause difficulties in setting standard thresholds for quantification, and therefore tissue was instead stained for proliferating cell nuclear antigen (PCNA) which resulted in more consistent staining. Examples of the staining achieved are shown in Figure 4.11A. In collaboration with other members of the group (Eoghan O'Duibhir, Phil Starkey-Lewis and Alex Raven), we trialled the Operetta screening system and accompanying Columbus analysis software to develop pipelines for detection of nuclear stains in liver tissue. The analysis 'pipeline' I used for all analysis of RFP or YFP and PCNA stained tissue is included in Appendix 1. Quantification of the proportion of RFP positive cells that were PCNA positive fell in the *Krt19CreER*^{T}*;RCL*^{tdT} mice receiving DAPT from 32% to 13.5% (Figure 4.11B).

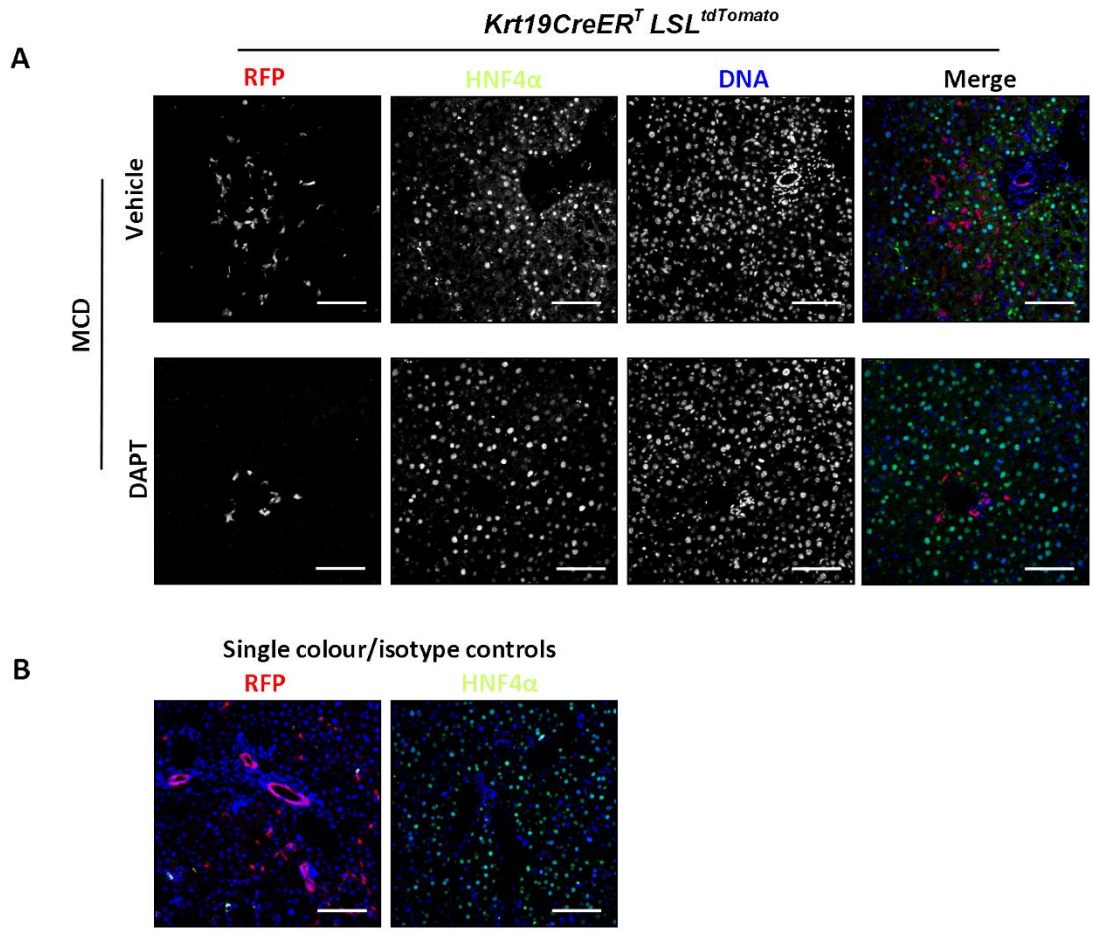

Figure 4.10: Loss of ductular cells in DAPT-treated animals is not due to hepatocytic differentiation: (A) Immunohistochemistry for RFP (red) and HNF4a (green) in *Krt19-CreER^{T};RCL-tdT* animals treated with DAPT or vehicle while receiving MCD diet to induce hepatocellular injury. Ductular lineage-traced hepatocyte remained at negligible frequency in both groups (0-1 cells per section). **(B)** Single stain/isotype controls. Photomicrograph scale bars: 100uM.

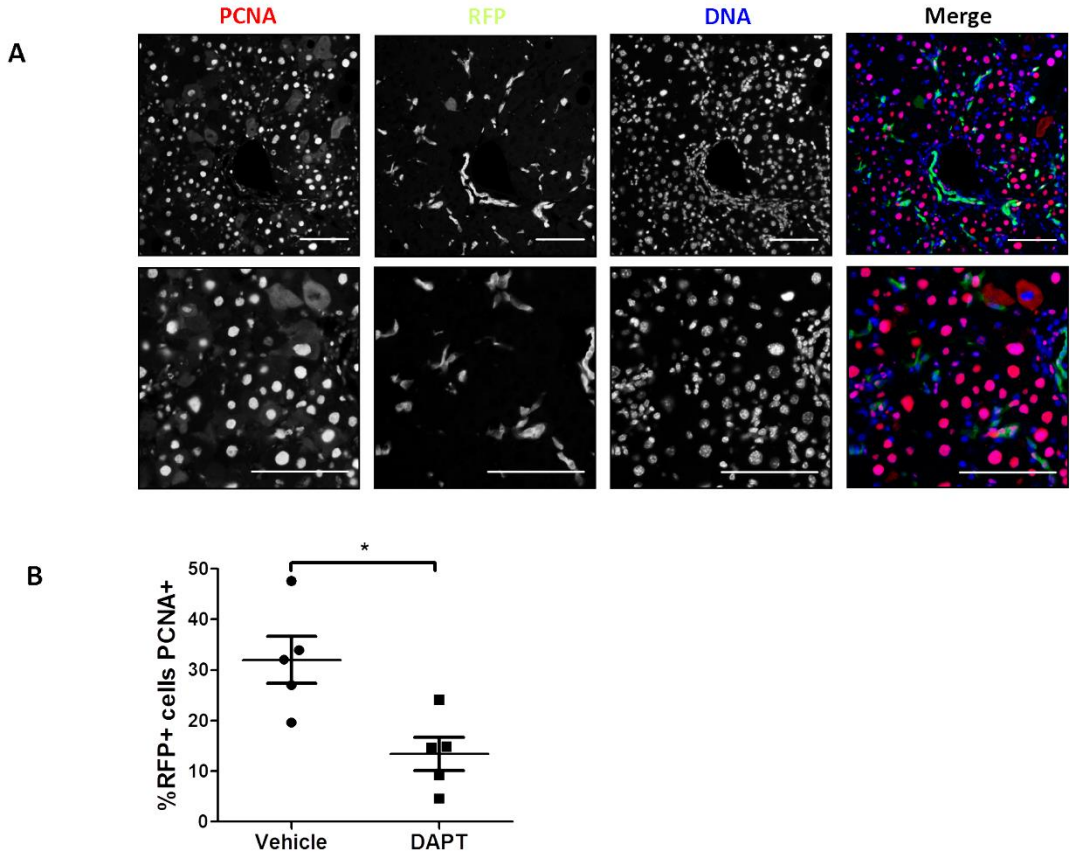

Figure 4.11: Notch signalling drives proliferation of the ductular reaction after hepatocellular injury: (A) Representative Immunohistochemistry for PCNA (red) and RFP (green) in *Krt19-CreER^{T};RCL-tdT* strain administered MCD diet to induce hepatocellular injury. **(B)** Quantification of RFP-positive cell number (left) and PCNA positive proportion (right) in *Krt19-CreER^{T};RCL-tdT* strain administered DAPT or vehicle during MCD diet (*n*=5 per group). Data are presented as mean ± SEM. Mann Whitney test was used. *p<0.05; **p<0.01. Photomicrograph scale bars: 100uM.

I designed an experiment using the *OPN-iCreER^{T2};R26R^{YFP}* strain and the previously established CDE-recovery protocol (56) with the initial intention of identifying whether in this system DAPT administration has an effect on HPC differentiation. However, having now clearly established a role for Notch in the proliferation of DRs, I was not sure if any effect on differentiation could be assessed without considering the impact of proliferation, clearly a

necessary part of the response. This animal experiment was performed by Noemi van Hul from the Leclercq lab at Universite Catholique de Louvaine in Belgium, to my experimental protocol, pending the rederivation of the strain into our animal unit. I performed all subsequent analysis. *OPN-iCreER^{T2};R26R^{YFP}* mice received three doses of DAPT or vehicle per week during the 'recovery' period (Figure 4.12A). In the vehicle treated group patches of YFP positive hepatocytes of ductular origin could be detected, however these were absent in the DAPT treated group (Figure 4.12B). Few labelled hepatocytes were seen but this was barely above the frequency of aberrant recombination events seen in uninjured animals 7 weeks after tamoxifen administration (Figure 4.12F). After the recovery period, serum ALT levels in both groups had returned to normal Figure 4.12D). Further animals underwent the CDE-recovery protocol with groups taken off at the end of injury (day 0), and after 3 and 7 days of recovery. The proportion of YFP positive cells that were proliferating (PCNA positive) were quantified in all groups and proliferation rate remained high (27%, 19% and 17% respectively) (Figure 4.12E). Given the persisting high rate of DR proliferation during the first part of the recovery period, the sensitivity of DR proliferation to Notch and the requirement for cell division during differentiation, ascertaining a direct effect of Notch on differentiation in a complex *in vivo* model is extremely difficult.

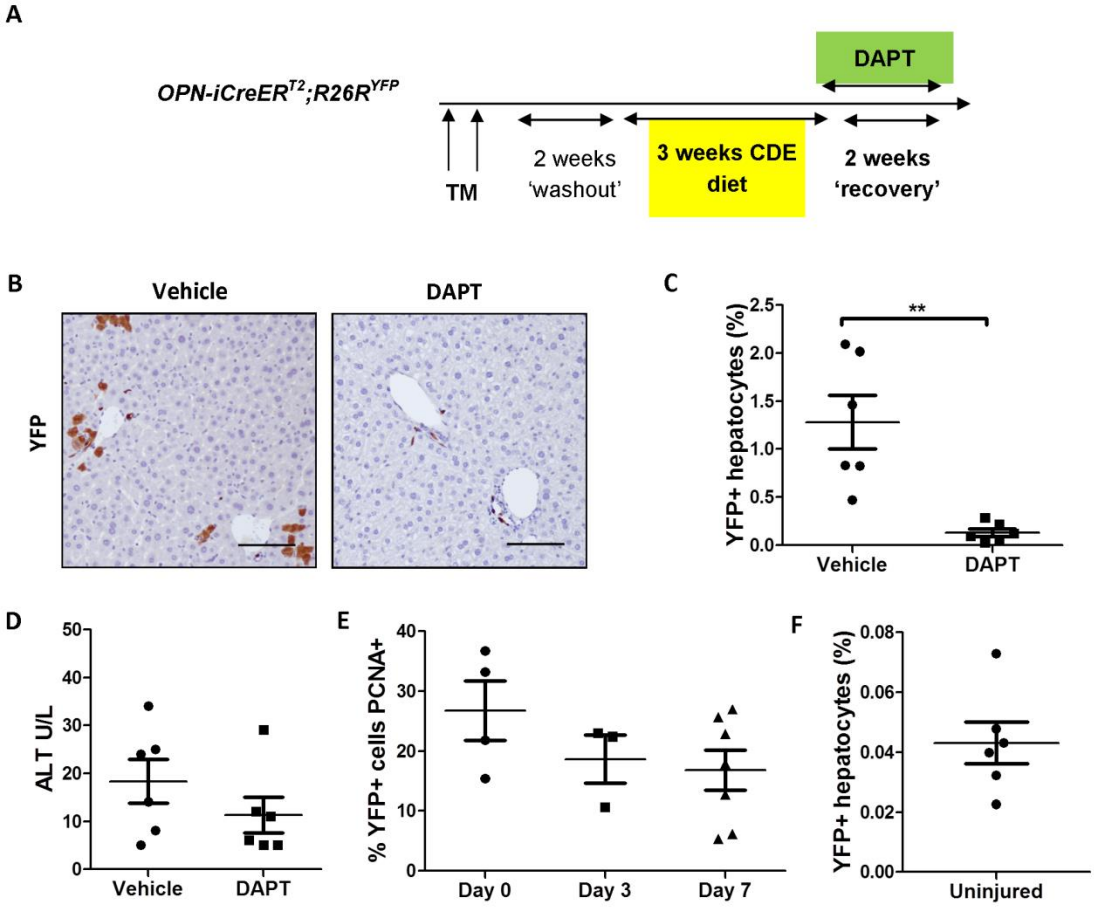

Figure 4.12: Notch inhibition results in a reduction in lineage-labelled hepatocytes using the CDE-STOP regimen: (A) Schematic of experimental strategy for assessing the effect on generation of biliary lineage-derived hepatocytes of Notch inhibition with DAPT using *OPN-iCreER^{T2};R26R^{YFP}* strain and the CDE-STOP protocol to induce differentiation. **(B)** Representative images of YFP staining from the experiment. **(C)** Quantification of resultant YFP-positive hepatocytes and serum ALT levels **(D)** (n=6 per group). **(E)** Quantification of proportion of YFP+ cells PCNA-positive at the end of 3 weeks CDE diet (Day 0 *n*=4), and after 3 and 7 days of recovery (Day 3 *n*=3, Day 7 *n*=7). **(F)** Proportion of YFP-labelled hepatocytes 7 weeks after tamoxifen induction in uninjured mice. Data are presented as mean ± SEM. Mann Whitney test was used for experiments with two groups. *p<0.05; **p<0.01; ***p<0.001. Photomicrograph scale bars: 100uM.

4.4.3 Effects of Notch on ductular response are receptor specific

I had identified in HPC lines that the Notch-related proliferation effect was mediated by Notch1 and Notch3. Given the dynamic expression patterns of these receptors *in vivo* I wanted to see if these were the important receptors for the proliferation phenotype *in vivo*.

I administered the Notch1, Notch2 and control antibodies used in Figure 4.2 to *AhCre MDM2*$^{fl/fl}$ mice one day after Cre induction with BNF (Figure 4.13A). This was to cover the time when *Notch1* expression was high. As *Notch2* expression did not change over the time-course, it seemed most appropriate to administer it over this same time period as this coincides with high levels of Notch driven H2B:venus expression. Ductular cell number fell in animals receiving either clone of Notch1 blocking antibody (Figure 4.13C), as did their proliferation rate from 28.6% to 9.8 and 10.1%. Blocking Notch2 had no effect on ductular cell number or proliferation. Initial injury levels as determined by serum ALT values were consistent.

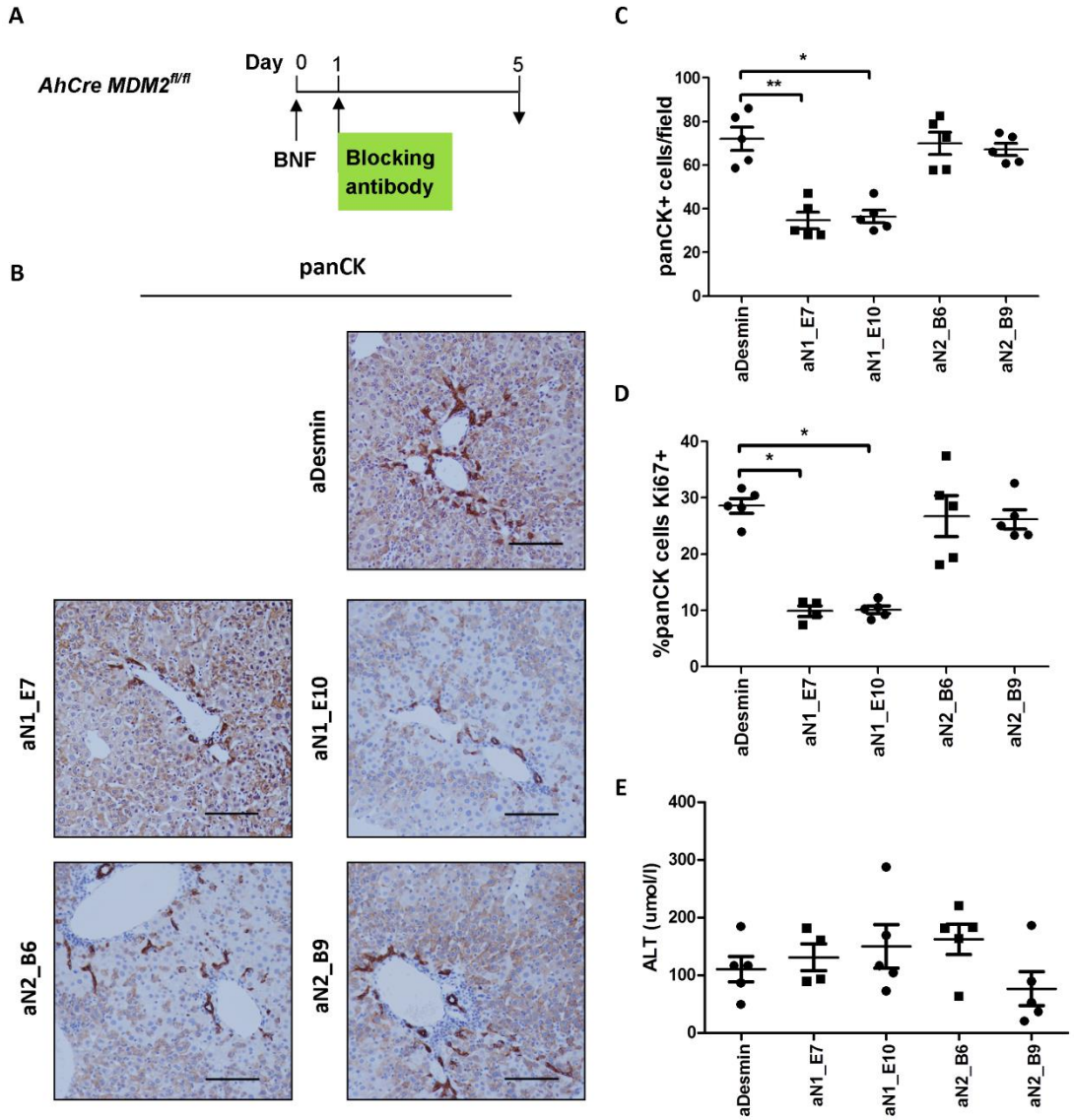

Figure 4.13: Notch1 but not Notch2 drives expansion of the ductular reaction after hepatocellular injury: (A) Schematic representing strategy for blocking antibody-mediated Notch inhibition with one of two clones of Notch1 (aN1_7 or aN1_E10) or Notch2 (aN2_B6 or aN2_B9) blocking antibody or control antibody (to intracellular epitope of desmin aDesmin) in the *AhCre MDM2$^{fl/fl}$* model. **(B)** Representative immunohistochemistry of panCK staining from the experiment. **(C)** Quantification of effect on ductular response in terms of panCK-positive cell number (p=0.0015) and **(D)** Ki67 positive proportion (p=0.0024). **(E)** Serum ALT values. (*n*=5 per group). Data are presented as mean ± SEM. Kruskal-Wallis test was used for comparison of multiple groups (p value shown in legend above) with Dunn's multiple comparison post-test analysis included in the figure. *p<0.05; **p<0.01. Photomicrograph scale bar: 100uM.

In order to investigate the role of Notch3 in the ductular response, in the absence of available Notch3 blocking antibodies, or specific small molecule inhibitors, I used a genetic knock-out approach. As there is no floxed allele for Notch3 available, I used a Notch3 null strain *Notch3*$^{-/-}$ (321), recognising the limitation that as with the Notch1 and Notch2 blocking antibodies, it would not limit the effect to the ductular compartment. No liver developmental phenotype has been identified in this strain (317, 321) and there are no published reports of its response to liver injury. Studies using mice with the Notch3 null mutation to examine muscle regeneration had observed an unusual phenotype. While muscle appeared to have developed normally, when injured the Notch3 null strain demonstrated a hypertrophic response (318). This was due to increased proliferation of muscle progenitors which is largely dependent on Notch1 and thus Notch3 was thought to provide negative regulation of Notch1-driven proliferation by inducing Notch inhibitor *Nrarp*. I was therefore particularly intrigued to see the effect on liver regeneration of the loss of Notch3 and could anticipate no phenotype if it was truly redundant, impaired regeneration if it was required or enhanced progenitor activity if the role of Notch3 was to regulate Notch1.

For further experiments I crossed the *Notch3*$^{-/-}$ strain with the *AhCre MDM2*$^{fl/fl}$ and *OPN-iCreER*^{T2}*;R26R*^{YFP} strains. While these new strains were being bred, I used the *Notch3*$^{-/-}$ colony to identify if I would likely require homozygous knockout rather than haploinsufficiency to observe any phenotype. Given the marked variation in background strain sensitivities to dietary injury, in particular CDE diet, I put groups of *Notch3*$^{+/+}$, *Notch3*$^{+/-}$ and *Notch3*$^{-/-}$ animals on the DDC biliary injury diet to assess the response (Figure 4.14A). Although the focus of this thesis is hepatocellular injury, this diet model was chosen for this experiment because 1. It is a rapid and reliable inducer of DRs, 2. Given the published literature on the role of Notch after liver disease, an effect of loss of any of the receptors would be predicted to be most marked in a biliary injury model. If no effect was seen with the different genotypes with CDE diet it would not be clear whether this related to alterations in the background strain and thus sensitivity to injury or if Notch3 had no functional role. There was no change in ductular cell number between *Notch3*$^{+/+}$ and *Notch3*$^{+/-}$ mice, however there was a significant reduction in cell number in the homozygous

knockout (Figure 4.14C). Using this information to direct my breeding strategy for the other *Notch3* knockout strains, I bred *AhCre MDM2*$^{fl/fl}$ *Notch3*$^{+/+}$ and *AhCre MDM2*$^{fl/fl}$ *Notch3*$^{-/-}$ strain and *OPN-iCreER*^{T2}*;R26R*^{YFP}*;Notch3*$^{+/+}$ and *OPN-iCreER*^{T2}*;R26R*^{YFP}*;Notch3*$^{-/-}$ strains for further experiments.

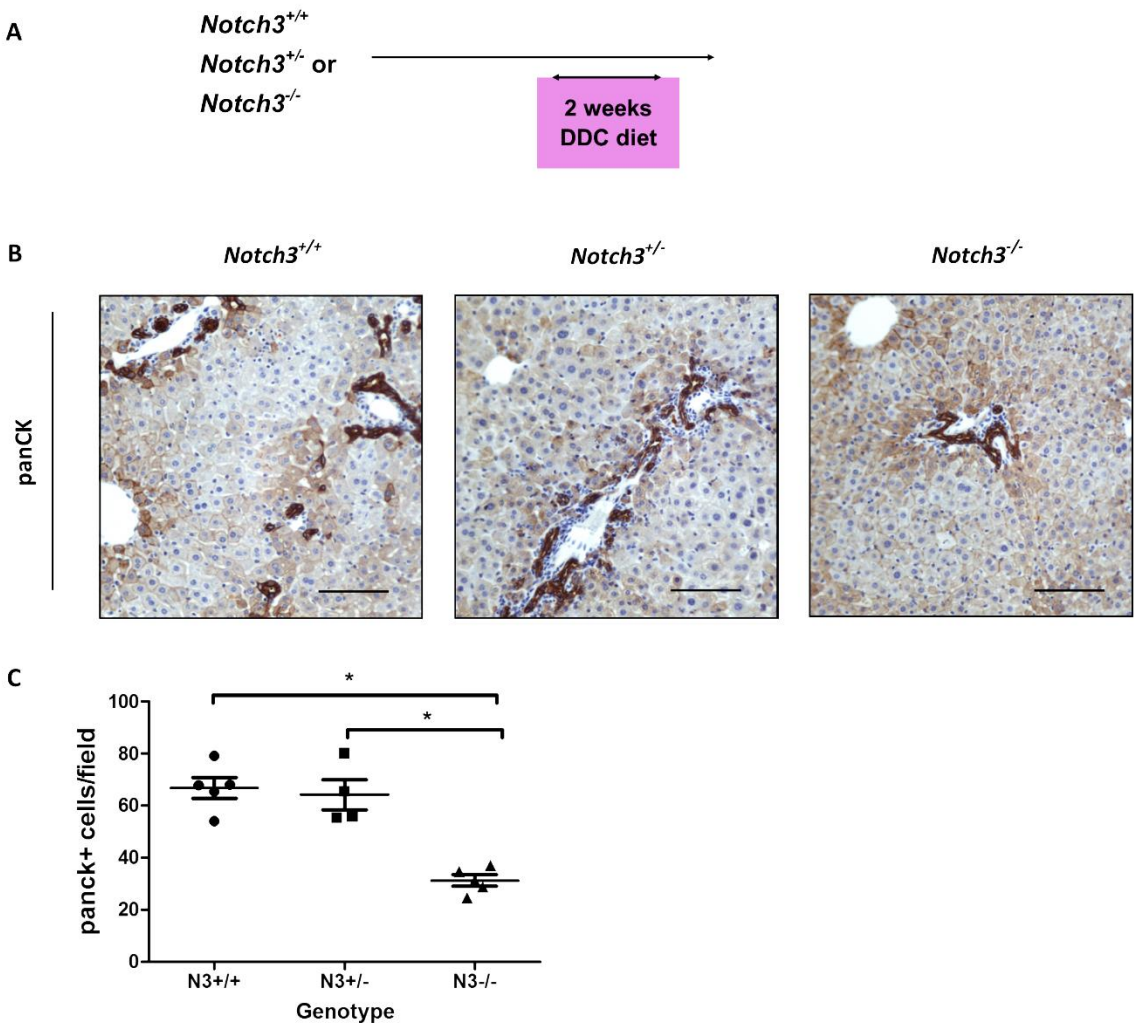

Figure 4.14: Homozygous loss of Notch3 attenuates ductular response to biliary injury: (A) Schematic demonstrating experimental strategy for assessment of the effect on the ductular reaction of genetic Notch3 loss using *Notch3*$^{+/+}$, *Notch3*$^{+/-}$ and *Notch3*$^{-/-}$ animals with DDC diet to induce biliary injury. **(B)** Representative immunohistochemistry for panCK. **(C)** Quantification of ductular cells in each group. P=0.0110. (*n*=5 per group). Data are presented as mean ± SEM. Kruskal-Wallis test was used for comparison of multiple groups (p value shown in legend above) with Dunn's multiple comparison post-test analysis included in the figure. *p<0.05. Photomicrograph scale bar: 100uM.

I administered BNF to induce Cre expression in *AhCre MDM2$^{fl/fl}$ Notch3$^{+/+}$* and *AhCre MDM2$^{fl/fl}$ Notch3$^{-/-}$* mice and harvested tissue 7 days later (Figure 4.15A). I chose this time period to cover when *Notch3* expression should be at its peak. Cell number and proliferation rate was reduced in the *AhCre MDM2$^{fl/fl}$ Notch3$^{-/-}$* mice (Figure 4.15C and D). Serum ALT values were much higher in this experiment than in other *AhCre MDM2$^{fl/fl}$* experiments (Figure 4.15E). This may reflect a variation in concentration in the BNF administered, a difference in response due to the alteration in background strain following the cross, an effect of loss of Notch3 from other cell types or potentially a protective effect of a ductular reaction.

Having established that loss of Notch3 attenuates the DR and that this appears to be due to a loss in proliferation, I wanted to be sure that cell loss due to precocious hepatocyte differentiation was not contributing. Using *OPN-iCreER^{T2};R26R^{YFP};Notch3$^{+/+}$* and *OPN-iCreER^{T2};R26R^{YFP};Notch3$^{-/-}$* strains, groups of animals received 3 weeks of CDE diet to induce a ductular response two weeks after Cre induction with tamoxifen (Figure 4.16A). Again there was a marked loss in ductular lineage labelled cells. The number of lineage labelled hepatocytes was small and in fact lower in the *iCreER^{T2};R26R^{YFP};Notch3$^{-/-}$* strain and therefore hepatocyte differentiation does not explain the loss of ductular cells.

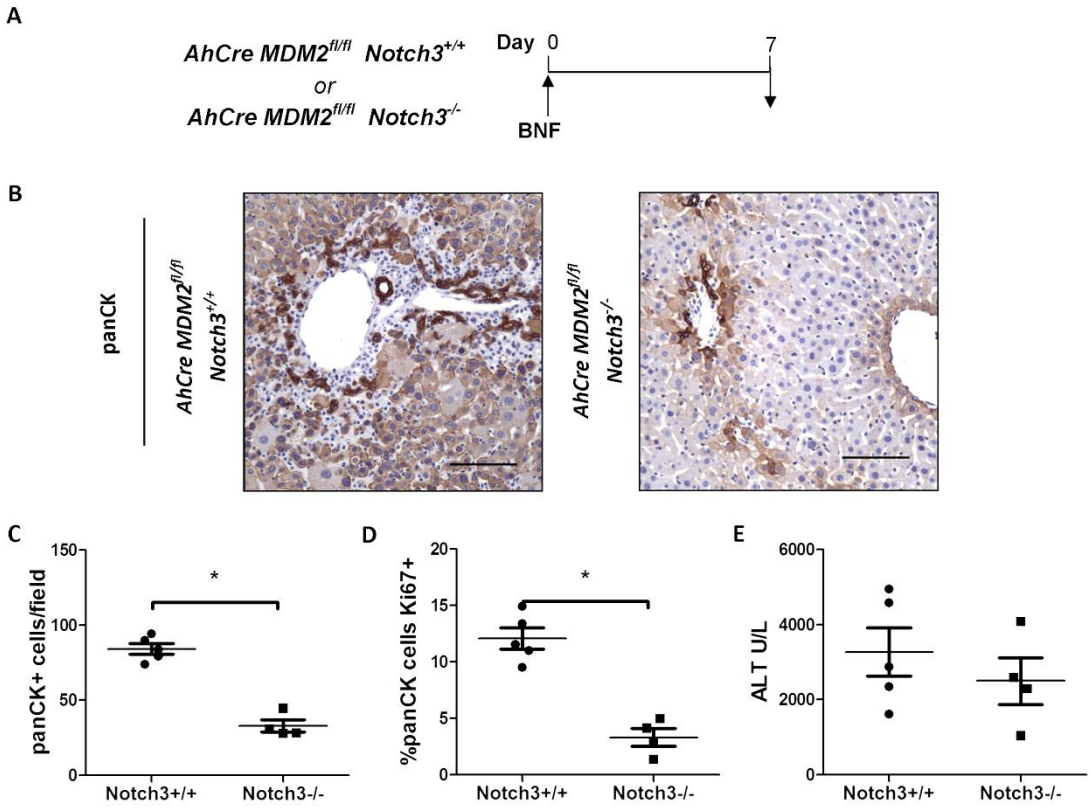

Figure 4.15: Notch3 drives expansion of the ductular reaction after hepatocellular injury: **(A)** Schematic represents experimental design for assessing the effect on ductular response of loss of Notch3 in MDM2-mediated hepatocyte injury. *AhCre MDM2$^{fl/fl}$ Notch3$^{+/+}$* n=5, *AhCre MDM2$^{fl/fl}$ Notch3$^{-/-}$* n=4. **(B)** Representative immunohistochemistry of panCK staining from the experiment. **(C)** Quantification of effect on ductular response in terms of panCK-positive cell number and (D) Ki67 positive proportion. **(E)** Serum ALT values. Data are presented as mean ± SEM. Mann Whitney test was used for experiments with two groups. *p<0.05. Photomicrograph scale bar: 100uM.

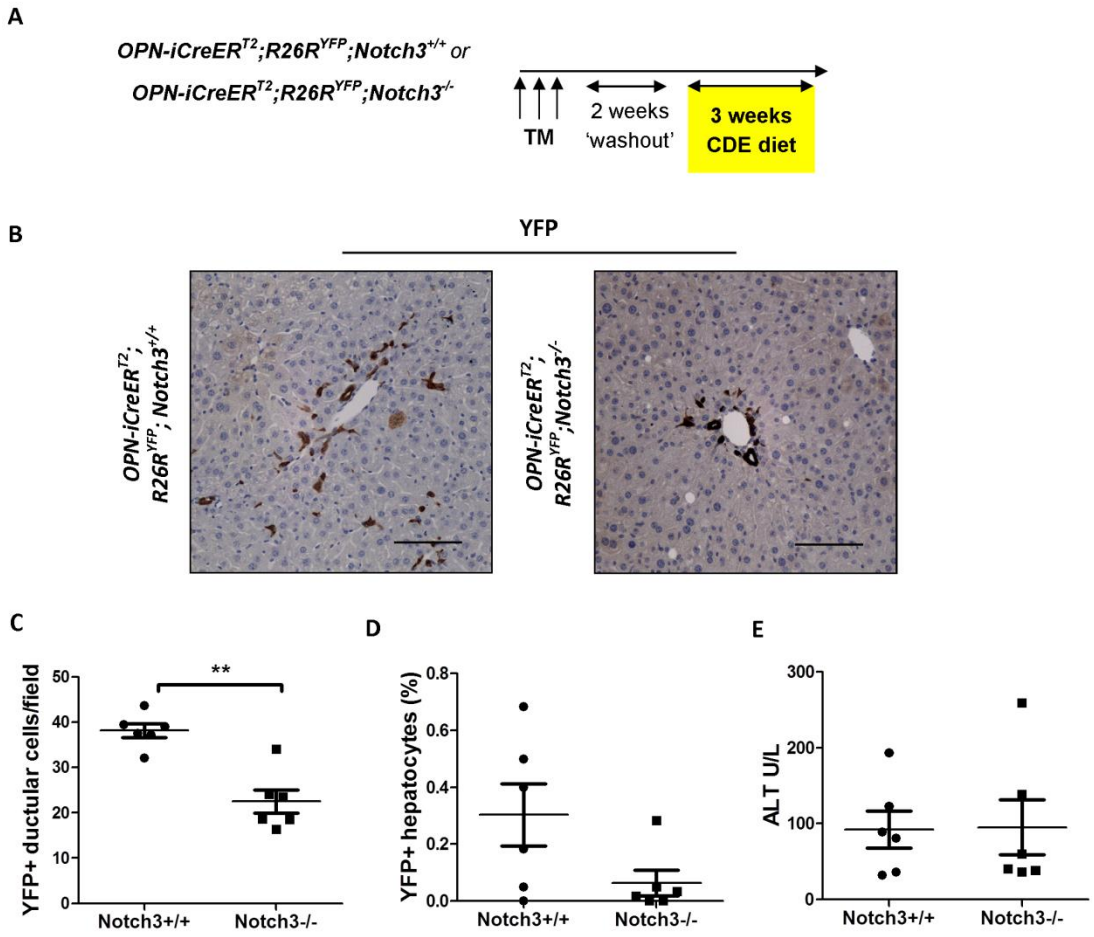

Figure 4.16: Loss of ductular cells in Notch3$^{-/-}$ animals is not due to increased hepatocyte differentiation: (A) Schematic of experimental design to assess effect of loss of Notch3 on the ductular response hepatocellular injury induced with choline deficient ethionine supplemented (CDE) diet using *OPN-iCreER^{T2};R26R^{YFP};Notch3$^{+/+}$* and *OPN-iCreER^{T2};R26R^{YFP};Notch3$^{-/-}$* strains (*n*=6 per group). **(B)** Representative images for YFP staining. **(C)** Quantification of YFP-positive ductular cell number confirming loss of ductular cells in Notch3$^{-/-}$ animals and **(D)** Proportion of hepatocytes YFP-positive (p=0.1062). **(E)** Serum ALT values. Data are presented as mean ± SEM. Mann Whitney test was used for experiments with two groups. **p<0.01. Photomicrograph scale bar: 100uM.

4.5 Discussion

Macrophage-derived Wnt promotes proliferation of DRs after hepatocyte injury (123), however when the liver is depleted of macrophages HPCs remain able to expand but fail to migrate into the parenchyma instead forming 'duct like' structures (342). The persisting ability to expand suggests alternative signals are involved in their initial proliferation. Important signals identified to date in HPC activation and proliferation include HGF/c-met, EGFR, Shh, TWEAK and TGF-β (343-345). In this chapter I have established a role for Notch signalling in ductular proliferation in response to hepatocyte injury.

Using HPC lines I have demonstrated that their proliferation is Notch sensitive. Pan-Notch inhibition with DAPT (222) or using a mouse strain where RBPJK is conditionally deleted in the ductular compartment (58) has confirmed a role for Notch in proliferation of DRs after biliary injury *in vivo*. By designing experiments to coincide administering Notch inhibition with the dynamic changes in Notch pathway expression in the *AhCre MDM2*$^{fl/fl}$ model shown in chapter 3, I have confirmed that these changes reflect functionality of the Notch pathway and control of DR proliferation after hepatocellular injury. When Notch was inhibited while Notch1 expression was high and when Notch pathway reporter was expressed, there was a reduction in proliferation of DRs. This phenotype was also demonstrated by inhibiting Notch when Notch3 expression was at its peak. When Notch receptor and Notch pathway reporter expression was low, Notch inhibition did not affect DR proliferation.

This is the first description of a role of Notch in regeneration from biliary compartment after hepatocellular injury in mouse. He et al (52) performed complex experiments in zebrafish where the hepatocyte compartment was genetically ablated. They determined nearly all the biliary cells lost their tubular morphology, proliferated and expressed hepatocyte-specific markers. Lineage tracing demonstrated that most new hepatocytes arose from the biliary compartment and this required Notch signalling. Regenerating cells expressed a Notch reporter and delivery of DAPT concurrent with hepatocyte injury resulted in a marked reduction in formation of new hepatocytes. The authors also proposed that activation of early endoderm and hepatoblast markers indicated biliary transdifferentiation included a step of de-differentiation into a bi-potential intermediate

involving activation of Sox9 which was Notch-dependent, however the relative contribution of different paralogs was not examined.

I performed experiments using blocking antibodies and demonstrated that when growing in isolation, proliferation of HPCs is governed by Notch1 but not Notch2 or the Notch ligand Jagged1. As I have shown that BMOL and SWA cells do not express Jagged1, then Jagged1 blocking antibody would not be anticipated to have an effect on HPC proliferation. I have demonstrated that HPCs express instead Dll1 and this may be the source of Notch ligand in BMOL and SWA monocultures. By reducing expression of Notch3 in the BMOL cell line using siRNA, I was also able to demonstrate a role for Notch3 in proliferation of HPCs. The use of cell lines for these experiments has both advantages and disadvantages. A cell line that has undergone spontaneous immortalisation may not behave in the same was as primary cells with regard to proliferation, conducting similar experiments with primary cells may overcome this, however when cultured in the absence of niche-derived ligands, the biology of these cells too may be altered, particularly with regard to sensitivity to those same niche-derived ligands. The number of cells required for this work would require many more experimental mice to be used. In addition determining which primary HPCs to isolate and from which time points after injury would markedly increase the complexity of experiments and potentially impede interpretation of results.

Boulter et al (123) co-cultured HPCs with Jagged1 expressing myofibroblasts. When Notch inhibitor DAPT was added to block Notch signalling, expression of Notch responsive Hes and Hey genes fell, as did biliary genes HNF6 and gamma-glutamyltranspeptidase (GGT), supporting a role for Notch signalling via Jagged1 in promoting biliary differentiation of HPCs. Kim et al (91) have shown that after biliary injury, the interaction between Jagged1 expressed on myofibroblasts and Notch1 expressed within the DR results in proliferation. CCN1, a matricellular protein that binds distinct cell surface integrin receptors, binds integrin $\alpha_v\beta_5/\alpha_v\beta_5$ on myofibroblasts activating NK-kB leading to Jagged1 expression. A further interesting finding in this paper is that when knock-in mice expressing a CCN1 mutant that is unable to bind $\alpha_v\beta_5/\alpha_v\beta_5$ undergo biliary injury by bile duct ligation (BDL), there is an impaired DR which leads to massive hepatocyte collapse and mortality; this can be rescued by administration of soluble Jagged1. This further emphasises the importance of DRs and ductular Notch signalling in supporting liver regeneration, even when not directly

providing new hepatocytes. In order to determine if this Jagged1-Notch1 interaction is specific to biliary disease or if proliferation of my HPC lines derived from hepatocellular injury models could be promoted by Jagged1, they could be co-cultured with Jagged1 expressing myofibroblasts in the presence or absence of anti-Jagged1 or as a monoculture in the presence of soluble Jagged1. I have demonstrated that *in vivo* Jagged1 and Jagged2 ligand are available and intimately associated with the DR. Administration of the anti-Jagged1 antibody *in vivo* could permit observation of an effect on proliferation of the DR, and would suggest but would not confirm a direct effect of interrupting signalling between Jagged1 expressing myofibroblasts and cells of the DR. It may be that the involvement of multiple ligands builds redundancy into this system and/or potential for paired ligand and Notch paralog signals like the specific Jagged1-Notch1 interaction demonstrated by Kim et al (91).

By using the anti-Notch1 and anti-Notch2 blocking antibodies *in vivo* I confirmed a role for Notch1 but not Notch2 in the proliferation of DRs. I had found no dynamic changes in expression of Notch2 therefore this combined with the lack of effect on proliferation of DRs of Notch2 blockade suggests this paralog has no role in DR proliferation after hepatocellular injury. This may reflect functional redundancy however would also be consistent with divergent roles for Notch1 and Notch2. Interfering with pan-Notch signalling or the specific interaction between Jagged1 and Notch1 limits proliferation of DRs after biliary injury (91, 222). Overexpression of Notch1 in the hepatocytes of newborn and adult mice results in their transdifferentiation to cholangiocytes (103, 215). Loss of Notch2 but not Notch1 in development compromises intrahepatic duct development (213). Loss of Notch2 in biliary injury does not limit accumulation of DRs but instead they fail to progress to mature ducts (222). Together this suggests the role of Notch2 is primarily related to determination of biliary fate, with potentially a wider range of actions for Notch1.

As a Notch3 blocking antibody was not available, I used genetic deletion to investigate if this paralog has a role in proliferation of DRs *in vivo* as suggested by the siRNA experiment *in vitro.* Mice that were null for Notch3 failed to generate appropriate DRs in response to both CDE diet and MDM2-mediated hepatocyte injury and DDC diet induced biliary injury. Further analysis of the *AhCre MDM2$^{fl/fl}$ Notch3$^{+/+}$* and *AhCre MDM2$^{fl/fl}$ Notch3$^{-/-}$* strains confirmed a loss of proliferation within the DR. Silencing of Notch3 in the liver by virus

mediated transfer of shRNA reduced fibrosis in response to CCl4 in rats associated with reduction in activated stellate cells and transforming growth factor beta-1 (TGFb1) (226). As the CCl4 model does not induce a DR, whether the observed effect was a primary effect related to loss of activated myofibroblasts or loss of biliary activation is unclear. Likewise it would be pure speculation to suggest the phenotype observed in my *Notch3*$^{-/-}$ mice resulted from loss of activated myofibroblasts to support a DR rather than a direct effect on the DR itself. In human foetal liver, interactions between Jagged1, expressed on the embryonic ductal plate, and Notch3, expressed on the adjacent portal tract mesenchyme and hepatic arterial endothelium, are thought to play a role in the process of ductal plate remodelling and the subsequent development of the intrahepatic biliary tree (346). Although there is no reported developmental phenotype in the *Notch3*$^{-/-}$ mice, it remains possible that there may be a defect in biliary development or development of cells with HPC capability that would only be revealed after the administration of liver injury (318, 321). As Notch3 is also expressed by blood vessels in the liver, an indirect effect on DRs from loss of vascular Notch3 cannot be excluded. To demonstrate a direct effect on HPCs *in vivo* and corroborate the proliferation effect seen *in vitro* would require experiments with a mouse strain where the Notch3 alleles were flanked by loxP site so could be specifically targeted to the biliary compartment in adult mice. The direct effect on proliferation in the cell line monoculture, would suggest at least part of the proliferative effects on HPCs of signalling via Notch3 were direct.

A potential role for Notch signalling from the vascular compartment in general and endothelium in particular on DRs is intriguing. Conditional deletion of Notch1 from all liver cell compartments causes the generation of lesions similar to nodular regenerative hyperplasia (NRH) (347). This phenotype is related not to a direct effect on hepatocytes but rather loss of pan-Notch (via RBP-JK) or Notch1 inactivation within liver sinusoidal endothelial cells (LSECs) resulted in their dedifferentiation and proliferation with formation of abnormal vessels and veno-occlusive disease. There was subsequent hepatocyte apoptosis and reduced proliferation after partial hepatectomy (219, 220). This highlights further the importance of both context and cell-type specificity of Notch signalling in the liver and how altering Notch activity levels in the vascular compartment may have multiple indirect effects on other cell compartments (156).

Notch signalling can play a role in cell migration and invasion (207, 341), triggering epithelial-mesenchymal transition by mechanisms including upregulation of Snail1. When I exposed HPC lines to Notch inhibition with DAPT there was no effect on cell migration, therefore it is likely that this pathway is not involved directly in migration of HPCs generated in response to hepatocellular injury. Attempting to confirm this *in vivo* presents difficulty: when cells proliferate, unless sequentially smaller cells are generated, the space they occupy will increase. This will give the appearance of cells further from the starting point in the absence of any true migration. As Notch drives proliferation of the DR, distinguishing a change in migration from proliferation is further hampered. Inhibiting proliferation of the DR, while preserving Notch signal and not altering hepatocyte or other cell type behaviour is beyond the limits of current models. Further inference of a lack of effect on HPC migration could be sought from examining if at a time when Notch is not directing proliferation, Notch inhibition results in less migratory DRs. Examining distance of DRs from the portal tract in animals given DAPT or vehicle in the *AhCre MDM2*$^{fl/fl}$ 'late' experiment showed no difference (data not shown) however as the *AhCre MDM2*$^{fl/fl}$; *CBF:H2B-venus* data suggests Notch pathway is not active at this time, any effect or lack of it cannot be attributed to Notch signalling. Generation of a computer simulation that could determine predicted distance from portal tract based on number of cell divisions and thus assess whether Notch inhibition results in less than expected movement could be a way around this predicament.

Due to the key role of Notch in fate determination, I wanted to ensure that loss of DRs was principally due to loss of proliferation, not hepatocytic differentiation. Using two independent strains I performed lineage tracing experiments in two models of hepatocellular injury. First to more closely replicate the conditions of the *AhCre MDM2*$^{fl/fl}$ model, I gave MCD diet to induce hepatocellular injury in *Krt19CreER*^{T}*;RCL*^{tdT} animals and administered DAPT throughout the injury period. The continuous nature of the injury meant classification of injury into early and late was not practical. In this model there was again a reduction in DRs and their proliferation, however this time I could confirm that loss of cells was not due to differentiation into heptaocytes as *Krt19* lineage labelled hepatocytes appeared only at negligible frequencies in treatment and control groups. Similarly using *OPN-iCreER*^{T2}*;R26R*^{YFP}*;Notch3*$^{+/+}$ and *OPN-iCreER*^{T2}*;R26R*^{YFP}*;Notch3*$^{-/-}$ strains, loss of Notch3 was associated with a diminished ductular response to CDE diet, without the

appearance of frequent OPN lineage labelled hepatocytes. As previous work has suggested significant hepatocytic differentiation of HPCs only occurs after a period of recovery from injury, I also administered DAPT to animals in the recovery phase of the CDE-recovery model. Contrary to seeing an increase in lineage labelled hepatocytes due to Notch inhibition, the number of labelled cells fell markedly. This can best be explained by viewing the proliferation rate of DRs during the recovery period. This remained high and thus if Notch-driven proliferation was prevented, the number of lineage labelled hepatocytes resulting would also decrease. The intimate association of cell division with differentiation where the same signal can govern both processes presents a significant obstacle. Using a system where downstream mediators of Notch driven proliferation could be targeted such as Notch-dependent cyclin genes or AKT signalling may permit direct differentiation related effects of Notch to be further studied, however loss of cell division may prevent differentiation from occurring.

In summary this chapter describes a functional role for Notch signalling that is tied temporally to the stage of regenerative response. Notch1 and Notch3 specifically are responsible for mediating this action.

5 The functional role of Wnt signalling in progenitor mediated hepatocellular regeneration

5.1 Introduction

Canonical Wnt signalling is initiated by binding of soluble Wnt ligand to cell surface Frizzled and low-density lipoprotein receptor-related protein (LRP) 5 or 6 (see Figure 1.4). A key event in the transduction of the Wnt signal inside the cell is the stabilization of cytoplasmic β-catenin. In the absence of ligand binding, beta-catenin is recruited by the destruction complex that includes axin, adenomatous polyposis coli (APC), and glycogen synthase kinase-3b (GSK3b) where it is phosphorylated by casein kinase I and GSK3b which targets it for ubiquitination and proteasomal degradation (238). Binding of Wnts to their receptors results in inhibition of the destruction complex. This permits accumulation of non-phosphorylated beta-catenin in the cytoplasm and its resultant translocation to the nucleus. In the nucleus beta-catenin forms a complex with members of the T-cell factor/lymphoid enhancer-binding factor (TCF/LEF) family of transcriptional factors. This complex recruits transcriptional co-activators including cAMP response element-binding (CREB)-binding protein (CBP) or its homolog p300 as well as other components of the transcription machinery. Together, these events turn TCF/LEF from transcriptional repressor into transcriptional activator, thereby initiating transcription of Wnt target genes (238, 348).

The actions of beta-catenin in liver development are complex, with roles in expansion of hepatoblasts and biliary cells and hepatocyte maturation (253, 333, 349-352). Depending on the time of transgene activation, loss of negative regulator of beta-catenin APC results in failure of expansion of foetal hepatoblasts and constitutively activated beta-catenin causes failure of liver development (350); yet when beta-catenin is deleted, hepatoblasts fail to proliferate, apoptose and fail to differentiate into hepatocytes (254). Inappropriate over activation of beta-catenin can also result in hepatocyte hyperplasia, hyper-proliferation and ultimately animal death (353). Thus during ontogeny there is a requirement for careful temporal regulation with of Wnt signal for effective liver development.

The requirement for Wnt does not end at birth. Recently Wang et al have demonstrated that Wnt-responsive pericentral (zone 3) hepatocytes are responsible for producing new hepatocytes during homeostatic renewal (150). Central vein endothelial cells provide Wnt ligand that maintains pericentral hepatocytes in a state where they express early liver progenitor marker Tbx3, Wnt-responsive gene *Axin2* and are diploid (unlike mature hepatocytes which are mostly polyploid). These cells also express glutamine synthetase (GS), another Wnt-responsive gene that also is used to distinguish zone 3 hepatocytes (354). In terms of roles of Wnt in HPC-mediated regeneration, in rats when a potent HPC response induced by 2-acetylaminofluorine (2AAF) and two-thirds partial hepatectomy (2/3PH), there is a marked increase in active beta-catenin, localising to ductular reactions and occurs when HPCs are proliferating rapidly (262). Murine HPCs have been shown to report Wnt activity after biliary injury (DDC) diet and respond to administration of Wnt3a by proliferating (263) and deletion of beta-catenin diminishes the ductular response to the same dietary injury model (262). An adult HPC line derived from DDC diet fed animals also demonstrated increased proliferation in response to GSK3b inhibitor BIO which mimics activation of canonical Wnt signalling by suppressing GSK3b-mediated phosphorylation and subsequent degradation of beta-catenin (355). Lineage tracing using the Wnt-dependent stem cell marker Lgr5 has also identified expansion of Lgr5 positive periductal cells after liver injury and these cells can be lineage traced into hepatocytes after hepatocellular damage or isolated, expanded then differentiated in media containing Wnt agonist and Lgr5 ligand R-spondin prior to transplantation where they behave as functional hepatocytes in a non-competitive transplantation model (*Fah*$^{-/-}$ mice) (77). Taken together these studies all support Wnt signalling as being of key importance in HPC-mediated regeneration.

Having demonstrated Wnt pathway activity in ductular cells after MDM2-mediated hepatocyte injury, and that this activity appeared to be dynamic, I wanted to confirm if this reflected dynamic functionality of the Wnt pathway. As studies have identified proliferation as a key function of Wnt signalling in liver development and after biliary injury, and the rat 2AAF 2/3PH model has suggested a role in HPC proliferation in response to hepatocellular injury, I focused in this chapter on examining a potential role for Wnt signalling in proliferation of ductular cells after hepatocyte injury.

5.2 Wnt signalling promotes proliferation of HPC lines

Using a similar approach as I had in determining the role of Notch signalling, I again used a MTT assay to determine if there was a dose-response effect to Wnt inhibition in my HPC cell lines. I used increasing doses of the small molecule inhibitor ICG001 (356) which selectively inhibits the CBP/beta-catenin/TCF/LEF interaction and found a dose-dependent loss in viable cell number (Figure 5.1A). To determine if this reduction in cell number was caused by a drop in proliferation rate, rather than cell death, I selected a concentration of ICG001 that from the dose-response curve reduced absorbance in both lines by approximately 50% (5uM) and performed an EdU incorporation assay. After incubation for 48 hours, EdU incorporation in BMOLs was reduced from 48.2% to 11.7% and in SWAs from 47.5% to 9.8% (Figure 5.1B). To confirm this reduction in rate related to Wnt inhibition, I measured expression of classical Wnt effector genes *Lef1* and *cyclin E1 (CCne1)* in cells treated with the same dose of inhibitor and found significant reductions in expression (Figure 5.2).

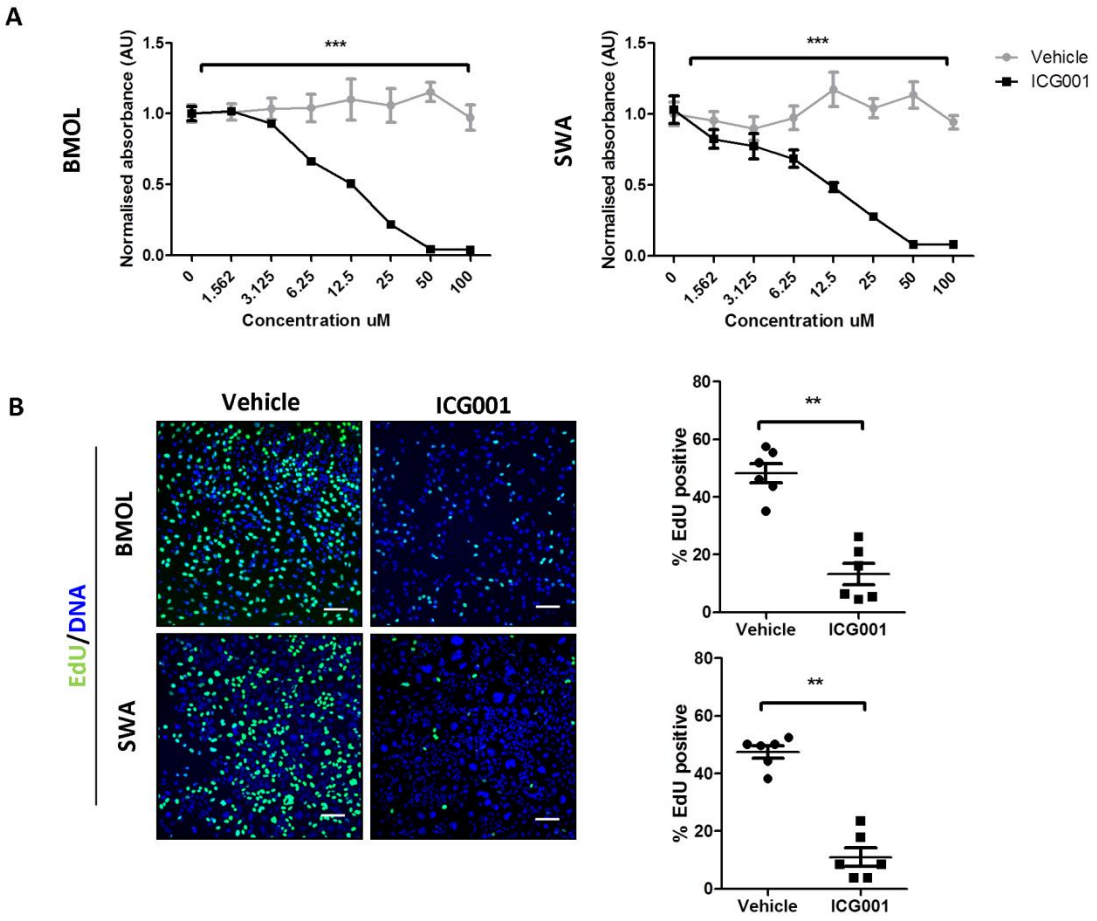

Figure 5.1: Wnt inhibition with small molecule inhibitor ICG001 reduces proliferation of HPC lines: (A) MTT assay using BMOL (left) and SWA (right) lines treated with increasing concentrations of ICG001 or vehicle. Data presented as mean ± SEM of 6 experimental replicates, experiment was repeated twice. **(B)** Representative images and quantification of EdU incorporation in BMOL (upper panel) and SWA (lower panel) lines treated with ICG001 or vehicle (*n*=6 per group). Data are presented as mean ± SEM. ICG001 dose-response experiments were analysed by 2-way ANOVA. Mann Whitney test was used for experiments with two groups. **p<0.01; ***p<0.001. Photomicrograph scale bars: 100uM.

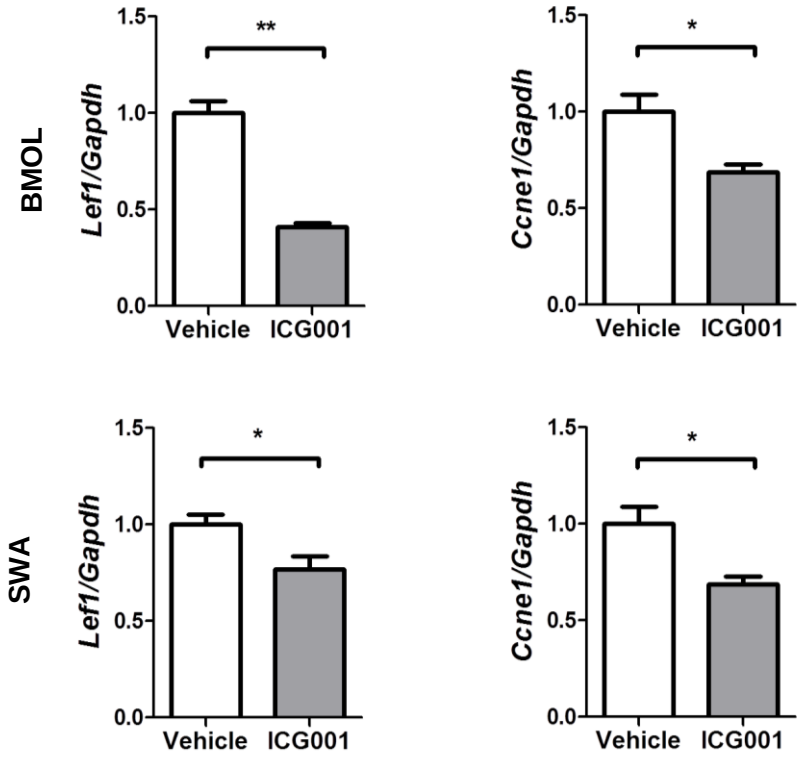

Figure 5.2: Small molecule inhibitor ICG001 reduces expression of Wnt target genes in HPC lines: Gene expression of Wnt target genes *Lef1* (left) and CyclinE1 *(Ccne1)* (right) relative to *Gapdh* in cell lines BMOL (upper panels) and SWA (lower panels) treated with ICG001 compared to vehicle (*n*=6 per group). Data are presented as mean ± SEM. Mann Whitney test was used for experiments with two groups. *p<0.05; **p<0.01.

5.3 Wnt signal controls HPC migration *in vitro*

Functions of Wnt can include migration (357-360). In order to determine if Wnt signalling causes migration of HPCs I performed the same migration assay as described in Chapter 4.3 (and Figure 4.4), blocking proliferation of cells with mitomycin C to exclude the influence of cell expansion upon apparent migration. While Notch inhibition did not influence migration of the HPCs into the centre of the well, exposure to ICG001 impaired migration in both cell lines. This supports the theory that while Notch and Wnt can have similar functions, these functions are highly context-dependent, and temporal regulation of these signals can assist in generating a program of HPC activation, proliferation, migration and hepatocytic differentiation after injury.

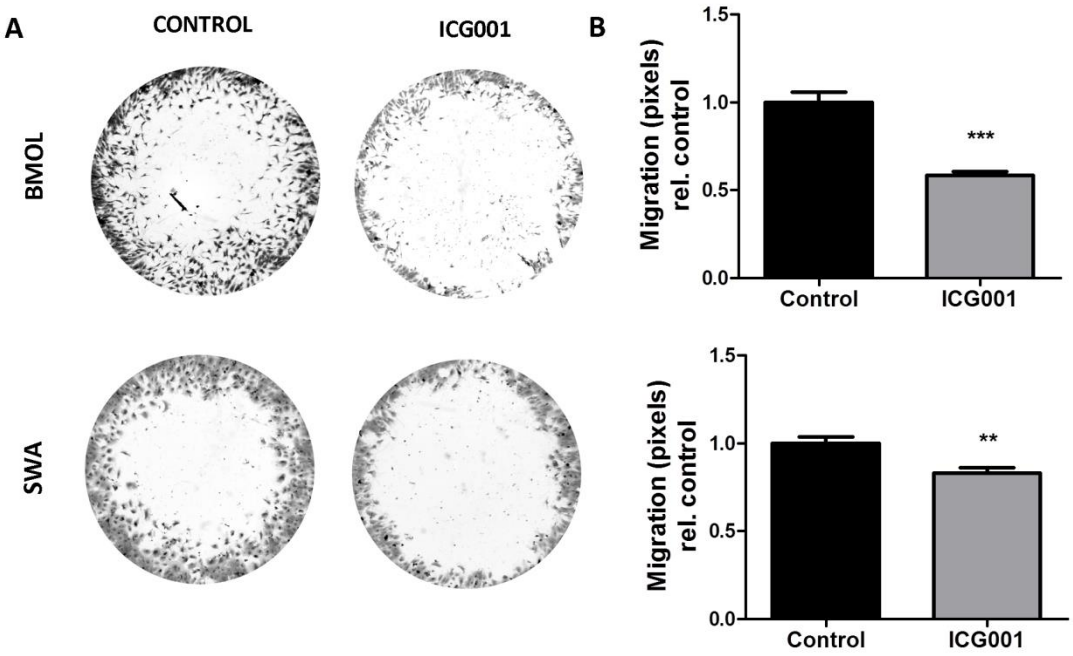

Figure 5.3: Wnt inhibition prevents migration of HPC lines: (A) Representative images of migration assay of BMOLs (upper panel) and SWA (lower panel). Migration of cells towards centre of well was assessed after proliferation had been inhibited with mitomycin C and cells exposed to ICG001 5uM (right) or control media containing an equivalent volume of DMSO (left). **(B)** Quantification of cell migration by pixel analysis normalised to control conditions. *n*=8 per group. Data are presented as mean ± SEM. Statistical analysis by Student's 2-tailed t test. **p<0.01; ***p<0.001.

5.4 Wnt pathway is functionally active during the HPC response *in vivo* and directs HPC proliferation

Having established a functional role for Wnt signalling in the proliferation of HPC lines *in vitro*, I sought to confirm this effect *in vivo*. As I have identified temporal changes in expression of Wnt pathway components and Wnt reporter activity in the *AhCre MDM2*$^{fl/fl}$ strains, I designed experiments to assess the functional relevance of these changes to the expansion of the DR.

Experiments were designed to reflect the apparent time-sensitive nature of Wnt signalling after hepatocellular injury. *AhCre MDM2*$^{fl/fl}$ mice received ICG001 or vehicle by daily i.p.

injection to coincide with falling levels of expression of Wnt effectors and H2B-GFP (days 1-4, 'early'). Further groups received ICG001 or vehicle days 6-9 ('late') when Wnt effector and H2B-GFP expression was rising. I then designed a further experiment using an alternative Wnt inhibitor C59, which prevents palmitoylation and secretion of Wnt ligand by inhibiting porcupine (361), to ensure any observed effect was not inhibitor specific (Figure 5.4). Animals were harvested 24 hours after the final dose.

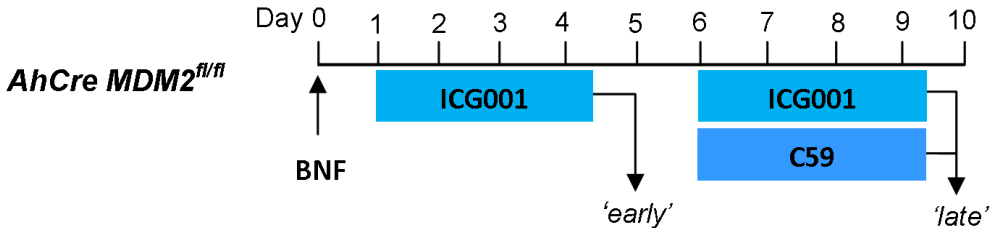

Figure 5.4: Schematic depicting experimental design for Wnt inhibition experiments in *AhCre MDM2$^{fl/fl}$* strain: Wnt inhibitor ICG001 or vehicle was administered days 1-4 ('early') post Cre-induction to coincide with falling levels of expression of Wnt effectors and TCF/LEF:H2B-GFP, and days 6-9 ('late') when Wnt effector expression was rising and TCF/LEF:H2B-GFP expression was high. A second small molecule Wnt inhibitor which prevents secretion of Wnt, the porcupine inhibitor C59 or vehicle was then given to a second group of animals at the 'late' time-point. Animals were harvested 24 hours after the final dose. (*n*=5 per group).

'Early' inhibition of Wnt (Figure 5.5) did not result in any change in ductular cell number. Cell proliferation was also unchanged. Serum ALT levels were similar indicating comparable initiating injury levels.

In contrast 'late' inhibition of Wnt (Figure 5.6) resulted in loss of ductular cells (Figure 5.6B and C). Staining for proliferation marker Ki67 confirmed this loss reflected a reduced proliferation rate (Figure 5.6D). Serum ALT levels remained consistent (Figure 5.6E).

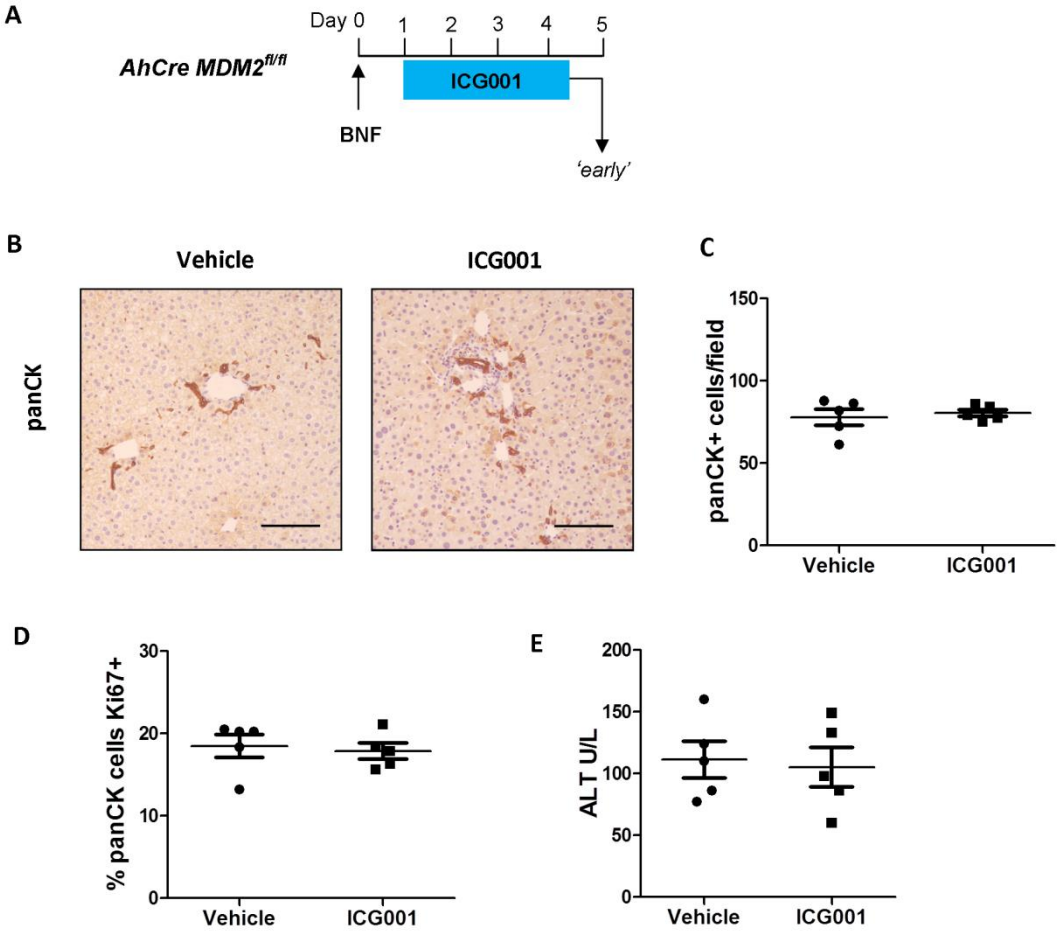

Figure 5.5: Wnt signalling does not drive ductular proliferation early after hepatocellular injury: (A) Schematic demonstrates the strategy for time-dependent treatment with Wnt inhibitor ICG001 or vehicle following MDM2-mediated hepatocyte injury. **(B)** Representative images of panCK staining in ICG001 and vehicle-treated animals. **(C)** Quantification of effect on ductular response of Wnt inhibition in terms of panCK-positive cell number (centre) and **(D)** Ki67 positive proportion (right) (*n*=5 per group) **(E)** Serum ALT values were equivalent. Data are presented as mean ± SEM. Mann Whitney test was used. Photomicrograph scale bar: 100uM.

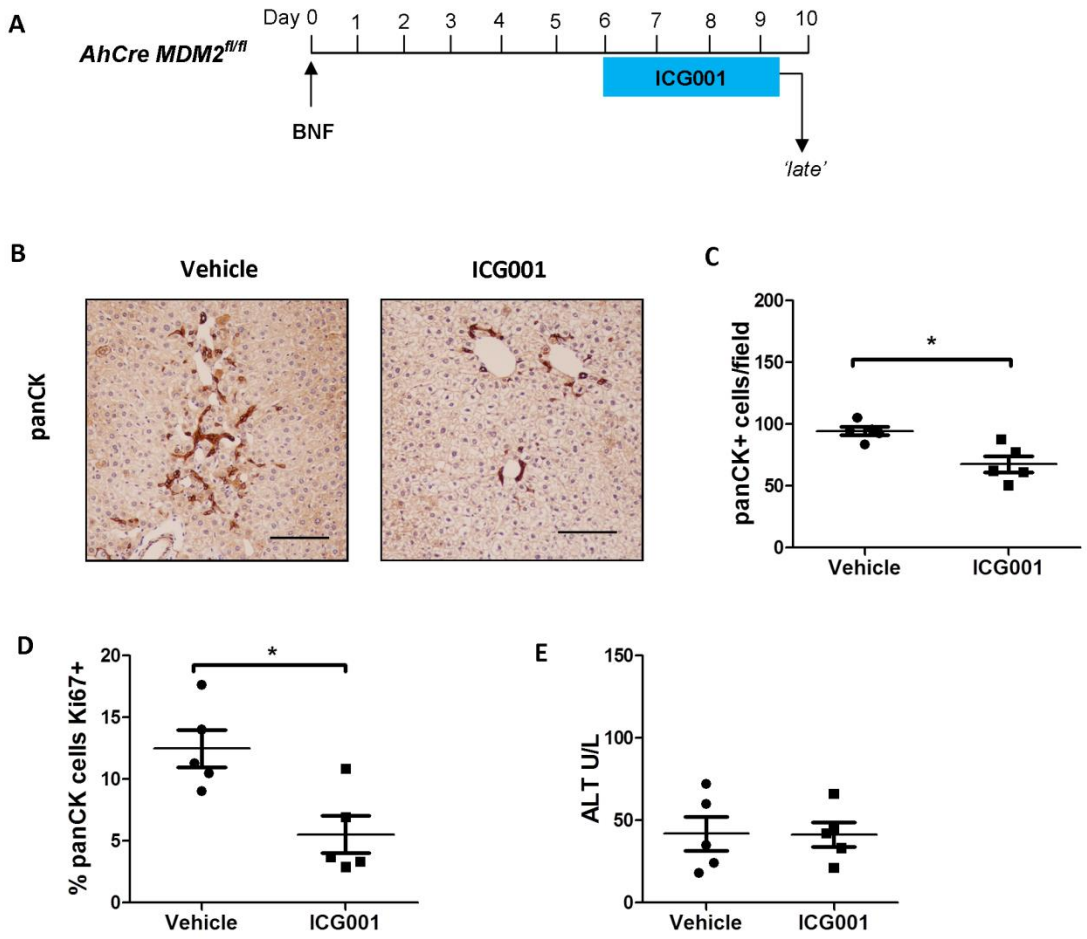

Figure 5.6: Wnt signalling drives ductular proliferation late after hepatocellular injury: (A) Schematic demonstrates the strategy for time-dependent treatment with Wnt inhibitor ICG001 or vehicle following MDM2-mediated hepatocyte injury. **(B)** Representative images of panCK staining in ICG001 and vehicle-treated animals. **(C)** Quantification of effect on ductular response of Wnt inhibition in terms of panCK-positive cell number (centre) and **(D)** Ki67 positive proportion (right) (*n*=5 per group). **(E)** Serum ALT values were equivalent. Data are presented as mean ± SEM. Mann Whitney test was used. *p<0.05. Photomicrograph scale bar: 100uM.

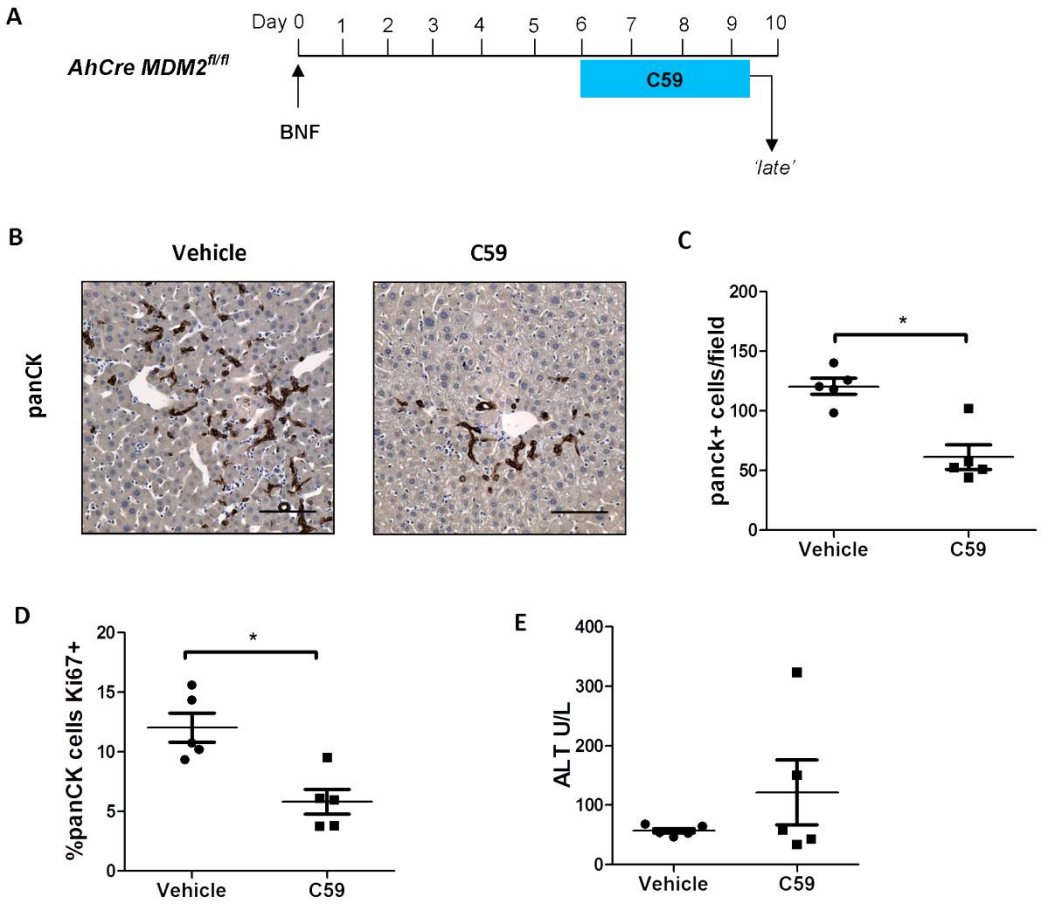

Figure 5.7: Use of a second Wnt inhibitor C59 confirms Wnt signalling drives ductular proliferation late after hepatocellular injury: (A) Schematic demonstrates the strategy for time-dependent treatment with Wnt secretion inhibitor C59 or vehicle following MDM2-mediated hepatocyte injury. **(B)** Representative images of panCK staining in C59 and vehicle-treated animals. **(C)** Quantification of effect on ductular response of Wnt inhibition with C59 in terms of panCK-positive cell number (centre) and **(D)** Ki67 positive proportion (right) (*n*=5 per group) **(E)** Serum ALT values were equivalent. Data are presented as mean ± SEM. Mann Whitney test was used. *p<0.05. Photomicrograph scale bar: 100uM.

When I administered the alternative Wnt inhibitor, C59, there was also a reduction in ductular cells (Figure 5.7A and B). Staining for proliferation marker ki67 confirmed again this was due to a reduced proliferation rate (Figure 5.7D). Serum ALT levels were constant (Figure 5.7E).

Taken together these data suggest that:

1. The *AhCre MDM2$^{fl/fl}$; TCF/LEF:H2B-GFP* strain accurately reports active Wnt signalling and
2. Ductular proliferation in the late but not early phase of the ductular response is Wnt-sensitive.

5.5 Loss of DR is due to loss of proliferation capacity, not change in differentiation capacity when Wnt is inhibited

The experiments inhibiting Wnt in the *AhCre MDM2$^{fl/fl}$* strain support the loss of ductular cells being due to impaired proliferation. However the ductular cells are not lineage traced and so should there be a difference in their differentiation capacity, this would contribute to observed loss of cell number. As Wnt appears important in promoting the hepatocellular differentiation of HPCs (75-78, 123), it would be surprising if differentiation increased after Wnt inhibition. To ensure Wnt inhibition was not causing unexpected effects on differentiation I again employed the *Krt19-CreER^{T};RCL-tdT* and *OPN-iCreER^{T2};R26R^{YFP}* strains to lineage trace ductular cells after hepatocyte injury. Using the two strains I designed experiments to determine the effect of Wnt inhibition on the ability of DRs to generate hepatocytes, and to confirm in another model system the effects of Wnt on ductular proliferation after hepatocellular injury.

Groups of *Krt19-CreER^{T};RCL-tdT* mice received three doses of tamoxifen i.p. at 5-6 weeks old to induce Cre recombination. After a two week washout period to reduce the chance of any residual tamoxifen inappropriately labelling non-ductular cells in response to injury, mice received 2 weeks of MCD diet to induce steatohepatitis and a DR. As the dietary injury models involve continuous exposure to the toxin, ICG001 was administered three doses per week for the duration of the injury diet (Figure 5.8A). I then stained the tissue for the RFP lineage label and quantified the cells. There was a marked reduction in lineage labelled cells (Figure 5.8B and C) and this could not be explained by differences in the level of liver injury as determined by serum ALT levels (Figure 5.8D). The RFP cells all appeared to be of ductular morphology and subsequent co-staining of tissue for RFP with hepatocyte marker HNF4a failed to identify lineage labelled hepatocytes above a negligible frequency (0-1 per section examined) (Figure 5.9B). Having established that the RFP positive cells remained ductular and were not hepatocytes, I wanted to confirm if the loss in cell number was due to loss of proliferation consistent with the *AhCre MDM2$^{fl/fl}$* model. I again used the Operetta high-content analysis system (described in Appendix 1) to quantify the proliferation rate of the RFP-reporter positive cells and confirmed a reduction in proliferation from 32% to 18.7% (Figure 5.9A).

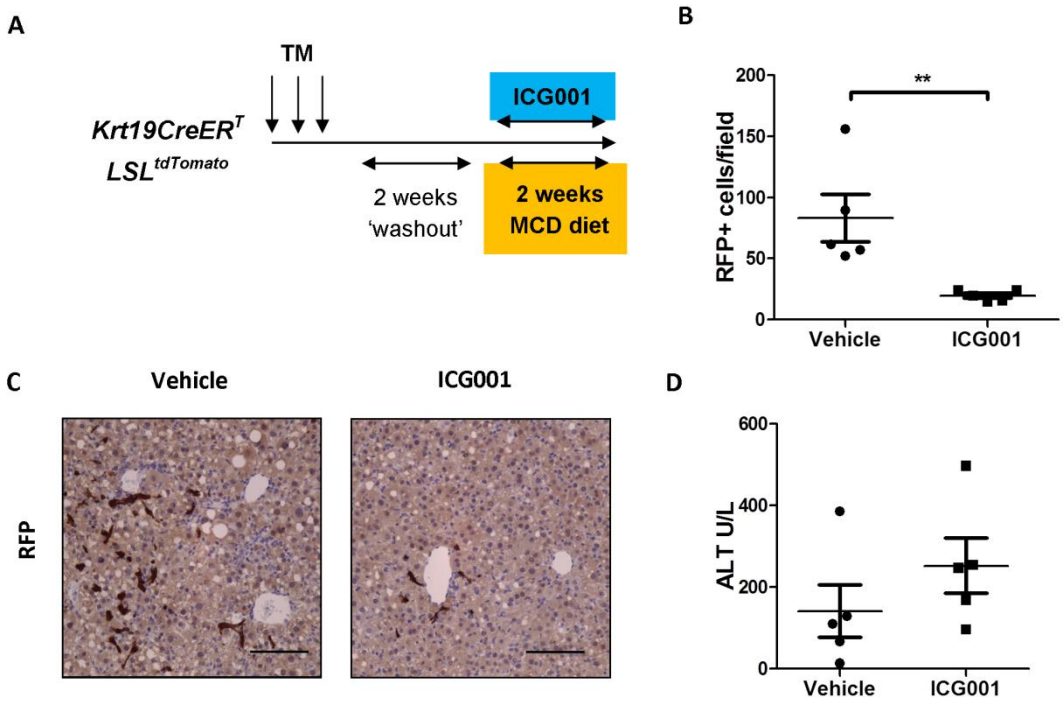

Figure 5.8: Lineage tracing confirms loss of ductular cells after Wnt inhibition in hepatocellular injury: (A) Schematic demonstrating experimental strategy for assessment of the effect on the ductular reaction of Wnt inhibition using *Krt19-CreER^T;RCL-tdT* strain with MCD diet to induce hepatocellular injury. **(B)** Quantification of effect of Wnt inhibition on RFP-positive (lineage labelled) cell number. **(C)** Representative immunohistochemistry for RFP label. **(D)** Serum ALT levels were equivalent. (*n*=5 per group). Data are presented as mean ± SEM. Mann Whitney test was used. **p<0.01. Photomicrograph scale bars: 100uM.

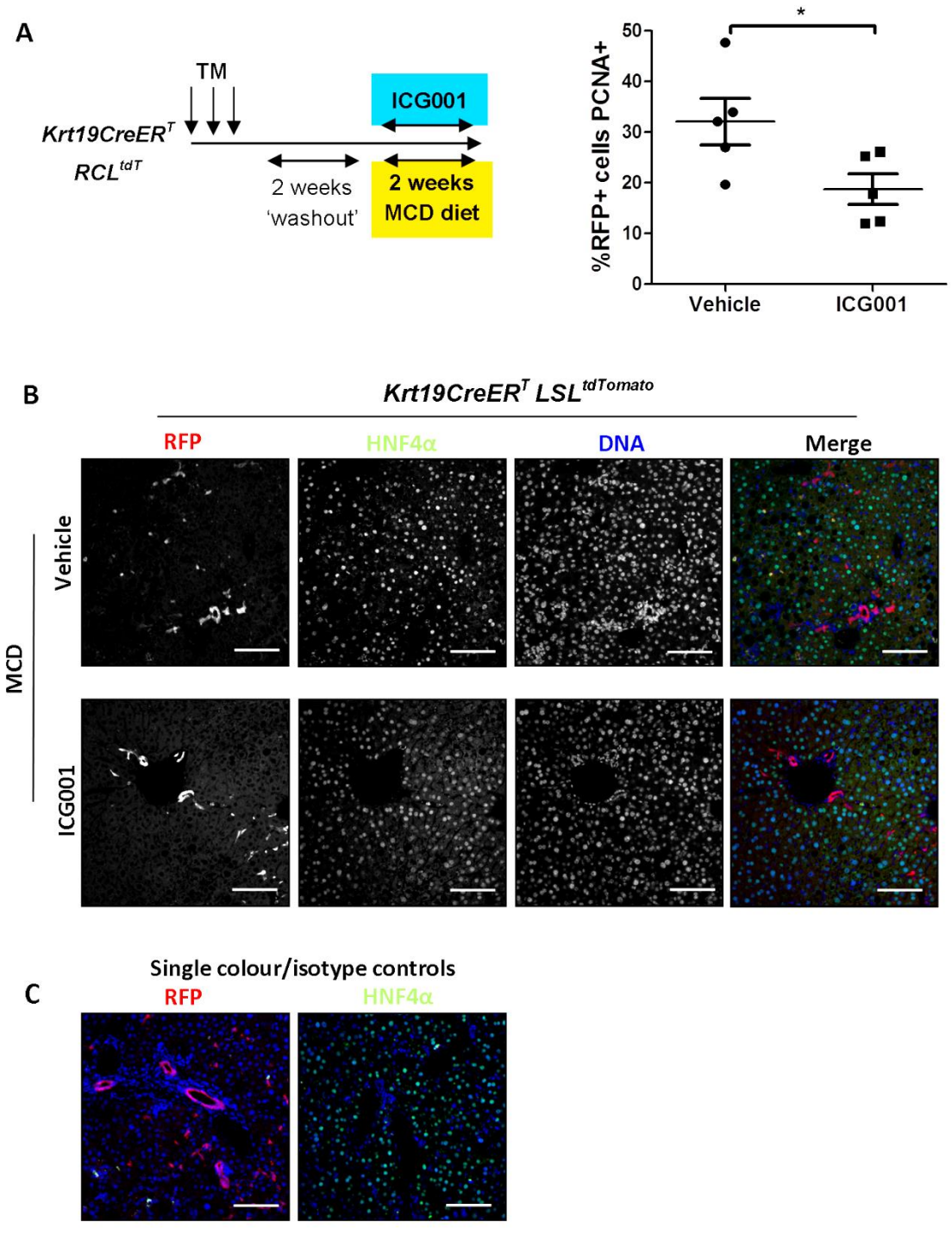
A
TM
Krt19CreER^T
RCL^tdT
2 weeks
'washout'
ICG001
2 weeks
MCD diet
%RFP+ cells PCNA+
50
40
30
20
10
0
*
Vehicle
ICG001
B
Krt19CreER^T LSL^tdTomato
RFP
HNF4α
DNA
Merge
MCD
Vehicle
ICG001
C
Single colour/isotype controls
RFP
HNF4α

Figure 5.9: Lineage tracing confirms loss of ductular cells after Wnt inhibition is due to loss of proliferation: (A) Quantification of effect of Wnt inhibition on PCNA-positive (proliferating) proportion of lineage labelled RFP-positive cells in *Krt19-CreER^{T};RCL-tdT* strain administered ICG001 or vehicle during MCD diet to induce hepatocellular injury (with experimental schematic left). (*n*=5 per group). **(B)** Representative immunohistochemistry for RFP (red) and HNF4a (green) in these animals. Ductular lineage-traced hepatocyte remained at negligible frequency in both groups (0-1 cells per section). **(C)** Single stain/isotype controls. Data are presented as mean ± SEM. Mann Whitney test was used. *p<0.05. Photomicrograph scale bars: 100uM.

Using the *OPN-iCreER^{T2};R26R^{YFP}* strain and the previously established CDE-recovery protocol (56) I designed an experiment where Wnt inhibitor ICG001 was administered during the two week recovery period, to ascertain the effect on hepatocellular differentiation of DRs (Figure 5.10A). As with the Notch inhibitor experiment, this was performed at Universite Catholique de Louvaine in Belgium, to my experimental protocol, pending the rederivation of the strain into our animal unit. I performed all subsequent analysis. From the Notch experiment, I had established that proliferation remained ongoing during the recovery period, therefore the effect of Wnt inhibition during this same period on differentiation capability was difficult to predict. Loss of Wnt may impair differentiation and thus number of labelled hepatocytes, however if DR proliferation was inhibited, the resultant number of differentiated hepatocytes may fall further. As ICG001 specifically blocks CBP/beta-catenin function there may be a net increase in beta-catenin-mediated p300 activation, with potential effects on proliferation and differentiation (see discussion). If Wnt inhibition resulted in reduction in Wnt-dependent production of Notch inhibitor Numb, then Notch-mediated effects on proliferation may be higher and potentially result in increased lineage labelled hepatocytes, as would potentially any imbalance between any other Notch and Wnt-sensitive nodes. Ultimately the mean proportion of labelled hepatocytes did not change significantly, although trending to rise. The variation in number of labelled hepatocytes did increase (range 0.5-2.1% to 0.1-4.2%) (Figure 5.10B and C). This increased variation in outcome may reflect the precise balance of these competing determinants in each animal.

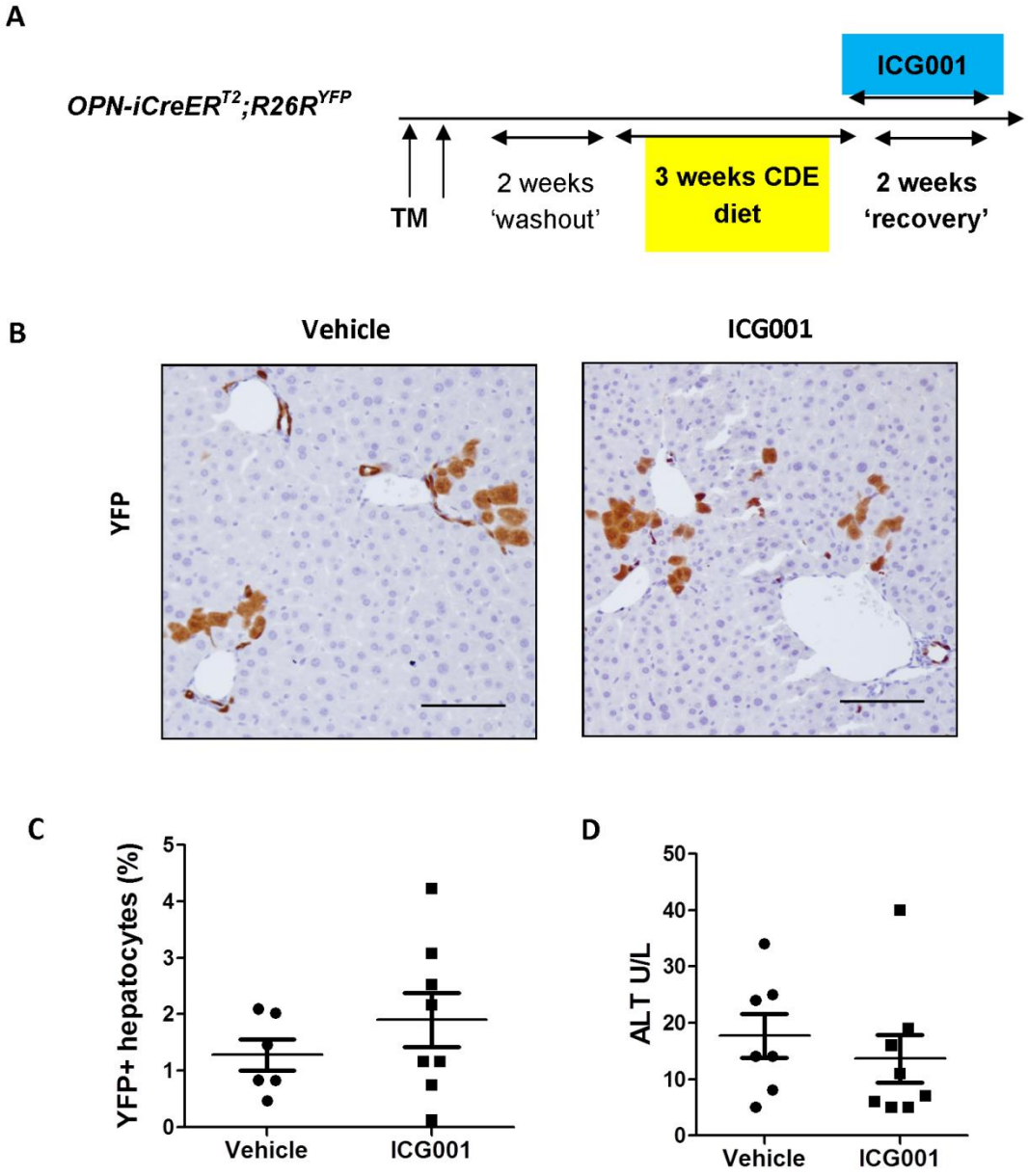

Figure 5.10: Wnt inhibition did not result in a change in lineage-labelled hepatocytes using the CDE-STOP regimen: (A) Schematic of experimental strategy for assessing the effect on generation of biliary lineage-derived hepatocytes of Wnt inhibition with ICG001 using *OPN-iCreER^{T2};R26R^{YFP}* strain. **(B)** Representative images of YFP positive cells generated from the experiment. **(C)** Quantification of resultant YFP-positive hepatocytes after Wnt inhibition and serum ALT levels **(D).** (*n*=6 for vehicle group, *n*=8 for ICG001 group). For proliferation rates of labelled ductular cells during the recovery period see Figure 4.12E. Data are presented as mean ± SEM. Mann Whitney test was used for experiments with two groups. Photomicrograph scale bars: 100uM.

5.6 Discussion

Careful temporal regulation of Wnt signalling is crucial for proper liver development (254, 333, 350, 351). In the adult it remains crucial for maintaining liver zonation and homeostasis (20, 150). In HPCs a role for Wnt in proliferation after biliary injury has been demonstrated (262, 263, 355) and a role for Wnt in expansion after hepatocellular injury is strongly suggested (77, 262), along with a role in hepatocytic differentiation (77, 78, 123, 269). In this chapter I establish a time-sensitive role for Wnt signalling in controlling the proliferation of HPCs in response to hepatocellular injury.

First using HPC lines I demonstrated that their proliferation is Wnt sensitive. By designing experiments to coincide administering Wnt inhibition with the dynamic changes in Wnt expression seen in the *AhCre MDM2*$^{fl/fl}$ model shown in chapter 3, I have confirmed that these changes reflect functionality of the Wnt pathway and control of DR proliferation after hepatocellular injury. When expression of Wnt target effectors and Wnt pathway reporter was low, inhibition had no effect on size or proliferation of the DR. When Wnt target gene expression was rising and ductular cells reported Wnt activity, administration of Wnt inhibitor prevented their proliferation.

Previous work by Hu et al also demonstrated that in response to Wnt3a, HPCs isolated from DDC treated livers would enter cell cycle and luciferase assays confirmed transcriptional activation via TCF/LEF (263). Apte et al studied Wnt in a classic model of potent HPC activation – 2AAF + partial hepatectomy (PH). They demonstrated increased expression of Wnt1 and beta-catenin on day 5 post PH which was lost by day 10 (262). Knockout of beta-catenin within both hepatocytes and biliary cells of mice resulted in a diminished HPC response after DDC diet; however these animals were not subject to a hepatocellular injury regimen. Williams et al also demonstrated increased expression of Wnt1 and beta-catenin in the rat 2AAF/PH model (269). They went on to propose that silencing Wnt1 resulted in failure of HPC differentiation and instead remained as atypical hyperplastic ducts. I have demonstrated that proliferation of HPCs after hepatocellular injury is Wnt-sensitive, and in addition that this sensitivity is temporally regulated. Use of a second Wnt inhibitor, inhibitor of Wnt secretion C59, confirmed this was not an effect specific to ICG001.

Benhamouche determined Wnt signalling antagonist APC maintains appropriate liver zonation, expressed in periportal hepatocytes preventing Wnt signalling, while zone 3

hepatocytes express Wnt target genes including GS. Their work also demonstrates active (dephosphorylated) beta-catenin in ductal cells (20). Wnt-responsive *Axin2* and GS-expressing pericentral hepatocytes have been identified as the cell responsible for homeostatic renewal of the liver, further supporting a critical role for Wnt in liver homeostasis (150). Recently detailed histological analysis of human tissue has described the origin and maturation of 'liver buds' derived from the stem/progenitor pathway in chronic liver disease (51). This study provides further support for the importance of this regenerative mechanism in human disease and of note they describe the first feature distinguishing a ductal cell capable of generating hepatocytes within a liver bud as expression of GS. This would strongly suggest Wnt signalling is involved in this process.

I went on to demonstrate using a lineage tracing approach that loss of DRs after treatment with Wnt inhibitor ICG001 was due to a loss of proliferation capacity. Lineage tracing of DRs using the *Krt19-CreER^{T};RCL-tdT* strain demonstrated a reduction in cell number after Wnt inhibition due to reduced proliferation rate with no unexpected effect on differentiation – lineage labelled hepatocytes remained negligible in treated and control animals.

In order for stem or progenitor cell mediated regeneration to proceed, cells must stop expanding, exit cell cycle, and initiate the process of differentiation. Evidence suggests CBP/beta-catenin-mediated transcription is essential for stem and/or progenitor cell maintenance and proliferation, whereas a switch to p300/beta-catenin mediated transcription is the critical step to initiate differentiation and a decrease in cellular potency (348, 362-364). Conversely p300 has been shown to promote cell cycle progression and prevent apoptosis in malignancy including prostate cancer and multiple myeloma (365, 366). It remains both possible and plausible that the ability of Wnt to promote both proliferation and hepatocytic differentiation of HPCs could be mediated through changes in underlying equilibrium between CBP/beta-catenin and p300/beta-catenin. This could potentially explain why when *OPN-iCreER^{T2};R26R^{YFP}* mice were treated with CBP inhibitor ICG001 during the recovery/differentiation phase of the CDE-STOP protocol, the number of lineage labelled hepatocytes did not fall but instead trended towards an increase, potentially mediated by a relative increase in p300 activity. Alternatively reduction in Wnt-dependent production of Notch inhibitor Numb may result in increased Notch activity, increasing the number of HPCs available to differentiate. The role of p300/beta-catenin

both in HPC proliferation and differentiation would be an interesting area for future research. Use of p300 inhibitors, or more interestingly, should they be developed, p300 agonists during CDE-recovery would be interesting and may specifically promote differentiation, and potentially of use in situations where there is a robust DR but poor or inadequate hepatocyte differentiation.

As Wnt signalling can induce cell migration, and migration into the parenchyma is key feature of HPCs after hepatocellular injury, I examined the effect of Wnt inhibition with CBP inhibitor ICG001. Using the same migration assay as described in Chapter 4.3, proliferation was prevented and then the migration of HPCs into the centre of a well was measured with and without ICG001. Assessing the role for Wnt in migration of HPCs *in vivo* is beset by the same pitfalls as discussed in chapter 4. Notch inhibition *in vitro* did not limit migration, but Wnt inhibition resulted in a failure to migrate. Notch and Wnt signalling can both cause cell migration but the differential actions of the two signalling pathways on HPCs may help explain how their temporal regulation may permit an effective and orderly regenerative response involving HPC activation, proliferation, migration and differentiation.

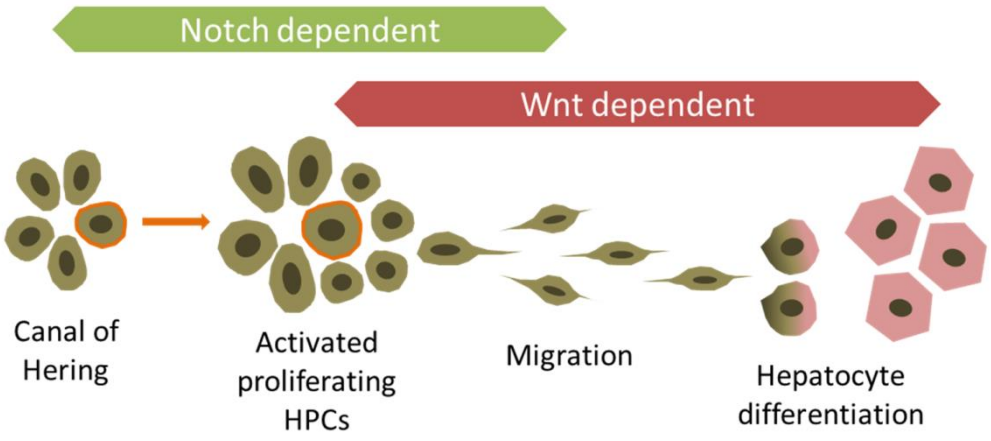

Figure 5.11: Notch and Wnt are required for an effective regenerative response: The early stage of activation and proliferation of the ductular reaction after hepatocellular injury is driven by Notch. For a period the Wnt pathway also becomes active and subsequently takes over control of proliferation and supports migration and differentiation of HPCs.

In summary, after hepatocellular injury there is temporally regulated activity of Notch and Wnt signalling that directs proliferation of HPCs (Figure 5.11). Quiescent bile ducts show evidence of active Notch signalling. They also show evidence of active Wnt signalling, albeit at a lower level than the previously identified Wnt-responsive zone 3 hepatocytes. After hepatocellular injury there is marked expansion followed by migration into the parenchyma of DRs. This is accompanied by an upregulation of Notch pathway mediated by Notch1 and Notch3. This activity directs proliferation of the ductular reaction. The initial burst of Notch activity is followed by a rise in Wnt pathway activity, which appears to direct proliferation and potentially migration in the later part of the ductular response. As these two distinct signalling pathways appear to promote the same function (proliferation) and while one dominates the early and the other the late response, this suggests temporal segregation is a mechanism which prevents antagonistic activity and permits Notch-driven expansion of DRs pending arrival of the post-phagocytic macrophages known to supply Wnt ligand to HPCs (123). Notch/Wnt antagonism via Wnt-dependent Numb provides a mechanism to switch off Notch signalling ready for Wnt driven differentiation. Intriguingly the data presented here suggests Notch and Wnt can act on HPCs at the same time and even in the same cell, suggesting the development of a Notch/Wnt permissive state. This may be facilitated by the relative resistance of Notch3 to Numb-mediated degradation. In addition this suggests these pathways have the potential to be co-operative and agonistic. In the following chapter I sought to identify a node for their cooperation.

6 IGF1 axis: a Notch/Wnt-dependent node that controls HPC proliferation

6.1 Introduction

In the gut homeostasis requires both Wnt and Notch signal (41, 242, 270). Notch drives proliferation within the developing intestine and this requires an intact Wnt signalling cascade, making the cells 'competent' to respond to the Notch-dependent mitogenic stimulus (271). In muscle both Notch and Wnt signal are required for effective regeneration after injury from myogenic progenitors with a crucial switch from Notch driven proliferation to Wnt driven differentiation with crosstalk occurring via GSK3β. Having established that both Notch and Wnt have roles in the proliferation of HPCs after hepatocellular injury, I wanted to try and identify if there was a node representing cooperation between the two signalling pathways.

Growth hormone (GH) mediates its effects on growth and development both directly through the activation of GH receptors or indirectly by inducing production of insulin-like growth factor 1 (IGF1) principally by the liver (290-292). The effects of IGF1 can be modulated by IGF binding proteins (IGFBPs) which can regulate its biological actions by transporting IGF1 from the circulation to the tissue, maintain a reservoir of IGF1 in the circulation which can then potentiate or inhibit IGF1 action (293). IGF1 can be produced by many cell types and acts in a paracrine fashion in most tissues (294). Most actions of IGF1 are mediated through the type 1 IGF receptor (IGF1R), a transmembrane tyrosine kinase related to the insulin receptor (IR). Ligand binding causes activation of tyrosine kinase activity and autophosphorylation of the receptor. The phosphorylated receptor can bind several receptor substrates including the insulin receptor substrates (IRS) initiating phosphorylation cascades that transmit the IGF1R signal (see Figure 1.5) (294). This can cause activation of phosphatidylinositol 3-kinase (PI-3K) leading to activation of p70 S6K kinase which phosphorylates the S6 ribosomal protein and increases the ribosomal pool necessary for entry into the cell cycle, and protein kinase B (Akt) (367). Akt phosphorylation enhances pro-proliferative protein synthesis through mTOR activation (368, 369). In addition to the effects on PI3K, transduction of the IGF1R signal results in recruitment of Ras and activation of the Raf-1/MEK/ERK pathway and downstream factors resulting in

induction of cellular proliferation (296, 297). In muscle, where a role for both Notch and Wnt in regeneration has been described, IGF1 is also of key importance in muscle growth, proliferation and differentiation of satellite cells (muscle progenitor cells) (298). Given the powerful proliferative effects of IGF1/IGF1R signalling and that the dominant source of IGF1 is the liver, I was interested in exploring further the relationship between HPC proliferation and this axis.

IGF1 is principally produced by mature hepatocytes (302, 370) however production has been identified in ductular cells after biliary injury (295). The IGF1-receptor (IGF1R) has been identified on ductular cells and been shown to be important in the development of DRs (295, 371). Administration or viral-induced expression of IGF1 in rats with carbon tetrachloride-induced cirrhosis (hepatocellular injury not associated with DRs) improved liver function and reduced fibrosis (372-374). Subsequently targeted overexpression of IGF1 by activated hepatic stellate cells or hepatocytes attenuated fibrogenesis and accelerated liver regeneration through effects on MMPs, HGF and TGFb (375, 376). Overexpression of IGF1 in hepatocytes of rats with TAA-induced cirrhosis (a model involving toxic damage to hepatocytes and typically DRs and a fibrotic response), resulted in reduction in fibrosis and improved liver biochemistry (376). Interestingly however when IGF1 was overexpressed in a model of chronic biliary injury, ductular proliferation and fibrosis increased (371). The first small scale clinical trial using short-term administration of recombinant IGF-1 in cirrhosis showed an improvement in a marker of liver function, albumin (307).

Several studies have demonstrated interactions between the IGF1 axis and Notch or Wnt signalling. The IGF1R is directly induced by Notch1 signalling under hypoxic conditions in adenocarcinoma of the lung, leading to activation of pro-survival Akt (299). Similarly in human T acute lymphoblastic leukaemia (T-ALL) initiating cells, IGF1R is a Notch1 target (300) and further promotes the mitogenic effects of IGF1 signalling through Hes induced inhibition of PTEN and thus enhanced PI3K/Akt/mTOR action. The relationship between Wnt signalling and the IGF1 axis is complex, but suggests a close connection and a positive feedback loop between Wnt/beta-catenin and IGF1 signalling (377). Wnt signalling can induce phosphorylation of IGF1 signalling mediators including Akt and ERK in an IGF1R-dependent manner (301). IGF1 can stimulate TCF/LEF dependent transcription via activation of PI-3K and inhibition of negative regulator GSK3b and increasing cytoplasmic

levels of beta-catenin (303). In addition IGF1 can regulate the stability and transcriptional activity of beta-catenin (302). In some contexts Wnt signalling can induce expression of IGF1 (378), and IRS1, a principal intracellular mediator of IGF signalling (379). Thus I sought to determine if the IGF1 axis might represent a Notch/Wnt-sensitive node that drives proliferation of DRs, and see if this might explain the apparently contradictory results from liver based IGF studies.

6.2 The IGF1 axis is active in HPC lines and Wnt/Notch responsive

There are previous reports of expression of IGF1 and the IGF1 receptor (IGF1R) in ductular cells (295, 371). I began by staining my HPC lines for components of the IGF1 axis – IGF1, IGF1R and a third antibody raised against IGF1R phosphorylated at tyrosine 1161 (IGR1R pY1161). Following auto-phosphorylation, the tyrosine kinase function increases to a more active form. Both BMOL and SWA HPC lines stained positive for IGF1, IGF1R (the beta-subunit of the receptor) and IGF1R pY1161 (Figure 6.1).

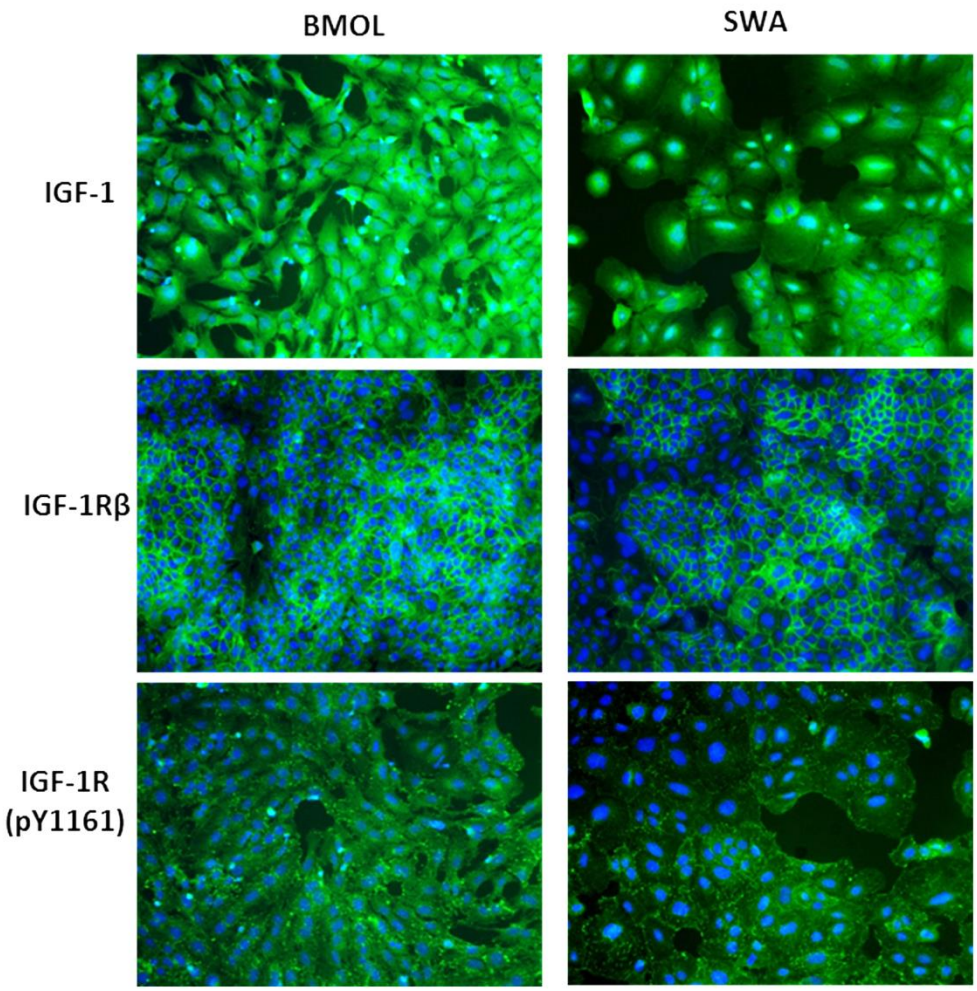

Figure 6.1: The IGF1 axis is expressed in HPC lines: Immunocytochemistry for IGF1 ligand (top), the beta-subunit of the IGF1 receptor (middle) and phosphorylated (more active) IGF1 receptor in HPC lines BMOL (left) and SWA (right).

I next wanted to determine if growth of the HPC lines was sensitive to IGF1 signalling. From the family of synthetic protein tyrosine kinase inhibitors known as tyrphostins, I chose a small molecule inhibitor AG1024 that is selective to IGF1R over other members of the insulin receptor family (380). Using a MTT assay, I performed a dose-response experiment with both HPC lines and found a clear drop in cell viability (Figure 6.2A), confirming these cells were sensitive to manipulation of the IGF1 axis. Next I added increasing doses of

recombinant murine IGF1 (rIGF1) to the media to see if this increased cell number (Figure 6.2B). There was no change in viable cell number. As the growth media contains serum, I wondered if this might be providing sufficient IGF1 to saturate the system, however when I repeated the experiment in serum free conditions, while there was a marked fall in growth rate, addition of IGF1 did not rescue this. Given my cell lines stained positive for IGF1 (Figure 6.1), I wondered if they might produce enough IGF1 ligand to drive their own growth through this pathway. I cultured cell lines for 48 hours in their usual growth media and collected the conditioned media, then the cells. I performed an ELISA test to quantify the secreted IGF1 and compared it to serum containing growth media. In both cases conditioned media contained far higher concentrations of IGF1 than the regular media (Figure 6.2C). In order to compare the production of IGF1 between cell lines, I lysed the collected cells and quantified total cellular protein using a Bradford protein assay as a proxy for cell number and normalised the secreted IGF1 level to this and found both lines produced very similar levels of IGF1 (Figure 6.2D). Production of IGF1 and IGF1R by HPCs suggests that they may utilise this axis to drive their own proliferation.

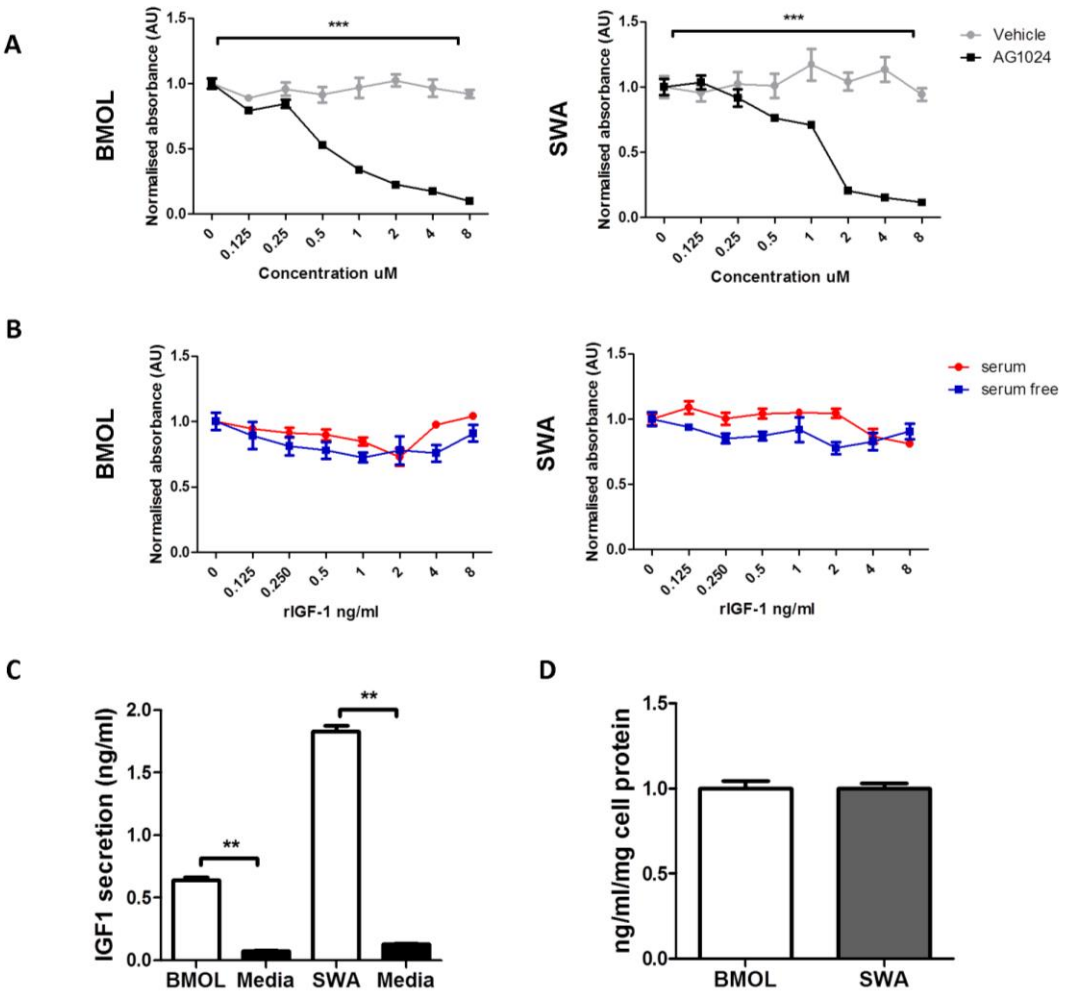

Figure 6.2: HPC lines are sensitive to manipulation of the IGF1 axis: (A) MTT assay using BMOL (left) and SWA (right) cell lines treated with increasing concentrations of small molecule IGF1-receptor (IGF1R) inhibitor AG1024 or vehicle. **(B)** MTT assay using BMOL (left) and SWA (right) treated with increasing combinations of recombinant murine IGF1 (rIGF1) in ordinary growth media (red) and serum free (blue) media, normalised to lowest concentration. **(C)** Absolute quantification of secreted IGF1 from BMOL and SWA cells compared to growth media ($p<0.0001$). **(D)** Secreted IGF1 concentration normalised to total cell protein as a surrogate for cell number ($n=6$ per group). Data are presented as mean ± SEM. Dose-response experiments were analysed by 2-way ANOVA. Kruskal-Wallis test was used for comparison of multiple groups (p value shown in legend above) with Dunn's multiple comparison post-test analysis included in the figure; Mann Whitney test was used for experiments with two groups. **p<0.01; ***p<0.001.

In order to determine if Wnt signalling might be driving IGF1 production in HPCs, I treated cells with ICG001 or vehicle for 48 hours, collected the conditioned media and then the cells. Gene expression of *Igf1* was reduced in treated cells (Figure 6.3A). Using ELISA, I established the concentration of IGF1 in the conditioned media and confirmed a marked reduction in IGF1 secretion (Figure 6.3B). In order to determine if this Wnt mediated effect was specific to IGF1, I quantified gene expression of *Igf1R* in the same samples and found no effect (Figure 6.3C).

To identify if Notch signalling might be driving IGF1R expression in HPCs, I treated cells with DAPT or vehicle for 48 hours and collected the cells. Gene expression of *Igf1R* was reduced in treated cells (Figure 6.4A). Protein expression was determined using western blotting. Using cell lysates from the experiment I performed, Ben Dwyer (a post-doc in the lab) performed the blot and I analysed the results. Expression of IGF1R was reduced in BMOL cells treated with Notch inhibitor DAPT (Figure 6.4B). There was no reduction in detectable IGF1R pY1161 in SWA cells (Figure 6.4C). The range of densitometry was 24.3-52.4 for SWA and 53.7-63.07 for BMOLs, and discrepancy remained even after correction for protein loading (beta-actin). This difference in expression and detection may reflect a difference in auto-phosphorylation in this cell line. Repeating the blot with a less specific antibody may help resolve this. Again I confirmed the effect of Notch on IGF1R expression was specific by quantifying gene expression of *Igf1* in the same samples and found no change in either cell line (Figure 6.4D).

I have established that Notch and Wnt both drive proliferation of HPC lines. Notch-driven production of IGF1 receptor in the BMOL line and Wnt-driven production of IGF1 ligand in both cell lines sets up a node for cooperation between signalling systems and the capacity for HPCs to drive their own proliferation.

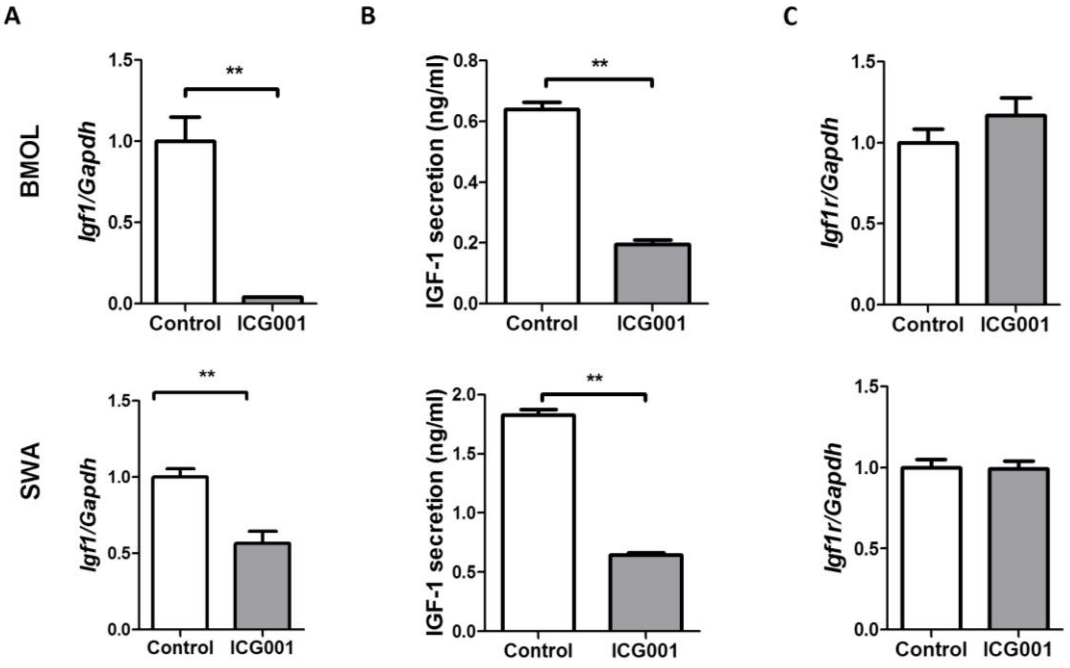

Figure 6.3: Wnt inhibition reduces expression of IGF1 but not IGF1 receptor in HPC lines: (A) Gene expression of *Igf1* relative to *Gapdh* in BMOL (upper panel) and SWA (lower panel) cell lines treated with ICG001. **(B)** Quantification of absolute levels of IGF1 protein secretion per ml of media from BMOL (upper panel) and SWA (lower panel) cell lines treated with ICG001 (*n*=6 per group). **(C)** Gene expression of *Igf1-receptor* relative to *Gapdh* in BMOL (upper panel) and SWA (lower panel) cell lines treated with with ICG001 (right). *n*=6 per group. Data are presented as mean ± SEM. Mann Whitney test was used for experiments with two groups. **p<0.01.

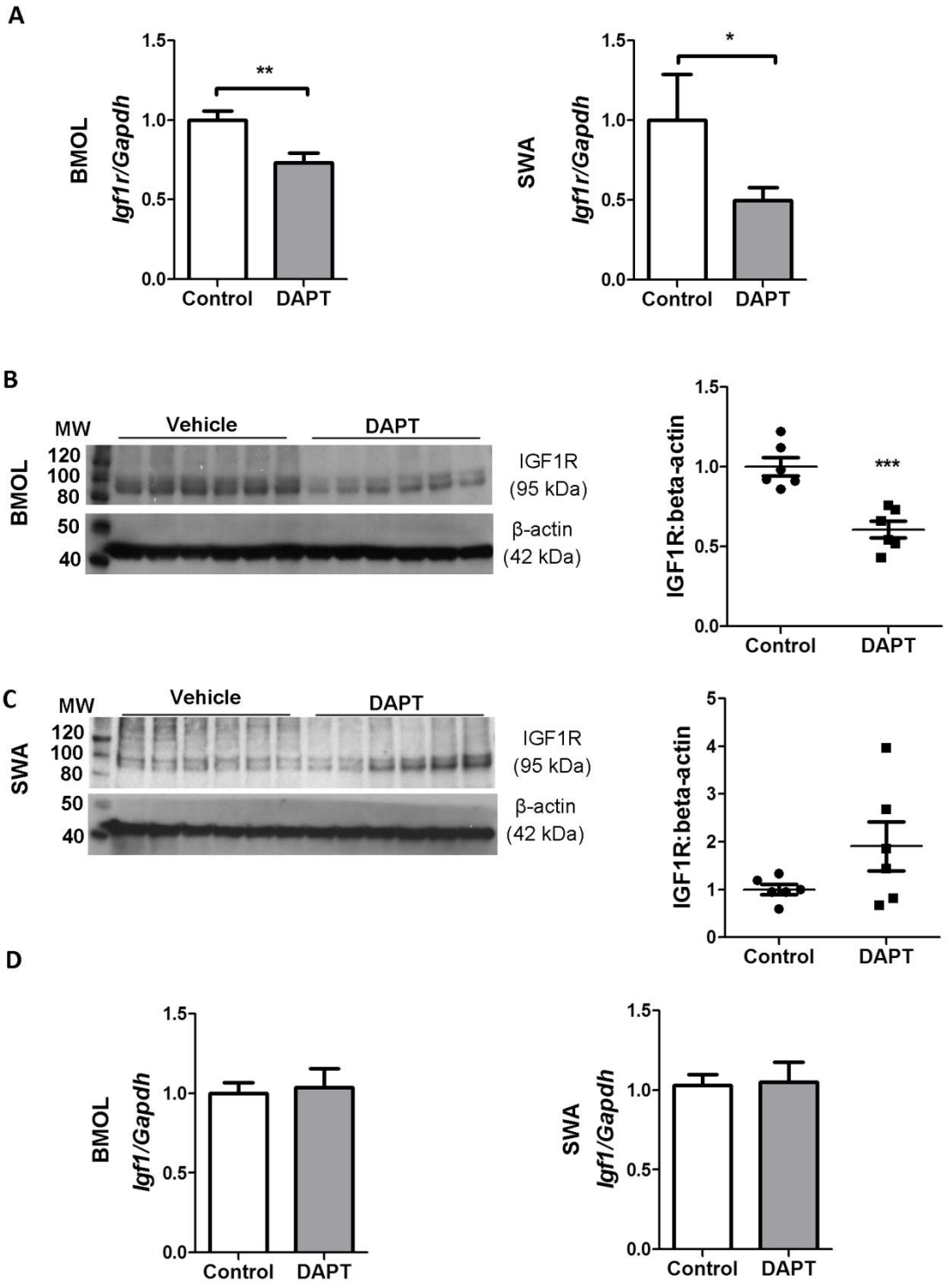
A
BMOL
Igf1r/Gapdh
1.5
1.0
0.5
0.0
**
Control
DAPT
SWA
Igf1r/Gapdh
*
B
MW
Vehicle
DAPT
BMOL
120
100
80
50
40
IGF1R
(95 kDa)
β-actin
(42 kDa)
IGF1R:beta-actin
***
C
SWA
D
Igf1/Gapdh

Figure 6.4: Notch inhibition reduces expression of IGF1 receptor but not IGF1: (A) Gene expression of *Igf1-receptor* relative to *Gapdh* in BMOL (left) and SWA (right) cell lines treated with DAPT. **(B)** Expression of IGF1 receptor phosphorylated at tyrosine position 1161 (IGF1R pY1161) in BMOL cells treated with DAPT or vehicle by western blot (left) and quantification of densitometry normalised to beta actin expression (right). **(C)** Expression of IGF1 receptor phosphorylated at tyrosine position 1161 (IGF1R pY1161) in SWA cells treated with DAPT or vehicle by western blot (left) and quantification of densitometry normalised to beta actin expression (right). **(D)** Gene expression of *Igf1* relative to *Gapdh* in BMOL (left) and SWA (right) cell lines treated with DAPT. *n*=6 per group. Data are presented as mean ± SEM. Mann Whitney test was used for experiments with two groups. *p<0.05; **p<0.01.

6.3 The IGF axis is present in DRs and is Notch/Wnt responsive

IGF1 production within ducts has previously been reported (295) and I wanted to confirm this remained the case in the *AhCre MDM2*$^{fl/fl}$ model. By performing immunohistochemistry for IGF1 I was able to localise its expression with ductular marker CK19 (Figure 6.5A). When I analysed gene expression of *Igf1* over the *AhCre MDM2*$^{fl/fl}$ model time-course, the expression profile followed the expression dynamics of the Wnt expression 'signature', suggesting that *in vivo* IGF1 expression may also be under the control of Wnt signalling (Figure 6.5B).

The DRs in the *AhCre MDM2*$^{fl/fl}$ model stained positive for IGF1R (Figure 6.6A). The receptor was also detected in blood vessels. Gene analysis over the time-course revealed the expression profile of *Igf1R* mirrored that of the Notch expression 'signature', again suggesting its expression may be under control of Notch (Figure 6.6B).

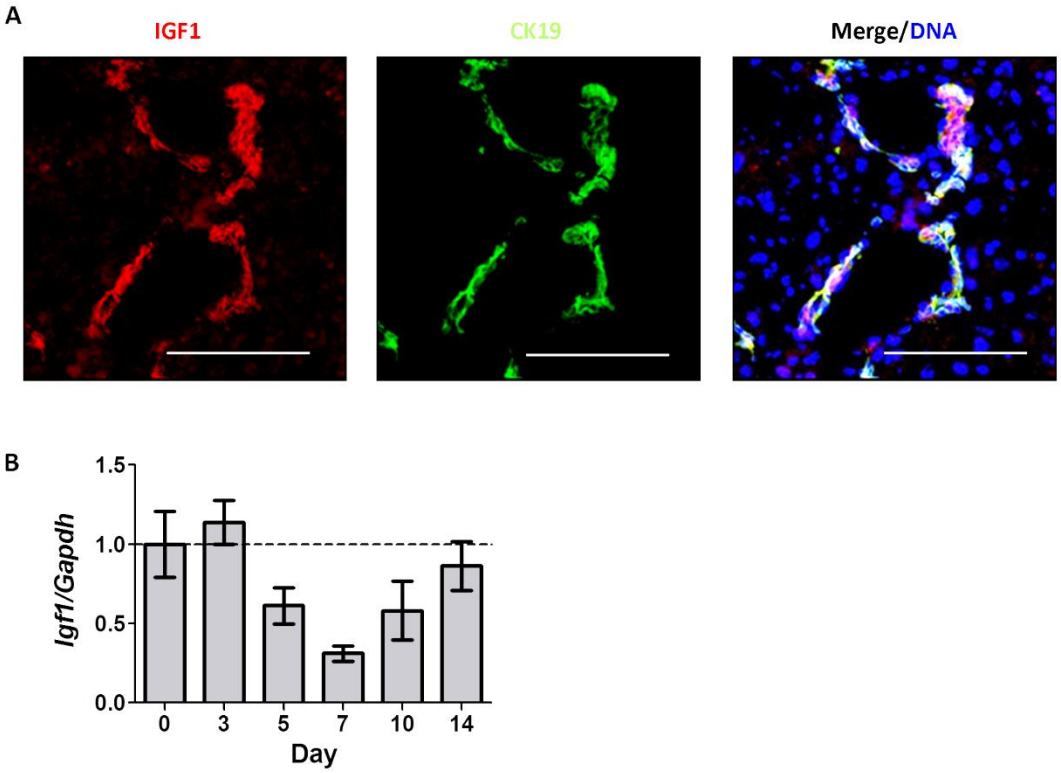

Figure 6.5: Ductular cells express IGF1 and the expression profile after hepatocellular injury follows the Wnt 'signature': (A) Immunohistochemistry for Igf1 (red) and CK19 (green) in *AhCre MDM2*$^{fl/fl}$ model. **(B)** Gene expression of *Igf1* following Cre induction relative to *Gapdh* normalised to day 0 levels in *AhCre MDM2*$^{fl/fl}$ model (*n*=5-8 per time point). Data are presented as mean ± SEM. Photomicrograph scale bars: 100uM.

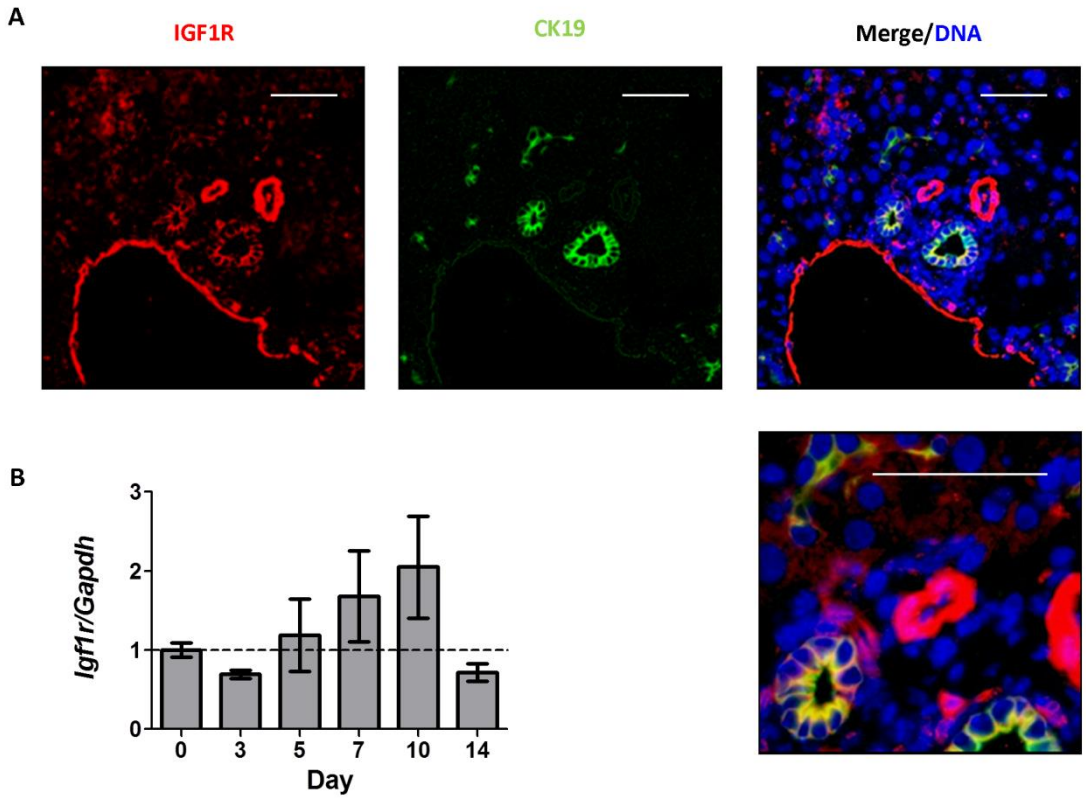

Figure 6.6: Ductular cells express IGF1 receptor and the expression profile after hepatocellular injury follows the Notch 'signature': (A) Immunohistochemistry for phosphorylated Igf1 receptor (Igf1RpY1161) (red), CK19 (green) in day 7 of *AhCre MDM2*$^{fl/fl}$ model**. (B)** Gene expression of *Igf1-receptor* following Cre induction relative to *Gapdh* normalised to day 0 levels in *AhCre MDM2*$^{fl/fl}$ model (*n*=5-8 per time point). Data are presented as mean ± SEM. Photomicrograph scale bars: 50uM.

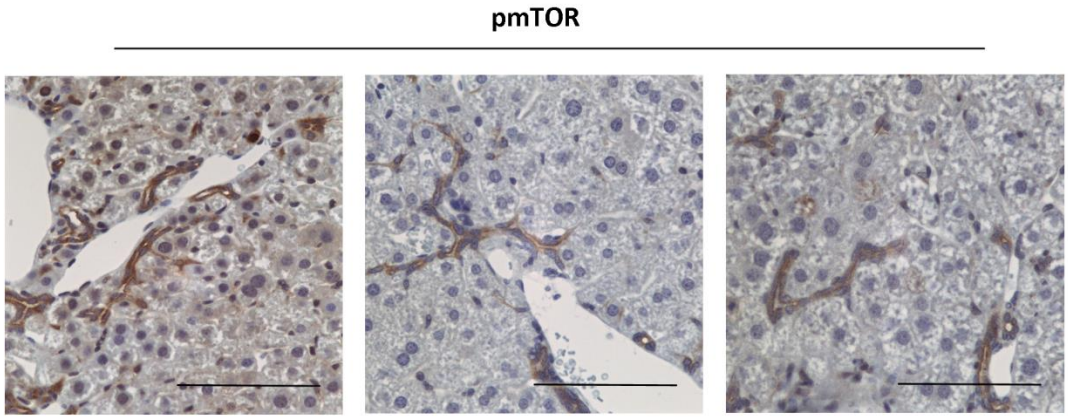

Figure 6.7: mTOR signalling is active in the ductular reaction after hepatocellular injury: Representative photomicrographs of phospho-mTOR staining of day 7 (left panel) and day 10 (centre and right panel) *AhCre MDM2*$^{fl/fl}$ model. Photomicrograph scale bars: 100uM.

Downstream of IGF1 and its receptor are PI3K/Akt/mTOR activation (294, 367). In order to confirm downstream pro-proliferative mediators were present within the DRs of the *AhCre MDM2*$^{fl/fl}$ model I performed immunohistochemistry for phosphorylated (active) mTOR (Figure 6.7). The staining localised to the DRs.

To determine if IGF1 an IGF1R remained sensitive to Notch and Wnt signal *in vivo* and that this effect remained specific, I treated mice with Notch inhibitor DAPT and Wnt inhibitor ICG001 and analysed expression of *Igf1* and *Igf1R*. Consistent with findings in the HPC lines, Wnt inhibition reduced expression of *Igf1* but not *Igf1R* and Notch inhibition reduced expression of the receptor *Igf1R* but not the ligand *Igf1*.

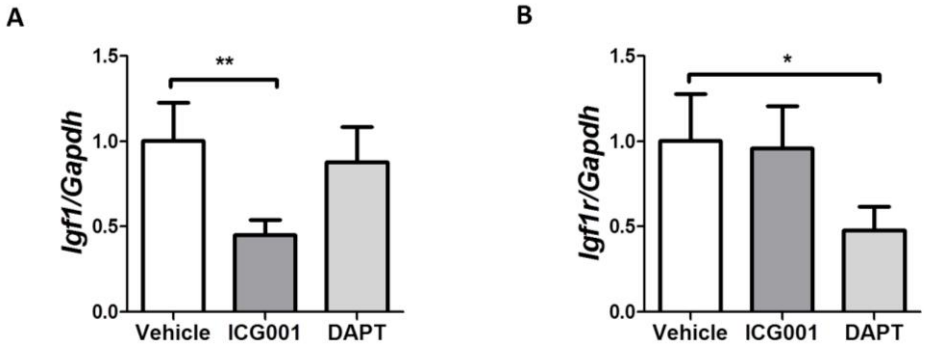

Figure 6.8: Expression of Igf1 and IGF1 receptor is Notch/Wnt responsive *in vivo*: (A) Gene expression of *Igf1* relative to *Gapdh* in animals treated with ICG001 and DAPT (p=0.0128) demonstrates sensitivity of expression of *Igf1* to Wnt but not Notch inhibition. **(B)** Gene expression of *Igf1-receptor* relative to *Gapdh* in animals treated with ICG001 and DAPT demonstrates sensitivity of *Igf1R* to Notch inhibition but not Wnt inhibition (p=0.0068). (*n*=5 per group). Data are presented as mean ± SEM. Kruskal-Wallis test was used for comparison of multiple groups (p value shown in legend above) with Dunn's multiple comparison post-test analysis included in the figure. *p<0.05; **p<0.01.

Having established that a Notch/Wnt responsive IGF1 axis is expressed in DRs after hepatocellular injury, I wanted to confirm if it was functionally active in driving DR proliferation. Using the *AhCre MDM2*$^{fl/fl}$ model, I designed an experiment where specific IGF1R inhibitor AG1024 was administered by i.p. injection daily for days 6-9 (Figure 6.9A). Mice were harvested 24 hours after the final dose. There was a marked reduction in size of DRs (Figure 6.9B and C). Analysis of proliferation rate confirmed this loss was due to failure of proliferation (Figure 6.9D). Level of initial injury as inferred from serum ALT levels remaining constant between groups (Figure 6.9E).

Further importance of this axis in driving the DR was demonstrated through a second experiment where the experimental protocol was repeated but instead of inhibition at the point of IGF1R, the mTOR inhibitor rapamycin was administered (Figure 6.10A). As mTOR does not mediate proliferation solely due to IGF1/IGF1R signalling, rapamycin could potentially reduce proliferation of hepatocytes. As the size of the DR in this model relates

to the degree of failure of hepatocyte replication, mTOR inhibition could potentially increase the stimulus for the DR. Administration of rapamycin in the *AhCre MDM2*$^{fl/fl}$ model resulted in a reduced DR in terms of both cell number and proliferation therefore any increased stimulus relating to an effect on hepatocytes was insufficient to overcome the importance of mTOR activity in DR proliferation (Figure 6.10B-D).

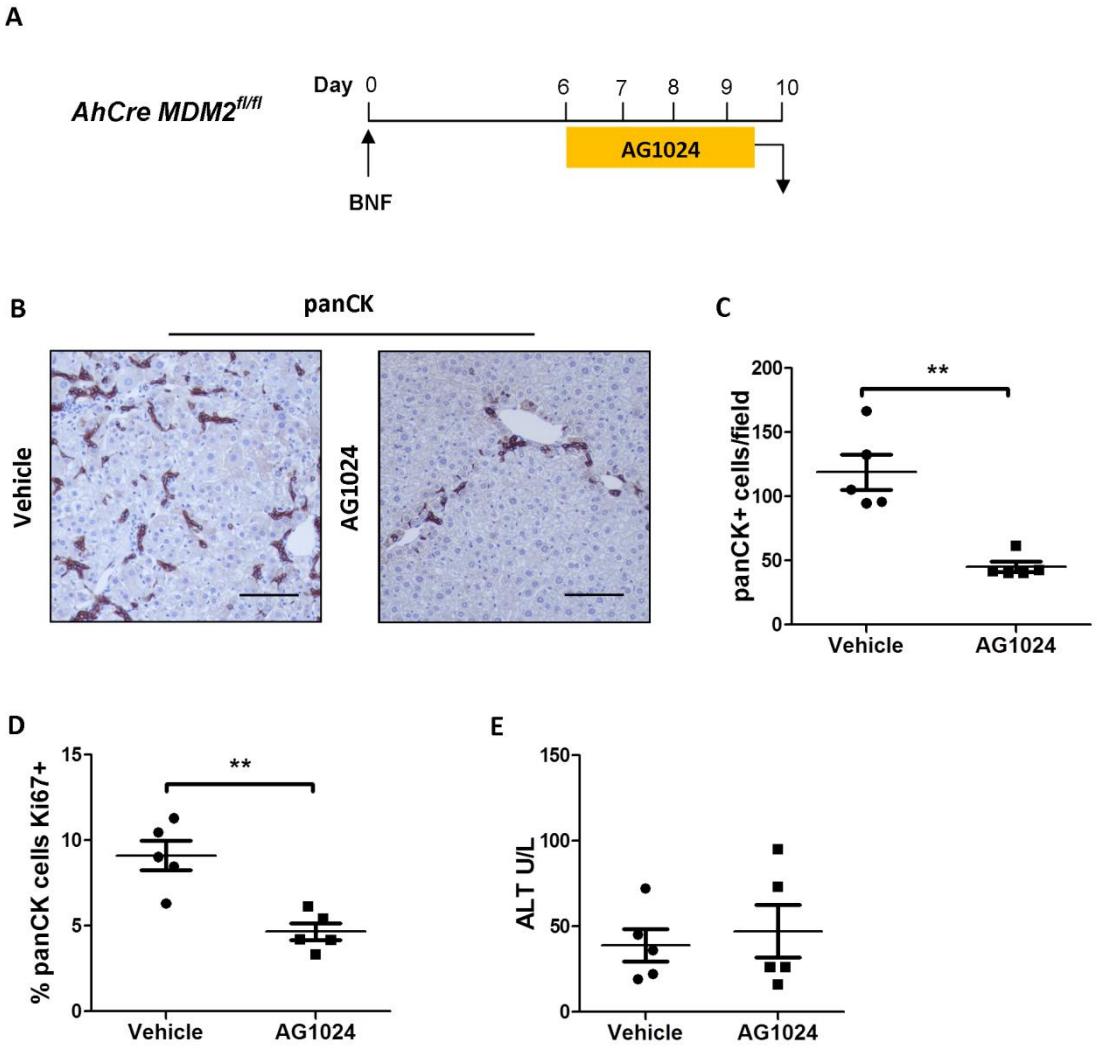

Figure 6.9: The IGF1 axis drives ductular expansion after hepatocellular injury: (A) Schematic (left) demonstrates the experimental design for treatment with Igf1-receptor inhibitor AG1024 or vehicle following MDM2-mediated hepatocyte injury. **(B)** Representative images of panCK staining. **(C)** Quantification of effect on ductular response in terms of panCK-positive cell number and **(D)** Ki67 positive proportion. **(E)** Serum ALT values. (*n*=5 per group). Data are presented as mean ± SEM. Mann Whitney test was used for experiments with two groups. **p<0.01. Photomicrograph scale bars: 100uM.

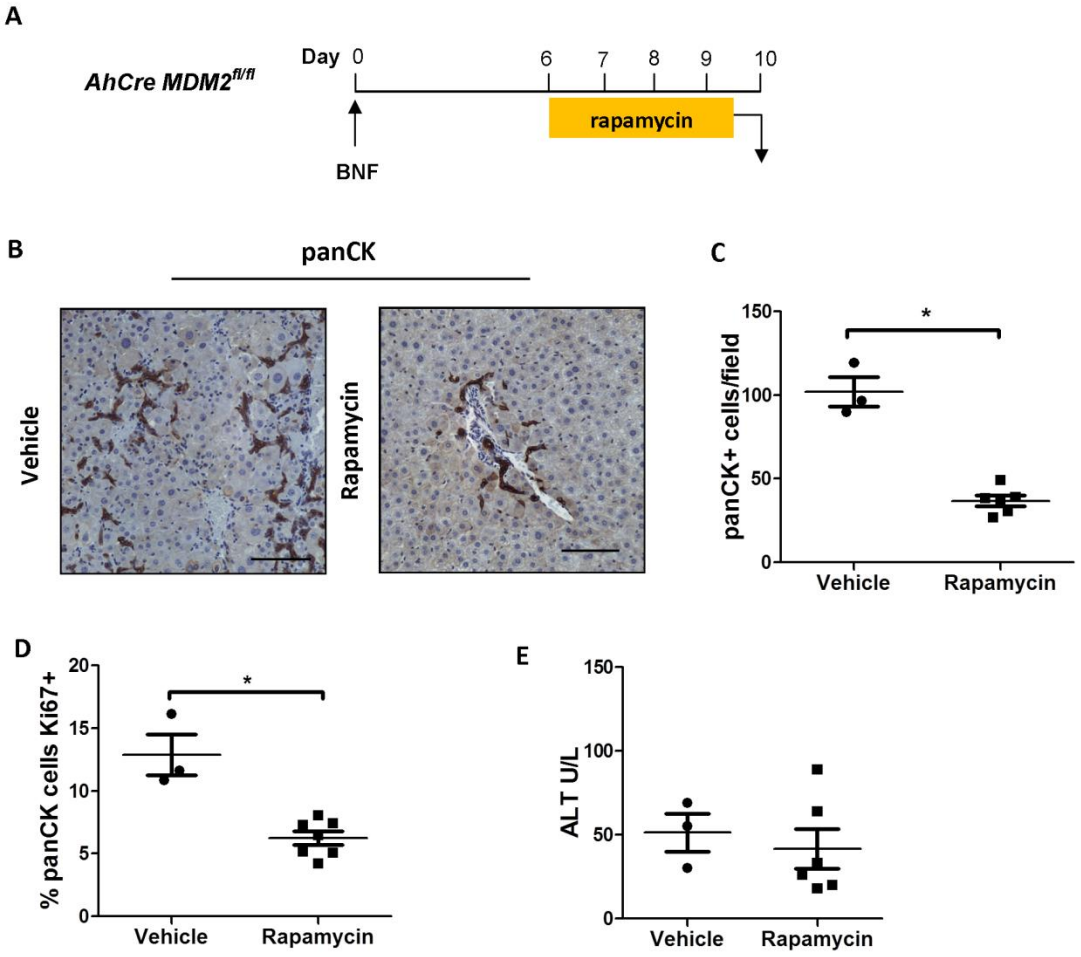

Figure 6.10: Inhibition of the IGF1 axis downstream at mTOR further supports functionality of this pathway in generating the ductular reaction: (A) Schematic demonstrates the strategy for treatment with rapamycin or vehicle following MDM2-mediated hepatocyte injury. **(B)** Representative images of panCK staining. **(C)** Quantification of effect on ductular response in terms of panCK-positive cell number and Ki67 positive proportion **(D). (E)** Serum ALT values. (*n*=3 vehicle group, *n*=6 treatment group). Data are presented as mean ± SEM. Mann Whitney test was used for experiments with two groups. *p<0.05. Photomicrograph scale bars: 100uM.

Positive staining of the DRs for phosphor-mTOR (Figure 6.7), and the data from the HPC lines, suggests the DR is a specific site for this active pathway. However it remains possible that use of IGF1 axis inhibitors might influence other components of the HPC niche – macrophages and myofibroblasts – and changes in their function might result in differences in the signals they deliver to the DR and thus indirectly impair DR proliferation. In order to determine a direct role for the IGF1 axis in driving DRs *in vivo* I generated a strain where *Igf1R* could be specifically deleted in ductular cells. I crossed mice with *loxP* sites flanking exon 3 of the *Igf1r* gene (326) with the *OPN-iCreER^{T2};R26R^{YFP}* strain to generate *OPN-iCreER^{T2};R26R^{YFP};Igf1r$^{fl/fl}$* and *OPN-iCreER^{T2};R26R^{YFP};Igf1r$^{wt/wt}$* strains. Following tamoxifen administration and a two week tamoxifen 'washout' period, mice received 3 weeks of CDE diet to induce hepatocellular injury and DRs (Figure 6.11A). There was a marked reduction in the number of YFP-positive (and thus conditionally lacking *Igf1r*) ductular cells in the *OPN-iCreER^{T2};R26R^{YFP};Igf1r$^{fl/fl}$* group (Figure 6.11B and C). Analysis of PCNA expression confirmed a reduction in proliferation capacity (Figure 6.11D). The number of lineage traced hepatocytes remained negligible in both groups and level of injury (as inferred by serum ALT) was consistent (Figure 6.11E-F).

6.4 Disruption of the IGF axis disrupts proliferation of DRs

Having established that in the CDE model of hepatocellular injury, conditional loss of *Igf1r* within the biliary compartment resulted in loss of DRs, I wanted to test this in a second model to confirm the effect. Further groups of animals received two weeks of MCD diet (Figure 6.12A). In this model there was also a reduction in DRs and their proliferation (Figure 6.12B-D). The number of lineage labelled hepatocytes remained low in both groups except for one animal in the *OPN-iCreER^{T2};R26R^{YFP};Igf1r$^{wt/wt}$* group which showed approximately 12% labelled hepatocytes. This may reflect inadvertent liver injury either at time of tamoxifen administration or prior to the initiation of MCD diet thus combining a 'recovery' model with an active injury model and seeing expansion of pre-labelled hepatocytes with MCD diet.

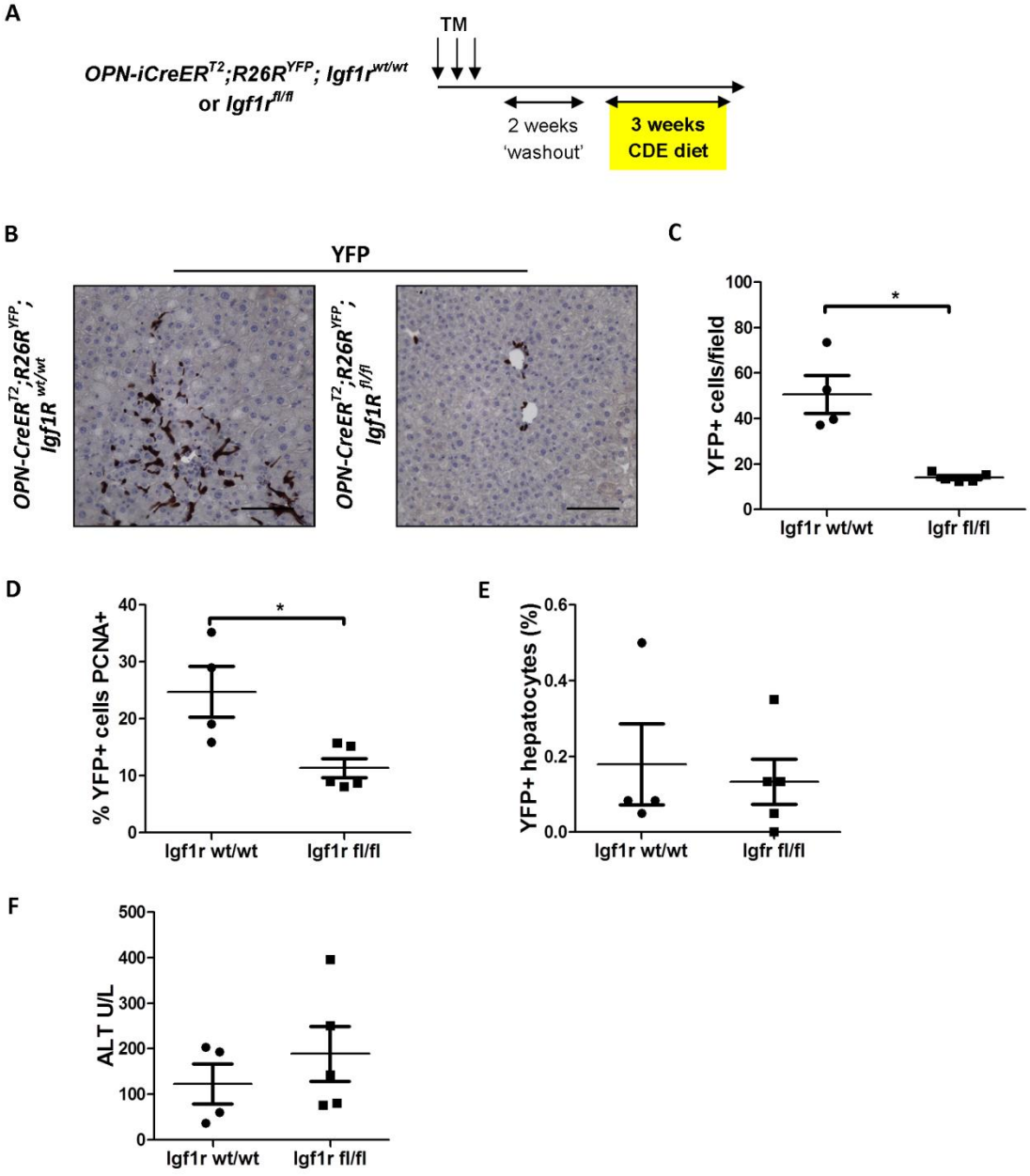
A
TM
OPN-iCreER^{T2};R26R^{YFP}; Igf1r$^{wt/wt}$
or Igf1r$^{fl/fl}$
2 weeks
'washout'
3 weeks
CDE diet
B
YFP
OPN-CreER^{T2};R26R^{YFP}; Igf1R$^{wt/wt}$
OPN-CreER^{T2};R26R^{YFP}; Igf1R$^{fl/fl}$
C
YFP+ cells/field
100
80
60
40
20
0
*
Igf1r wt/wt
Igfr fl/fl
D
% YFP+ cells PCNA+
40
30
20
10
0
*
Igf1r wt/wt
Igf1r fl/fl
E
YFP+ hepatocytes (%)
0.6
0.4
0.2
0.0
Igf1r wt/wt
Igfr fl/fl
F
ALT U/L
500
400
300
200
100
0
Igf1r wt/wt
Igf1r fl/fl

Figure 6.11: Conditional loss of *Igf1r* leads to loss of expansion of the ductular reaction after hepatocellular injury: (A) Schematic of experimental design to assess effect of loss of Igf1-receptor on the ductular response to CDE diet injury using *OPN-iCreER^{T2};R26R^{YFP};Igf1r$^{fl/fl}$* (*n*=5) and *OPN-iCreER^{T2};R26R^{YFP};Igf1r$^{wt/wt}$* (*n*=4) *s*trains. **(B)** Representative photomicrographs of YFP staining. **(C)** Quantification of effect on ductular reaction in terms of YFP-positive ductular cell number and **(D)** PCNA positive proportion. **(E)** The number of lineage traced hepatocytes in both groups remained minimal. **(F)** Serum ALT levels. Data are presented as mean ± SEM. Mann Whitney test was used for experiments with two groups. *p<0.05. Photomicrograph scale bars: 100uM.

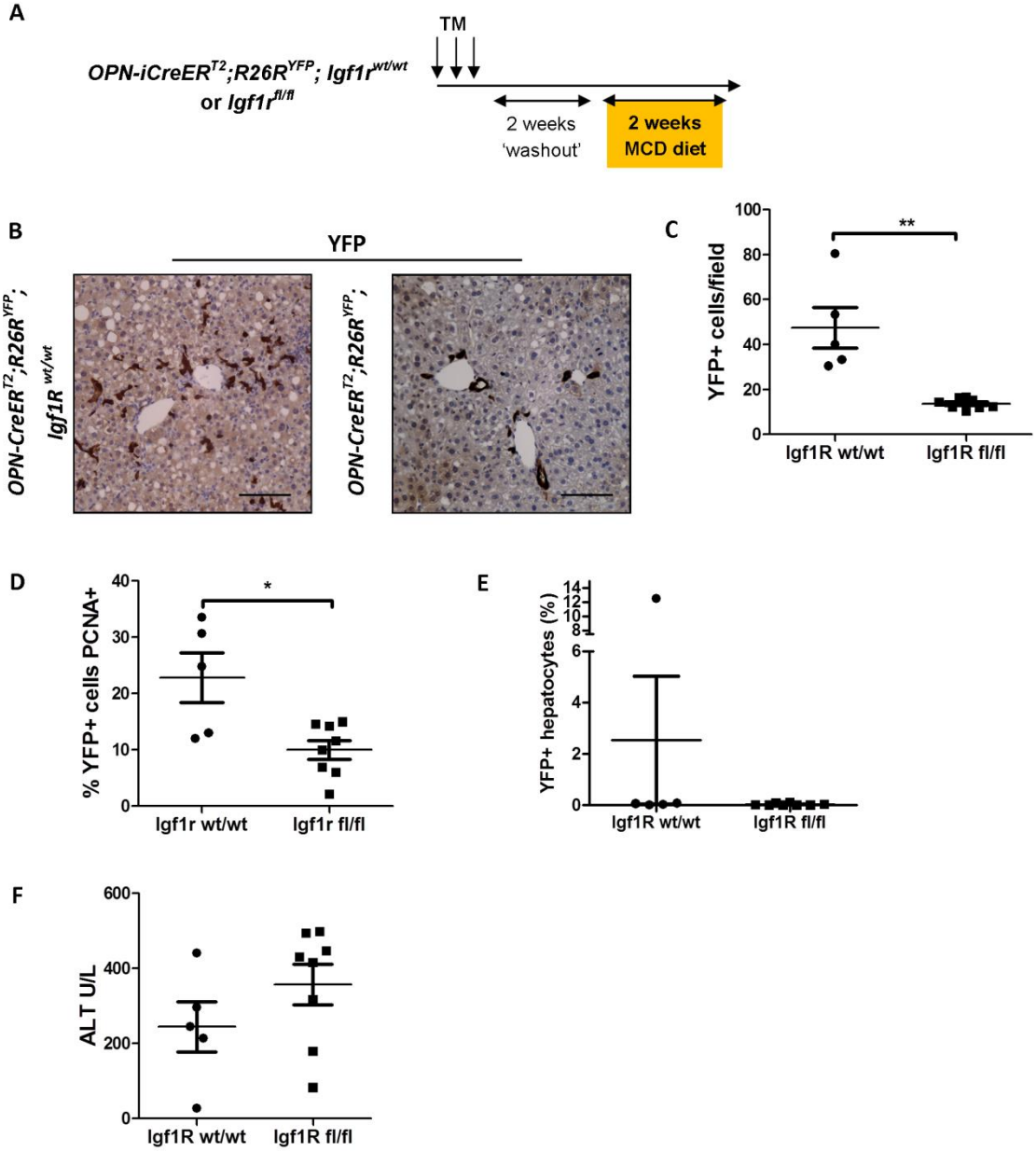
A
OPN-iCreER^{T2};R26R^{YFP}; Igf1r$^{wt/wt}$
or Igf1r$^{fl/fl}$
TM
2 weeks
'washout'
2 weeks
MCD diet
B
YFP
OPN-CreER^{T2};R26R^{YFP}; Igf1R$^{wt/wt}$
OPN-CreER^{T2};R26R^{YFP};
C
YFP+ cells/field
100
80
60
40
20
0
**
Igf1R wt/wt
Igf1R fl/fl
D
% YFP+ cells PCNA+
40
30
20
10
0
*
Igf1r wt/wt
Igf1r fl/fl
E
YFP+ hepatocytes (%)
14
12
10
8
6
4
2
0
Igf1R wt/wt
Igf1R fl/fl
F
ALT U/L
600
400
200
0
Igf1R wt/wt
Igf1R fl/fl

Figure 6.12: A second model of hepatocellular injury (MCD diet) further confirms *Igf1r* required for expansion of the ductular reaction: (A) Schematic of experimental design to assess effect of loss of Igf1-receptor (IGF1R) on the ductular response to MCD diet injury using *OPN-iCreER^{T2};R26R^{YFP};Igf1r$^{fl/fl}$* (*n*=8) and *OPN-iCreER^{T2};R26R^{YFP};Igf1r$^{wt/wt}$* (*n*=5) strains. **(B)** Representative photomicrographs of YFP staining. **(C)** Quantification of effect on DR in terms of YFP-positive ductular cell number and **(D)** PCNA positive proportion. **(E)** The number of lineage traced hepatocytes in both groups remained minimal except for one animal in the *wt/wt* group that showed approximately 12% labelled hepatocytes. **(F)** Serum ALT levels. Data are presented as mean ± SEM. Mann Whitney test was used for experiments with two groups. *p<0.05; **p<0.01. Photomicrograph scale bars: 100uM.

As this data supports a specific effect on the DR of the IGF1 axis in driving proliferation, I wanted to see what the effect was on the DR *in vivo* of administering additional IGF1. In the HPC lines, additional IGF1 did not increase proliferation, however in these spontaneously immortalised cell lines the proliferation rate is extremely high and therefore may not be amenable to further increases. Even when the growth rate was reduced by enforcing serum free conditions, additional IGF1 did not enhance growth. IGF1 production in both cell lines was extremely high and the system may have been saturated. The *AhCre MDM2$^{fl/fl}$* model results in generation of robust DRs that have a high proliferation rate. It was not clear if it would be possible to influence this with additional IGF1. I designed an experiment where recombinant murine IGF1 (rIGF1) or vehicle was administered daily days 6-9 after Cre induction (Figure 6.13A). At this time-point post Cre-induction while the absolute number of ductular cells is rising rapidly, their proliferation rate is falling. Despite the high number of ductular cells in the vehicle group, there was a small increase in number in the animals receiving rIGF1 (Figure 6.13B and C). When I assessed the proliferation rate of the cells however there was a marked increase from 6.5% to 21.3%, restoring proliferation rate to peal levels seen in the first few days of the ductular response (Figure 6.13D). If the animals had been left longer it is reasonable to predict the expansion of the DR would have continued.

Given the conflicting evidence from previous studies regarding the effect of IGF1 on causing fibrosis (371, 373, 375, 376) and the debate regarding whether HPCs drive fibrosis (86) I

went on to examine fibrosis in this model. Picrosirius red (PSR) stains collagen I and III deposited during the fibrotic response. PSR stain in this experiment showed collagen deposition in fact fell in the IGF1 treated animals, supporting that enhancing HPC function need not necessarily lead to increased fibrosis.

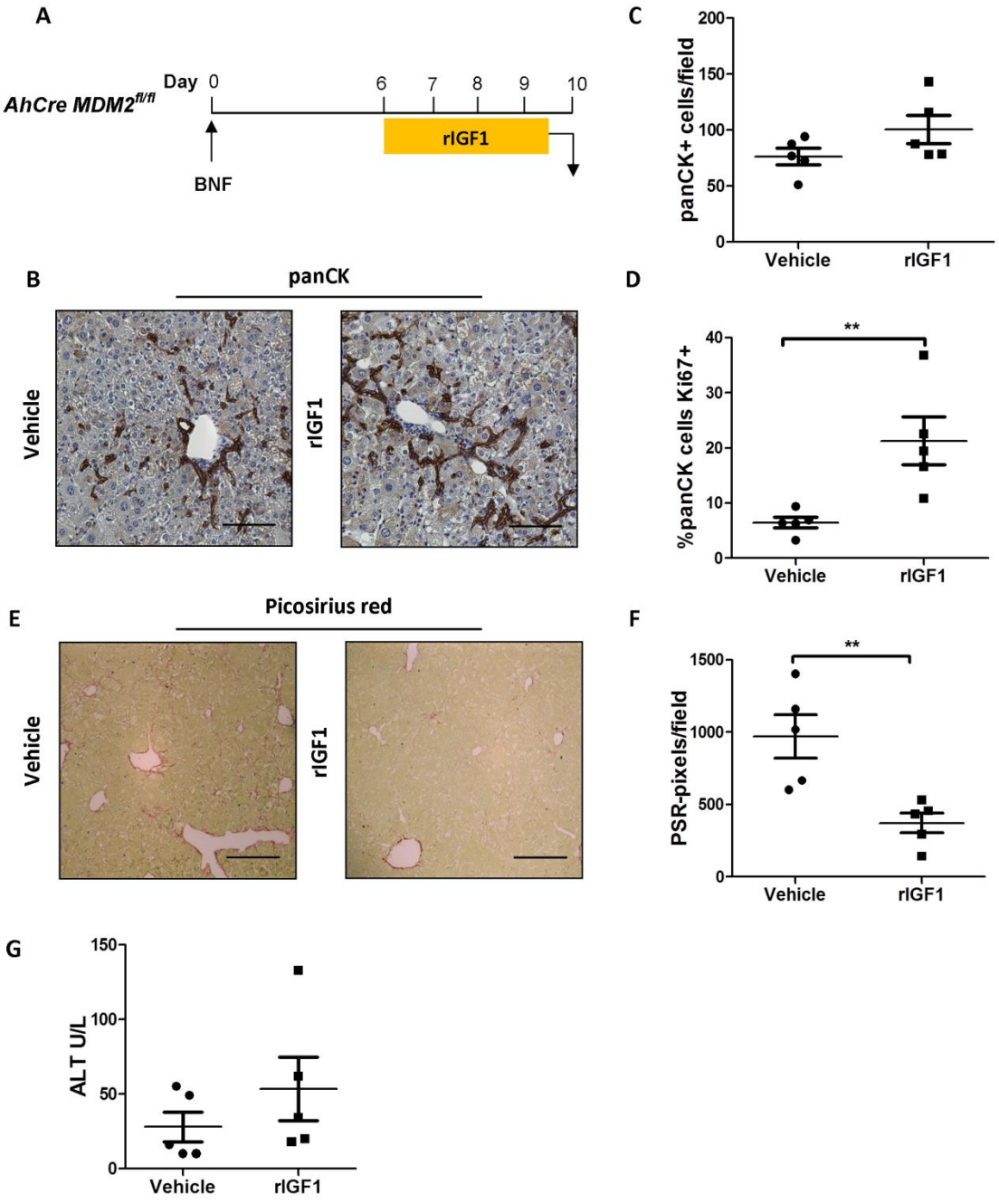
A
AhCre MDM2fl/fl
Day 0 6 7 8 9 10
rIGF1
BNF
B
panCK
Vehicle
rIGF1
C
panCK+ cells/field
200
150
100
50
0
Vehicle
rIGF1
D
%panCK cells Ki67+
**
40
30
20
10
0
Vehicle
rIGF1
E
Picosirius red
Vehicle
rIGF1
F
PSR-pixels/field
**
1500
1000
500
0
Vehicle
rIGF1
G
ALT U/L
150
100
50
0
Vehicle
rIGF1

Figure 6.13: Administration of recombinant IGF1 enhances the ductular reaction without causing fibrosis: **(A)** Schematic demonstrates the strategy for administration of recombinant murine Igf1 or vehicle following MDM2-mediated hepatocyte injury. **(B)** Representative images of panCK staining**. (C)** Quantification of effect on ductular response in terms of panCK-positive cell number and **(D)** Ki67 positive proportion. **(E)** Representative photomicrographs of picosirius red (PSR) staining from this experiment. **(F)** Quantification of PSR staining. **(G)** Serum ALT levels. *n*=5 per group. Data are presented as mean ± SEM. Mann Whitney test was used for experiments with two groups. **p<0.01. Photomicrograph scale bars: 100uM.

6.5 Discussion

In this chapter I have examined the IGF1 axis as a driver for DRs and a potential node for cooperation between Notch and Wnt signalling after hepatocellular injury. Synergy between Notch signalling and the IGF1 axis has been demonstrated with Notch1 directly driving expression of IGF1R and via Hes1 enhancing action of IGF1 axis signalling intermediaries (299, 300). Wnt and IGF1 cooperate in a positive feedback loop with IGF1 stimulating TCF/LEF dependent transcription and both increasing the stability and transcriptional activity of beta-catenin (377). In addition Wnt signalling can drive expression of both IGF1 and the principal intracellular mediator of IGF signalling IRS1 (378, 379).

I have demonstrated that two independent HPC lines express both IGF1 ligand and receptor. I went on to show growth of both these lines is sensitive to disruption of IGF1 signalling. I have demonstrated that both cell lines are the dominant source of IGF1 ligand that governs their growth. In both cell lines production of IGF1 at the gene and protein level was Wnt-sensitive. In both cell lines expression of IGF1R was Notch sensitive at the gene level, although I could not detect a reduction at the protein level of IGF1R with a specific phosphorylation status. I confirmed this Notch-Wnt sensitivity was a specific effect as Notch inhibition had no effect on IGF1 ligand production and Wnt inhibition had no effect on receptor production.

IGF1 production by ductular cells after biliary injury has been previously demonstrated (295). The IGF1-receptor (IGF1R) has also been identified on ductular cells (295, 371). I confirmed that both ligand and receptor were expressed in the ductular reactions after MDM2-mediated hepatocellular injury. I also confirmed downstream signalling was active by localising (active) phosphorylated mTOR within DRs. I have shown that expression of IGF1 in the *AhCre MDM2*$^{fl/fl}$ model time-course follows the Wnt target gene expression 'signature' and that IGF1R expression follows the Notch target gene expression 'signature', suggesting that *in vivo* too IGF1 axis expression is Notch/Wnt sensitive. This was further confirmed as specific by identifying reduced expression of *Igf1* but not *Igf1R* in animals treated with Wnt inhibitor ICG001. Animals treated with Notch inhibitor DAPT had reduced expression of *Igf1R* but not *Igf1*.

I consistently found that disrupting the IGF1 axis after hepatocellular injury diminished DRs. Using the *AhCre MDM2*$^{fl/fl}$ model I inhibited the IGF1R with a small molecule AG1024

resulting in failure of DR proliferation. A previous study demonstrated that cholagniocytes isolated from rats undergoing bile duct ligation (BDL) to induce liver injury expressed both IGF1 and IGF1R and their proliferation could be inhibited with a IGF1R blocking antibody or downstream inhibition of PI3K activity (295). Similarly I found inhibiting the IGF1 axis downstream at the point of mTOR resulted in a similar effect on proliferation as blocking IGF1R. Using Cre-lox technology to target IGF1 axis disruption to the biliary compartment I generated *OPN-iCreER^{T2};R26R^{YFP};Igf1r$^{fl/fl}$* and *OPN-iCreER^{T2};R26R^{YFP};Igf1r$^{wt/wt}$* strains and put these animals through two different hepatocellular injury models, CDE and MCD diet. In both cases there was a marked reduction in generation of labelled (and thus *Igf1R* lacking) ductular cells, and failure of their proliferation.

I went on to assess the effects of administering an excess of IGF1 to animals after hepatocellular injury. Using the *AhCre MDM2$^{fl/fl}$* model I administered recombinant IGF1 at a similar time to previous inhibitory experiments. At this point DRs are well established and while total ductular cell number is still increasing, their proliferation rate is falling. In this experiment administration of IGF1 was able to increase cell number and restore proliferation rate to maximal levels. Fibrosis in these animals also decreased.

Several studies have examined the link between IGF1 and CCl4-induced fibrosis in the liver. Administration of recombinant IGF1, viral-mediated gene transfer and genetic over expression have been used. Recombinant IGF1 administered to rats with CCl4 induced cirrhosis showed a number of beneficial effects. Hepatocellular function (serum albumin and clotting factors) and hepatocyte proliferation improved and oxidative stress and fibrosis were reduced. Livers showed lower hydroxyproline content and activity, fewer activated stellate cells and reduced expression of collagen I and III (372, 373, 381). In addition there were positive effects on the extrahepatic manifestations of cirrhosis with increased food intake, muscle mass and bone density (382). Transgenic mice that expressed IGF1 under an aSMA promotor (i.e. overexpress IGF1 on activation of stellate cells) were shown to recover more rapidly from acute liver injury caused by administration of CCl4. Accompanying improved transaminases and reduced area of necrosis was an enhanced expression of HGF, and reduced expression of TGFb1 and collagen Ia (375). Administration of a recombinant simian viral vector encoding IGF1 (rSVIGF-1) was found to prevent progression of CCl4-induced cirrhosis in rats (376) and mice (374). This was associated with

reduced serum bilirubin, improved transaminases, an increase in expression of matrix metalloproteinases (MMPs) and HGF and reduced tissue inhibitors of MMPs (TIMPs) and TGFb. The CCl4 injury model is not associated with DRs, and has not been shown to involve HPC-mediated hepatocellular regeneration, and therefore it is difficult to infer an effect on generation of DRs.

Sokolovic and colleagues investigated the effect of overexpression of IGF1 in a model of biliary injury (371). They used the genetic *Abcb4*$^{-/-}$ model (also known as *Mdr2*$^{-/-}$) in which excretion of phospholipids into bile, a requirement to neutralise bile acid toxicity, is limited. This strain was crossed with the model described above where IGF1 overexpression is driven by an aSMA promotor. Contrary to the observed positive effects in animals with hepatocyte injury, these animals showed increased fibrosis. Collagen staining increased, as did the expression of TGFb and TIMPs. DRs were also larger. Only one previous study has looked at the effects of IGF1 administration after hepatocellular injury associated with DRs. In this study rSVIGF-1 was administered to rats with thioacetamide (TAA)-induced cirrhosis. Oral administration of thioacetamide results in formation of toxic metabolites within zone 3 (pericentral) hepatocytes (112, 113). Prolonged administration results in ductular reaction, hepatic fibrosis and cirrhosis in mice and ultimately dysplasia and biliary carcinoma in rats (114). In this rSVIGF-1 TAA study fibrosis also fell, HGF and MMPs increased and TIMPs fell (376). Interestingly Irvine et al have recently demonstrated that when the secretion of Wnt from macrophages was prevented, fibrosis was increased in mice receiving TAA (383). DRs continued to expand (presumably via Notch and other signals such as TWEAK) but they were unable to demonstrate any direct effect on fibroblasts numbers or rate of collagen deposition. There was however an associated reduction in expression of MMPs and increase in expression of TIMPs. IGF1 was not examined but reduced Wnt-driven IGF1 expression could explain their findings.

In this chapter I propose a model for cooperation of Notch and Wnt in controlling proliferation of DRs in which Notch signalling can drive proliferation via induction of pro-proliferative genes or direct interaction with PI3K/Akt signalling. It can also drive expression of IGF1R, upstream of Akt and mTOR. Wnt signalling can drive proliferation via induction of pro-proliferative genes including IGF1. This can then in turn re-inforce Wnt signalling and cement the Wnt programme within HPCs to favour differentiation into hepatocytes (Figure

6.14). It may be that apparently contradictory effects of IGF1 demonstrated in previous studies can be explained when considered in the context of Notch and Wnt signalling. In chronic biliary injury where there is a high and persistent level of Notch signalling governing DR proliferation (58, 384), cholangiocytic differentiation (123) and transformation of hepatic stellate cells into myofibroblasts and resultant fibrosis (283), the addition of IGF1 results in further over-activity of this system and fibrosis ensues. In situations where there is hepatocyte injury, fibrosis and no DR, such as CCl4-induced injury, IGF1 can be hepatoprotective and pro-regenerative via induction of HGF, and limiting fibrosis through a direct or indirect effect on myofibroblasts. In contexts where there is the potential for DRs to generate HPCs capable of hepatocyte differentiation, then increased IGF1, promotion of the 'Wnt program', including potentially anti-fibrotic pathways, HPC migration and subsequent differentiation, may improve regeneration. This further highlights the importance of understanding the mechanisms involved in disease development in order for both the rational design of therapies and their appropriate usage.

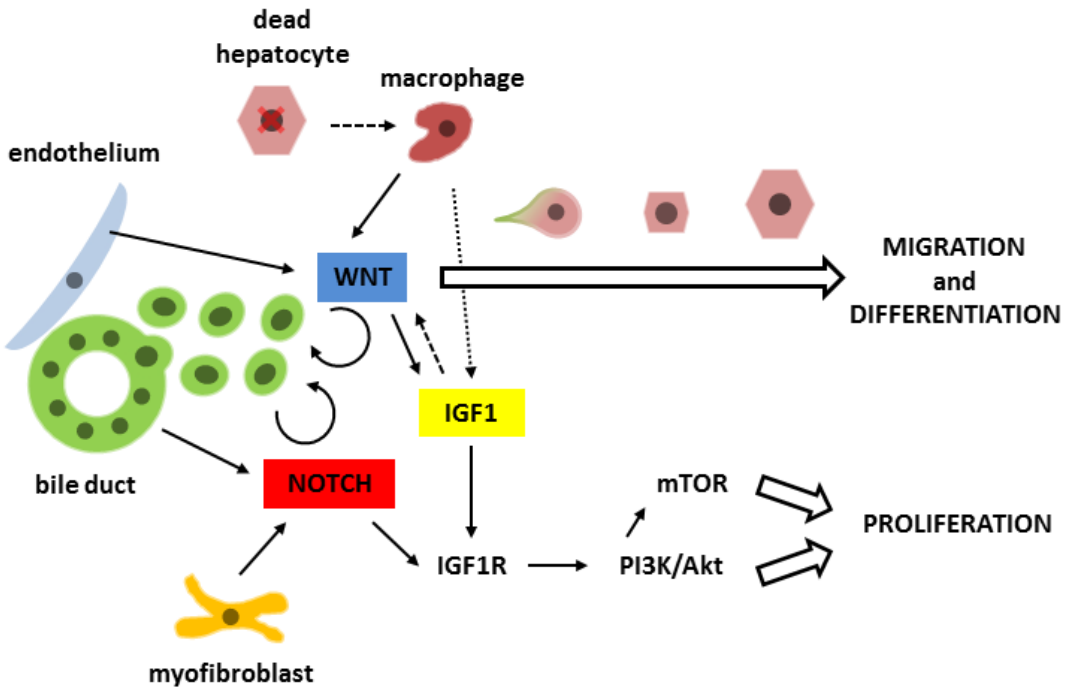

Figure 6.14: Proposed model for cooperation of Notch and Wnt in controlling HPC response to hepatocellular injury: Notch ligand produced by activated myofibroblasts and potentially bile ducts/HPCs themselves can drive HPC expansion via induction of pro-proliferative genes or direct interaction with PI3K/Akt signalling. In addition, Notch can drive expression of type 1 IGF receptor, upstream of Akt and mTOR. Wnt ligands produced by macrophages in response to engulfment of dead hepatocyte material and potentially endothelial-derived ligand can drive HPC proliferation via induction of pro-proliferative genes, including IGF1. IGF1 then further reinforces the Wnt program within HPCs resulting in their migration and hepatocytic differentiation.

In a pilot randomised clinical trial IGF1 was administered to individuals with cirrhosis (307). The trial was limited to those with alcoholic liver disease (ALD) or primary biliary cirrhosis (PBC) as their aetiology because of reports of growth promoting and anti-apoptotic properties of IGF1 and may be associated with the development certain tumours and/or their progression (385). Therefore those with a higher risk of developing hepatocellular carcinoma (HCC) such as haemochromatosis or chronic viral hepatitis were excluded. The level of IGF1 replacement was low and serum levels remained below normal values in treated patients. There was a significant increase in serum albumin concentration in the IGF1 treated group, consistent with improved liver function. There was also a trend towards improvement of Child-Pugh score which assesses the prognosis of liver disease. The benefits were most evident in patients with alcoholic liver disease (where injury is predominantly hepatocellular in nature and DRs can be seen (61, 386)) compared with individuals with biliary injury.

While IGF-II has been associated with HCC (387-390), a link between IGF1 and HCC is not established and low serum IGF1 may in fact predict risk of developing HCC, probably serving as a biomarker for severity of liver disease (391). Patients with non-alcoholic fatty liver disease have insulin resistance and chronic hyperinsulinaemia which in turn results in upregulation of IGF1 and potential involvement in hepatocarcinogenesis, (392) although which part of this cascade is directly or principally responsible is yet to be clarified, as is any deleterious effect of raising IGF1 levels in this setting. If serum levels of IGF1 were increased to supra-physiological levels, this could potentially increase the risk of non-liver malignancies associated with IGF1, particularly breast (393) and prostate cancer (394). In addition recombinant IGF1 is extremely costly and the dose and duration required for cirrhotic patients would render this an unrealistic therapeutic solution at present (395). Studies in animals with hepatocellular injury using gene transfer of IGF1 have shown encouraging results in terms of slowing the development of cirrhosis and even regression (374, 376). IGF1 levels were shown to increase in the liver without circulating levels rising above normal. Development of gene transfer or targeted cell therapies in humans may represent a viable strategy for delivery of IGF1 to patients with hepatocellular disease.

7 Conclusions and future perspectives

The importance of Notch and Wnt in liver regeneration is well recognised but remains incompletely understood. Differences in expression of Notch and Wnt have been documented in end liver stage disease and key roles for Notch in biliary and Wnt in hepatocellular fate determination have been demonstrated. However the roles of Notch and Wnt in driving the regenerative response, particular after hepatocellular injury, are not known.

Establishing how the liver regenerates, from which cell types and the potency of those cells has been hotly debated in recent years (33). The development of inducible, tissue specific Cre-lox labelling systems has not conclusively settled the matter (95). Potential reasons behind contradictory results include unexpected effects of tamoxifen on hepatocyte biology and difficulty in labelling lineages which share common ancestry due to transient expression of adult fate-specific genes such as albumin in developmental precursors as well as adult progenitors. In addition there is limited ability of our available models to meaningfully recapitulate the human disease picture of gross hepatocyte turnover, exhaustion and senescence. Rodent dietary models attempt to mirror human chronic hepatocellular damage, however age and background strain sensitivity, along with further variability related to individual animal units' pathogen levels, make reproducibility of findings between groups a further challenge. Further controversy regarding liver regeneration likely relates to consideration of only a single key recovery mechanism – either mature hepatocytes or a stem or progenitor cell – and further by the degree of rigidity of definitions of stemness applied. In an organ if one mature cell type can regenerate itself as well as another cell type can it be a stem cell? Is it transdifferentiation? And if this process involves transition through an intermediate bipotential progenitor cell then is this de-differentiation of a mature cell, or an apparently terminally differentiated cell acting as a facultative (stem) cell of origin for progenitor cells? As an organ whose key role is detoxification of both expected and unknown insults, high plasticity and multiple potential regenerative strategies for the liver would seem an evolutionary necessity. In order to develop new treatments for advanced liver disease, where prognosis is dismal and therapies are limited, all potential regenerative avenues must be considered for exploitation. Multiple studies have now demonstrated that cells from the biliary

compartment can generate hepatocytes after liver injury in the zebrafish, rat and mouse (52, 53, 56-58, 262, 396), behaving as facultative stem cells, and there is recent supportive evidence of this process occurring in human disease (51). The challenge remains to fully understand this process and identify ways of enhancing an important endogenous repair pathway.

The best characterised models of liver regeneration are 2/3 partial hepatectomy and acetaminophen poisoning whereby a single insult is applied and the dynamics of the response studied, however these injuries are not typically associated with regenerative DRs. Combining administration of 2 acetylaminofluorene (AAF), which causes DNA damage and increased expression of p21 leading to hepatocyte cell-cycle arrest, with partial hepatectomy in rats (2AAF/PH model) has provided compelling evidence of a biliary origin for hepatocyte-regenerating DRs. While this model permits time-sensitive study of the regenerative response (262, 269), current genetic technology does not however permit robust lineage tagging, signalling pathway reporter gene expression or cell type specific genetic loss or gain of function. A mouse model has the potential to overcome some of these limitations. Classic murine dietary injury models can induce a ductular reaction in which lineage labelling has confirmed a biliary origin of both HPCs and a proportion of new hepatocytes generated after injury (56-58). The disadvantage of these models is that the continuous nature of the injury means our ability to study what signals may drive a DR over time are limited and real-time analysis of regenerative pathways is not possible. The *AhCreMDM2*$^{fl/fl}$ strain, through Cre-mediated deletion of MDM2, results in high levels of hepatocyte p53 expression and subsequent senescence with p21 expression (59). Cells from the DRs of these animals are able to differentiate down either the hepatocyte or biliary route, be isolated, expanded, transplanted and then functionally repopulate the parenchyma. When the ability of these animals to generate DRs is lost, the animals die, confirming both the importance and potency of ductular derived HPCs. Crucially, as injury is administered as a 'single hit', this model has the potential for scrutiny to be applied to the temporal dynamics of injury and regeneration.

I have demonstrated that after severe hepatocyte injury and induction of senescence using the *AhCreMDM2*$^{fl/fl}$ model, a robust DR develops that can be studied over time. There is highly predictable activation, expansion and migration of DRs. I also studied the

proliferation dynamics, confirming a highly proliferative cell type. I used this system to study Notch and Wnt signalling, but clearly this model has potential for the study of many other signalling systems. Isolation of cellular components – hepatocytes, HPCs, fibroblasts or macrophages would enable relative contribution of cell populations to expression profiles and also assist in the identification of further therapeutic targets.

The major limitation of this system is that the biliary compartment is not lineage tagged. This means direct positive lineage tracing evidence of large scale contribution to hepatocyte replacement cannot be demonstrated. This would require a method to induce similar hepatocyte injury not using Cre-lox technology, enabling Cre-mediated lineage labelling of the biliary compartment. Viral induced overexpression of p21 in hepatocytes may be an effective strategy and is currently being developed in the Forbes laboratory. In addition to permitting positive lineage tracing of ductular cells, Cre-mediated excision of key components of the signalling pathways could be used to determine the effects on generation of DRs and subsequent hepatocyte differentiation.

Using the *AhCreMDM2*$^{fl/fl}$ strain, complemented by biliary Cre lineage tracing systems, I went on to characterise the expression and activity of Notch and Wnt signalling pathways after hepatocellular injury. I identified changes in expression of Notch ligands and receptors after injury. Receptor expression localised to the DR. I measured the expression of a range of Notch target genes and identified a time-sensitive Notch expression 'signature'. By generating the *AhCreMDM2*$^{fl/fl}$*; CBF:H2B-venus* strain I was able to confirm ductular cells were in receipt of, and were acting on, canonical Notch signal. By evaluating changes in Notch reporter expression over time, I also confirmed that Notch pathway activity was dynamic after injury and lost as regeneration progressed. Experiments designed to reflect this dynamic expression revealed a time-sensitive role for Notch in driving the proliferation of DRs. I went on to demonstrate that this phenotype was driven by the dynamically expressed Notch receptors, Notch1 and Notch3. Using *Krt19* and *OPN* Cre strains I was further able to further prove Notch-dependent proliferation of DRs in more traditional diet based liver injury models.

I have demonstrated changes in Wnt pathway activity over time after MDM2-mediated hepatocyte injury. Similar to Notch effector expression, I identified a characteristic time-sensitive expression profile or 'signature' for Wnt target genes. After injury I observed a

loss of expression of Wnt target genes and Wnt pathway activity reporter, which was subsequently restored as the DR developed. Using additional experiments designed to reflect this dynamic expression profile I went on to demonstrate that proliferation of DRs in this later phase was Wnt driven. Furthermore, using the *Krt19* Cre strain I was able to prove Wnt-dependent proliferation of DRs in diet based liver injury models.

Having identified roles for both Notch and Wnt in controlling proliferation of DRs, I went on to investigate if there was a node of cooperation between the two pathways. I identified Notch driven expression of IGF1 receptor and Wnt driven expression of IGF1 ligand,. I went on to demonstrate the significance of this axis in proliferation of the DR in multiple mouse models, including genetic disruption of this axis specific to the biliary compartment. Importantly I demonstrated that administration of additional IGF1 could both enhance proliferation of the DR and reduce fibrosis, thus potentially enhancing HPC mediated regeneration without negative effects.

Previous studies in livers from mice with CDE-induced injury in which macrophages (and therefore secreted factors such as Wnt ligands and TWEAK) were depleted there was no change in expansion of ductular cells, but these HPCs did not migrate into the parenchyma instead forming periportal aggregates akin to bile ducts (342). Similarly silencing of Wnt1 resulted in expanded proliferating atypical ducts in the rat 2AAF/PH model (269). The persisting ability of DRs to expand suggests alternative signals are also involved in their proliferation. Important signals identified to date in HPC activation and proliferation include HGF/c-met, EGFR, Shh, TWEAK and TGF-β (343-345). Notch is a key signal in biliary specification of the hepatoblast. It is required for effective arborisation of the developing biliary tree and when over-expressed in hepatocytes has the potential to convert their fate to cholangiocytes with roles proposed for both Notch1 and Notch2 (156, 170, 171, 211, 213, 222, 397). I found no dynamic changes in expression of Notch2 after hepatocellular injury. In addition blockade of Notch2 did not affect DR proliferation. This may reflect functional redundancy, however recent work identified specific Jagged1-Notch1 interaction as important for proliferation of DRs after injury by bile duct injury, further supporting discrete roles for Notch1 and Notch2 in cholangiocyte proliferation and differentiation (91, 213).

The functions of Notch3 are less well characterised. It may have a role in activation of stellate cells (226) and is expressed by the vasculature (398) and therefore could have indirect actions to the ductular proliferation phenotype I observed. My *in vivo* data, combined with the effect of *Notch3* knock down in my HPC line, is highly supportive of a direct effect upon biliary proliferation. As the Notch receptors are not equivalent targets for Numb inhibition with structural differences rendering Notch3 relatively resistant (197, 284), this paralog is ideally placed to permit persisting Notch activity in HPCs at a time of rising Wnt; a 'permitted' Notch. I have not examined the relative roles of the different paralog on the production of IGF1R and this would be interesting to pursue.

A particularly interesting finding in the section of work describing Wnt pathway expression was the identification of *Axin2* and *TCF/LEF:H2B-GFP* in the ducts of uninjured animals. Previous studies have reported *Axin2* RNA expression to be restricted to zone 3 hepatocytes (20, 150) however in these studies images suggest there may be some ductular expression. Similarly a beta-galactosidase (beta-gal) TCF/LEF reporter system has reported hepatocyte zone 3 beta-gal activity, with minimal (but detectable) reporter activity in the portal region of non-injured animals. The sensitivity of the RNAScope system I employed to identify *Axin2* is high and may explain apparently differing results. Similarly the *TCF/LEF:H2B-GFP* construct is both highly sensitive (with six TCF/LEF binding sites) and encodes a very bright fluorescent reporter permitting high resolution reporting. This also enabled co-staining of *TCF/LEF:H2B-GFP* reporting cells to confirm they were ductular. Demonstrating Wnt activity in the uninjured biliary tree may reflect a basal 'stem potential' of ductular cells consistent with a 'Wnt responsive' stem cell model as present in tissues such as the intestine, stomach, skin and mammary gland (233) and most recently in pericentral hepatocytes (150).

I saw gross upregulation of *Ascl2* accompanying DR activation after hepatocellular injury, preceding *Lgr5* upregulation, reflecting both a Wnt program but also potentially further interaction between Notch and Wnt. Transcription factor Ascl2 occupies an interesting position between the two signalling pathways. In epidermal development, Notch signalling can both induce Ascl2 expression and repress it via Hes-1 (289). As a direct target of canonical Wnt signalling, Ascl2 is required for maintenance of the Lgr5 stem cell pool in adult intestinal epithelium (286, 287). I did not give Wnt inhibitor to *AhCreMDM2*$^{fl/fl}$ animals

at the time of Cre-induction or pre-treat them with Wnt inhibitor. This would help determine if the low level of Wnt signalling reported in uninjured ducts was required for subsequent cell activation and generation of the DR and if in this system *Ascl2* expression was dependent on Wnt, Notch or both signals. I have not investigated the source of Wnt ligand providing Wnt signal to ductular cell in the absence or after injury. Infiltrating bone marrow derived macrophages have been demonstrated to be a source of Wnt ligand in mice after CDE diet (123) and in mice and rats after chronic thioacetamide (TAA) administration (115). Hepatocytes were found to be a source of Wnt1, providing paracrine signal to DRs in the 2AAF/PH hepatectomy rat model (262, 269). Central vein endothelial cells have been shown to provide Wnt signals to maintain the Wnt-responsive pericentral *Axin2* positive hepatocytes responsible for homeostatic renewal (150). It may be that zone 1 hepatocytes or portal tract vessels provide local tonic Wnt signal to ductal cells in the resting state and after injury infiltrating macrophages, injured or peri-injury hepatocytes, or even sinusoidal endothelilal cells in response to pressure changes related to hepatocyte damage can provide Wnt ligand as the DR develops. Changing sources and patterns of Wnt ligand expression and the factors controlling this would be an interesting area for further study.

As mentioned above the requirement for induction of Cre to prompt loss of MDM2 in hepatocytes makes further tissue-specific genetic alterations difficult. Should viral mediated overexpression of p21 in hepatocytes produce a similar phenotype to the *AhCreMDM2*$^{fl/fl}$ strain, then future work could focus on functional effects of deletion of specific Notch receptors or Wnt receptors or mediators such as beta-catenin from the biliary compartment, or potential ligand expression targeted to biliary cells or other niche components such as fibroblasts, endothelia or macrophages.

The output of Notch signalling is context-dependent, and the proper timing and spatial regulation of activation is crucial for normal embryonic developmental processes and often involves cross-talk with other developmental signals Wnt and Shh (155). In the adult, experiments on damaged muscle identified that the correct sequence of Notch and Wnt signal was essential for effective regeneration with this ‘molecular switch’ achieved by changes in phosphorylation status of GSK3b (279). I identified a similar paradigm with both signals influencing HPC proliferation. It is likely that Wnt is in addition responsible for the

migration of HPCs in vivo given the phenotypic change accompanying onset of Wnt signalling and the previous finding of loss of HPC migration when macrophages (and their secreted Wnt) are obliterated (342). This would be further supported by my observation of loss of migration of HPC lines exposed to Wnt but not Notch inhibition.

Improving the generation of hepatocytes from ductular derived HPCs represents a key therapeutic goal. Previous work would suggest inhibiting Notch signalling in favour of Wnt would promote hepatocytic differentiation (123). Jors et al performed elegant experiments to see if conditional knock out of canonical Notch intermediary Rbpjk and over expression of beta-catenin could fate switch DRs during biliary injury, an injury model that normally does not result in generation of ductular-derived hepatocytes (58). They found no fate switch by altering these alleles, either alone or simultaneously, however did observe in all cases a loss of proliferation of affected cells, most marked in the tandem allele strain. There are a number of possible reasons why inhibiting Notch at the same time as over-expressing the Wnt pathway may result in a loss of proliferation: it may reflect a requirement for both these signals to be received in the correct sequence, over expression of Wnt might result in an excess of Notch antagonism by Numb, or even an imbalance in the IGF1/IGF1R axis.

A previous study found Notch pathway was active in the rat 2AAF/PH model and administering a gamma secretase inhibitor during peak HPC response demonstrated a requirement for Notch in the proper regulation of differentiation of HPCs, albeit in the absence of direct lineage tracing (399). I also found that inhibiting Notch in a model where HPCs are known to differentiate into hepatocytes resulted in a significantly reduced number of lineage labelled HPC derived hepatocytes, rather than enhanced differentiation as might have been expected. This is likely to be secondary to a failure of HPC proliferation. This suggests that viewing only differentiation related actions of Notch would be short-sighted and attempting to improve hepatocyte regeneration by Notch inhibition would be unsuccessful.

In addition I found inhibiting Wnt in the same model did not reduce the number of HPC-derived hepatocytes, which might have been expected if it is important for hepatocytic differentiation. Again this is potentially explained by interference with carefully controlled HPC proliferation or alternatively differing proliferation versus differentiation outputs of Wnt signalling. Given the experience from ex vivo differentiation protocols, it remains

highly likely that Wnt is required for hepatocytic differentiation (75, 77, 78). Resolving this may ultimately require unpicking of the differential functions of Wnt signalling and how this might be mediated. Previous work has suggested CBP/beta-catenin mediated transcription is essential for stem and/or progenitor maintenance and proliferation, whereas a switch to p300/beta-catenin mediated transcription is a critical step to initiate differentiation (348, 362-364). Future work could focus on exploring the differential actions of beta-catenin/TCF/LEF dependent transcriptional co-activators CBP versus p300 in HPCs. Using CBP inhibitor ICG001 I have demonstrated CBP-dependent roles in proliferation and migration. It may be differentiation of HPCs relates to p300 activity and permits use of the same signal to promote multiple phases in the regenerative response. This would be of particular benefit in chronic injury where newly activated DRs could be directed to proliferate and migrate while mature DRs are directed to differentiate. This could be further explored using specific p300 inhibitors, and should they be identified, p300 agonists may promote differentiation.

I have demonstrated that CBP inhibition reduces IGF1 expression in HPCs but I have not explored any effect related to p300 activity. Wnt and IGF1 cooperate in a positive feedback loop with IGF1 stimulating TCF/LEF dependent transcription and both increasing the stability and transcriptional activity of beta-catenin (377), acting to 'wind up' and reinforce the Wnt programme. Whether this influences the balance of CBP/p300 activity has not been established.

The data presented here combined with that from previous studies suggest IGF1 therapy is potentially beneficial to individuals with hepatocellular liver disease. Delivery of IGF1 to the HPC niche however is not without difficulty. Recombinant IGF1 is prohibitively expensive, especially when the dose and duration of therapy is considered. Systemic administration also carries a theoretical risk of malignancy; especially should supra-physiological levels be reached. Delivering direct gene transfer to the liver is another therapeutic option for future study, as is ex vivo manipulation of isolated HPCs to enhance IGF1 production, which could then be transplanted to exert a positive local effect on the endogenous response. I have principally examined autologous Wnt-responsive IGF1 expression of IGF1 by HPCs and biliary cells, however the major non-liver source of IGF1 is believed to be macrophages where its production is stimulated in response to colony stimulating factor (CSF)-1 (400). As

infiltrating macrophages have already been demonstrated to provide Wnt ligand to HPCs after hepatocellular injury, clearly they could also provide IGF1 and thus further promote the Wnt programme. This also suggests an alternative future therapeutic strategy involving cell therapy with engineered macrophages as an alternative to enhancing hepatocyte or HPC IGF1 production or systemic administration. As macrophages do not produce IGF binding partners the effect of secreted IGF1 is likely to be local with little systemic activity and so potentially carrying lower risk of inducing tumorigenesis.

In conclusion this work describes the identification of temporally regulated Notch and Wnt signalling after hepatocellular injury. Following injury the DR is associated with a marked increase in Notch activity and inhibition of this pathway attenuates this response by affecting ductular proliferation. Once the reaction has developed, ductular Wnt signalling becomes dominant and further drives proliferation, as the effects of Notch diminish. I demonstrate that these signalling pathways can operate independently and cooperatively to drive proliferation of regenerative DRs. This work supports the paradigm of a Notch/Wnt permissive state within HPCs and one where both functional antagonism (for example with relation to differentiation via Numb) and agonism (for example proliferation via the IGF1 axis and relative Numb resistance of Notch3) can occur. Exploration of the roles and interactions of these signalling systems helps identify the complex networks at play and identify key target pathways for the rational design of novel disease and context-specific therapies to optimise liver regeneration.

8 References

1. Mokdad, A.A., Lopez, A.D., Shahraz, S., Lozano, R., Mokdad, A.H., Stanaway, J., Murray, C.J., and Naghavi, M. 2014. Liver cirrhosis mortality in 187 countries between 1980 and 2010: a systematic analysis. *BMC Med* 12:145.
2. Ratib, S., West, J., Crooks, C.J., and Fleming, K.M. 2014. Diagnosis of liver cirrhosis in England, a cohort study, 1998-2009: a comparison with cancer. *Am J Gastroenterol* 109:190-198.
3. Theise, N.D., Saxena, R., Portmann, B.C., Thung, S.N., Yee, H., Chiriboga, L., Kumar, A., and Crawford, J.M. 1999. The canals of Hering and hepatic stem cells in humans. *Hepatology* 30:1425-1433.
4. Gualdi, R., Bossard, P., Zheng, M., Hamada, Y., Coleman, J.R., and Zaret, K.S. 1996. Hepatic specification of the gut endoderm in vitro: cell signaling and transcriptional control. *Genes Dev* 10:1670-1682.
5. Jung, J., Zheng, M., Goldfarb, M., and Zaret, K.S. 1999. Initiation of mammalian liver development from endoderm by fibroblast growth factors. *Science* 284:1998-2003.
6. Watanabe, T., Nakagawa, K., Ohata, S., Kitagawa, D., Nishitai, G., Seo, J., Tanemura, S., Shimizu, N., Kishimoto, H., Wada, T., et al. 2002. SEK1/MKK4-mediated SAPK/JNK signaling participates in embryonic hepatoblast proliferation via a pathway different from NF-kappaB-induced anti-apoptosis. *Dev Biol* 250:332-347.
7. Nitou, M., Sugiyama, Y., Ishikawa, K., and Shiojiri, N. 2002. Purification of fetal mouse hepatoblasts by magnetic beads coated with monoclonal anti-e-cadherin antibodies and their in vitro culture. *Exp Cell Res* 279:330-343.
8. Tanimizu, N., Nishikawa, M., Saito, H., Tsujimura, T., and Miyajima, A. 2003. Isolation of hepatoblasts based on the expression of Dlk/Pref-1. *J Cell Sci* 116:1775-1786.
9. Shiojiri, N., and Sugiyama, Y. 2004. Immunolocalization of extracellular matrix components and integrins during mouse liver development. *Hepatology* 40:346-355.
10. Rossi, J.M., Dunn, N.R., Hogan, B.L., and Zaret, K.S. 2001. Distinct mesodermal signals, including BMPs from the septum transversum mesenchyme, are required in combination for hepatogenesis from the endoderm. *Genes Dev* 15:1998-2009.
11. Lemaigre, F.P. 2009. Mechanisms of liver development: concepts for understanding liver disorders and design of novel therapies. *Gastroenterology* 137:62-79.
12. Antoniou, A., Raynaud, P., Cordi, S., Zong, Y., Tronche, F., Stanger, B.Z., Jacquemin, P., Pierreux, C.E., Clotman, F., and Lemaigre, F.P. 2009. Intrahepatic bile ducts develop according to a new mode of tubulogenesis regulated by the transcription factor SOX9. *Gastroenterology* 136:2325-2333.
13. Crawford, A.R., Lin, X.Z., and Crawford, J.M. 1998. The normal adult human liver biopsy: a quantitative reference standard. *Hepatology* 28:323-331.
14. Carpentier, R., Suner, R.E., van Hul, N., Kopp, J.L., Beaudry, J.B., Cordi, S., Antoniou, A., Raynaud, P., Lepreux, S., Jacquemin, P., et al. 2011. Embryonic ductal plate cells

give rise to cholangiocytes, periportal hepatocytes, and adult liver progenitor cells. *Gastroenterology* 141:1432-1438, 1438 e1431-1434.
15. Kyrmizi, I., Hatzis, P., Katrakili, N., Tronche, F., Gonzalez, F.J., and Talianidis, I. 2006. Plasticity and expanding complexity of the hepatic transcription factor network during liver development. *Genes Dev* 20:2293-2305.
16. Jungermann, K., and Katz, N. 1989. Functional specialization of different hepatocyte populations. *Physiol Rev* 69:708-764.
17. Jungermann, K. 1988. Metabolic zonation of liver parenchyma. *Semin Liver Dis* 8:329-341.
18. Moorman, A.F., Vermeulen, J.L., Charles, R., and Lamers, W.H. 1989. Localization of ammonia-metabolizing enzymes in human liver: ontogenesis of heterogeneity. *Hepatology* 9:367-372.
19. Gebhardt, R., and Matz-Soja, M. 2014. Liver zonation: Novel aspects of its regulation and its impact on homeostasis. *World J Gastroenterol* 20:8491-8504.
20. Benhamouche, S., Decaens, T., Godard, C., Chambrey, R., Rickman, D.S., Moinard, C., Vasseur-Cognet, M., Kuo, C.J., Kahn, A., Perret, C., et al. 2006. Apc tumor suppressor gene is the "zonation-keeper" of mouse liver. *Dev Cell* 10:759-770.
21. Inagaki, T., Choi, M., Moschetta, A., Peng, L., Cummins, C.L., McDonald, J.G., Luo, G., Jones, S.A., Goodwin, B., Richardson, J.A., et al. 2005. Fibroblast growth factor 15 functions as an enterohepatic signal to regulate bile acid homeostasis. *Cell Metab* 2:217-225.
22. Mleczko-Sanecka, K., Casanovas, G., Ragab, A., Breitkopf, K., Muller, A., Boutros, M., Dooley, S., Hentze, M.W., and Muckenthaler, M.U. 2010. SMAD7 controls iron metabolism as a potent inhibitor of hepcidin expression. *Blood* 115:2657-2665.
23. Pajvani, U.B., Shawber, C.J., Samuel, V.T., Birkenfeld, A.L., Shulman, G.I., Kitajewski, J., and Accili, D. 2011. Inhibition of Notch signaling ameliorates insulin resistance in a FoxO1-dependent manner. *Nat Med* 17:961-967.
24. Pajvani, U.B., Qiang, L., Kangsamaksin, T., Kitajewski, J., Ginsberg, H.N., and Accili, D. 2013. Inhibition of Notch uncouples Akt activation from hepatic lipid accumulation by decreasing mTorc1 stability. *Nat Med* 19:1054-1060.
25. Valenti, L., Mendoza, R.M., Rametta, R., Maggioni, M., Kitajewski, C., Shawber, C.J., and Pajvani, U.B. 2013. Hepatic notch signaling correlates with insulin resistance and nonalcoholic fatty liver disease. *Diabetes* 62:4052-4062.
26. Kaibori, M., Kwon, A.H., Oda, M., Kamiyama, Y., Kitamura, N., and Okumura, T. 1998. Hepatocyte growth factor stimulates synthesis of lipids and secretion of lipoproteins in rat hepatocytes. *Hepatology* 27:1354-1361.
27. Goodnough, J.B., Ramos, E., Nemeth, E., and Ganz, T. 2012. Inhibition of hepcidin transcription by growth factors. *Hepatology* 56:291-299.
28. Matz-Soja, M., Hovhannisyan, A., and Gebhardt, R. 2013. Hedgehog signalling pathway in adult liver: a major new player in hepatocyte metabolism and zonation? *Med Hypotheses* 80:589-594.
29. Michalopoulos, G.K. 2007. Liver regeneration. *J Cell Physiol* 213:286-300.
30. Miyaoka, Y., Ebato, K., Kato, H., Arakawa, S., Shimizu, S., and Miyajima, A. 2012. Hypertrophy and unconventional cell division of hepatocytes underlie liver regeneration. *Curr Biol* 22:1166-1175.
31. Lee, V.M., Cameron, R.G., and Archer, M.C. 1998. Zonal location of compensatory hepatocyte proliferation following chemically induced hepatotoxicity in rats and humans. *Toxicol Pathol* 26:621-627.

32. Grompe, M. 2014. Liver stem cells, where art thou? *Cell Stem Cell* 15:257-258.
33. Michalopoulos, G.K., and Khan, Z. 2015. Liver Stem Cells: Experimental Findings and Implications for Human Liver Disease. *Gastroenterology* 149:876-882.
34. Kato, A., Bamba, H., Shinohara, M., Yamauchi, A., Ota, S., Kawamoto, C., and Yoshida, Y. 2005. Relationship between expression of cyclin D1 and impaired liver regeneration observed in fibrotic or cirrhotic rats. *J Gastroenterol Hepatol* 20:1198-1205.
35. Kanta, J., and Chlumska, A. 1991. Regenerative ability of hepatocytes is inhibited in early stages of liver fibrosis. *Physiol Res* 40:453-458.
36. Gouw, A.S., Clouston, A.D., and Theise, N.D. 2011. Ductular reactions in human liver: diversity at the interface. *Hepatology* 54:1853-1863.
37. Marshall, A., Rushbrook, S., Davies, S.E., Morris, L.S., Scott, I.S., Vowler, S.L., Coleman, N., and Alexander, G. 2005. Relation between hepatocyte G1 arrest, impaired hepatic regeneration, and fibrosis in chronic hepatitis C virus infection. *Gastroenterology* 128:33-42.
38. Weissman, I.L., Anderson, D.J., and Gage, F. 2001. Stem and progenitor cells: origins, phenotypes, lineage commitments, and transdifferentiations. *Annu Rev Cell Dev Biol* 17:387-403.
39. Weissman, I.L. 2000. Stem cells: units of development, units of regeneration, and units in evolution. *Cell* 100:157-168.
40. Gage, F.H. 2000. Mammalian neural stem cells. *Science* 287:1433-1438.
41. Barker, N., van Es, J.H., Kuipers, J., Kujala, P., van den Born, M., Cozijnsen, M., Haegebarth, A., Korving, J., Begthel, H., Peters, P.J., et al. 2007. Identification of stem cells in small intestine and colon by marker gene Lgr5. *Nature* 449:1003-1007.
42. Snippert, H.J., Haegebarth, A., Kasper, M., Jaks, V., van Es, J.H., Barker, N., van de Wetering, M., van den Born, M., Begthel, H., Vries, R.G., et al. 2010. Lgr6 marks stem cells in the hair follicle that generate all cell lineages of the skin. *Science* 327:1385-1389.
43. Till, J.E., and Mc, C.E. 1961. A direct measurement of the radiation sensitivity of normal mouse bone marrow cells. *Radiat Res* 14:213-222.
44. Uchida, N., and Weissman, I.L. 1992. Searching for hematopoietic stem cells: evidence that Thy-1.1lo Lin- Sca-1+ cells are the only stem cells in C57BL/Ka-Thy-1.1 bone marrow. *J Exp Med* 175:175-184.
45. Chan, C.K., Seo, E.Y., Chen, J.Y., Lo, D., McArdle, A., Sinha, R., Tevlin, R., Seita, J., Vincent-Tompkins, J., Wearda, T., et al. 2015. Identification and specification of the mouse skeletal stem cell. *Cell* 160:285-298.
46. Cotsarelis, G., Sun, T.T., and Lavker, R.M. 1990. Label-retaining cells reside in the bulge area of pilosebaceous unit: implications for follicular stem cells, hair cycle, and skin carcinogenesis. *Cell* 61:1329-1337.
47. Takeda, N., Jain, R., LeBoeuf, M.R., Wang, Q., Lu, M.M., and Epstein, J.A. 2011. Interconversion between intestinal stem cell populations in distinct niches. *Science* 334:1420-1424.
48. Tian, H., Biehs, B., Warming, S., Leong, K.G., Rangell, L., Klein, O.D., and de Sauvage, F.J. 2011. A reserve stem cell population in small intestine renders Lgr5-positive cells dispensable. *Nature* 478:255-259.
49. Yan, K.S., Chia, L.A., Li, X., Ootani, A., Su, J., Lee, J.Y., Su, N., Luo, Y., Heilshorn, S.C., Amieva, M.R., et al. 2012. The intestinal stem cell markers Bmi1 and Lgr5 identify two functionally distinct populations. *Proc Natl Acad Sci U S A* 109:466-471.

50. Yoon, S.M., Gerasimidou, D., Kuwahara, R., Hytiroglou, P., Yoo, J.E., Park, Y.N., and Theise, N.D. 2011. Epithelial cell adhesion molecule (EpCAM) marks hepatocytes newly derived from stem/progenitor cells in humans. *Hepatology* 53:964-973.
51. Stueck, A.E., and Wanless, I.R. 2015. Hepatocyte buds derived from progenitor cells repopulate regions of parenchymal extinction in human cirrhosis. *Hepatology* 61:1696-1707.
52. He, J., Lu, H., Zou, Q., and Luo, L. 2014. Regeneration of liver after extreme hepatocyte loss occurs mainly via biliary transdifferentiation in zebrafish. *Gastroenterology* 146:789-800 e788.
53. Choi, T.Y., Ninov, N., Stainier, D.Y., and Shin, D. 2014. Extensive conversion of hepatic biliary epithelial cells to hepatocytes after near total loss of hepatocytes in zebrafish. *Gastroenterology* 146:776-788.
54. Evarts, R.P., Nagy, P., Marsden, E., and Thorgeirsson, S.S. 1987. A precursor-product relationship exists between oval cells and hepatocytes in rat liver. *Carcinogenesis* 8:1737-1740.
55. Yovchev, M.I., Grozdanov, P.N., Zhou, H., Racherla, H., Guha, C., and Dabeva, M.D. 2008. Identification of adult hepatic progenitor cells capable of repopulating injured rat liver. *Hepatology* 47:636-647.
56. Espanol-Suner, R., Carpentier, R., Van Hul, N., Legry, V., Achouri, Y., Cordi, S., Jacquemin, P., Lemaigre, F., and Leclercq, I.A. 2012. Liver progenitor cells yield functional hepatocytes in response to chronic liver injury in mice. *Gastroenterology* 143:1564-1575 e1567.
57. Rodrigo-Torres, D., Affo, S., Coll, M., Morales-Ibanez, O., Millan, C., Blaya, D., Alvarez-Guaita, A., Rentero, C., Lozano, J.J., Maestro, M.A., et al. 2014. The biliary epithelium gives rise to liver progenitor cells. *Hepatology* 60:1367-1377.
58. Jors, S., Jeliazkova, P., Ringelhan, M., Thalhammer, J., Durl, S., Ferrer, J., Sander, M., Heikenwalder, M., Schmid, R.M., Siveke, J.T., et al. 2015. Lineage fate of ductular reactions in liver injury and carcinogenesis. *J Clin Invest* 125:2445-2457.
59. Lu, W.Y., Bird, T.G., Boulter, L., Tsuchiya, A., Cole, A.M., Hay, T., Guest, R.V., Wojtacha, D., Man, T.Y., Mackinnon, A., et al. 2015. Hepatic progenitor cells of biliary origin with liver repopulation capacity. *Nat Cell Biol* 17:971-983.
60. Demetris, A.J., Seaberg, E.C., Wennerberg, A., Ionellie, J., and Michalopoulos, G. 1996. Ductular reaction after submassive necrosis in humans. Special emphasis on analysis of ductular hepatocytes. *Am J Pathol* 149:439-448.
61. Desmet, V., Roskams, T., and Van Eyken, P. 1995. Ductular reaction in the liver. *Pathol Res Pract* 191:513-524.
62. Roskams, T.A., Theise, N.D., Balabaud, C., Bhagat, G., Bhathal, P.S., Bioulac-Sage, P., Brunt, E.M., Crawford, J.M., Crosby, H.A., Desmet, V., et al. 2004. Nomenclature of the finer branches of the biliary tree: canals, ductules, and ductular reactions in human livers. *Hepatology* 39:1739-1745.
63. Paku, S., Schnur, J., Nagy, P., and Thorgeirsson, S.S. 2001. Origin and structural evolution of the early proliferating oval cells in rat liver. *Am J Pathol* 158:1313-1323.
64. Kaneko, K., Kamimoto, K., Miyajima, A., and Itoh, T. 2015. Adaptive remodeling of the biliary architecture underlies liver homeostasis. *Hepatology* 61:2056-2066.
65. Shinozuka, H., Lombardi, B., Sell, S., and Iammarino, R.M. 1978. Early histological and functional alterations of ethionine liver carcinogenesis in rats fed a choline-deficient diet. *Cancer Res* 38:1092-1098.

66. Sell, S. 1978. Distribution of alpha-fetoprotein- and albumin-containing cells in the livers of Fischer rats fed four cycles of N-2-fluorenylacetamide. *Cancer Res* 38:3107-3113.
67. Jelnes, P., Santoni-Rugiu, E., Rasmussen, M., Friis, S.L., Nielsen, J.H., Tygstrup, N., and Bisgaard, H.C. 2007. Remarkable heterogeneity displayed by oval cells in rat and mouse models of stem cell-mediated liver regeneration. *Hepatology* 45:1462-1470.
68. Falkowski, O., An, H.J., Ianus, I.A., Chiriboga, L., Yee, H., West, A.B., and Theise, N.D. 2003. Regeneration of hepatocyte 'buds' in cirrhosis from intrabiliary stem cells. *J Hepatol* 39:357-364.
69. Kuwahara, R., Kofman, A.V., Landis, C.S., Swenson, E.S., Barendswaard, E., and Theise, N.D. 2008. The hepatic stem cell niche: identification by label-retaining cell assay. *Hepatology* 47:1994-2002.
70. Furuyama, K., Kawaguchi, Y., Akiyama, H., Horiguchi, M., Kodama, S., Kuhara, T., Hosokawa, S., Elbahrawy, A., Soeda, T., Koizumi, M., et al. 2011. Continuous cell supply from a Sox9-expressing progenitor zone in adult liver, exocrine pancreas and intestine. *Nat Genet* 43:34-41.
71. Lowes, K.N., Brennan, B.A., Yeoh, G.C., and Olynyk, J.K. 1999. Oval cell numbers in human chronic liver diseases are directly related to disease severity. *Am J Pathol* 154:537-541.
72. Trautwein, C., Will, M., Kubicka, S., Rakemann, T., Flemming, P., and Manns, M.P. 1999. 2-acetaminofluorene blocks cell cycle progression after hepatectomy by p21 induction and lack of cyclin E expression. *Oncogene* 18:6443-6453.
73. Dolle, L., Best, J., Mei, J., Al Battah, F., Reynaert, H., van Grunsven, L.A., and Geerts, A. 2010. The quest for liver progenitor cells: a practical point of view. *J Hepatol* 52:117-129.
74. Dorrell, C., Erker, L., Schug, J., Kopp, J.L., Canaday, P.S., Fox, A.J., Smirnova, O., Duncan, A.W., Finegold, M.J., Sander, M., et al. 2011. Prospective isolation of a bipotential clonogenic liver progenitor cell in adult mice. *Genes Dev* 25:1193-1203.
75. Suzuki, A., Sekiya, S., Onishi, M., Oshima, N., Kiyonari, H., Nakauchi, H., and Taniguchi, H. 2008. Flow cytometric isolation and clonal identification of self-renewing bipotent hepatic progenitor cells in adult mouse liver. *Hepatology* 48:1964-1978.
76. Okabe, M., Tsukahara, Y., Tanaka, M., Suzuki, K., Saito, S., Kamiya, Y., Tsujimura, T., Nakamura, K., and Miyajima, A. 2009. Potential hepatic stem cells reside in EpCAM+ cells of normal and injured mouse liver. *Development* 136:1951-1960.
77. Huch, M., Dorrell, C., Boj, S.F., van Es, J.H., Li, V.S., van de Wetering, M., Sato, T., Hamer, K., Sasaki, N., Finegold, M.J., et al. 2013. In vitro expansion of single Lgr5+ liver stem cells induced by Wnt-driven regeneration. *Nature* 494:247-250.
78. Huch, M., Gehart, H., van Boxtel, R., Hamer, K., Blokzijl, F., Verstegen, M.M., Ellis, E., van Wenum, M., Fuchs, S.A., de Ligt, J., et al. 2015. Long-term culture of genome-stable bipotent stem cells from adult human liver. *Cell* 160:299-312.
79. Sell, S. 1998. Comparison of liver progenitor cells in human atypical ductular reactions with those seen in experimental models of liver injury. *Hepatology* 27:317-331.
80. Zhou, H., Rogler, L.E., Teperman, L., Morgan, G., and Rogler, C.E. 2007. Identification of hepatocytic and bile ductular cell lineages and candidate stem cells in bipolar ductular reactions in cirrhotic human liver. *Hepatology* 45:716-724.

81. Roskams, T., Yang, S.Q., Koteish, A., Durnez, A., DeVos, R., Huang, X., Achten, R., Verslype, C., and Diehl, A.M. 2003. Oxidative stress and oval cell accumulation in mice and humans with alcoholic and nonalcoholic fatty liver disease. *Am J Pathol* 163:1301-1311.
82. Clouston, A.D., Powell, E.E., Walsh, M.J., Richardson, M.M., Demetris, A.J., and Jonsson, J.R. 2005. Fibrosis correlates with a ductular reaction in hepatitis C: roles of impaired replication, progenitor cells and steatosis. *Hepatology* 41:809-818.
83. Wood, M.J., Gadd, V.L., Powell, L.W., Ramm, G.A., and Clouston, A.D. 2014. Ductular reaction in hereditary hemochromatosis: the link between hepatocyte senescence and fibrosis progression. *Hepatology* 59:848-857.
84. Xiao, S.Y., Lu, L., and Wang, H.L. 2008. Fibrosing cholestatic hepatitis: clinicopathologic spectrum, diagnosis and pathogenesis. *Int J Clin Exp Pathol* 1:396-402.
85. Clouston, A.D., Jonsson, J.R., and Powell, E.E. 2009. Hepatic progenitor cell-mediated regeneration and fibrosis: chicken or egg? *Hepatology* 49:1424-1426.
86. Williams, M.J., Clouston, A.D., and Forbes, S.J. 2014. Links between hepatic fibrosis, ductular reaction, and progenitor cell expansion. *Gastroenterology* 146:349-356.
87. Jakubowski, A., Ambrose, C., Parr, M., Lincecum, J.M., Wang, M.Z., Zheng, T.S., Browning, B., Michaelson, J.S., Baetscher, M., Wang, B., et al. 2005. TWEAK induces liver progenitor cell proliferation. *J Clin Invest* 115:2330-2340.
88. Kuramitsu, K., Sverdlov, D.Y., Liu, S.B., Csizmadia, E., Burkly, L., Schuppan, D., Hanto, D.W., Otterbein, L.E., and Popov, Y. 2013. Failure of fibrotic liver regeneration in mice is linked to a severe fibrogenic response driven by hepatic progenitor cell activation. *Am J Pathol* 183:182-194.
89. Novoyatleva, T., Schymura, Y., Janssen, W., Strobl, F., Swiercz, J.M., Patra, C., Posern, G., Wietelmann, A., Zheng, T.S., Schermuly, R.T., et al. 2013. Deletion of Fn14 receptor protects from right heart fibrosis and dysfunction. *Basic Res Cardiol* 108:325.
90. Dohi, T., and Burkly, L.C. 2012. The TWEAK/Fn14 pathway as an aggravating and perpetuating factor in inflammatory diseases: focus on inflammatory bowel diseases. *J Leukoc Biol* 92:265-279.
91. Kim, K.H., Chen, C.C., Alpini, G., and Lau, L.F. 2015. CCN1 induces hepatic ductular reaction through integrin alphavbeta(5)-mediated activation of NF-kappaB. *J Clin Invest* 125:1886-1900.
92. Van Hul, N.K., Abarca-Quinones, J., Sempoux, C., Horsmans, Y., and Leclercq, I.A. 2009. Relation between liver progenitor cell expansion and extracellular matrix deposition in a CDE-induced murine model of chronic liver injury. *Hepatology* 49:1625-1635.
93. Thomas, J.A., Pope, C., Wojtacha, D., Robson, A.J., Gordon-Walker, T.T., Hartland, S., Ramachandran, P., Van Deemter, M., Hume, D.A., Iredale, J.P., et al. 2011. Macrophage therapy for murine liver fibrosis recruits host effector cells improving fibrosis, regeneration, and function. *Hepatology* 53:2003-2015.
94. Evarts, R.P., Hu, Z., Omori, N., Omori, M., Marsden, E.R., and Thorgeirsson, S.S. 1996. Precursor-product relationship between oval cells and hepatocytes: comparison between tritiated thymidine and bromodeoxyuridine as tracers. *Carcinogenesis* 17:2143-2151.
95. Lemaigre, F.P. 2015. Determining the fate of hepatic cells by lineage tracing: facts and pitfalls. *Hepatology* 61:2100-2103.

96. Ireland, H., Kemp, R., Houghton, C., Howard, L., Clarke, A.R., Sansom, O.J., and Winton, D.J. 2004. Inducible Cre-mediated control of gene expression in the murine gastrointestinal tract: effect of loss of beta-catenin. *Gastroenterology* 126:1236-1246.
97. Tanimizu, N., Nishikawa, Y., Ichinohe, N., Akiyama, H., and Mitaka, T. 2014. Sry HMG box protein 9-positive (Sox9+) epithelial cell adhesion molecule-negative (EpCAM-) biphenotypic cells derived from hepatocytes are involved in mouse liver regeneration. *J Biol Chem* 289:7589-7598.
98. Kuhn, R., Schwenk, F., Aguet, M., and Rajewsky, K. 1995. Inducible gene targeting in mice. *Science* 269:1427-1429.
99. Tarlow, B.D., Finegold, M.J., and Grompe, M. 2014. Clonal tracing of Sox9+ liver progenitors in mouse oval cell injury. *Hepatology* 60:278-289.
100. Chevalier, C., Nicolas, J.F., and Petit, A.C. 2014. Preparation and delivery of 4-hydroxy-tamoxifen for clonal and polyclonal labeling of cells of the surface ectoderm, skin, and hair follicle. *Methods Mol Biol* 1195:239-245.
101. Brake, R.L., Simmons, P.J., and Begley, C.G. 2004. Cross-contamination with tamoxifen induces transgene expression in non-exposed inducible transgenic mice. *Genet Mol Res* 3:456-462.
102. Malato, Y., Naqvi, S., Schurmann, N., Ng, R., Wang, B., Zape, J., Kay, M.A., Grimm, D., and Willenbring, H. 2011. Fate tracing of mature hepatocytes in mouse liver homeostasis and regeneration. *J Clin Invest* 121:4850-4860.
103. Yanger, K., Zong, Y., Maggs, L.R., Shapira, S.N., Maddipati, R., Aiello, N.M., Thung, S.N., Wells, R.G., Greenbaum, L.E., and Stanger, B.Z. 2013. Robust cellular reprogramming occurs spontaneously during liver regeneration. *Genes Dev* 27:719-724.
104. Sekiya, S., and Suzuki, A. 2014. Hepatocytes, rather than cholangiocytes, can be the major source of primitive ductules in the chronically injured mouse liver. *Am J Pathol* 184:1468-1478.
105. Yang, L., Jung, Y., Omenetti, A., Witek, R.P., Choi, S., Vandongen, H.M., Huang, J., Alpini, G.D., and Diehl, A.M. 2008. Fate-mapping evidence that hepatic stellate cells are epithelial progenitors in adult mouse livers. *Stem Cells* 26:2104-2113.
106. Mederacke, I., Hsu, C.C., Troeger, J.S., Huebener, P., Mu, X., Dapito, D.H., Pradere, J.P., and Schwabe, R.F. 2013. Fate tracing reveals hepatic stellate cells as dominant contributors to liver fibrosis independent of its aetiology. *Nat Commun* 4:2823.
107. Michelotti, G.A., Xie, G., Swiderska, M., Choi, S.S., Karaca, G., Kruger, L., Premont, R., Yang, L., Syn, W.K., Metzger, D., et al. 2013. Smoothened is a master regulator of adult liver repair. *J Clin Invest* 123:2380-2394.
108. Clawson, G.A. 1989. Mechanisms of carbon tetrachloride hepatotoxicity. *Pathol Immunopathol Res* 8:104-112.
109. Yanger, K., Knigin, D., Zong, Y., Maggs, L., Gu, G., Akiyama, H., Pikarsky, E., and Stanger, B.Z. 2014. Adult hepatocytes are generated by self-duplication rather than stem cell differentiation. *Cell Stem Cell* 15:340-349.
110. Lee, W.M., and Seremba, E. 2008. Etiologies of acute liver failure. *Curr Opin Crit Care* 14:198-201.
111. Kofman, A.V., Morgan, G., Kirschenbaum, A., Osbeck, J., Hussain, M., Swenson, S., and Theise, N.D. 2005. Dose- and time-dependent oval cell reaction in acetaminophen-induced murine liver injury. *Hepatology* 41:1252-1261.

112. Morley, C.G., and Boyer, J.L. 1977. Stimulation of hepatocellular proliferation by a serum factor from thioacetamide-treated rats. *Biochim Biophys Acta* 477:165-176.
113. Chieli, E., and Malvaldi, G. 1984. Role of the microsomal FAD-containing monooxygenase in the liver toxicity of thioacetamide S-oxide. *Toxicology* 31:41-52.
114. Yeh, C.N., Maitra, A., Lee, K.F., Jan, Y.Y., and Chen, M.F. 2004. Thioacetamide-induced intestinal-type cholangiocarcinoma in rat: an animal model recapitulating the multi-stage progression of human cholangiocarcinoma. *Carcinogenesis* 25:631-636.
115. Boulter, L., Guest, R.V., Kendall, T.J., Wilson, D.H., Wojtacha, D., Robson, A.J., Ridgway, R.A., Samuel, K., Van Rooijen, N., Barry, S.T., et al. 2015. WNT signaling drives cholangiocarcinoma growth and can be pharmacologically inhibited. *J Clin Invest* 125:1269-1285.
116. Guest, R.V., Boulter, L., Kendall, T.J., Minnis-Lyons, S.E., Walker, R., Wigmore, S.J., Sansom, O.J., and Forbes, S.J. 2014. Cell lineage tracing reveals a biliary origin of intrahepatic cholangiocarcinoma. *Cancer Res* 74:1005-1010.
117. Ohlson, L.C., Koroxenidou, L., and Hallstrom, I.P. 1998. Inhibition of in vivo rat liver regeneration by 2-acetylaminofluorene affects the regulation of cell cycle-related proteins. *Hepatology* 27:691-696.
118. Nagy, P., Bisgaard, H.C., and Thorgeirsson, S.S. 1994. Expression of hepatic transcription factors during liver development and oval cell differentiation. *J Cell Biol* 126:223-233.
119. Sell, S. 1994. Liver stem cells. *Mod Pathol* 7:105-112.
120. Golding, M., Sarraf, C.E., Lalani, E.N., Anilkumar, T.V., Edwards, R.J., Nagy, P., Thorgeirsson, S.S., and Alison, M.R. 1995. Oval cell differentiation into hepatocytes in the acetylaminofluorene-treated regenerating rat liver. *Hepatology* 22:1243-1253.
121. DeBaun, J.R., Rowley, J.Y., Miller, E.C., and Miller, J.A. 1968. Sulfotransferase activation of N-hydroxy-2-acetylaminofluorene in rodent livers susceptible and resistant to this carcinogen. *Proc Soc Exp Biol Med* 129:268-273.
122. Akhurst, B., Croager, E.J., Farley-Roche, C.A., Ong, J.K., Dumble, M.L., Knight, B., and Yeoh, G.C. 2001. A modified choline-deficient, ethionine-supplemented diet protocol effectively induces oval cells in mouse liver. *Hepatology* 34:519-522.
123. Boulter, L., Govaere, O., Bird, T.G., Radulescu, S., Ramachandran, P., Pellicoro, A., Ridgway, R.A., Seo, S.S., Spee, B., Van Rooijen, N., et al. 2012. Macrophage-derived Wnt opposes Notch signaling to specify hepatic progenitor cell fate in chronic liver disease. *Nat Med* 18:572-579.
124. Guest, I., Ilic, Z., and Sell, S. 2010. Age dependence of oval cell responses and bile duct carcinomas in male fischer 344 rats fed a cyclic choline-deficient, ethionine-supplemented diet. *Hepatology* 52:1750-1757.
125. Schaub, J.R., Malato, Y., Gormond, C., and Willenbring, H. 2014. Evidence against a stem cell origin of new hepatocytes in a common mouse model of chronic liver injury. *Cell Rep* 8:933-939.
126. Shin, S., Upadhyay, N., Greenbaum, L.E., and Kaestner, K.H. 2015. Ablation of Foxl1-Cre-labeled hepatic progenitor cells and their descendants impairs recovery of mice from liver injury. *Gastroenterology* 148:192-202 e193.
127. Passman, A.M., Strauss, R.P., McSpadden, S.B., Finch-Edmondson, M.L., Woo, K.H., Diepeveen, L.A., London, R., Callus, B.A., and Yeoh, G.C. 2015. A modified choline-

deficient, ethionine-supplemented diet reduces morbidity and retains a liver progenitor cell response. *Dis Model Mech*.

128. Rinella, M.E., Elias, M.S., Smolak, R.R., Fu, T., Borensztajn, J., and Green, R.M. 2008. Mechanisms of hepatic steatosis in mice fed a lipogenic methionine choline-deficient diet. *J Lipid Res* 49:1068-1076.
129. Leclercq, I.A., Farrell, G.C., Field, J., Bell, D.R., Gonzalez, F.J., and Robertson, G.R. 2000. CYP2E1 and CYP4A as microsomal catalysts of lipid peroxides in murine nonalcoholic steatohepatitis. *J Clin Invest* 105:1067-1075.
130. Rinella, M.E., and Green, R.M. 2004. The methionine-choline deficient dietary model of steatohepatitis does not exhibit insulin resistance. *J Hepatol* 40:47-51.
131. Machado, M.V., Michelotti, G.A., Xie, G., Almeida Pereira, T., Boursier, J., Bohnic, B., Guy, C.D., and Diehl, A.M. 2015. Mouse models of diet-induced nonalcoholic steatohepatitis reproduce the heterogeneity of the human disease. *PLoS One* 10:e0127991.
132. Wang, X., Foster, M., Al-Dhalimy, M., Lagasse, E., Finegold, M., and Grompe, M. 2003. The origin and liver repopulating capacity of murine oval cells. *Proc Natl Acad Sci U S A* 100 Suppl 1:11881-11888.
133. Tarlow, B.D., Pelz, C., Naugler, W.E., Wakefield, L., Wilson, E.M., Finegold, M.J., and Grompe, M. 2014. Bipotential adult liver progenitors are derived from chronically injured mature hepatocytes. *Cell Stem Cell* 15:605-618.
134. Kountouras, J., Billing, B.H., and Scheuer, P.J. 1984. Prolonged bile duct obstruction: a new experimental model for cirrhosis in the rat. *Br J Exp Pathol* 65:305-311.
135. Tuchweber, B., Desmouliere, A., Bochaton-Piallat, M.L., Rubbia-Brandt, L., and Gabbiani, G. 1996. Proliferation and phenotypic modulation of portal fibroblasts in the early stages of cholestatic fibrosis in the rat. *Lab Invest* 74:265-278.
136. Desmouliere, A., Darby, I., Costa, A.M., Raccurt, M., Tuchweber, B., Sommer, P., and Gabbiani, G. 1997. Extracellular matrix deposition, lysyl oxidase expression, and myofibroblastic differentiation during the initial stages of cholestatic fibrosis in the rat. *Lab Invest* 76:765-778.
137. Fickert, P., Fuchsbichler, A., Wagner, M., Zollner, G., Kaser, A., Tilg, H., Krause, R., Lammert, F., Langner, C., Zatloukal, K., et al. 2004. Regurgitation of bile acids from leaky bile ducts causes sclerosing cholangitis in Mdr2 (Abcb4) knockout mice. *Gastroenterology* 127:261-274.
138. Popov, Y., Patsenker, E., Fickert, P., Trauner, M., and Schuppan, D. 2005. Mdr2 (Abcb4)-/- mice spontaneously develop severe biliary fibrosis via massive dysregulation of pro- and antifibrogenic genes. *J Hepatol* 43:1045-1054.
139. Curado, S., Anderson, R.M., Jungblut, B., Mumm, J., Schroeter, E., and Stainier, D.Y. 2007. Conditional targeted cell ablation in zebrafish: a new tool for regeneration studies. *Dev Dyn* 236:1025-1035.
140. Fu, L., Zhu, X., Yi, F., Liu, G.H., and Izpisua Belmonte, J.C. 2014. Regenerative medicine: transdifferentiation in vivo. *Cell Res* 24:141-142.
141. Michalopoulos, G.K. 2014. The liver is a peculiar organ when it comes to stem cells. *Am J Pathol* 184:1263-1267.
142. Miyajima, A., Tanaka, M., and Itoh, T. 2014. Stem/progenitor cells in liver development, homeostasis, regeneration, and reprogramming. *Cell Stem Cell* 14:561-574.
143. Alison, M.R., and Lin, W.R. 2015. Diverse routes to liver regeneration. *J Pathol*.

144. Huch, M. 2015. Regenerative biology: The versatile and plastic liver. *Nature* 517:155-156.
145. Hindley, C.J., Mastrogiovanni, G., and Huch, M. 2014. The plastic liver: differentiated cells, stem cells, every cell? *J Clin Invest* 124:5099-5102.
146. Zajicek, G., Oren, R., and Weinreb, M., Jr. 1985. The streaming liver. *Liver* 5:293-300.
147. Turner, R., Lozoya, O., Wang, Y., Cardinale, V., Gaudio, E., Alpini, G., Mendel, G., Wauthier, E., Barbier, C., Alvaro, D., et al. 2011. Human hepatic stem cell and maturational liver lineage biology. *Hepatology* 53:1035-1045.
148. Fellous, T.G., Islam, S., Tadrous, P.J., Elia, G., Kocher, H.M., Bhattacharya, S., Mears, L., Turnbull, D.M., Taylor, R.W., Greaves, L.C., et al. 2009. Locating the stem cell niche and tracing hepatocyte lineages in human liver. *Hepatology* 49:1655-1663.
149. Font-Burgada, J., Shalapour, S., Ramaswamy, S., Hsueh, B., Rossell, D., Umemura, A., Taniguchi, K., Nakagawa, H., Valasek, M.A., Ye, L., et al. 2015. Hybrid Periportal Hepatocytes Regenerate the Injured Liver without Giving Rise to Cancer. *Cell* 162:766-779.
150. Wang, B., Zhao, L., Fish, M., Logan, C.Y., and Nusse, R. 2015. Self-renewing diploid Axin2(+) cells fuel homeostatic renewal of the liver. *Nature* 524:180-185.
151. Guidotti, J.E., Bregerie, O., Robert, A., Debey, P., Brechot, C., and Desdouets, C. 2003. Liver cell polyploidization: a pivotal role for binuclear hepatocytes. *J Biol Chem* 278:19095-19101.
152. Comai, L. 2005. The advantages and disadvantages of being polyploid. *Nat Rev Genet* 6:836-846.
153. Sigal, S.H., Rajvanshi, P., Gorla, G.R., Sokhi, R.P., Saxena, R., Gebhard, D.R., Jr., Reid, L.M., and Gupta, S. 1999. Partial hepatectomy-induced polyploidy attenuates hepatocyte replication and activates cell aging events. *Am J Physiol* 276:G1260-1272.
154. Magami, Y., Azuma, T., Inokuchi, H., Kokuno, S., Moriyasu, F., Kawai, K., and Hattori, T. 2002. Cell proliferation and renewal of normal hepatocytes and bile duct cells in adult mouse liver. *Liver* 22:419-425.
155. Andersson, E.R., Sandberg, R., and Lendahl, U. 2011. Notch signaling: simplicity in design, versatility in function. *Development* 138:3593-3612.
156. Geisler, F., and Strazzabosco, M. 2015. Emerging roles of Notch signaling in liver disease. *Hepatology* 61:382-392.
157. D'Souza, B., Meloty-Kapella, L., and Weinmaster, G. 2010. Canonical and non-canonical Notch ligands. *Curr Top Dev Biol* 92:73-129.
158. Bachmann, E., Krogh, T.N., Hojrup, P., Skjodt, K., and Teisner, B. 1996. Mouse fetal antigen 1 (mFA1), the circulating gene product of mdlk, pref-1 and SCP-1: isolation, characterization and biology. *J Reprod Fertil* 107:279-285.
159. Baladron, V., Ruiz-Hidalgo, M.J., Nueda, M.L., Diaz-Guerra, M.J., Garcia-Ramirez, J.J., Bonvini, E., Gubina, E., and Laborda, J. 2005. dlk acts as a negative regulator of Notch1 activation through interactions with specific EGF-like repeats. *Exp Cell Res* 303:343-359.
160. Komatsu, H., Chao, M.Y., Larkins-Ford, J., Corkins, M.E., Somers, G.A., Tucey, T., Dionne, H.M., White, J.Q., Wani, K., Boxem, M., et al. 2008. OSM-11 facilitates LIN-12 Notch signaling during Caenorhabditis elegans vulval development. *PLoS Biol* 6:e196.

161. Gibson, M.A., Hatzinikolas, G., Kumaratilake, J.S., Sandberg, L.B., Nicholl, J.K., Sutherland, G.R., and Cleary, E.G. 1996. Further characterization of proteins associated with elastic fiber microfibrils including the molecular cloning of MAGP-2 (MP25). *J Biol Chem* 271:1096-1103.
162. Sakamoto, K., Yamaguchi, S., Ando, R., Miyawaki, A., Kabasawa, Y., Takagi, M., Li, C.L., Perbal, B., and Katsube, K. 2002. The nephroblastoma overexpressed gene (NOV/ccn3) protein associates with Notch1 extracellular domain and inhibits myoblast differentiation via Notch signaling pathway. *J Biol Chem* 277:29399-29405.
163. Martinez Arias, A., Zecchini, V., and Brennan, K. 2002. CSL-independent Notch signalling: a checkpoint in cell fate decisions during development? *Curr Opin Genet Dev* 12:524-533.
164. Liu, J., Sato, C., Cerletti, M., and Wagers, A. 2010. Notch signaling in the regulation of stem cell self-renewal and differentiation. *Curr Top Dev Biol* 92:367-409.
165. Hori, K., Sen, A., and Artavanis-Tsakonas, S. 2013. Notch signaling at a glance. *J Cell Sci* 126:2135-2140.
166. Kurooka, H., Kuroda, K., and Honjo, T. 1998. Roles of the ankyrin repeats and C-terminal region of the mouse notch1 intracellular region. *Nucleic Acids Res* 26:5448-5455.
167. Beatus, P., Lundkvist, J., Oberg, C., Pedersen, K., and Lendahl, U. 2001. The origin of the ankyrin repeat region in Notch intracellular domains is critical for regulation of HES promoter activity. *Mech Dev* 104:3-20.
168. Bellavia, D., Checquolo, S., Campese, A.F., Felli, M.P., Gulino, A., and Screpanti, I. 2008. Notch3: from subtle structural differences to functional diversity. *Oncogene* 27:5092-5098.
169. McDaniell, R., Warthen, D.M., Sanchez-Lara, P.A., Pai, A., Krantz, I.D., Piccoli, D.A., and Spinner, N.B. 2006. NOTCH2 mutations cause Alagille syndrome, a heterogeneous disorder of the notch signaling pathway. *Am J Hum Genet* 79:169-173.
170. Oda, T., Elkahloun, A.G., Pike, B.L., Okajima, K., Krantz, I.D., Genin, A., Piccoli, D.A., Meltzer, P.S., Spinner, N.B., Collins, F.S., et al. 1997. Mutations in the human Jagged1 gene are responsible for Alagille syndrome. *Nat Genet* 16:235-242.
171. Li, L., Krantz, I.D., Deng, Y., Genin, A., Banta, A.B., Collins, C.C., Qi, M., Trask, B.J., Kuo, W.L., Cochran, J., et al. 1997. Alagille syndrome is caused by mutations in human Jagged1, which encodes a ligand for Notch1. *Nat Genet* 16:243-251.
172. Bonafe, L., Giunta, C., Gassner, M., Steinmann, B., and Superti-Furga, A. 2003. A cluster of autosomal recessive spondylocostal dysostosis caused by three newly identified DLL3 mutations segregating in a small village. *Clin Genet* 64:28-35.
173. Joutel, A., Vahedi, K., Corpechot, C., Troesch, A., Chabriat, H., Vayssiere, C., Cruaud, C., Maciazek, J., Weissenbach, J., Bousser, M.G., et al. 1997. Strong clustering and stereotyped nature of Notch3 mutations in CADASIL patients. *Lancet* 350:1511-1515.
174. Joutel, A., Monet, M., Domenga, V., Riant, F., and Tournier-Lasserve, E. 2004. Pathogenic mutations associated with cerebral autosomal dominant arteriopathy with subcortical infarcts and leukoencephalopathy differently affect Jagged1 binding and Notch3 activity via the RBP/JK signaling Pathway. *Am J Hum Genet* 74:338-347.

175. Hicks, C., Johnston, S.H., diSibio, G., Collazo, A., Vogt, T.F., and Weinmaster, G. 2000. Fringe differentially modulates Jagged1 and Delta1 signalling through Notch1 and Notch2. *Nat Cell Biol* 2:515-520.
176. Kato, T.M., Kawaguchi, A., Kosodo, Y., Niwa, H., and Matsuzaki, F. 2010. Lunatic fringe potentiates Notch signaling in the developing brain. *Mol Cell Neurosci* 45:12-25.
177. Fortini, M.E. 2009. Notch signaling: the core pathway and its posttranslational regulation. *Dev Cell* 16:633-647.
178. del Alamo, D., Rouault, H., and Schweisguth, F. 2011. Mechanism and significance of cis-inhibition in Notch signalling. *Curr Biol* 21:R40-47.
179. Micchelli, C.A., Rulifson, E.J., and Blair, S.S. 1997. The function and regulation of cut expression on the wing margin of Drosophila: Notch, Wingless and a dominant negative role for Delta and Serrate. *Development* 124:1485-1495.
180. Miller, A.C., Lyons, E.L., and Herman, T.G. 2009. cis-Inhibition of Notch by endogenous Delta biases the outcome of lateral inhibition. *Curr Biol* 19:1378-1383.
181. Sprinzak, D., Lakhanpal, A., Lebon, L., Santat, L.A., Fontes, M.E., Anderson, G.A., Garcia-Ojalvo, J., and Elowitz, M.B. 2010. Cis-interactions between Notch and Delta generate mutually exclusive signalling states. *Nature* 465:86-90.
182. Dunwoodie, S.L., Henrique, D., Harrison, S.M., and Beddington, R.S. 1997. Mouse Dll3: a novel divergent Delta gene which may complement the function of other Delta homologues during early pattern formation in the mouse embryo. *Development* 124:3065-3076.
183. Ladi, E., Nichols, J.T., Ge, W., Miyamoto, A., Yao, C., Yang, L.T., Boulter, J., Sun, Y.E., Kintner, C., and Weinmaster, G. 2005. The divergent DSL ligand Dll3 does not activate Notch signaling but cell autonomously attenuates signaling induced by other DSL ligands. *J Cell Biol* 170:983-992.
184. Konishi, J., Kawaguchi, K.S., Vo, H., Haruki, N., Gonzalez, A., Carbone, D.P., and Dang, T.P. 2007. Gamma-secretase inhibitor prevents Notch3 activation and reduces proliferation in human lung cancers. *Cancer Res* 67:8051-8057.
185. Sansone, P., Storci, G., Tavolari, S., Guarnieri, T., Giovannini, C., Taffurelli, M., Ceccarelli, C., Santini, D., Paterini, P., Marcu, K.B., et al. 2007. IL-6 triggers malignant features in mammospheres from human ductal breast carcinoma and normal mammary gland. *J Clin Invest* 117:3988-4002.
186. Kageyama, R., Ohtsuka, T., Shimojo, H., and Imayoshi, I. 2009. Dynamic regulation of Notch signaling in neural progenitor cells. *Curr Opin Cell Biol* 21:733-740.
187. Radtke, F., Fasnacht, N., and Macdonald, H.R. 2010. Notch signaling in the immune system. *Immunity* 32:14-27.
188. Rao, P., and Kadesch, T. 2003. The intracellular form of notch blocks transforming growth factor beta-mediated growth arrest in Mv1Lu epithelial cells. *Mol Cell Biol* 23:6694-6701.
189. Cohen, B., Shimizu, M., Izrailit, J., Ng, N.F., Buchman, Y., Pan, J.G., Dering, J., and Reedijk, M. 2010. Cyclin D1 is a direct target of JAG1-mediated Notch signaling in breast cancer. *Breast Cancer Res Treat* 123:113-124.
190. Rangarajan, A., Talora, C., Okuyama, R., Nicolas, M., Mammucari, C., Oh, H., Aster, J.C., Krishna, S., Metzger, D., Chambon, P., et al. 2001. Notch signaling is a direct determinant of keratinocyte growth arrest and entry into differentiation. *EMBO J* 20:3427-3436.

191. Ong, C.T., Cheng, H.T., Chang, L.W., Ohtsuka, T., Kageyama, R., Stormo, G.D., and Kopan, R. 2006. Target selectivity of vertebrate notch proteins. Collaboration between discrete domains and CSL-binding site architecture determines activation probability. *J Biol Chem* 281:5106-5119.
192. Itoh, M., Kim, C.H., Palardy, G., Oda, T., Jiang, Y.J., Maust, D., Yeo, S.Y., Lorick, K., Wright, G.J., Ariza-McNaughton, L., et al. 2003. Mind bomb is a ubiquitin ligase that is essential for efficient activation of Notch signaling by Delta. *Dev Cell* 4:67-82.
193. Jeffries, S., Robbins, D.J., and Capobianco, A.J. 2002. Characterization of a high-molecular-weight Notch complex in the nucleus of Notch(ic)-transformed RKE cells and in a human T-cell leukemia cell line. *Mol Cell Biol* 22:3927-3941.
194. Wu, L., Sun, T., Kobayashi, K., Gao, P., and Griffin, J.D. 2002. Identification of a family of mastermind-like transcriptional coactivators for mammalian notch receptors. *Mol Cell Biol* 22:7688-7700.
195. Rhyu, M.S., Jan, L.Y., and Jan, Y.N. 1994. Asymmetric distribution of numb protein during division of the sensory organ precursor cell confers distinct fates to daughter cells. *Cell* 76:477-491.
196. Zhong, W., Jiang, M.M., Weinmaster, G., Jan, L.Y., and Jan, Y.N. 1997. Differential expression of mammalian Numb, Numblike and Notch1 suggests distinct roles during mouse cortical neurogenesis. *Development* 124:1887-1897.
197. Beres, B.J., George, R., Lougher, E.J., Barton, M., Verrelli, B.C., McGlade, C.J., Rawls, J.A., and Wilson-Rawls, J. 2011. Numb regulates Notch1, but not Notch3, during myogenesis. *Mech Dev* 128:247-257.
198. McGill, M., and McGlade, C. 2003. Mammalian numb proteins promote notch1 receptor ubiquitination and degradation of the notch1 intracellular domain. *J Biol Chem* 278:23196-23203.
199. McGill, M.A., Dho, S.E., Weinmaster, G., and McGlade, C.J. 2009. Numb regulates post-endocytic trafficking and degradation of Notch1. *J Biol Chem* 284:26427-26438.
200. Espinosa, L., Ingles-Esteve, J., Aguilera, C., and Bigas, A. 2003. Phosphorylation by glycogen synthase kinase-3 beta down-regulates Notch activity, a link for Notch and Wnt pathways. *J Biol Chem* 278:32227-32235.
201. Foltz, D.R., Santiago, M.C., Berechid, B.E., and Nye, J.S. 2002. Glycogen synthase kinase-3beta modulates notch signaling and stability. *Curr Biol* 12:1006-1011.
202. Le Bras, S., Loyer, N., and Le Borgne, R. 2011. The multiple facets of ubiquitination in the regulation of notch signaling pathway. *Traffic* 12:149-161.
203. Coleman, M.L., McDonough, M.A., Hewitson, K.S., Coles, C., Mecinovic, J., Edelmann, M., Cook, K.M., Cockman, M.E., Lancaster, D.E., Kessler, B.M., et al. 2007. Asparaginyl hydroxylation of the Notch ankyrin repeat domain by factor inhibiting hypoxia-inducible factor. *J Biol Chem* 282:24027-24038.
204. Derynck, R., and Zhang, Y.E. 2003. Smad-dependent and Smad-independent pathways in TGF-beta family signalling. *Nature* 425:577-584.
205. Blokzijl, A., Dahlqvist, C., Reissmann, E., Falk, A., Moliner, A., Lendahl, U., and Ibanez, C.F. 2003. Cross-talk between the Notch and TGF-beta signaling pathways mediated by interaction of the Notch intracellular domain with Smad3. *J Cell Biol* 163:723-728.
206. Diez, H., Fischer, A., Winkler, A., Hu, C.J., Hatzopoulos, A.K., Breier, G., and Gessler, M. 2007. Hypoxia-mediated activation of Dll4-Notch-Hey2 signaling in endothelial progenitor cells and adoption of arterial cell fate. *Exp Cell Res* 313:1-9.

207. Sahlgren, C., Gustafsson, M.V., Jin, S., Poellinger, L., and Lendahl, U. 2008. Notch signaling mediates hypoxia-induced tumor cell migration and invasion. *Proc Natl Acad Sci U S A* 105:6392-6397.
208. Gustafsson, M.V., Zheng, X., Pereira, T., Gradin, K., Jin, S., Lundkvist, J., Ruas, J.L., Poellinger, L., Lendahl, U., and Bondesson, M. 2005. Hypoxia requires notch signaling to maintain the undifferentiated cell state. *Dev Cell* 9:617-628.
209. Li, X., Zhang, X., Leathers, R., Makino, A., Huang, C., Parsa, P., Macias, J., Yuan, J.X., Jamieson, S.W., and Thistlethwaite, P.A. 2009. Notch3 signaling promotes the development of pulmonary arterial hypertension. *Nat Med* 15:1289-1297.
210. Yeung, T.M., Gandhi, S.C., and Bodmer, W.F. 2011. Hypoxia and lineage specification of cell line-derived colorectal cancer stem cells. *Proc Natl Acad Sci U S A* 108:4382-4387.
211. McCright, B., Lozier, J., and Gridley, T. 2002. A mouse model of Alagille syndrome: Notch2 as a genetic modifier of Jag1 haploinsufficiency. *Development* 129:1075-1082.
212. Sparks, E.E., Huppert, K.A., Brown, M.A., Washington, M.K., and Huppert, S.S. 2010. Notch signaling regulates formation of the three-dimensional architecture of intrahepatic bile ducts in mice. *Hepatology* 51:1391-1400.
213. Geisler, F., Nagl, F., Mazur, P.K., Lee, M., Zimber-Strobl, U., Strobl, L.J., Radtke, F., Schmid, R.M., and Siveke, J.T. 2008. Liver-specific inactivation of Notch2, but not Notch1, compromises intrahepatic bile duct development in mice. *Hepatology* 48:607-616.
214. Hofmann, J.J., Zovein, A.C., Koh, H., Radtke, F., Weinmaster, G., and Iruela-Arispe, M.L. 2010. Jagged1 in the portal vein mesenchyme regulates intrahepatic bile duct development: insights into Alagille syndrome. *Development* 137:4061-4072.
215. Zong, Y., Panikkar, A., Xu, J., Antoniou, A., Raynaud, P., Lemaigre, F., and Stanger, B.Z. 2009. Notch signaling controls liver development by regulating biliary differentiation. *Development* 136:1727-1739.
216. Ortica, S., Tarantino, N., Aulner, N., Israël, A., and Gupta-Rossi, N. 2014. The 4 Notch receptors play distinct and antagonistic roles in the proliferation and hepatocytic differentiation of liver progenitors. *The FASEB Journal* 28:603-614.
217. Raynaud, P., Carpentier, R., Antoniou, A., and Lemaigre, F.P. 2011. Biliary differentiation and bile duct morphogenesis in development and disease. *Int J Biochem Cell Biol* 43:245-256.
218. Kohler, C., Bell, A.W., Bowen, W.C., Monga, S.P., Fleig, W., and Michalopoulos, G.K. 2004. Expression of Notch-1 and its ligand Jagged-1 in rat liver during liver regeneration. *Hepatology* 39:1056-1065.
219. Wang, L., Wang, C.M., Hou, L.H., Dou, G.R., Wang, Y.C., Hu, X.B., He, F., Feng, F., Zhang, H.W., Liang, Y.M., et al. 2009. Disruption of the transcription factor recombination signal-binding protein-Jkappa (RBP-J) leads to veno-occlusive disease and interfered liver regeneration in mice. *Hepatology* 49:268-277.
220. Dill, M.T., Rothweiler, S., Djonov, V., Hlushchuk, R., Tornillo, L., Terracciano, L., Meili-Butz, S., Radtke, F., Heim, M.H., and Semela, D. 2012. Disruption of Notch1 induces vascular remodeling, intussusceptive angiogenesis, and angiosarcomas in livers of mice. *Gastroenterology* 142:967-977 e962.
221. Spee, B., Carpino, G., Schotanus, B.A., Katoonizadeh, A., Vander Borght, S., Gaudio, E., and Roskams, T. 2010. Characterisation of the liver progenitor cell niche in liver diseases: potential involvement of Wnt and Notch signalling. *Gut* 59:247-257.

222. Fiorotto, R., Raizner, A., Morell, C.M., Torsello, B., Scirpo, R., Fabris, L., Spirli, C., and Strazzabosco, M. 2013. Notch signaling regulates tubular morphogenesis during repair from biliary damage in mice. *J Hepatol* 59:124-130.
223. Fabris, L., Cadamuro, M., Guido, M., Spirli, C., Fiorotto, R., Colledan, M., Torre, G., Alberti, D., Sonzogni, A., Okolicsanyi, L., et al. 2007. Analysis of liver repair mechanisms in Alagille syndrome and biliary atresia reveals a role for notch signaling. *Am J Pathol* 171:641-653.
224. Jeliazkova, P., Jors, S., Lee, M., Zimber-Strobl, U., Ferrer, J., Schmid, R.M., Siveke, J.T., and Geisler, F. 2013. Canonical Notch2 signaling determines biliary cell fates of embryonic hepatoblasts and adult hepatocytes independent of Hes1. *Hepatology* 57:2469-2479.
225. Sawitza, I., Kordes, C., Reister, S., and Haussinger, D. 2009. The niche of stellate cells within rat liver. *Hepatology* 50:1617-1624.
226. Zheng, S.P., Chen, Y.X., Guo, J.L., Qi, D., Zheng, S.J., Zhang, S.L., and Weng, Z.H. 2013. Recombinant adeno-associated virus-mediated transfer of shRNA against Notch3 ameliorates hepatic fibrosis in rats. *Exp Biol Med (Maywood)* 238:600-609.
227. Fan, B., Malato, Y., Calvisi, D.F., Naqvi, S., Razumilava, N., Ribback, S., Gores, G.J., Dombrowski, F., Evert, M., Chen, X., et al. 2012. Cholangiocarcinomas can originate from hepatocytes in mice. *J Clin Invest* 122:2911-2915.
228. Sekiya, S., and Suzuki, A. 2012. Intrahepatic cholangiocarcinoma can arise from Notch-mediated conversion of hepatocytes. *J Clin Invest* 122:3914-3918.
229. Raggi, C., Invernizzi, P., and Andersen, J.B. 2015. Impact of microenvironment and stem-like plasticity in cholangiocarcinoma: molecular networks and biological concepts. *J Hepatol* 62:198-207.
230. Mu, X., Espanol-Suner, R., Mederacke, I., Affo, S., Manco, R., Sempoux, C., Lemaigre, F.P., Adili, A., Yuan, D., Weber, A., et al. 2015. Hepatocellular carcinoma originates from hepatocytes and not from the progenitor/biliary compartment. *J Clin Invest* 125:3891-3903.
231. Villanueva, A., Alsinet, C., Yanger, K., Hoshida, Y., Zong, Y., Toffanin, S., Rodriguez-Carunchio, L., Sole, M., Thung, S., Stanger, B.Z., et al. 2012. Notch signaling is activated in human hepatocellular carcinoma and induces tumor formation in mice. *Gastroenterology* 143:1660-1669 e1667.
232. Dill, M.T., Tornillo, L., Fritzius, T., Terracciano, L., Semela, D., Bettler, B., Heim, M.H., and Tchorz, J.S. 2013. Constitutive Notch2 signaling induces hepatic tumors in mice. *Hepatology* 57:1607-1619.
233. Clevers, H., Loh, K.M., and Nusse, R. 2014. Stem cell signaling. An integral program for tissue renewal and regeneration: Wnt signaling and stem cell control. *Science* 346:1248012.
234. Najdi, R., Proffitt, K., Sprowl, S., Kaur, S., Yu, J., Covey, T.M., Virshup, D.M., and Waterman, M.L. 2012. A uniform human Wnt expression library reveals a shared secretory pathway and unique signaling activities. *Differentiation* 84:203-213.
235. Alexandre, C., Baena-Lopez, A., and Vincent, J.P. 2014. Patterning and growth control by membrane-tethered Wingless. *Nature* 505:180-185.
236. Koo, B.K., and Clevers, H. 2014. Stem cells marked by the R-spondin receptor LGR5. *Gastroenterology* 147:289-302.
237. Bullions, L.C., and Levine, A.J. 1998. The role of beta-catenin in cell adhesion, signal transduction, and cancer. *Curr Opin Oncol* 10:81-87.

238. Clevers, H., and Nusse, R. 2012. Wnt/beta-catenin signaling and disease. *Cell* 149:1192-1205.
239. Kinzler, K.W., Nilbert, M.C., Su, L.K., Vogelstein, B., Bryan, T.M., Levy, D.B., Smith, K.J., Preisinger, A.C., Hedge, P., McKechnie, D., et al. 1991. Identification of FAP locus genes from chromosome 5q21. *Science* 253:661-665.
240. Nishisho, I., Nakamura, Y., Miyoshi, Y., Miki, Y., Ando, H., Horii, A., Koyama, K., Utsunomiya, J., Baba, S., and Hedge, P. 1991. Mutations of chromosome 5q21 genes in FAP and colorectal cancer patients. *Science* 253:665-669.
241. Leblond, C.P., and Stevens, C.E. 1948. The constant renewal of the intestinal epithelium in the albino rat. *Anat Rec* 100:357-377.
242. Korinek, V., Barker, N., Moerer, P., van Donselaar, E., Huls, G., Peters, P.J., and Clevers, H. 1998. Depletion of epithelial stem-cell compartments in the small intestine of mice lacking Tcf-4. *Nat Genet* 19:379-383.
243. Fevr, T., Robine, S., Louvard, D., and Huelsken, J. 2007. Wnt/beta-catenin is essential for intestinal homeostasis and maintenance of intestinal stem cells. *Mol Cell Biol* 27:7551-7559.
244. Kim, K.A., Kakitani, M., Zhao, J., Oshima, T., Tang, T., Binnerts, M., Liu, Y., Boyle, B., Park, E., Emtage, P., et al. 2005. Mitogenic influence of human R-spondin1 on the intestinal epithelium. *Science* 309:1256-1259.
245. van Amerongen, R., Bowman, A.N., and Nusse, R. 2012. Developmental stage and time dictate the fate of Wnt/beta-catenin-responsive stem cells in the mammary gland. *Cell Stem Cell* 11:387-400.
246. Plaks, V., Brenot, A., Lawson, D.A., Linnemann, J.R., Van Kappel, E.C., Wong, K.C., de Sauvage, F., Klein, O.D., and Werb, Z. 2013. Lgr5-expressing cells are sufficient and necessary for postnatal mammary gland organogenesis. *Cell Rep* 3:70-78.
247. Lim, X., Tan, S.H., Koh, W.L., Chau, R.M., Yan, K.S., Kuo, C.J., van Amerongen, R., Klein, A.M., and Nusse, R. 2013. Interfollicular epidermal stem cells self-renew via autocrine Wnt signaling. *Science* 342:1226-1230.
248. Bowman, A.N., van Amerongen, R., Palmer, T.D., and Nusse, R. 2013. Lineage tracing with Axin2 reveals distinct developmental and adult populations of Wnt/beta-catenin-responsive neural stem cells. *Proc Natl Acad Sci U S A* 110:7324-7329.
249. Yokoyama, N., and Malbon, C.C. 2009. Dishevelled-2 docks and activates Src in a Wnt-dependent manner. *J Cell Sci* 122:4439-4451.
250. Inoki, K., Ouyang, H., Zhu, T., Lindvall, C., Wang, Y., Zhang, X., Yang, Q., Bennett, C., Harada, Y., Stankunas, K., et al. 2006. TSC2 integrates Wnt and energy signals via a coordinated phosphorylation by AMPK and GSK3 to regulate cell growth. *Cell* 126:955-968.
251. Laplante, M., and Sabatini, D.M. 2012. mTOR signaling in growth control and disease. *Cell* 149:274-293.
252. Goessling, W., North, T.E., Lord, A.M., Ceol, C., Lee, S., Weidinger, G., Bourque, C., Strijbosch, R., Haramis, A.P., Puder, M., et al. 2008. APC mutant zebrafish uncover a changing temporal requirement for wnt signaling in liver development. *Dev Biol* 320:161-174.
253. Ober, E.A., Verkade, H., Field, H.A., and Stainier, D.Y. 2006. Mesodermal Wnt2b signalling positively regulates liver specification. *Nature* 442:688-691.
254. Tan, X., Yuan, Y., Zeng, G., Apte, U., Thompson, M.D., Cieply, B., Stolz, D.B., Michalopoulos, G.K., Kaestner, K.H., and Monga, S.P. 2008. Beta-catenin deletion in

hepatoblasts disrupts hepatic morphogenesis and survival during mouse development. *Hepatology* 47:1667-1679.

255. Cordi, S., Godard, C., Saandi, T., Jacquemin, P., Monga, S.P., Colnot, S., and Lemaigre, F. 2016. Role of beta-catenin in development of bile ducts. In *Differentiation*.
256. Monga, S.P., Pediaditakis, P., Mule, K., Stolz, D.B., and Michalopoulos, G.K. 2001. Changes in WNT/beta-catenin pathway during regulated growth in rat liver regeneration. *Hepatology* 33:1098-1109.
257. Block, G.D., Locker, J., Bowen, W.C., Petersen, B.E., Katyal, S., Strom, S.C., Riley, T., Howard, T.A., and Michalopoulos, G.K. 1996. Population expansion, clonal growth, and specific differentiation patterns in primary cultures of hepatocytes induced by HGF/SF, EGF and TGF alpha in a chemically defined (HGM) medium. *J Cell Biol* 132:1133-1149.
258. Patijn, G.A., Lieber, A., Schowalter, D.B., Schwall, R., and Kay, M.A. 1998. Hepatocyte growth factor induces hepatocyte proliferation in vivo and allows for efficient retroviral-mediated gene transfer in mice. *Hepatology* 28:707-716.
259. Borowiak, M., Garratt, A.N., Wustefeld, T., Strehle, M., Trautwein, C., and Birchmeier, C. 2004. Met provides essential signals for liver regeneration. *Proc Natl Acad Sci U S A* 101:10608-10613.
260. Paranjpe, S., Bowen, W.C., Bell, A.W., Nejak-Bowen, K., Luo, J.H., and Michalopoulos, G.K. 2007. Cell cycle effects resulting from inhibition of hepatocyte growth factor and its receptor c-Met in regenerating rat livers by RNA interference. *Hepatology* 45:1471-1477.
261. Monga, S.P., Mars, W.M., Pediaditakis, P., Bell, A., Mule, K., Bowen, W.C., Wang, X., Zarnegar, R., and Michalopoulos, G.K. 2002. Hepatocyte growth factor induces Wnt-independent nuclear translocation of beta-catenin after Met-beta-catenin dissociation in hepatocytes. *Cancer Res* 62:2064-2071.
262. Apte, U., Thompson, M.D., Cui, S., Liu, B., Cieply, B., and Monga, S.P. 2008. Wnt/beta-catenin signaling mediates oval cell response in rodents. *Hepatology* 47:288-295.
263. Hu, M., Kurobe, M., Jeong, Y.J., Fuerer, C., Ghole, S., Nusse, R., and Sylvester, K.G. 2007. Wnt/beta-catenin signaling in murine hepatic transit amplifying progenitor cells. *Gastroenterology* 133:1579-1591.
264. de La Coste, A., Romagnolo, B., Billuart, P., Renard, C.A., Buendia, M.A., Soubrane, O., Fabre, M., Chelly, J., Beldjord, C., Kahn, A., et al. 1998. Somatic mutations of the beta-catenin gene are frequent in mouse and human hepatocellular carcinomas. *Proc Natl Acad Sci U S A* 95:8847-8851.
265. Giles, R.H., van Es, J.H., and Clevers, H. 2003. Caught up in a Wnt storm: Wnt signaling in cancer. *Biochim Biophys Acta* 1653:1-24.
266. Colnot, S., Decaens, T., Niwa-Kawakita, M., Godard, C., Hamard, G., Kahn, A., Giovannini, M., and Perret, C. 2004. Liver-targeted disruption of Apc in mice activates beta-catenin signaling and leads to hepatocellular carcinomas. *Proc Natl Acad Sci U S A* 101:17216-17221.
267. Liu, J., Ding, X., Tang, J., Cao, Y., Hu, P., Zhou, F., Shan, X., Cai, X., Chen, Q., Ling, N., et al. 2011. Enhancement of canonical Wnt/beta-catenin signaling activity by HCV core protein promotes cell growth of hepatocellular carcinoma cells. *PLoS One* 6:e27496.

268. Ong, C.K., Subimerb, C., Pairojkul, C., Wongkham, S., Cutcutache, I., Yu, W., McPherson, J.R., Allen, G.E., Ng, C.C., Wong, B.H., et al. 2012. Exome sequencing of liver fluke-associated cholangiocarcinoma. *Nat Genet* 44:690-693.
269. Williams, J.M., Oh, S.H., Jorgensen, M., Steiger, N., Darwiche, H., Shupe, T., and Petersen, B.E. 2010. The role of the Wnt family of secreted proteins in rat oval "stem" cell-based liver regeneration: Wnt1 drives differentiation. *Am J Pathol* 176:2732-2742.
270. Pellegrinet, L., Rodilla, V., Liu, Z., Chen, S., Koch, U., Espinosa, L., Kaestner, K.H., Kopan, R., Lewis, J., and Radtke, F. 2011. Dll1- and dll4-mediated notch signaling are required for homeostasis of intestinal stem cells. *Gastroenterology* 140:1230-1240 e1231-1237.
271. Fre, S., Pallavi, S.K., Huyghe, M., Lae, M., Janssen, K.P., Robine, S., Artavanis-Tsakonas, S., and Louvard, D. 2009. Notch and Wnt signals cooperatively control cell proliferation and tumorigenesis in the intestine. *Proc Natl Acad Sci U S A* 106:6309-6314.
272. van Es, J.H., Jay, P., Gregorieff, A., van Gijn, M.E., Jonkheer, S., Hatzis, P., Thiele, A., van den Born, M., Begthel, H., Brabletz, T., et al. 2005. Wnt signalling induces maturation of Paneth cells in intestinal crypts. *Nat Cell Biol* 7:381-386.
273. Andreu, P., Colnot, S., Godard, C., Gad, S., Chafey, P., Niwa-Kawakita, M., Laurent-Puig, P., Kahn, A., Robine, S., Perret, C., et al. 2005. Crypt-restricted proliferation and commitment to the Paneth cell lineage following Apc loss in the mouse intestine. *Development* 132:1443-1451.
274. Pinto, D., Gregorieff, A., Begthel, H., and Clevers, H. 2003. Canonical Wnt signals are essential for homeostasis of the intestinal epithelium. *Genes Dev* 17:1709-1713.
275. van Es, J.H., van Gijn, M.E., Riccio, O., van den Born, M., Vooijs, M., Begthel, H., Cozijnsen, M., Robine, S., Winton, D.J., Radtke, F., et al. 2005. Notch/gamma-secretase inhibition turns proliferative cells in intestinal crypts and adenomas into goblet cells. *Nature* 435:959-963.
276. VanDussen, K.L., Carulli, A.J., Keeley, T.M., Patel, S.R., Puthoff, B.J., Magness, S.T., Tran, I.T., Maillard, I., Siebel, C., Kolterud, A., et al. 2012. Notch signaling modulates proliferation and differentiation of intestinal crypt base columnar stem cells. *Development* 139:488-497.
277. Tian, H., Biehs, B., Chiu, C., Siebel, C.W., Wu, Y., Costa, M., de Sauvage, F.J., and Klein, O.D. 2015. Opposing activities of Notch and Wnt signaling regulate intestinal stem cells and gut homeostasis. *Cell Rep* 11:33-42.
278. Conboy, I.M., and Rando, T.A. 2002. The regulation of Notch signaling controls satellite cell activation and cell fate determination in postnatal myogenesis. *Dev Cell* 3:397-409.
279. Brack, A.S., Conboy, I.M., Conboy, M.J., Shen, J., and Rando, T.A. 2008. A temporal switch from notch to Wnt signaling in muscle stem cells is necessary for normal adult myogenesis. *Cell Stem Cell* 2:50-59.
280. Katoh, M., and Katoh, M. 2006. NUMB is a break of WNT-Notch signaling cycle. *Int J Mol Med* 18:517-521.
281. Dho, S.E., French, M.B., Woods, S.A., and McGlade, C.J. 1999. Characterization of four mammalian numb protein isoforms. Identification of cytoplasmic and membrane-associated variants of the phosphotyrosine binding domain. *J Biol Chem* 274:33097-33104.

282. Di Marcotullio, L., Ferretti, E., Greco, A., De Smaele, E., Po, A., Sico, M.A., Alimandi, M., Giannini, G., Maroder, M., Screpanti, I., et al. 2006. Numb is a suppressor of Hedgehog signalling and targets Gli1 for Itch-dependent ubiquitination. *Nat Cell Biol* 8:1415-1423.
283. Xie, G., Karaca, G., Swiderska-Syn, M., Michelotti, G.A., Kruger, L., Chen, Y., Premont, R.T., Choi, S.S., and Diehl, A.M. 2013. Cross-talk between Notch and Hedgehog regulates hepatic stellate cell fate in mice. *Hepatology* 58:1801-1813.
284. Jia, L., Yu, G., Zhang, Y., and Wang, M.M. 2009. Lysosome-dependent degradation of Notch3. *Int J Biochem Cell Biol* 41:2594-2598.
285. Ortica, S., Tarantino, N., Aulner, N., Israel, A., and Gupta-Rossi, N. 2014. The 4 Notch receptors play distinct and antagonistic roles in the proliferation and hepatocytic differentiation of liver progenitors. *FASEB J* 28:603-614.
286. Van der Flier, L.G., Sabates-Bellver, J., Oving, I., Haegebarth, A., De Palo, M., Anti, M., Van Gijn, M.E., Suijkerbuijk, S., Van de Wetering, M., Marra, G., et al. 2007. The Intestinal Wnt/TCF Signature. *Gastroenterology* 132:628-632.
287. van der Flier, L.G., van Gijn, M.E., Hatzis, P., Kujala, P., Haegebarth, A., Stange, D.E., Begthel, H., van den Born, M., Guryev, V., Oving, I., et al. 2009. Transcription factor achaete scute-like 2 controls intestinal stem cell fate. *Cell* 136:903-912.
288. Schuijers, J., Junker, J.P., Mokry, M., Hatzis, P., Koo, B.K., Sasselli, V., van der Flier, L.G., Cuppen, E., van Oudenaarden, A., and Clevers, H. 2015. Ascl2 acts as an R-spondin/Wnt-responsive switch to control stemness in intestinal crypts. *Cell Stem Cell* 16:158-170.
289. Moriyama, M., Durham, A.D., Moriyama, H., Hasegawa, K., Nishikawa, S., Radtke, F., and Osawa, M. 2008. Multiple roles of Notch signaling in the regulation of epidermal development. *Dev Cell* 14:594-604.
290. Giustina, A., Mazziotti, G., and Canalis, E. 2008. Growth hormone, insulin-like growth factors, and the skeleton. *Endocr Rev* 29:535-559.
291. Laviola, L., Natalicchio, A., Perrini, S., and Giorgino, F. 2008. Abnormalities of IGF-I signaling in the pathogenesis of diseases of the bone, brain, and fetoplacental unit in humans. *Am J Physiol Endocrinol Metab* 295:E991-999.
292. Ohlsson, C., Mohan, S., Sjogren, K., Tivesten, A., Isgaard, J., Isaksson, O., Jansson, J.O., and Svensson, J. 2009. The role of liver-derived insulin-like growth factor-I. *Endocr Rev* 30:494-535.
293. Jones, J.I., and Clemmons, D.R. 1995. Insulin-like growth factors and their binding proteins: biological actions. *Endocr Rev* 16:3-34.
294. Perrini, S., Laviola, L., Carreira, M.C., Cignarelli, A., Natalicchio, A., and Giorgino, F. 2010. The GH/IGF1 axis and signaling pathways in the muscle and bone: mechanisms underlying age-related skeletal muscle wasting and osteoporosis. *J Endocrinol* 205:201-210.
295. Alvaro, D., Metalli, V.D., Alpini, G., Onori, P., Franchitto, A., Barbaro, B., Glaser, S.S., Francis, H., Cantafora, A., Blotta, I., et al. 2005. The intrahepatic biliary epithelium is a target of the growth hormone/insulin-like growth factor 1 axis. *J Hepatol* 43:875-883.
296. Grey, A., Chen, Q., Xu, X., Callon, K., and Cornish, J. 2003. Parallel phosphatidylinositol-3 kinase and p42/44 mitogen-activated protein kinase signaling pathways subserve the mitogenic and antiapoptotic actions of insulin-like growth factor I in osteoblastic cells. *Endocrinology* 144:4886-4893.

297. Hermanto, U., Zong, C.S., and Wang, L.H. 2000. Inhibition of mitogen-activated protein kinase kinase selectively inhibits cell proliferation in human breast cancer cells displaying enhanced insulin-like growth factor I-mediated mitogen-activated protein kinase activation. *Cell Growth Differ* 11:655-664.
298. Ten Broek, R.W., Grefte, S., and Von den Hoff, J.W. 2010. Regulatory factors and cell populations involved in skeletal muscle regeneration. *J Cell Physiol* 224:7-16.
299. Eliasz, S., Liang, S., Chen, Y., De Marco, M.A., Machek, O., Skucha, S., Miele, L., and Bocchetta, M. 2010. Notch-1 stimulates survival of lung adenocarcinoma cells during hypoxia by activating the IGF-1R pathway. *Oncogene* 29:2488-2498.
300. Medyouf, H., Gusscott, S., Wang, H., Tseng, J.C., Wai, C., Nemirovsky, O., Trumpp, A., Pflumio, F., Carboni, J., Gottardis, M., et al. 2011. High-level IGF1R expression is required for leukemia-initiating cell activity in T-ALL and is supported by Notch signaling. *J Exp Med* 208:1809-1822.
301. Palsgaard, J., Emanuelli, B., Winnay, J.N., Sumara, G., Karsenty, G., and Kahn, C.R. 2012. Cross-talk between insulin and Wnt signaling in preadipocytes: role of Wnt co-receptor low density lipoprotein receptor-related protein-5 (LRP5). *J Biol Chem* 287:12016-12026.
302. Playford, M.P., Bicknell, D., Bodmer, W.F., and Macaulay, V.M. 2000. Insulin-like growth factor 1 regulates the location, stability, and transcriptional activity of beta-catenin. *Proc Natl Acad Sci U S A* 97:12103-12108.
303. Desbois-Mouthon, C., Cadoret, A., Blivet-Van Eggelpoel, M.J., Bertrand, F., Cherqui, G., Perret, C., and Capeau, J. 2001. Insulin and IGF-1 stimulate the beta-catenin pathway through two signalling cascades involving GSK-3beta inhibition and Ras activation. *Oncogene* 20:252-259.
304. Scharf, J.G., Schmitz, F., Frystyk, J., Skjaerbaek, C., Moesus, H., Blum, W.F., Ramadori, G., and Hartmann, H. 1996. Insulin-like growth factor-I serum concentrations and patterns of insulin-like growth factor binding proteins in patients with chronic liver disease. *J Hepatol* 25:689-699.
305. Caufriez, A., Reding, P., Urbain, D., Golstein, J., and Copinschi, G. 1991. Insulin-like growth factor I: a good indicator of functional hepatocellular capacity in alcoholic liver cirrhosis. *J Endocrinol Invest* 14:317-321.
306. Donaghy, A., Ross, R., Wicks, C., Hughes, S.C., Holly, J., Gimson, A., and Williams, R. 1997. Growth hormone therapy in patients with cirrhosis: a pilot study of efficacy and safety. *Gastroenterology* 113:1617-1622.
307. Conchillo, M., de Knegt, R.J., Payeras, M., Quiroga, J., Sangro, B., Herrero, J.I., Castilla-Cortazar, I., Frystyk, J., Flyvbjerg, A., Yoshizawa, C., et al. 2005. Insulin-like growth factor I (IGF-I) replacement therapy increases albumin concentration in liver cirrhosis: results of a pilot randomized controlled clinical trial. *J Hepatol* 43:630-636.
308. Munoz-Descalzo, S., Sanders, P.G., Montagne, C., Johnson, R.I., Balayo, T., and Arias, A.M. 2010. Wingless modulates the ligand independent traffic of Notch through Dishevelled. *Fly (Austin)* 4:182-193.
309. Estrach, S., Ambler, C.A., Lo Celso, C., Hozumi, K., and Watt, F.M. 2006. Jagged 1 is a beta-catenin target gene required for ectopic hair follicle formation in adult epidermis. *Development* 133:4427-4438.
310. Hayward, P., Brennan, K., Sanders, P., Balayo, T., DasGupta, R., Perrimon, N., and Martinez Arias, A. 2005. Notch modulates Wnt signalling by associating with

Armadillo/beta-catenin and regulating its transcriptional activity. *Development* 132:1819-1830.

311. Shimizu, T., Kagawa, T., Inoue, T., Nonaka, A., Takada, S., Aburatani, H., and Taga, T. 2008. Stabilized beta-catenin functions through TCF/LEF proteins and the Notch/RBP-Jkappa complex to promote proliferation and suppress differentiation of neural precursor cells. *Mol Cell Biol* 28:7427-7441.
312. Rallis, C., Pinchin, S.M., and Ish-Horowicz, D. 2010. Cell-autonomous integrin control of Wnt and Notch signalling during somitogenesis. *Development* 137:3591-3601.
313. Saint Just Ribeiro, M., Hansson, M.L., Lindberg, M.J., Popko-Scibor, A.E., and Wallberg, A.E. 2009. GSK3beta is a negative regulator of the transcriptional coactivator MAML1. *Nucleic Acids Res* 37:6691-6700.
314. Alves-Guerra, M.C., Ronchini, C., and Capobianco, A.J. 2007. Mastermind-like 1 Is a specific coactivator of beta-catenin transcription activation and is essential for colon carcinoma cell survival. *Cancer Res* 67:8690-8698.
315. Krebs, L.T., Deftos, M.L., Bevan, M.J., and Gridley, T. 2001. The Nrarp gene encodes an ankyrin-repeat protein that is transcriptionally regulated by the notch signaling pathway. *Dev Biol* 238:110-119.
316. Lamar, E., Deblandre, G., Wettstein, D., Gawantka, V., Pollet, N., Niehrs, C., and Kintner, C. 2001. Nrarp is a novel intracellular component of the Notch signaling pathway. *Genes Dev* 15:1885-1899.
317. Kitamoto, T., Takahashi, K., Takimoto, H., Tomizuka, K., Hayasaka, M., Tabira, T., and Hanaoka, K. 2005. Functional redundancy of the Notch gene family during mouse embryogenesis: analysis of Notch gene expression in Notch3-deficient mice. *Biochem Biophys Res Commun* 331:1154-1162.
318. Kitamoto, T., and Hanaoka, K. 2010. Notch3 null mutation in mice causes muscle hyperplasia by repetitive muscle regeneration. *Stem Cells* 28:2205-2216.
319. Ishitani, T., Matsumoto, K., Chitnis, A.B., and Itoh, M. 2005. Nrarp functions to modulate neural-crest-cell differentiation by regulating LEF1 protein stability. *Nat Cell Biol* 7:1106-1112.
320. Phng, L.K., Potente, M., Leslie, J.D., Babbage, J., Nyqvist, D., Lobov, I., Ondr, J.K., Rao, S., Lang, R.A., Thurston, G., et al. 2009. Nrarp coordinates endothelial Notch and Wnt signaling to control vessel density in angiogenesis. *Dev Cell* 16:70-82.
321. Krebs, L.T., Xue, Y., Norton, C.R., Sundberg, J.P., Beatus, P., Lendahl, U., Joutel, A., and Gridley, T. 2003. Characterization of Notch3-deficient mice: normal embryonic development and absence of genetic interactions with a Notch1 mutation. *Genesis* 37:139-143.
322. Nowotschin, S., Xenopoulos, P., Schrode, N., and Hadjantonakis, A.K. 2013. A bright single-cell resolution live imaging reporter of Notch signaling in the mouse. *BMC Dev Biol* 13:15.
323. Ferrer-Vaquer, A., Piliszek, A., Tian, G., Aho, R.J., Dufort, D., and Hadjantonakis, A.K. 2010. A sensitive and bright single-cell resolution live imaging reporter of Wnt/ss-catenin signaling in the mouse. *BMC Dev Biol* 10:121.
324. Means, A.L., Xu, Y., Zhao, A., Ray, K.C., and Gu, G. 2008. A CK19(CreERT) knockin mouse line allows for conditional DNA recombination in epithelial cells in multiple endodermal organs. *Genesis* 46:318-323.
325. Madisen, L., Zwingman, T.A., Sunkin, S.M., Oh, S.W., Zariwala, H.A., Gu, H., Ng, L.L., Palmiter, R.D., Hawrylycz, M.J., Jones, A.R., et al. 2010. A robust and high-

throughput Cre reporting and characterization system for the whole mouse brain. *Nat Neurosci* 13:133-140.

326. Dietrich, P., Dragatsis, I., Xuan, S., Zeitlin, S., and Efstratiadis, A. 2000. Conditional mutagenesis in mice with heat shock promoter-driven cre transgenes. *Mamm Genome* 11:196-205.
327. Falk, R., Falk, A., Dyson, M.R., Melidoni, A.N., Parthiban, K., Young, J.L., Roake, W., and McCafferty, J. 2012. Generation of anti-Notch antibodies and their application in blocking Notch signalling in neural stem cells. *Methods* 58:69-78.
328. Tsuchiya, A., Heike, T., Fujino, H., Shiota, M., Umeda, K., Yoshimoto, M., Matsuda, Y., Ichida, T., Aoyagi, Y., and Nakahata, T. 2005. Long-term extensive expansion of mouse hepatic stem/progenitor cells in a novel serum-free culture system. *Gastroenterology* 128:2089-2104.
329. Liu, Y., Meyer, C., Xu, C., Weng, H., Hellerbrand, C., ten Dijke, P., and Dooley, S. 2013. Animal models of chronic liver diseases. *Am J Physiol Gastrointest Liver Physiol* 304:G449-468.
330. Tirnitz-Parker, J.E., Tonkin, J.N., Knight, B., Olynyk, J.K., and Yeoh, G.C. 2007. Isolation, culture and immortalisation of hepatic oval cells from adult mice fed a choline-deficient, ethionine-supplemented diet. *Int J Biochem Cell Biol* 39:2226-2239.
331. Hofmann, J.J., and Iruela-Arispe, M.L. 2007. Notch signaling in blood vessels: who is talking to whom about what? *Circ Res* 100:1556-1568.
332. Tan, X., Behari, J., Cieply, B., Michalopoulos, G.K., and Monga, S.P. 2006. Conditional deletion of beta-catenin reveals its role in liver growth and regeneration. *Gastroenterology* 131:1561-1572.
333. Burke, Z.D., Reed, K.R., Phesse, T.J., Sansom, O.J., Clarke, A.R., and Tosh, D. 2009. Liver zonation occurs through a beta-catenin-dependent, c-Myc-independent mechanism. *Gastroenterology* 136:2316-2324 e2311-2313.
334. Chen, Y., Zheng, S., Qi, D., Zheng, S., Guo, J., Zhang, S., and Weng, Z. 2012. Inhibition of Notch signaling by a gamma-secretase inhibitor attenuates hepatic fibrosis in rats. *PLoS One* 7:e46512.
335. Li, X., Zhao, X., Fang, Y., Jiang, X., Duong, T., Fan, C., Huang, C.C., and Kain, S.R. 1998. Generation of destabilized green fluorescent protein as a transcription reporter. *J Biol Chem* 273:34970-34975.
336. Corish, P., and Tyler-Smith, C. 1999. Attenuation of green fluorescent protein half-life in mammalian cells. *Protein Eng* 12:1035-1040.
337. Kodama, Y., Hijikata, M., Kageyama, R., Shimotohno, K., and Chiba, T. 2004. The role of notch signaling in the development of intrahepatic bile ducts. *Gastroenterology* 127:1775-1786.
338. Vanderpool, C., Sparks, E.E., Huppert, K.A., Gannon, M., Means, A.L., and Huppert, S.S. 2012. Genetic interactions between hepatocyte nuclear factor-6 and Notch signaling regulate mouse intrahepatic bile duct development in vivo. *Hepatology* 55:233-243.
339. Aujla, P.K., Bora, A., Monahan, P., Sweedler, J.V., and Raetzman, L.T. 2011. The Notch effector gene Hes1 regulates migration of hypothalamic neurons, neuropeptide content and axon targeting to the pituitary. *Dev Biol* 353:61-71.
340. Xie, J., Wang, W., Si, J.W., Miao, X.Y., Li, J.C., Wang, Y.C., Wang, Z.R., Ma, J., Zhao, X.C., Li, Z., et al. 2013. Notch signaling regulates CXCR4 expression and the migration of mesenchymal stem cells. *Cell Immunol* 281:68-75.

341. Bolos, V., Mira, E., Martinez-Poveda, B., Luxan, G., Canamero, M., Martinez, A.C., Manes, S., and de la Pompa, J.L. 2013. Notch activation stimulates migration of breast cancer cells and promotes tumor growth. *Breast Cancer Res* 15:R54.
342. Van Hul, N., Lanthier, N., Espanol Suner, R., Abarca Quinones, J., van Rooijen, N., and Leclercq, I. 2011. Kupffer cells influence parenchymal invasion and phenotypic orientation, but not the proliferation, of liver progenitor cells in a murine model of liver injury. *Am J Pathol* 179:1839-1850.
343. Duncan, A.W., Dorrell, C., and Grompe, M. 2009. Stem cells and liver regeneration. *Gastroenterology* 137:466-481.
344. Martinez-Palacian, A., del Castillo, G., Herrera, B., Fernandez, M., Roncero, C., Fabregat, I., and Sanchez, A. 2012. EGFR is dispensable for c-Met-mediated proliferation and survival activities in mouse adult liver oval cells. *Cell Signal* 24:505-513.
345. Ishikawa, T., Factor, V.M., Marquardt, J.U., Raggi, C., Seo, D., Kitade, M., Conner, E.A., and Thorgeirsson, S.S. 2012. Hepatocyte growth factor/c-met signaling is required for stem-cell-mediated liver regeneration in mice. *Hepatology* 55:1215-1226.
346. Flynn, D.M., Nijjar, S., Hubscher, S.G., de Goyet Jde, V., Kelly, D.A., Strain, A.J., and Crosby, H.A. 2004. The role of Notch receptor expression in bile duct development and disease. *J Pathol* 204:55-64.
347. Croquelois, A., Blindenbacher, A., Terracciano, L., Wang, X., Langer, I., Radtke, F., and Heim, M.H. 2005. Inducible inactivation of Notch1 causes nodular regenerative hyperplasia in mice. *Hepatology* 41:487-496.
348. Takahashi-Yanaga, F., and Kahn, M. 2010. Targeting Wnt signaling: can we safely eradicate cancer stem cells? *Clin Cancer Res* 16:3153-3162.
349. Micsenyi, A., Tan, X., Sneddon, T., Luo, J.H., Michalopoulos, G.K., and Monga, S.P. 2004. Beta-catenin is temporally regulated during normal liver development. *Gastroenterology* 126:1134-1146.
350. Decaens, T., Godard, C., de Reynies, A., Rickman, D.S., Tronche, F., Couty, J.P., Perret, C., and Colnot, S. 2008. Stabilization of beta-catenin affects mouse embryonic liver growth and hepatoblast fate. *Hepatology* 47:247-258.
351. Monga, S.P., Monga, H.K., Tan, X., Mule, K., Pediaditakis, P., and Michalopoulos, G.K. 2003. Beta-catenin antisense studies in embryonic liver cultures: role in proliferation, apoptosis, and lineage specification. *Gastroenterology* 124:202-216.
352. Reed, K.R., Athineos, D., Meniel, V.S., Wilkins, J.A., Ridgway, R.A., Burke, Z.D., Muncan, V., Clarke, A.R., and Sansom, O.J. 2008. B-catenin deficiency, but not Myc deletion, suppresses the immediate phenotypes of APC loss in the liver. *Proc Natl Acad Sci U S A* 105:18919-18923.
353. Cadoret, A., Ovejero, C., Saadi-Kheddouci, S., Souil, E., Fabre, M., Romagnolo, B., Kahn, A., and Perret, C. 2001. Hepatomegaly in transgenic mice expressing an oncogenic form of beta-catenin. *Cancer Res* 61:3245-3249.
354. Cadoret, A., Ovejero, C., Terris, B., Souil, E., Levy, L., Lamers, W.H., Kitajewski, J., Kahn, A., and Perret, C. 2002. New targets of beta-catenin signaling in the liver are involved in the glutamine metabolism. *Oncogene* 21:8293-8301.
355. Itoh, T., Kamiya, Y., Okabe, M., Tanaka, M., and Miyajima, A. 2009. Inducible expression of Wnt genes during adult hepatic stem/progenitor cell response. *FEBS Lett* 583:777-781.

356. Emami, K.H., Nguyen, C., Ma, H., Kim, D.H., Jeong, K.W., Eguchi, M., Moon, R.T., Teo, J.L., Kim, H.Y., Moon, S.H., et al. 2004. A small molecule inhibitor of beta-catenin/CREB-binding protein transcription [corrected]. *Proc Natl Acad Sci U S A* 101:12682-12687.
357. Aman, A., and Piotrowski, T. 2008. Wnt/beta-catenin and Fgf signaling control collective cell migration by restricting chemokine receptor expression. *Dev Cell* 15:749-761.
358. Vlad-Fiegen, A., Langerak, A., Eberth, S., and Muller, O. 2012. The Wnt pathway destabilizes adherens junctions and promotes cell migration via beta-catenin and its target gene cyclin D1. *FEBS Open Bio* 2:26-31.
359. Schlessinger, K., Hall, A., and Tolwinski, N. 2009. Wnt signaling pathways meet Rho GTPases. *Genes Dev* 23:265-277.
360. Bilir, B., Kucuk, O., and Moreno, C.S. 2013. Wnt signaling blockage inhibits cell proliferation and migration, and induces apoptosis in triple-negative breast cancer cells. *J Transl Med* 11:280.
361. Barrott, J.J., Cash, G.M., Smith, A.P., Barrow, J.R., and Murtaugh, L.C. 2011. Deletion of mouse Porcn blocks Wnt ligand secretion and reveals an ectodermal etiology of human focal dermal hypoplasia/Goltz syndrome. *Proc Natl Acad Sci U S A* 108:12752-12757.
362. Kawasaki, H., Eckner, R., Yao, T.P., Taira, K., Chiu, R., Livingston, D.M., and Yokoyama, K.K. 1998. Distinct roles of the co-activators p300 and CBP in retinoic-acid-induced F9-cell differentiation. *Nature* 393:284-289.
363. Rebel, V.I., Kung, A.L., Tanner, E.A., Yang, H., Bronson, R.T., and Livingston, D.M. 2002. Distinct roles for CREB-binding protein and p300 in hematopoietic stem cell self-renewal. *Proc Natl Acad Sci U S A* 99:14789-14794.
364. Ma, H., Nguyen, C., Lee, K.S., and Kahn, M. 2005. Differential roles for the coactivators CBP and p300 on TCF/beta-catenin-mediated survivin gene expression. *Oncogene* 24:3619-3631.
365. Yan, G., Eller, M.S., Elm, C., Larocca, C.A., Ryu, B., Panova, I.P., Dancy, B.M., Bowers, E.M., Meyers, D., Lareau, L., et al. 2013. Selective inhibition of p300 HAT blocks cell cycle progression, induces cellular senescence, and inhibits the DNA damage response in melanoma cells. *J Invest Dermatol* 133:2444-2452.
366. Santer, F.R., Hoschele, P.P., Oh, S.J., Erb, H.H., Bouchal, J., Cavarretta, I.T., Parson, W., Meyers, D.J., Cole, P.A., and Culig, Z. 2011. Inhibition of the acetyltransferases p300 and CBP reveals a targetable function for p300 in the survival and invasion pathways of prostate cancer cell lines. *Mol Cancer Ther* 10:1644-1655.
367. Giorgetti, S., Ballotti, R., Kowalski-Chauvel, A., Tartare, S., and Van Obberghen, E. 1993. The insulin and insulin-like growth factor-I receptor substrate IRS-1 associates with and activates phosphatidylinositol 3-kinase in vitro. *J Biol Chem* 268:7358-7364.
368. Petley, T., Graff, K., Jiang, W., Yang, H., and Florini, J. 1999. Variation among cell types in the signaling pathways by which IGF-I stimulates specific cellular responses. *Horm Metab Res* 31:70-76.
369. Muise-Helmericks, R.C., Grimes, H.L., Bellacosa, A., Malstrom, S.E., Tsichlis, P.N., and Rosen, N. 1998. Cyclin D expression is controlled post-transcriptionally via a phosphatidylinositol 3-kinase/Akt-dependent pathway. *J Biol Chem* 273:29864-29872.

370. Butler, A.A., and LeRoith, D. 2001. Minireview: tissue-specific versus generalized gene targeting of the igf1 and igf1r genes and their roles in insulin-like growth factor physiology. *Endocrinology* 142:1685-1688.
371. Sokolovic, A., Rodriguez-Ortigosa, C.M., Bloemendaal, L.T., Oude Elferink, R.P., Prieto, J., and Bosma, P.J. 2013. Insulin-like growth factor 1 enhances bile-duct proliferation and fibrosis in Abcb4(-/-) mice. *Biochim Biophys Acta* 1832:697-704.
372. Castilla-Cortazar, I., Garcia, M., Muguerza, B., Quiroga, J., Perez, R., Santidrian, S., and Prieto, J. 1997. Hepatoprotective effects of insulin-like growth factor I in rats with carbon tetrachloride-induced cirrhosis. *Gastroenterology* 113:1682-1691.
373. Muguerza, B., Castilla-Cortazar, I., Garcia, M., Quiroga, J., Santidrian, S., and Prieto, J. 2001. Antifibrogenic effect in vivo of low doses of insulin-like growth factor-I in cirrhotic rats. *Biochim Biophys Acta* 1536:185-195.
374. Vera, M., Sobrevals, L., Zaratiegui, M., Martinez, L., Palencia, B., Rodriguez, C.M., Prieto, J., and Fortes, P. 2007. Liver transduction with a simian virus 40 vector encoding insulin-like growth factor I reduces hepatic damage and the development of liver cirrhosis. *Gene Ther* 14:203-210.
375. Sanz, S., Pucilowska, J.B., Liu, S., Rodriguez-Ortigosa, C.M., Lund, P.K., Brenner, D.A., Fuller, C.R., Simmons, J.G., Pardo, A., Martinez-Chantar, M.L., et al. 2005. Expression of insulin-like growth factor I by activated hepatic stellate cells reduces fibrogenesis and enhances regeneration after liver injury. *Gut* 54:134-141.
376. Sobrevals, L., Rodriguez, C., Romero-Trevejo, J.L., Gondi, G., Monreal, I., Paneda, A., Juanarena, N., Arcelus, S., Razquin, N., Guembe, L., et al. 2010. Insulin-like growth factor I gene transfer to cirrhotic liver induces fibrolysis and reduces fibrogenesis leading to cirrhosis reversion in rats. *Hepatology* 51:912-921.
377. Malaguarnera, R., and Belfiore, A. 2014. The emerging role of insulin and insulin-like growth factor signaling in cancer stem cells. *Front Endocrinol (Lausanne)* 5:10.
378. Longo, K.A., Kennell, J.A., Ochocinska, M.J., Ross, S.E., Wright, W.S., and MacDougald, O.A. 2002. Wnt signaling protects 3T3-L1 preadipocytes from apoptosis through induction of insulin-like growth factors. *J Biol Chem* 277:38239-38244.
379. Bommer, G.T., Feng, Y., Iura, A., Giordano, T.J., Kuick, R., Kadikoy, H., Sikorski, D., Wu, R., Cho, K.R., and Fearon, E.R. 2010. IRS1 regulation by Wnt/beta-catenin signaling and varied contribution of IRS1 to the neoplastic phenotype. *J Biol Chem* 285:1928-1938.
380. Parrizas, M., Gazit, A., Levitzki, A., Wertheimer, E., and LeRoith, D. 1997. Specific inhibition of insulin-like growth factor-1 and insulin receptor tyrosine kinase activity and biological function by tyrphostins. *Endocrinology* 138:1427-1433.
381. Mirpuri, E., Garcia-Trevijano, E.R., Castilla-Cortazar, I., Berasain, C., Quiroga, J., Rodriguez-Ortigosa, C., Mato, J.M., Prieto, J., and Avila, M.A. 2002. Altered liver gene expression in CCl4-cirrhotic rats is partially normalized by insulin-like growth factor-I. *Int J Biochem Cell Biol* 34:242-252.
382. Picardi, A., de Oliveira, A.C., Muguerza, B., Tosar, A., Quiroga, J., Castilla-Cortazar, I., Santidrian, S., and Prieto, J. 1997. Low doses of insulin-like growth factor-I improve nitrogen retention and food efficiency in rats with early cirrhosis. *J Hepatol* 26:191-202.
383. Irvine, K.M., Clouston, A.D., Gadd, V.L., Miller, G.C., Wong, W.Y., Melino, M., Maradana, M.R., MacDonald, K., Lang, R.A., Sweet, M.J., et al. 2015. Deletion of

Wntless in myeloid cells exacerbates liver fibrosis and the ductular reaction in chronic liver injury. *Fibrogenesis Tissue Repair* 8:19.

384. Lorenzini, S., Bird, T.G., Boulter, L., Bellamy, C., Samuel, K., Aucott, R., Clayton, E., Andreone, P., Bernardi, M., Golding, M., et al. 2010. Characterisation of a stereotypical cellular and extracellular adult liver progenitor cell niche in rodents and diseased human liver. *Gut* 59:645-654.
385. Samani, A.A., Yakar, S., LeRoith, D., and Brodt, P. 2007. The role of the IGF system in cancer growth and metastasis: overview and recent insights. *Endocr Rev* 28:20-47.
386. Uchida, T., and Peters, R.L. 1983. The nature and origin of proliferated bile ductules in alcoholic liver disease. *Am J Clin Pathol* 79:326-333.
387. Cariani, E., Lasserre, C., Seurin, D., Hamelin, B., Kemeny, F., Franco, D., Czech, M.P., Ullrich, A., and Brechot, C. 1988. Differential expression of insulin-like growth factor II mRNA in human primary liver cancers, benign liver tumors, and liver cirrhosis. *Cancer Res* 48:6844-6849.
388. Lamas, E., Le Bail, B., Housset, C., Boucher, O., and Brechot, C. 1991. Localization of insulin-like growth factor-II and hepatitis B virus mRNAs and proteins in human hepatocellular carcinomas. *Lab Invest* 64:98-104.
389. D'Errico, A., Grigioni, W.F., Fiorentino, M., Baccarini, P., Lamas, E., De Mitri, S., Gozzetti, G., Mancini, A.M., and Brechot, C. 1994. Expression of insulin-like growth factor II (IGF-II) in human hepatocellular carcinomas: an immunohistochemical study. *Pathol Int* 44:131-137.
390. Iizuka, N., Oka, M., Tamesa, T., Hamamoto, Y., and Yamada-Okabe, H. 2004. Imbalance in expression levels of insulin-like growth factor 2 and H19 transcripts linked to progression of hepatocellular carcinoma. *Anticancer Res* 24:4085-4089.
391. Mazziotti, G., Sorvillo, F., Morisco, F., Carbone, A., Rotondi, M., Stornaiuolo, G., Precone, D.F., Cioffi, M., Gaeta, G.B., Caporaso, N., et al. 2002. Serum insulin-like growth factor I evaluation as a useful tool for predicting the risk of developing hepatocellular carcinoma in patients with hepatitis C virus-related cirrhosis: a prospective study. *Cancer* 95:2539-2545.
392. Starley, B.Q., Calcagno, C.J., and Harrison, S.A. 2010. Nonalcoholic fatty liver disease and hepatocellular carcinoma: a weighty connection. *Hepatology* 51:1820-1832.
393. Lann, D., and LeRoith, D. 2008. The role of endocrine insulin-like growth factor-I and insulin in breast cancer. *J Mammary Gland Biol Neoplasia* 13:371-379.
394. Roddam, A.W., Allen, N.E., Appleby, P., Key, T.J., Ferrucci, L., Carter, H.B., Metter, E.J., Chen, C., Weiss, N.S., Fitzpatrick, A., et al. 2008. Insulin-like growth factors, their binding proteins, and prostate cancer risk: analysis of individual patient data from 12 prospective studies. *Ann Intern Med* 149:461-471, W483-468.
395. Bonefeld, K., and Moller, S. 2011. Insulin-like growth factor-I and the liver. *Liver Int* 31:911-919.
396. Bird, T.G., Lorenzini, S., and Forbes, S.J. 2008. Activation of stem cells in hepatic diseases. *Cell Tissue Res* 331:283-300.
397. Lozier, J., McCright, B., and Gridley, T. 2008. Notch signaling regulates bile duct morphogenesis in mice. *PLoS One* 3:e1851.
398. Joutel, A., Andreux, F., Gaulis, S., Domenga, V., Cecillon, M., Battail, N., Piga, N., Chapon, F., Godfrain, C., and Tournier-Lasserve, E. 2000. The ectodomain of the Notch3 receptor accumulates within the cerebrovasculature of CADASIL patients. *J Clin Invest* 105:597-605.

399. Darwiche, H., Oh, S.H., Steiger-Luther, N.C., Williams, J.M., Pintilie, D.G., Shupe, T.D., and Petersen, B.E. 2011. Inhibition of Notch signaling affects hepatic oval cell response in rat model of 2AAF-PH. *Hepat Med* 3:89-98.
400. Gow, D.J., Sester, D.P., and Hume, D.A. 2010. CSF-1, IGF-1, and the control of postnatal growth and development. *J Leukoc Biol* 88:475-481.

9 Appendix: ‘Pipeline’ for the use of Operetta high-content analysis system

Appendix: 'Pipeline' for use of Operetta high-content analysis system for quantification of proliferating reporter-positive cells